



UNIVERSITY OF SIENA

Department of Biotechnology, Chemistry and Pharmacy
PHD SCHOOL IN BIOCHEMISTRY AND MOLECULAR
BIOLOGY – BIBIM 2.0, XXXV CYCLE

PhD coordinator: Prof.ssa Lorenza Trabalzini

Development of recombinant monoclonal antibodies as tools for functional characterization of structurally–complex transmembrane amino acid carrier

Tutor:
Prof. Rino Rappuoli

PhD student:
Andrea Avati

Academic year: 2021/2022

Index:

1	ABSTRACT	11
2	INTRODUCTION.....	13
2.1	MONOCLONAL ANTIBODIES: CHARACTERISTICS AND APPLICATIONS	13
2.2	HYBRIDOMA TECHNOLOGY.....	15
2.3	LIMITATIONS OF HYBRIDOMA TECHNOLOGY.....	19
2.4	LIMITATIONS OF MURINE MABS.....	20
2.5	DISPLAY TECHNOLOGIES	22
2.6	PHAGE DISPLAY TECHNOLOGY.....	24
2.7	LIMITATIONS OF DISPLAY TECHNOLOGIES	27
2.8	HU-IG TRANSGENIC MICE TECHNOLOGY	27
2.9	LIMITATIONS OF HU-IG TRANSGENIC MICE TECHNOLOGY	29
2.10	SINGLE B CELL TECHNOLOGIES	29
2.11	ANTIBODIES AGAINST STRUCTURALLY COMPLEX MEMBRANE PROTEINS	33
2.12	CHALLENGES FOR STRUCTURALLY COMPLEX MEMBRANE PROTEINS ANTIBODY DISCOVERY	35
3	AIMS AND SCOPE OF THE THESIS.....	37
4	MATERIALS AND METHODS	40
4.1	RECOMBINANT PLASMIDS CREATION	40
4.1.1	<i>Synthetic plasmids design.....</i>	<i>40</i>
4.1.2	<i>Synthetic DNA strings design</i>	<i>41</i>
4.1.3	<i>Plasmid DNA amplification (heat-shock bacterial transformation)</i>	<i>41</i>
4.1.4	<i>Plasmid DNA purification</i>	<i>42</i>
4.1.5	<i>Synthetic DNA strings amplification (PCR)</i>	<i>42</i>
4.1.6	<i>PCR products purification.....</i>	<i>44</i>
4.1.7	<i>Production of pcDNA3.4_TLS2Loop4-6His recombinant plasmid.....</i>	<i>44</i>
4.1.8	<i>Production of pcDNA5_TLS2-EGFP recombinant plasmid</i>	<i>46</i>
4.1.9	<i>Production of pcDNA5_TLS2-IRES-EGFP recombinant plasmid</i>	<i>48</i>
4.1.10	<i>Production of pcDNA3.4_cMyc-AP2 recombinant plasmid.....</i>	<i>49</i>
4.1.11	<i>Recombinant plasmids sequencing.....</i>	<i>50</i>
4.2	TLS2POLYP-HUIGFC POLY-EPITOPE AND TLS2LOOP4-6HIS RECOMBINANT FRAGMENT EXPRESSION	50
4.2.1	<i>Cell cultures.....</i>	<i>50</i>
4.2.2	<i>Expi293F™ cells transient transfection</i>	<i>51</i>
4.2.3	<i>Immunoaffinity chromatography</i>	<i>52</i>
4.2.4	<i>ExpiCHO-S™ cells transient transfection</i>	<i>52</i>
4.2.5	<i>Immobilized Metal Affinity Chromatography (IMAC).....</i>	<i>53</i>
4.2.6	<i>Purification control (SDS-PAGE).....</i>	<i>53</i>
4.2.7	<i>Desalting and protein quantification.....</i>	<i>54</i>
4.2.8	<i>Digestion with IdeZ protease.....</i>	<i>55</i>
4.3	TLS2-EGFP AND TLS2-IRES-EGFP/AP2 STABLE LINES GENERATION.....	55
4.3.1	<i>Cell cultures.....</i>	<i>55</i>
4.3.2	<i>Flp-In™ cell lines stable transfection.....</i>	<i>56</i>
4.3.3	<i>Confocal microscopy</i>	<i>57</i>
4.3.4	<i>Flow cytometry</i>	<i>58</i>
4.3.5	<i>Western Blot</i>	<i>59</i>
4.4	TLS2 ANTIBODIES PRODUCTION	60
4.4.1	<i>BALB/c mice immunization.....</i>	<i>60</i>
4.4.2	<i>Antibody titration.....</i>	<i>61</i>
		2

4.5	SELECTION AND IDENTIFICATION OF NEW TLS2 MABS.....	62
4.5.1	<i>Identification and isolation of TLS2-specific single ASCs</i>	62
4.5.2	<i>Recovery of V_H and V_L coding sequences from single antigen-specific ASC and “minigenes” assembly</i>	64
4.5.3	<i>Expi293FTM cells transient transfection into Deepwell plates</i>	74
4.5.4	<i>mAbs quantification and binding activity validation</i>	75
4.6	PRODUCTION AND CHARACTERIZATION OF TLS2 RECOMBINANT CHIMERIC MABS.....	77
4.6.1	<i>Cell cultures</i>	77
4.6.2	<i>V_H and V_L sequences cloning into expression vectors</i>	77
4.6.3	<i>Scale up of production and purification for selected TLS2 mAbs</i>	80
4.6.4	<i>Characterization of TLS2 chimeric mAbs</i>	80
5	RESULTS.....	82
5.1	GENERATION OF A POLY-EPI TOPE ANTIGEN AND A STABLE CELL LINE TO RAISE AND SCREEN ANTIBODY AGAINST TLS2.....	82
5.1.1	<i>Design and production of TLS2polyP-HuIgFc plasmid</i>	84
5.1.2	<i>TLS2polyP-HuIgFc protein expression and purification</i>	85
5.1.3	<i>HuIgFc-TAG removal and TLS2polyP purification</i>	87
5.1.4	<i>Design and production of pcDNA5_TLS2-EGFP recombinant plasmid</i>	88
5.1.5	<i>Generation and validation of a cell line stably expressing TLS2-EGFP</i>	91
5.1.6	<i>Mice immunization and antibody titer evaluation</i>	94
5.1.7	<i>Open questions and mitigation approaches</i>	98
5.2	REVISED APPROACH TO GENERATE MONOCLONAL ANTIBODIES RECOGNIZING CONFORMATIONAL EXTRACELLULAR EPITOPES OF TLS2.....	100
5.2.1	<i>Design and production of pcDNA3.4_TLS2Loop4-6His recombinant plasmid</i>	101
5.2.2	<i>TLS2Loop4-6His protein expression and purification</i>	103
5.2.3	<i>Design and production of a recombinant plasmid allowing the separate expression of TLS2 and EGFP from the same transcript (pcDNA5_TLS2-IRES-EGFP)</i>	105
5.2.4	<i>Design and production of pcDNA3.4_cMyc-AP2 recombinant plasmid</i>	109
5.2.5	<i>Generation and validation of a cell line stably expressing TLS2-IRES-EGFP and AP2</i>	112
5.2.6	<i>Mice immunization and antibody titer evaluation</i>	116
5.2.7	<i>Identification and isolation of TLS2-specific single ASCs</i>	119
5.2.8	<i>Recovery of V_H and V_L coding sequences from single antigen-specific ASCs and “minigenes” assembly</i>	121
5.2.9	<i>Transient mAbs production, quantification and binding activity validation</i>	124
5.2.10	<i>V_H and V_L sequences cloning into expression vectors</i>	126
5.2.11	<i>Scale up of production and purification for selected TLS2 mAbs</i>	127
5.2.12	<i>Characterization of the selected monoclonal antibodies</i>	129
6	DISCUSSION.....	135
7	REFERENCES.....	138
	APPENDIX-A.....	153
	APPENDIX-B.....	156

List of Figures:

Figure 2.1: Timeline from 1975 showing the successful development of therapeutic antibodies and their applications. Many biotech companies that promised antibodies as anticancer “magic bullets” were launched from 1981 to 1986. The height of the line and numerical annotations represent the estimated market value of mAb therapeutics in each indicated year (shown as billions of US dollars). Antibodies coloured in red represent the top 10 best-selling antibody drugs in 2018 (adapted from [25]).	15
Figure 2.2: Schematic depiction of the traditional hybridoma technology main stages: I. Animal immunization; II. B cells isolation and fusions; III. Hybridoma selection; IV. Hybridoma screening and expansion; V. mAb characterization.	17
Figure 2.3: Schematic depiction of antibody humanization from murine antibodies (red domains) to fully-human antibodies (blue domains): A. Murine antibody; B. Chimeric antibody: variable regions of murine origin and the rest of the chains are of human origin; C. Humanized antibody: only contain the complementary-determining regions (CDRs) of murine origin; D. Fully-human antibody.	21
Figure 2.4: Types of combinatorial antibody display libraries, distinguished by source and design: Naïve libraries: generated from a natural source of healthy or unimmunized donors, can be used for a wide variety of antigen; Immune libraries: amplified from B cell antibody repertoire of disease-infected or immunized donors, they are predisposed for a limited panel of antigens; Synthetic libraries: based on computational in silico design and genes synthesis, with a precisely defined and controlled design and composition of CDR loops; Semi-synthetic libraries: key subset of synthetic libraries, they comprise both CDRs from natural sources as well as in silico design of defined parts.	24
Figure 2.5: Schematic depiction of the phage display technology main stages: Target binding; Washing; Elution; Infection ± helper phage; DNA purification; Phage amplification.	26
Figure 2.6: Schematic depiction of the Hu-Ig transgenic mice technology main stages: Eggs collection and fertilization; Transgene microinjection; Transgenic zygote transfer; Implanted female pregnancy and delivery; Hybridoma development.	28
Figure 2.7: Schematic depiction of the single B cell technology main stages: I. Single B cells isolation; II. Single B cell antibodies sequencing and cloning; III. Antibodies reactivity screening.	31
Figure 3.1: Schematic depiction of human TLS2 amino acid transporter in plasma membrane. This human multi-pass membrane protein with a molar weight of approximately 70kDa is composed of 12 transmembrane α -helix domains (TM1–12) and 6 predicted extracellular loops of various sizes (Loop1–6).	38
Figure 5.1: Schematic depiction of TLS2-EGFP and TLS2 poly-epitope strategy experimental workflow.	83
Figure 5.2: Schematic depiction of TLS2polyP-HuIgFc synthetic plasmid.	84
Figure 5.3: Elution profile of TLS2polyP-HuIgFc. The red square indicates the single elution peak containing the poly-epitope (A); Purification control of TLS2polyP-HuIgFc. The red arrows indicate the presence of the poly-epitope in multimeric forms in the non-	

<i>reduced fraction and in monomeric form in the reduced fraction (with an expected molecular weight of approximately 63kDa) (B).</i>	86
Figure 5.4: SDS–PAGE of TLS2polyP fragment after the removal of HuIgFc–TAG. The red arrow indicates the TLS2poly fragment (with an expected molecular weight of approximately 25kDa).	87
Figure 5.5: Schematic depiction of TLS2Full synthetic plasmid (A) and pcDNA5–FRT–EGFP recombinant plasmid (B).	88
Figure 5.6: Schematic depiction of pcDNA–FRT–EGFP plasmid amplification product.	89
Figure 5.7: Schematic depiction of the ligase reaction between TLS2Full_HindIII+BamHI insert and pcDNA5–FRT–EGFP_HindIII+BamHI vector.	90
Figure 5.8: Schematic depiction of FRT recombination between Flp–In TM –293 genome and pcDNA5_TLS2–EGFP recombinant plasmid and generation of HEK293_TLS2–EGFP stable line.	92
Figure 5.9: The TLS2–EGFP associate with the cell membrane in HEK293 stable line. The association was visualized by the colocalization of the EGFP fluorescence with a plasma membrane marker labelled with TRITC in confocal microscopy.	93
Figure 5.10: Immunization and sampling timeline for TLS2polyP–HuIgFc.	94
Figure 5.11: Immunization of mice with TLS2polyP–HuIgFc poly–epitope induced a good antibody titer against the TLS2polyP fragment. The antigen–specific antibodies were revealed in an ELISA assay.	95
Figure 5.12: Flow cytometry recognition of the full–length TLS2 protein transiently expressed in HEK293 cells with individual mouse serum of mice immunized with TLS2polyP–HuIgFc poly–epitope.	96
Figure 5.13: Evaluation of the correct exposure of full–length TLS2 protein through flow cytometry test.	97
Figure 5.14: Schematic depiction of TLS2–IRES–EGFP+AP2 and TLS2Loop4 recombinant fragment strategy experimental workflow.	100
Figure 5.15: Schematic depiction of synthetic TLS2Loop4 DNA string (A) and pcDNA3.4–6His plasmid (B).	101
Figure 5.16: Schematic depiction of the ligase reaction between TLS2Loop4_HindIII+BamHI insert and pcDNA3.4–6His_HindIII+BamHI vector.	102
Figure 5.17: Elution profile of TLS2Loop4–6His. The red square indicates the single elution peak containing the recombinant fragment (A); Purification control of TLS2Loop4–6His. The red arrows indicate the presence of the recombinant fragment in multimeric forms in the non–reduced fraction and in monomeric form in the reduced fraction (with an expected molecular weight of approximately 18kDa) (B).	104
Figure 5.18: Schematic depiction of pAAV.CMV.Luc.IRES.EGFP.SV40 synthetic plasmid.	105
Figure 5.19: Schematic depiction of the ligase reaction between pIRES–EGFP_BamHI+NotI insert and pcDNA5_TLS2nostop_BamHI+NotI.	106
Figure 5.20: Schematic depiction of TLS2stopcodon–IRES–BstXI synthetic DNA string.	107
Figure 5.21: Schematic depiction of the ligase reaction between TLS2stopcodon–IRES_BstXI insert and pcDNA5_TLS2nostop–IRES–EGFP_BstXI vector.	108

Figure 5.22: Schematic depiction of cMyc–AP2 synthetic DNA string (A) and customized pcDNA3.4 plasmid (B).	110
Figure 5.23: Schematic depiction of the ligase reaction between cMyc–AP2_HindIII+NotI insert and pcDNA3.4_HindIII+NotI vector.	111
Figure 5.24: Schematic depiction of FRT recombination between Flp–In TM –CHO genome and pcDNA5_TLS2–IRES–EGFP recombinant plasmid and generation of CHO_TLS2–IRES–EGFP stable line.	112
Figure 5.25: pcDNA5_TLS2–IRES–EGFP expression validation in Flp–In TM –CHO stable line through fluorescence microscopy (B).	113
Figure 5.26: Flow cytometry recognition of the cMyc–tagged AP2 protein stably expressed in CHO_TLS2–IRES–EGFP cells with anti–cMyc mAb (Ab I ^o) and F(ab') ₂ –Goat anti–Mouse IgG (H+L) Cross-Adsorbed–Alexa Fluor TM 647 conjugated (Ab II ^o). The division into quadrants allows to identify the cMyc–AP2–expressing cells (top–right).	114
Figure 5.27: Western Blot recognition of TLS2 protein stably expressed in both CHO_TLS2–IRES–EGFP and CHO_TLS2–IRES–EGFP/AP2 cell lines. The red square indicates the presence of a band at the expected molecular weight for the TLS2 protein (approximately 70kDa).	115
Figure 5.28: Immunization and sampling timeline for Group A (CHO_TLS2–IRES–EGFP/AP2 stable line cells) (A) and Group B (TLS2Loop4–6His recombinant fragment) (B).	116
Figure 5.29: Immunization of mice with CHO_TLS2–IRES–EGFP/AP2 stable line (Group A) (A) or with TLS2Loop4–6His recombinant fragment (Group B) (B) induced a good antibody titer against TLS2Loop4–6His. The antigen–specific antibodies were revealed in an ELISA assay.	117
Figure 5.30: Immunization of mice with TLS2Loop4–6His recombinant fragment (Group B) induced a good antibody titer against full–length TLS2 protein expressed in CHO_TLS2–IRES–EGFP/AP2 stable line. The antigen–specific antibodies were revealed in a Western Blot assay. The red arrow indicates the presence of a band at the expected molecular weight for the TLS2 protein (approximately 70kDa).	118
Figure 5.31: Schematic depiction of the method used to isolate single antigen–specific CD138 ⁺ plasma cells.	120
Figure 5.32: Schematic depiction of the Transcriptionally Active PCR (TAP) minigenes assembly.	122
Figure 5.33: Schematic depiction of AbVec2.0–IGHG1 and AbVec1.1–IGKC plasmid.	123
Figure 5.34: Schematic depiction of the Polymerase Incomplete Primer Extension PCR (PIPE–PCR) method.	126
Figure 5.35: Elution profile of TLS2 mAb#51 and mAb#56. The red squares indicate the single elution peaks containing the monoclonal antibodies (A/C); Purification control of TLS2 mAb#51 and mAb#56. The red arrows indicate the presence of the monoclonal antibodies (with an expected molecular weight of approximately 150kDa) (B/D).	128
Figure 5.36: TLS2 mAb#51 and mAb#56 binding activity characterization against CHO_TLS2–IRES–EGFP/AP2 stable line and TLS2Loop4–6His recombinant fragment through Western Blot. The red squares indicate the presence of bands at the expected molecular weight for the TLS2 protein (approximately 70kDa).	129

Figure 5.37: TLS2 mAb#51 and mAb#56 binding activity characterization against CHO_TLS2-IRES-EGFP and CHO_TLS2-IRES-EGFP/AP2 stable lines through confocal analysis.....	130
Figure 5.38: TLS2 mAb#51 and mAb#56 binding activity characterization against CHO_TLS2-IRES-EGFP and CHO_TLS2-IRES-EGFP/AP2 stable lines through flow cytometry.....	132
Figure 5.39: TLS2 mAb#51 and mAb#56 binding activity characterization against HEL cell lines through flow cytometry.....	134
Figure A-1: Quality evaluation of the pcDNA5-FRT-EGFP recombinant plasmid amplification product. The red square highlights the presence of a band with dimension comparable to those expected for the amplified pcDNA5-FRT-EGFP vector (5808bps), which will be subsequently purified through QIAquick Gel Extraction Kit.	153
Figure A-2: TLS2Full synthetic plasmid and pcDNA5-FRT-EGFP amplified vector digested with HindIII + BamHI restriction enzymes. The red square highlights the band corresponding to TLS2Full_HindIII+BamHI insert (1914bps), while the green square highlights the band corresponding to pcDNA5-FRT-EGFP_HindIII+BamHI vector (5730bps), which will be subsequently purified through QIAquick Gel Extraction Kit....	154
Figure A-3: Colony PCR for the screening of DH5 α colonies transformed with pcDNA_TLS2-EGFP recombinant plasmid. The red squares highlight the bands corresponding to TLS2Full insert specific amplification product (1920bps).	155
Figure B-1: pAAV.CMV.Luc.IRES.EGFP.SV40 synthetic plasmid and pcDNA5_TLS2-EGFP recombinant plasmid digested with BamHI + NotI restriction enzymes. The red square highlights the band corresponding to pIRES-EGFP_BamHI+NotI insert (1316bps), while the green square highlights the band corresponding to pcDNA5_TLS2nostop_BamHI+NotI vector (6916bps), which will be subsequently purified through QIAquick Gel Extraction Kit.	159
Figure B- 2: Control digestion with HindIII restriction enzyme for the screening of DH5 α colonies transformed with pcDNA5_TLS2nostop-IRES-EGFP recombinant plasmid. The red squares highlight the bands corresponding to the correct cloning of pIRES-EGFP insert into pcDNA5_TLS2nostop vector (6082bps + 2150bps).	160
Figure B-3: TLS2stopcodon-IRES-BstXI synthetic DNA string and pcDNA5_TLS2nostop-IRES-EGFP recombinant plasmid digested with BstXI restriction enzyme. The red square highlights the band corresponding to TLS2stopcodon-IRES_BstXI insert (659bps), while the green square highlights the band corresponding to pcDNA5_TLS2nostop-IRES-EGFP_BstXI vector (7562bps), which will be subsequently purified through QIAquick Gel Extraction Kit.	162
Figure B- 4: Control digestion with XhoI restriction enzyme for the screening of DH5 α colonies transformed with pcDNA5_TLS2-IRES-EGFP recombinant plasmid. The red squares highlight the bands corresponding to the correct cloning of TLS2stopcodon-IRES insert into pcDNA5_TLS2nostop-IRES-EGFP vector (6904bps + 1328bps).	163
Figure B-5: Control digestion with XbaI and NotI restriction enzymes for the screening of DH5 α colonies transformed with pcDNA3.4_cMyc-AP2 recombinant plasmid. The red squares highlight the bands corresponding to the correct cloning of cMyc-AP2 insert into pcDNA3.4 vector (5998bps + 753bps).	166

Figure B-6: PCR amplification products for the creation of the human CMV promoter and human constant region fragment fused to a BGH poly-A signal (A); PCR II and PCR III (TAP) amplification products for the creation of complete mAb#51 and mAb#56 TAP V_H/V_L chimeric minigenes (B). 167

Figure B-7: Quality evaluation of mAb#51 PCR II products PIPE-amplification. The red and green squares highlight the presence of a band with dimension comparable to those expected for the amplified mAb_ V_H and mAb_ V_L inserts, respectively (A). Quality evaluation of mAb#26 PCR II products PIPE-amplification. The red and green squares highlight the presence of a band with dimension comparable to those expected for the amplified mAb_ V_H and mAb_ V_L inserts, respectively (B). Quality evaluation of mAb#56 PCR II products PIPE-amplification. The red and green squares highlight the presence of a band with dimension comparable to those expected for the amplified mAb_ V_H and mAb_ V_L inserts, respectively (C). Quality evaluation of AbVec2.0-IGHG1 and AbVec1.1-IGKC plasmids PIPE-amplification. The red and green squares highlight the presence of a band with dimension comparable to those expected for the amplified AbVec2.0-IGHG1 and AbVec1.1-IGKC vectors, respectively (D). 168

Figure B-8: Colony PCR and control digestion with EcoRI and HindIII restriction enzymes for the screening of Mach1 colonies transformed with mAb#51H/L insert + AbVec2.0-IGHG1/AbVec1.1-IGKC vector. The red square and green squares highlight the bands corresponding to the correct cloning of mAb#51_ V_H/V_L insert into AbVec2.0-IGHG1/AbVec1.1-IGKC vector, respectively (A). Colony PCR and control digestion with EcoRI and HindIII restriction enzymes for the screening of Mach1 colonies transformed with mAb#56H/L insert + AbVec2.0-IGHG1/AbVec1.1-IGKC vector. The red square and green squares highlight the bands corresponding to the correct cloning of mAb#56_ V_H/V_L insert into AbVec2.0-IGHG1/AbVec1.1-IGKC vector, respectively (B). 169

List of Tables:

Table 4.1: PCR Mix used for the amplification of TLS2Loop4–6His, TLS2stopcodon–IRES–BstXI and cMyc–AP2 synthetic DNA strings.	43
Table 4.2: Amplification profile used for TLS2Loop4–6His, TLS2stopcodon–IRES–BstXI and cMyc–AP2 synthetic DNA strings.....	43
Table 4.3: Colony PCR Mix.	45
Table 4.4: Amplification profile used for colony PCR.	45
Table 4.5: PCR Mix used for the amplification of pcDNA5–FRT–EGFP recombinant plasmid.	46
Table 4.6: Amplification profile used for pcDNA5–FRT–EGFP recombinant plasmid.	47
Table 4.7: TLS2–specific single CD138 ⁺ plasma cells Lysis Buffer.....	63
Table 4.8: RT–PCR Mix I.....	64
Table 4.9: RT–PCR Mix II.	65
Table 4.10: Amplification profile of RT–PCR.....	65
Table 4.11: preAmp–PCR Mix.	66
Table 4.12: Amplification profile used for cDNA pre–amplification.....	66
Table 4.13: PCR I/II Mix.....	67
Table 4.14: V _H and V _L PCR I primers.	68
Table 4.15: Amplification profile used for PCR I.	68
Table 4.16: PCR II primers.....	69
Table 4.17: Amplification profiles used for PCR II.	71
Table 4.18: V _H /V _L Vector PCR Mix.....	72
Table 4.19: V _H and V _L vectors PCR primers.....	72
Table 4.20: Amplification profile used for V _H and V _L vectors PCR.....	73
Table 4.21: TAP Mix.	73
Table 4.22: Amplification profiles used for TAP.	74
Table 4.23: PIPE–PCR Mix.	78
Table 4.24: V _H /V _L inserts and AbVec2.0–IGHG1/AbVec1.1–IGKC vectors PIPE–PCR primers.....	78
Table 4.25: Amplification profile used for PIPE–PCR.....	79
Table 5.1: Summary of TLS2 antigen–specific plasma cells isolation from bone marrow of mice immunized with CHO_TLS2–IRES–EGFP/AP2 stable line and TLS2Loop4 recombinant fragment.	121
Table 5.2: Summary of TLS2 antigen–specific plasma cells isolation, recovery of TAP minigenes and reactivity of chimeric mAbs.....	125
Table A–1: Bands generated through the enzymatic digestion of TLS2Full synthetic plasmid and amplified pcDNA5–EGFP vector.	154
Table B–1: Bands generated through the enzymatic digestion of synthetic TLS2Loop4 DNA string and pcDNA3.4–6His plasmid.	157

Table B-2: Bands generated through the enzymatic digestion of pAAV.CMV.Luc.IRES.EGFP.SV40 synthetic plasmid and pcDNA5_TLS2-EGFP recombinant plasmid.	159
Table B-3: Bands generated through the enzymatic digestion of pcDNA5_TLS2nostop-IRES-EGFP recombinant plasmid.	160
Table B-4: Bands generated through the enzymatic digestion of TLS2stopcodon-IRES-BstXI synthetic DNA string and pcDNA5_TLS2nostop-IRES-EGFP recombinant plasmid.	162
Table B-5: Bands generated through the enzymatic digestion of pcDNA5_TLS2-IRES-EGFP recombinant plasmid.	163
Table B-6: Bands generated through the enzymatic digestion of cMyc-AP2 synthetic DNA string and customized pcDNA3.4 plasmid.	165
Table B-7: Bands generated through the enzymatic digestion of pcDNA3-4_cMyc-AP2 recombinant plasmid.	166

1 Abstract

The high affinity and specificity of monoclonal antibodies (mAbs) against a single epitope, combined with the actual possibility to produce them in large quantities through different well-established technologies, make mAbs extremely important research tools for a broad spectrum of biochemistry, molecular and cellular biology applications and sharp devices in medical contexts, both for diagnostic and therapeutic purposes. However, the development of new approaches for the generation, isolation and production of mAbs is critical to address the limited ability of hybridoma technologies to represent the antibody repertoire diversity generated following immunization of wild type or Hu-Ig transgenic mice, or the display technologies propensity to lose the naturally selected heavy and light chains variable regions pairing.

Structurally-complex transmembrane protein families such as GPCRs, ion channels and solute carrier (SLC) membrane transporters are functional in many important cellular processes and involved in several pathological conditions. For these reasons they are very attractive targets for the development of monoclonal antibodies either for diagnostic or therapeutic applications. However, the technical difficulties encountered in their generation make these potential therapeutic targets still poorly exploited.

The aim of this PhD project is to define an effective method for the production of monoclonal antibodies targeting structurally-complex transmembrane proteins, in order to facilitate the development of potential diagnostics and therapeutics mAbs towards hard-to-target antigens.

Combining single antigen-specific Antibody Secreting Cells (ASCs) isolation and cloning of immunoglobulin (Ig) heavy- and light-chain variable regions (V_H and V_L) it was possible to identify monoclonal antibodies recognizing different epitopes and conformational structures of a complex multi-spanning membrane protein from mice immunized with the protein natively overexpressed on cell surface or with a recombinant fragment of it. One of the newly generated antibodies efficiently recognizes a cell-surface exposed conformational epitope on a cancer cell line. To date, there is no evidence in the literature of existing antibodies capable of specifically recognizing the selected target protein in its conformational form.

The results achieved allow the validation of the method described in this work. At the same time, the new developed molecular tool will be very useful for an in-depth functional characterization of a transmembrane amino acid carrier involved in several diseases; a tool that could be eventually further developed for diagnostic and therapeutic applications.

2 Introduction

2.1 Monoclonal antibodies: characteristics and applications

Since their first production in 1975 by Georges J. F. Köhler and César Milstein [1], through an innovative experimental procedure subsequently renamed “hybridoma technology”, the monoclonal antibodies (mAbs) have become essential tools for a broad spectrum of biochemical, molecular biology, and medical applications.

Unlike polyclonal antibodies (pAbs), which are immunoglobulins secreted by different plasma cell clones that recognize and bind a multiplicity of epitopes of the same antigen, mAbs are produced by a single B lymphoid cell clone and therefore have affinity for a unique antigenic determinant. This mono-specificity makes mAbs particularly suitable for structural analyses, evaluation of conformational, interactional, or post-translational modifications and identification of single antigen in a defined protein family.

Another difference between polyclonal and monoclonal antibodies lies in their reproducibility. pAbs are directly purified from the immune repertoire present in the blood serum of animals immunized with the antigen of interest. For this reason, their reactivity and titer significantly vary among different batches, with a production limited by the animal’s size and lifespan. On the other hand, both traditional (i.e., hybridoma) and novel techniques of mAbs development are based on the identification and the maintenance of the genetic information relative to the single monospecific antibody, thus generating a system for the constant production of antibodies with elevated specificity. This mAbs feature is useful for the establishment of immunoassay systems under safe and standardized conditions [2].

Overall, the possibility to produce large quantities of mAbs with highly specific binding make them extremely important tools for basic research and clinical applications, including:

- **Qualitative and/or quantitative analyses** to evaluate antigen presence and abundance in complex mixtures (e.g., enzyme-linked immunosorbent assay, ELISA [3], enzyme-linked immunospot, ELISPOT [4], immunoblot [5], immunoprecipitation [6], X-ray crystallography [7], proteome/antibody microarray [8], [9]), single-cell suspensions and sections of immobilized cells/tissue (e.g., immunofluorescence and immunohistochemistry [10], flow cytometry [11]), or even organisms *in vivo* (e.g., radioimmunoimaging [12]);

- **Purification and/or enrichment** of soluble antigen and antigen-associated molecules (e.g., immunoaffinity chromatography [13]) or subpopulations of antigen-expressing cells (e.g., magnetic-activated cell sorting, MACS [14], panning [15], fluorescence-activated cell sorting, FACS [11]);
- **Mediation and/or modulation** of physiological effects by targeting an antigen presented in an extracellular environment (e.g., abzymes [16]), in intact and viable cells (e.g., cell signalling activation [17] or neutralization [18] and intra-antibodies [19]) or in live animals and human patients (e.g., cell depletion [20], cell signalling neutralization [21] and immunotherapy [22]).

Given their high applicational versatility, the mAbs industry has managed to grow exponentially in recent years, with 115 potential mAbs therapeutics currently in late-stage clinical studies [23] and a global market of 126 approved antibody drugs by the US Food and Drug Administration (FDA) and EU European Medicines Agency (EMA) [24]. Recent data show that the mAbs market nearly quadrupled from the average of 1,6 new antibodies released per year in the period between 2002 and 2012, thanks also to a streamline in the approval process by the US and EU regulatory bodies and a good pipeline. In fact, 90 new mAbs have entered the market since 2013 and this trend is expected to continue in the future years, with a market value potentially reaching \$300 billion by 2025 [25].

Although mAbs have a stable niche of use in biochemistry, molecular and cellular biology, and in basic research as probes capable to recognize and bind a specific biomarker, the mAb industry has mainly focused on their development in medical contexts (e.g., oncology, immunology, haematology) both for diagnostic and therapeutic purposes [26]. It is evident that the importance of mAbs as therapeutic drugs has grown over the past years (Figure 2.1), making them the predominant treatment approach for several human diseases. During this period, there was also a strong interest of pharmaceutical companies in the repurposing of already existing mAbs to counteract any biosimilar effects and in the development of new technologies to make the discovery and the time-to-clinic processes of antibody therapies rapid and effective, including single-cell printing and cloning, high-throughput screening, selection of the best clones and culture in miniaturized bioreactor systems for improved scalability [26].

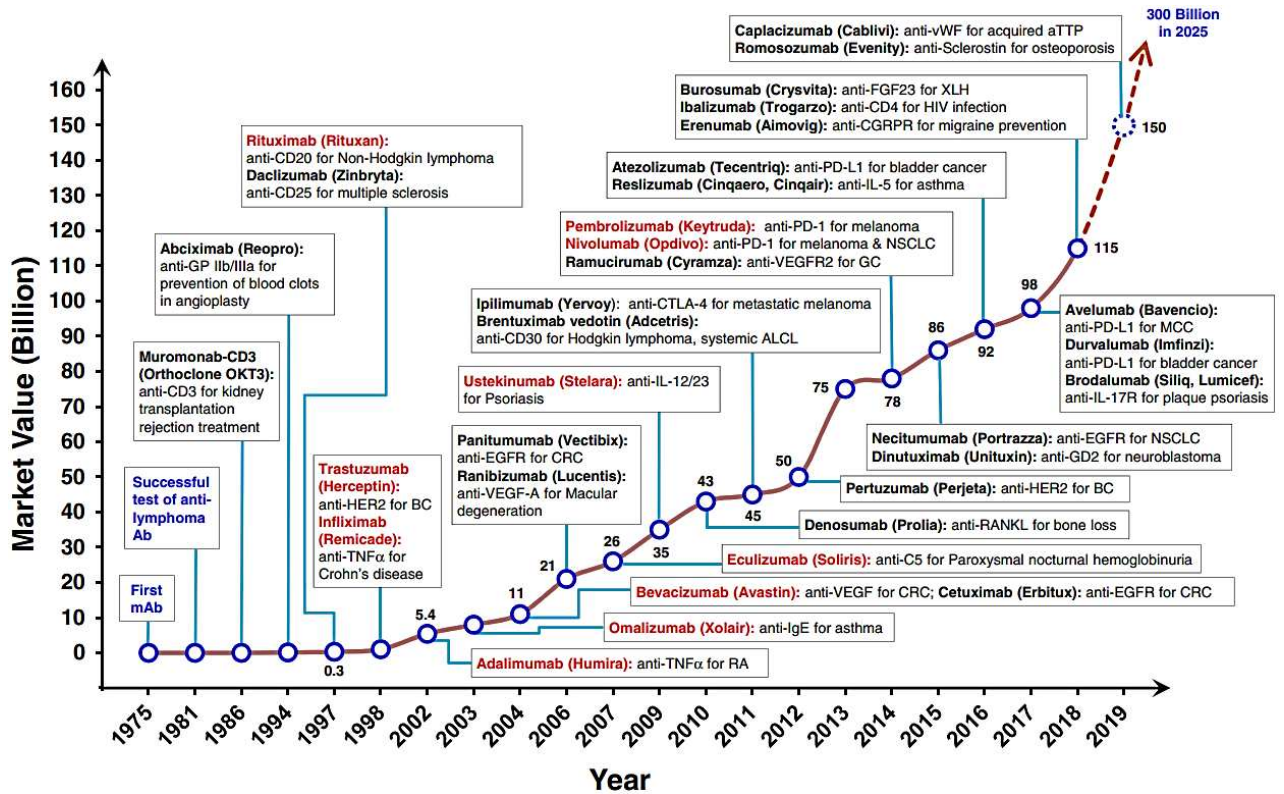


Figure 2.1: Timeline from 1975 showing the successful development of therapeutic antibodies and their applications. Many biotech companies that promised antibodies as anticancer “magic bullets” were launched from 1981 to 1986. The height of the line and numerical annotations represent the estimated market value of mAb therapeutics in each indicated year (shown as billions of US dollars). Antibodies coloured in red represent the top 10 best-selling antibody drugs in 2018 (adapted from [25]).

2.2 Hybridoma technology

The main purpose of the hybridoma development technique is to immortalize an isolated murine B cell capable of producing antibodies of single specificity, which would normally survive only a few days after isolation, so that it can be propagated in continuous cultures and obtain a virtually unlimited supply of high-quality murine mAbs.

mAbs production through hybridoma technologies can be divided in 5 main stages (Figure 2.2):

- I. **Animal immunization:** The antigen is presented as an immunogen capable of stimulating an immune response in the animal, in the form of a protein, short peptide coupled to a carrier protein (i.e., keyhole limpet hemocyanin, KLH [27]), synthetic multiple-antigenic peptide or antigen-expressing cells. The immunogen is typically administered through intraperitoneal or subcutaneous injection with a non-specific immune enhancer (e.g., complete/incomplete Freund’s adjuvant CFA/IFA). Regular boosters are required to increase the immune response and to induce class-switch

recombination (CSR) via somatic hypermutation, in order to generate higher affinity antibodies such as IgG, particularly appreciated for therapeutic applications due to their longer half-life (6 to 8 days) [28], [29]. The most commonly used mouse strain is the BALB/c, an exceptional model for immunology research due to its ability to produce plasma cell tumours within soft tissue and the easy activation of Th2 cells following immunization [30]. Other animal models that can be used for immunization are rabbits [31] and rats [32]. Although *in vivo* immunization is the most used approach, this step can also be performed *in vitro*, using cultured splenic cells and lower antigen amounts [33];

II. B cells isolation and fusion: After the identification of a mouse with an appropriate immune repertoire through antigen-specific antibody titration on serum samples, B-cells are aseptically removed from its lymphoid tissues (e.g., bone marrow, lymph nodes, spleen). The murine B lymphocytes thus obtained are fused with histocompatible myeloma cells (e.g., NS0, NS1, Sp2/0, X63Ag8.653 cell lines), derived from antibody-producing plasma cancer cells, through physical (i.e., pulsed UV laser microbeam [34]), chemical (i.e., polyethylene glycol PEG [35]) or electrochemical (i.e., electrofusion [36]) techniques. The myeloma fusion partners are previously selected in 8-azaguanine enriched medium [37] for a deficiency in hypoxanthine-guanine-phosphoribosyl transferase (HGPRT), an enzyme required for the salvage pathway for purine biosynthesis. The resulting HGPRT⁻ myeloma cells are therefore completely dependent on the *de novo* pathway to survive; which is extremely important during the selection of fused cells;

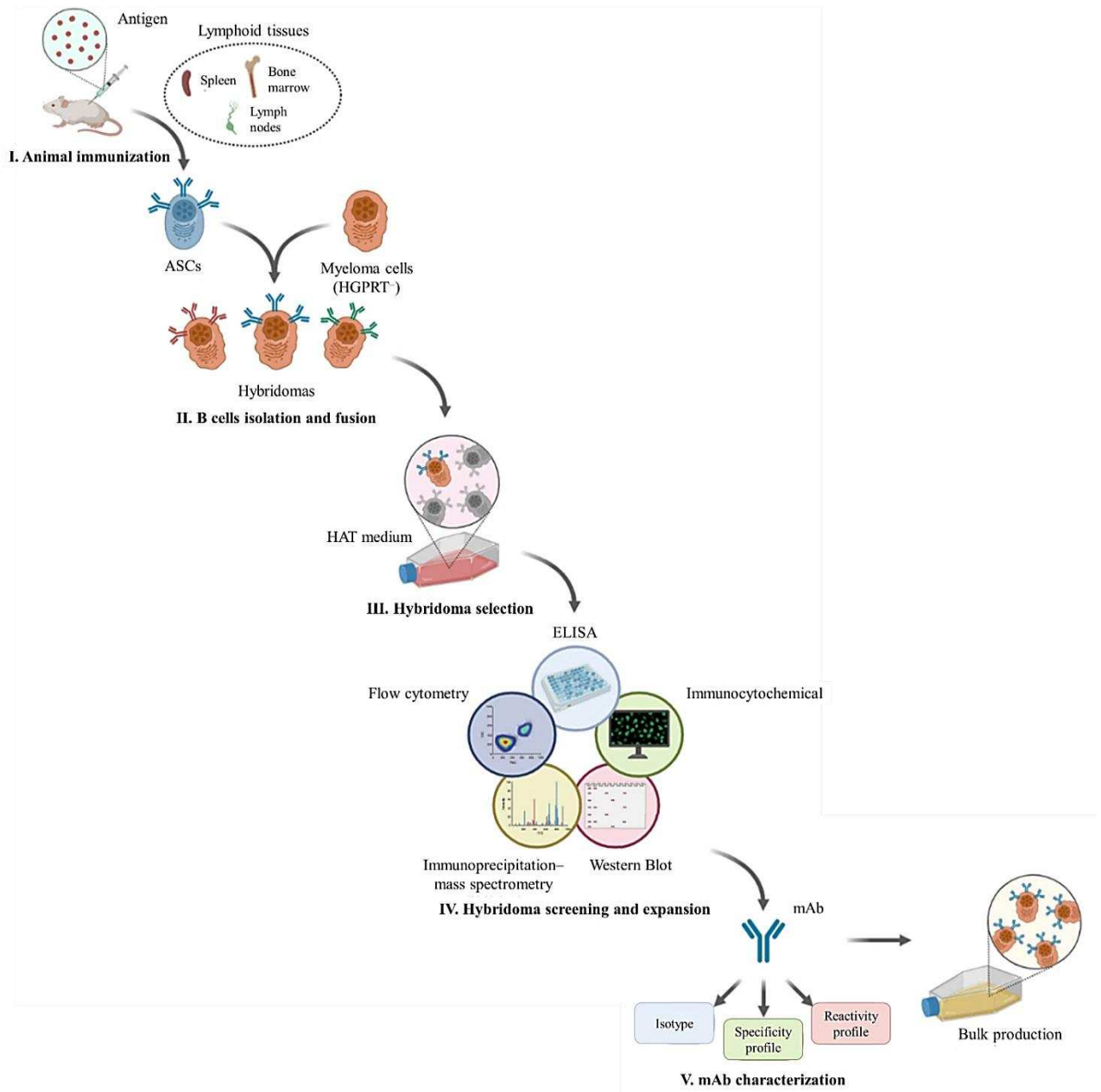


Figure 2.2: Schematic depiction of the traditional hybridoma technology main stages: **I.** Animal immunization; **II.** B cells isolation and fusions; **III.** Hybridoma selection; **IV.** Hybridoma screening and expansion; **V.** mAb characterization.

III. Hybridoma selection: Since fusion process has a low success rate, it is critical to remove any unfused myeloma cells, which can outgrow particularly unstable hybridomas. For this reason, the hybrid cells are seeded in tissue culture wells containing hypoxanthine–aminopterin–thymidine (HAT) selective medium. While hypoxanthine (a purine derivate) and thymidine are intermediates in the DNA synthesis, aminopterin is a folic acid analogue which inhibits dihydrofolate reductase

(DHFR), a key enzyme in the *de novo* pathway for purine biosynthesis. Hence, it is possible to select only B–myeloma fused cells, able to survive in HAT medium thanks to the salvage pathway enzyme supplied by the splenic B cells, compared to HGPRT[−] myeloma cells, fully auxotrophic for nucleic acids, and the spleen cells, limited in proliferation by a short lifespan. After a monitoring period of 20 to 30 days after transfection, in order to evaluate any regressions, consolidated hybridomas are propagated in multi–well plates with hypoxanthine–thymidine (HT) medium;

IV. Hybridoma screening and expansion: A primary screening of the culture supernatants is performed through immunoassay (e.g., ELISA, immunocytochemical, Western Blot, immunoprecipitation–mass spectrometry, flow cytometry). in order to identify the hybridomas that produce antigen–specific mAbs and eliminate the non–specific ones. To ensure that this screening maintains a good degree of equity among all the samples, hybridomas are tested after reaching a 75% cell confluence [38]. Samples showing a positive staining pattern are then re–cloned [39], [40], in order to isolate the individual hybridomas and prevent the colonies from being composed of multiple unrelated hybrids, and retested to confirm the previous immunoassay. Once the single positive hybridomas have been identified, they are recovered from the multi–well plates and expanded in tissue culture flasks, to obtain sufficient cells for cryopreservation and supernatants for further characterization. In the event that many hybridomas test positive at the screening, only those with a more intense staining are kept, while the less favoured ones are frozen and studied at a later date;

V. mAb characterization: During this stage, hybridomas undergo to an in–depth characterization of isotype, specificity, and reactivity of the mAbs produced against a wild panel of related antigens preparations [38]. The isotype determination is particularly important since, in addition to provide information on the immunoglobulin class and subclass, it allows to validate the presence of a single isotype and to evaluate the most suitable purification technique for the antibodies. Two crucial aspects that must be considered during mAbs characterization are the assay restriction [41], [42], that is how an assay system can bias the correct presentation of the target epitope to the antibody, and any problems of cross–reactivity or dual specificity [2], which can occur when the antibody recognizes

multiple antigenic determinants due to their structural or sequence similarity. These two phenomena make it necessary to rigorously ascertain the reactivity profiles of the monoclonal antibodies [43], which can be carried out through epitope mapping [44], cross-competition studies, recombinant phage methodologies or affinity measurements through surface plasmon resonance (SPR).

Once hybridomas with the desired characteristics of specificity and reactivity against the antigen of interest are identified, they are propagated in surface expanded tissue culture flasks or hollow fibre bioreactor systems, for a bulk production of the mAbs [38].

2.3 Limitations of hybridoma technology

Although the hybridoma development technology has been an indispensable platform for the production of high-binding specificity murine mAbs, capable of leading to a real revolution on their application in both research and clinical fields, it has several technical and applicational limitations.

As already mentioned, this methodology is based on the fusion of myeloma cells with antibody-secreting B cells, to immortalize the latter and propagate them over a prolonged period of time. However, its success is highly dependent on the myeloma conditions, so it becomes imperative to maintain cell cultures in optimal conditions, with strictly standardized protocol for routine passage and continuous checks for any mycoplasma contamination [45]. Despite this, fusion is still a very inefficient process and only a minimal number of the B cells can be immortalized and sampled (5×10^{-6} efficiency with chemical PEG fusion) [46], limiting the potential diversity of the immune repertoire generated by immunization and decreasing the chances of identifying and isolating infrequent antibodies with desired reactivity and specificity characteristics.

Another critical step during the hybridomas production is the screening stage, as it is strictly dependent on the hybrids growth rate. Slow-growing hybridomas, which are often the most stable, can take up to 25 to 30 days post-fusion to reach an acceptable confluence for the supernatant screening, while most are able to reach it in much less time. For this reason, the screening stage becomes an almost daily task, with a high workload and extremely time and materials-consuming [38].

Even once the antigen-specific hybridoma has been identified, there is still the risk of a low mAb expression due to hybrids (e.g., non-secreting variants, overgrown of unrelated hybrids) and genomic instability (e.g., onset of mutation, loss of chromosomes).

2.4 Limitations of murine mAbs

The use of murine mAbs in therapeutic fields is hampered by the recognition of these molecules as non-self by the host immune system, generating in turn an adverse response against them. In fact, murine mAbs have a reduced half-life in human blood stream, also as a consequence of a relatively weak binding with human major histocompatibility complex (MHC) class I-like Fc receptor (FcRn) [47]. Their administration can lead to the development of allergic reactions, with the consequent induction of anti-drug antibodies (ADAs) [48]. Finally, mAbs application in oncology therapy are limited by a poor recruitment of essential mechanism for tumour destruction, such as effector function, antibody-dependent cellular cytotoxicity (ADCC) and complement-dependent cytotoxicity (CDC) [49].

However, all these limitations have given a strong push towards the development of new techniques to replace the murine antibody sequences with functionally equivalent human amino acid sequences, in order to overcome the problems of decreasing immunological potential and allow their effective therapeutic use without altering their binding properties [50]. The advances in molecular biology, involving *in vitro* gene sequences manipulation and their expression in cell culture systems, have made possible to engineer new types mAb (Figure 2.3):

- **Chimeric mAbs:** these recombinant antibodies exhibit the variable region of a species (e.g., mouse), which will determinate its binding specificity against the antigen of interest, grafted to the constant region of a second species (e.g., human), towards which it will maintain its biological effector functions with a lower degree of immunogenicity [51]. While these antibodies can be used in therapeutic field, including a context of anticancer therapy (e.g., Rituximab [52]), the risk that the variable portion could lead to the development of ADAs by the host immune system still exists;
- **Humanized mAbs:** these recombinant antibodies are developed by replacing the complementary-determining regions (CDRs), responsible for generating the

antigen-binding site within each of the heavy and light chains variable regions, and possibly also other important amino acids in the framework region for activity and stability maintenance of a human antibody with those from a non-human species (e.g., mouse) [53]. Currently, chimeric and humanized antibodies are the main forms of human therapeutic antibodies, particularly important for diseases that require long-term treatment, such as cancer and autoimmune diseases [54]. Although humanized antibodies have a humanization proportion of about 85–90%, they are still not able to completely evade the human immune system due to their murine component, decreasing but not completely eliminating ADAs incidence.

Thanks to the push given by the excellent results in the engineering of monoclonal antibodies, new molecular approaches have been developed for the production and isolation of new mAbs directly derived from the gene sequences of human immunoglobulin. These technologies for the discovery of **fully-human mAbs (hmAbs)** can be grouped in the *in vitro* display technologies and in the immunization of transgenic mice expressing human immunoglobulins (Hu-Ig transgenic mice).

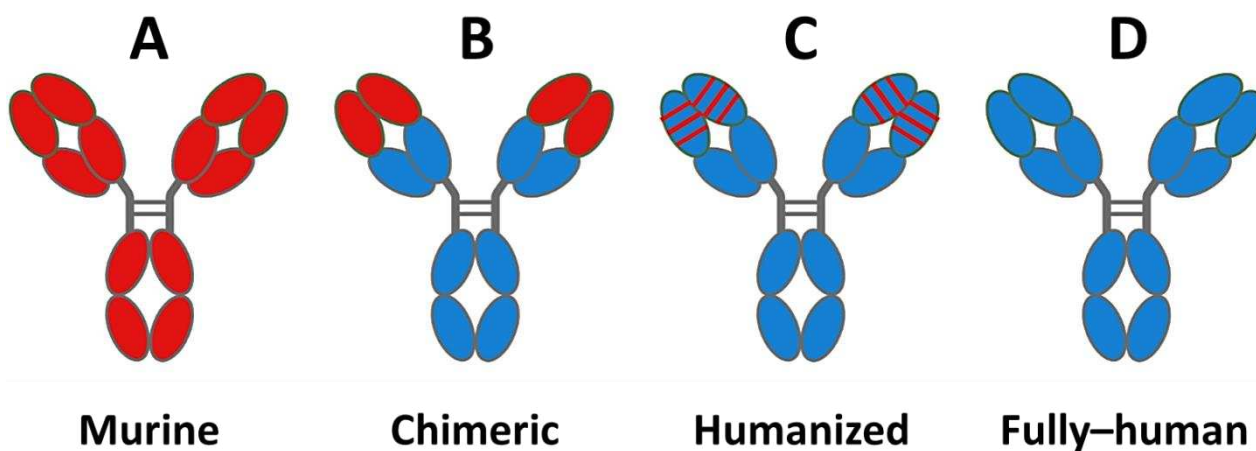


Figure 2.3: Schematic depiction of antibody humanization from murine antibodies (red domains) to fully-human antibodies (blue domains): **A.** Murine antibody; **B.** Chimeric antibody: variable regions of murine origin and the rest of the chains are of human origin; **C.** Humanized antibody: only contain the complementary-determining regions (CDRs) of murine origin; **D.** Fully-human antibody.

2.5 Display technologies

Since the first description of the phagic approach [55], display technologies have proved to be efficient tools for the creation and isolation of high affinity and specificity fully-human mAbs through a fine control of the selection and screening conditions.

All these methodologies are characterized by iterative cycles of selection and amplification on combinatorial antibody libraries, which can accurately mimic the natural human immune repertoire in terms of molecular diversity [56], [57], used to isolate the ligand of interest from them. According to the source of sequences, these libraries can be classified in (Figure 2.4):

- **Naïve libraries:** these libraries are generated by diverse variable regions of the immunoglobulin genes (i.e., single-chain variable fragment (scFv), antigen binding fragment (Fab), random combination of heavy and light chains variable regions (V_H and V_L)) cDNA obtained through reverse transcription-PCR (RT-PCR) from mRNA of a natural source, such as B cells of healthy or unimmunized donors. The amplification of heavy chain-related mRNA can be limited to the IgM isotype, in order to increase the diversity of independent clones in these libraries [58]. In contrast to immune libraries, a single naïve library exhibits high levels of unbiased sequence diversity enough to be used to isolate antibodies that recognize a wide range of antigens, including toxins and autoantigens [55];
- **Immune libraries:** these libraries are amplified from B cell antibody repertoire of disease-infected or immunized donors, so they are predisposed to a limited panel of immunogens [59], [60]. Smaller in size compared to naïve libraries due to their predisposition, immune libraries are not suitable to identify antibodies against a large antigen panel, in particular autoantigens. However, these libraries benefit from a great representation of antibody-secreting B lymphocytes, due to the higher IgH and IgL chain genes transcription, compared to other B cells. Of all the combinatorial libraries, the immune ones are the richest source of antibodies that bind a desired antigen with high selectivity and affinity [61];
- **Synthetic libraries:** these libraries are based on computational *in silico* design and synthesis of varying parts of the antibody's domains, with the introduction of defined and controlled sequence degeneration into the CDR loops to mimic the natural immune maturation and somatic hypermutation [62]. Similar in size compared to

naïve libraries, they are both known as ‘single-pot’ libraries, and even the synthetic ones can be used to isolate antibodies for different antigens [63], [64];

- **Semi-synthetic libraries:** these libraries are a key subset of synthetic libraries, composed by CDRs gene isolated from natural sources and subsequently inserted to a fixed framework sequence encoding the antibody backbone for a *in silico* design [65], [66]. In this way the diversity source still remains natural, unlike the synthetic libraries, but take advantage from the maturation processes of antibodies *in vivo* [67].

Before being able to pan and select the hmAbs that can specifically bind the antigen of interest, antibody libraries must be incorporated into a vector system to generate defined display-units, such as filamentous phages (i.e., phage display [55]), ribosomes (i.e., ribosome display [68]), or even cells (i.e., yeast display [69], bacterial display [70], mammalian cell display [71]). These units, each expressing and ‘displaying’ a single member of the corresponding antibody library of origin, can be screened against the antigen of interest, in order to identify the antibodies with high affinity for it. The display-units can therefore be isolated, thus recovering the hmAb-coding cDNAs which can be amplified and used for subsequent selection cycles. Consequently, the recognition and replication of the antibody is effectively linked to the coupling of phenotype (antibody) to genotype (cDNA), both easily identifiable through DNA sequencing, given by the display-unit.

After having identified the hmAbs able to bind the antigen of interest with the higher affinity, the corresponding cDNA are subcloned into mammalian expression vector for a bulk production.

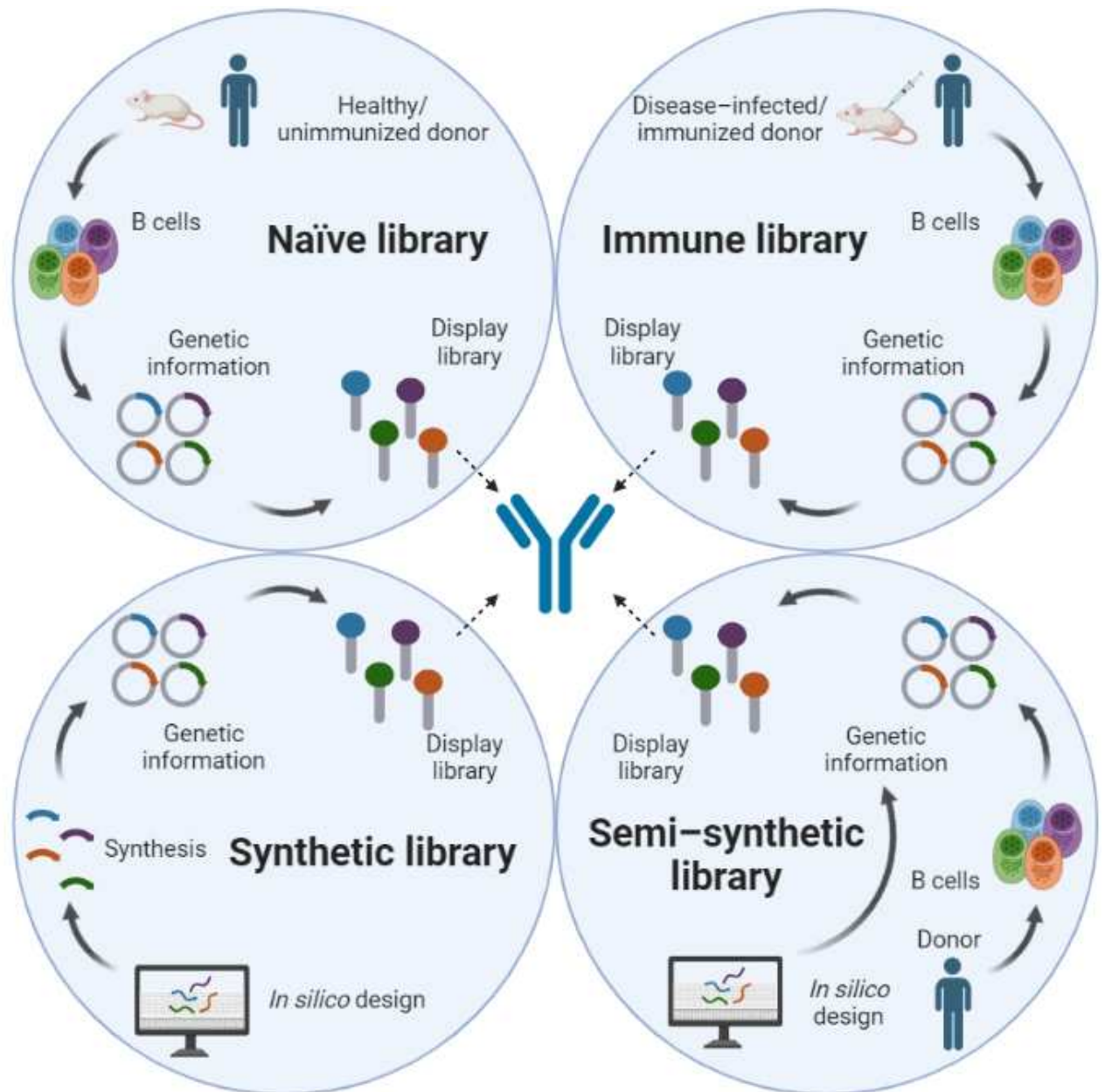


Figure 2.4: Types of combinatorial antibody display libraries, distinguished by source and design: Naïve libraries: generated from a natural source of healthy or unimmunized donors, can be used for a wide variety of antigen; Immune libraries: amplified from B cell antibody repertoire of disease-infected or immunized donors, they are predisposed for a limited panel of antigens; Synthetic libraries: based on computational *in silico* design and genes synthesis, with a precisely defined and controlled design and composition of CDR loops; Semi-synthetic libraries: key subset of synthetic libraries, they comprise both CDRs from natural sources as well as *in silico* design of defined parts.

2.6 Phage display technology

Among all the display technologies, the phage display is current the most widespread method for the selections of large collections of human mAbs and for the further engineering of the

selected ones [72], [73], which has allowed to generate nine fully-human antibody drugs approved by the US FDA. In this technique, the hmAb-coding cDNAs are inserted into a phage coat protein gene, causing the bacteriophage to exhibit the antibody-fragment on the surface of its capsid (Figure 2.5).

The most commonly used bacteriophage for phage display are members of the Ff family, such as M13, Fd and f1 [74], [75], however Enterobacteria phage λ [76] and Escherichia viruses T4 [77] and T7 [78] can also be used.

Regarding the fusion partners, the antibodies are usually merged with the N-terminus of M13 minor coat protein III (pIII) or a fragment of pIII, which facilitates its monovalent (3 + 3) display in phagemid systems and multivalent display in phage systems [79]. In the monovalent format the mAb-pIII fusion gene is carried on a phagemid vector, a 'minimal plasmid' containing only an antibiotic marker for its selection and M13 phage origin of replication for its rolling circle amplification, and the display is achieved by infecting the phagemid harbouring bacteria with a helper phage, containing the complete M13 genome to produce functional phage display-units. However, the use of a helper phage can be eliminated by using bacterial packaging cell line technology [80]. This display format is mostly preferred for the generation of hmAbs, as it involves a selection of high-affinity ligands, which are not distorted by avidity effects, which determines a greater transformation efficiency of the phagemid vectors [59], [79], [81]. Other multivalent display formats use M13 major coat protein VIII (pVIII) [82], and minor coat protein IX (pIX) [83].

Through an in vitro panning selection the desired mAb-pIII fusion protein is isolated from the phage libraries exploiting its binding affinity towards the antigen of interest (e.g., proteins, cell-surface glycans and receptors [84]) previously immobilized on solid surfaces such as nitrocellulose, magnetic beads, column matrices, polystyrene immunotubes and immunoplates, or expressed on the surface of living or fixed cells [63], [85]. After the incubation of the antibody libraries with the immobilized antigen for affinity capture, a washing step removes the unbound phages. The presence of positive clones among the phages recovered during the subsequent elution step is generally determined through ELISA [85].

Positive phages are then amplified through *Escherichia coli* infection onto selective plates (with or without the helper phage) and precipitated for reiterative panning rounds, until hmAbs with desired high binding affinity are obtained [86].

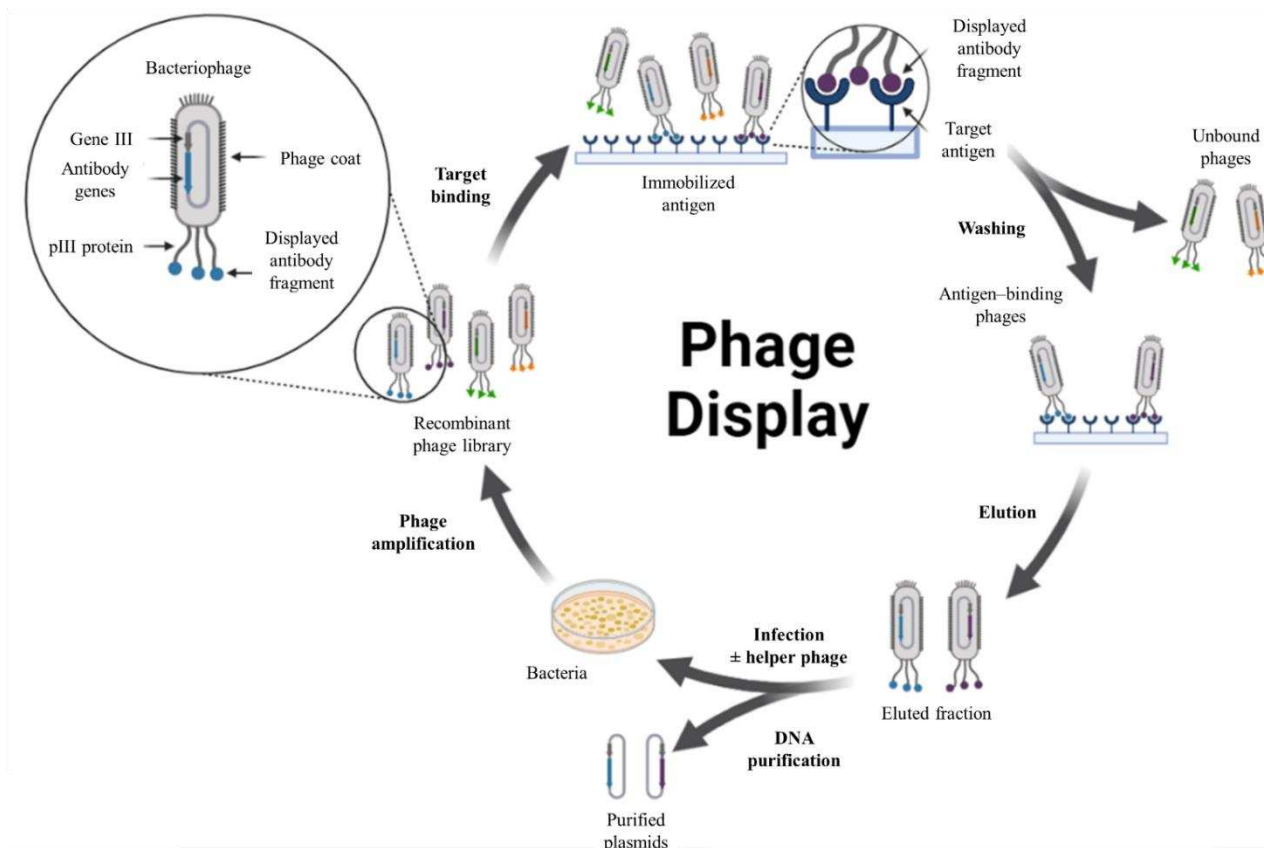


Figure 2.5: Schematic depiction of the phage display technology main stages: Target binding; Washing; Elution; Infection ± helper phage; DNA purification; Phage amplification.

The washing, elution and enrichment steps can be optimized to improve the phage libraries selection. In particular, the washing step can be modified to positively or negatively select some desirable properties for the antibodies, such as affinity, specificity, catalytic activity and manufacturability, through the introduction of different stringency degrees [58], [67]. A further tuning of the antibody characteristic is possible through site directed mutagenesis or depletion approaches. The elution step can be performed through the combination of acid–pH elution buffer and sonication, a method that allows to loosen the interaction of the antibody with the target antigen and its detachment from the immobilization surface, or ultrasound [87].

Finally, the genes of the specific antibodies are subcloned into whole human IgG expression vectors and transfected into mammalian cells, in order to produce fully human mAbs.

2.7 Limitations of display technologies

Despite their wide application for the rapid production of human recombinant mAbs, easily customizable for various downstream application in diagnostic [67] and therapeutics [88], display technologies have several drawbacks.

These methodologies are highly relying on the random combination of antibody variable region genes during the display libraries preparation, which determinates a reduced specific diversity due to loss of natural cognate heavy and light chain pairings normally evolved and selected during an *in vivo* immune response [89], [90]. Furthermore, this random pairing often requires several *in vitro* engineering steps for hmAbs isolated from naïve libraries before they can be used for therapeutic applications.

Another important limitation of these technologies is due to the display libraries screening. To perform the *in vitro* panning selection, it is essential to have the target antigen purified and immobilized on solid surfaces, which make this step strictly dependent on its quality and potentially challenging for some protein categories (e.g., glycosylated proteins, structurally–complex transmembrane proteins).

2.8 Hu–Ig transgenic mice technology

Although the Köhler and Milstein’s classic hybridoma technique has proved to be straightforward and highly reproducible, its applicational limitations in human, combined with the advanced technologies available for the production of fully–human mAbs, have led to the development of a new immunization methodology based on transgenic rodents, like HuMabMouse [91] or XenoMouse [92].

Hu–Ig transgenic mice are engineered for the silencing of the endogenous IgH and IgL chain gene repertoire and the introduction of their human counterpart at the germ line level, in order to effectively ‘humanize’ the murine immune system (Figure 2.6) [93]. Following Hu–Ig transgenic mice immunization against the antigen of interest, only human antibodies will be generated of. Single antibody–secreting B cells from the transgenic mice spleen are then recovered for the production of hmAbs through the conventional hybridoma technique. In addition to the several transgenic mice currently available on the market [94], several in progress studies aim to translate this methodology also on rat and bovine systems [95]. Similarly, a TransChromo (TC) MouseTM technology was developed through the

introduction of human chromosomes (hChrs) 14 and 2, bearing the IgH and Igk loci respectively, into IgH and IgL chain gene KO mice [96].

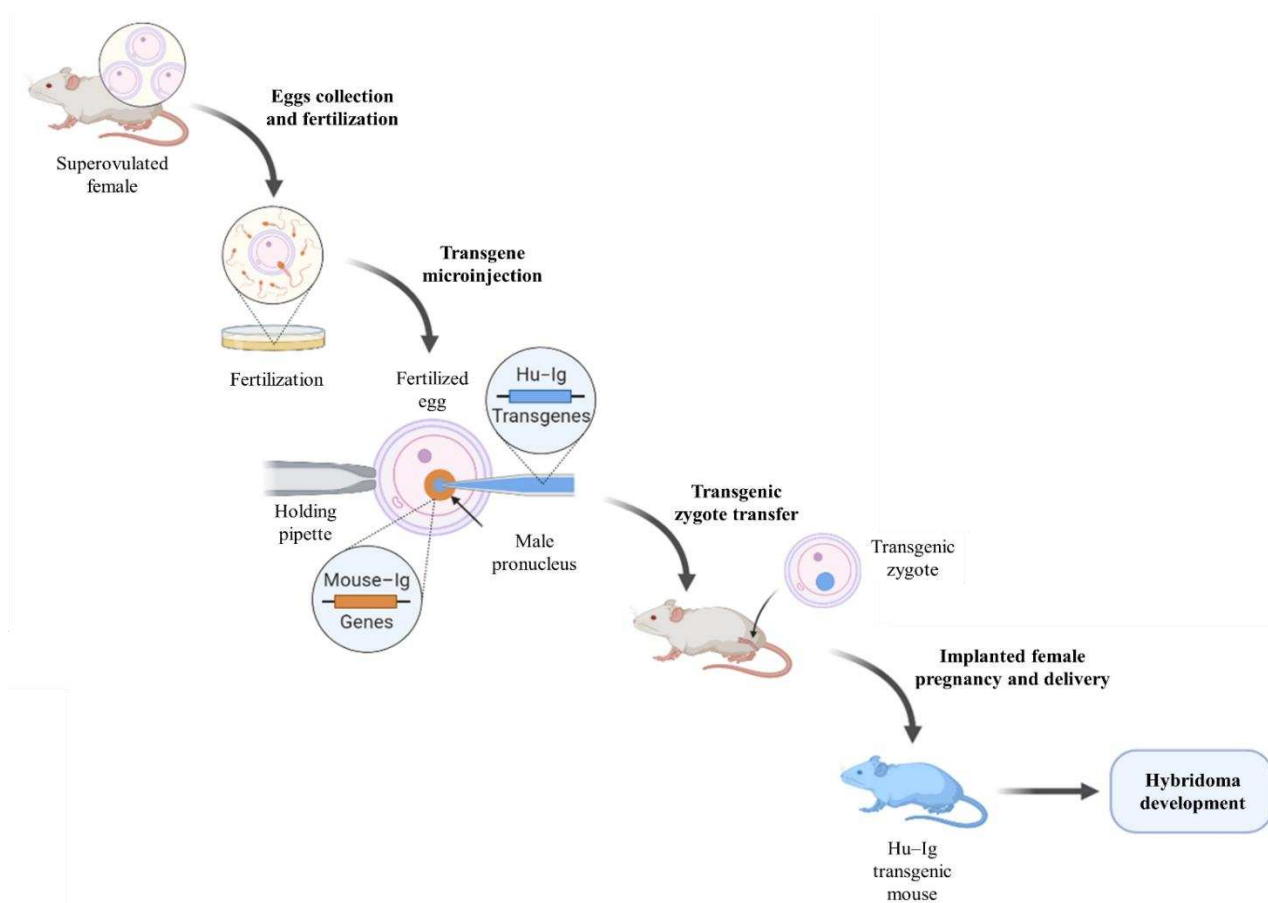


Figure 2.6: Schematic depiction of the Hu-Ig transgenic mice technology main stages: Eggs collection and fertilization; Transgene microinjection; Transgenic zygote transfer; Implanted female pregnancy and delivery; Hybridoma development.

Although display technologies are extremely faster, the transgenic mice approach exploits the natural immune selection of intact organisms, which allows the production of high affinity hmAbs without the necessity of further *in vitro* engineering steps [93], [97], [98]. Currently, 19 new fully-human antibody drugs approved by the US FDA have been obtained through this new molecular approach.

2.9 Limitations of Hu–Ig transgenic mice technology

Although this technology allows to easily produce a large quantity of hmAbs in a reproducible way, there are still some unsolved problems.

In fact, the Hu–Ig transgenic mice model cannot absolutely imitate a human immune response since, despite having lost the possibility of producing its own murine antibodies, it maintains its genetic background relating to the production of T cells, antigen processing and B cell regulation. Moreover, the antibody glycosylation will also be mouse–specific, limiting the application in immunotherapeutic context due to their recognition by anti–Gal1 α 1–3Gal antibodies present in human serum [99]. The durability of human chromosomal material containing the Hu–Ig genes, which in any case turn out to be incomplete, is another major concern related to this technology.

Another disadvantage of this methodology is the not easy accessibility of these Hu–Ig transgenic mice models, not freely available to the scientific community as they are owned by biological industries.

It should also be emphasized that the use of transgenic mice, despite solving several applicational problems of the classic hybridoma approach, is still hampered by the technical limitations linked to the dependence on obtaining a myeloma–antibody secreting B cell hybrid, on its growth rate and on its maintenance.

2.10 Single B cell technologies

Both the classical hybridoma development and the novel molecular approaches of display technologies and the use of Hu–Ig transgenic mice have proved to be excellent methods for the production of high affinity and specificity monoclonal antibodies.

However, the limited specificity diversity of the generable immune repertoire (hybridoma), the propensity to lose natural V_H and V_L pairing information (display technologies), or the inability to fully emulate the *in vivo* human immune response (Hu–Ig mice), have prompted to the development of new technological concepts based on isolation of Ig encoding genes from antigen–specific single B cells and their cloning into antibody expression vectors [90], [100].

Recently, there has been a rapid evolution of numerous strategies that allow the direct sampling of the immune repertoire from single B cells of human donors or immunized

animals [101]. mAbs production through single B cell technologies can be divided in 3 main stages (Figure 2.7):

- I. **Single B cells isolation:** Based on the type of future mAbs applications, single B cells can be isolated from lymphoid tissues or peripheral blood independently from their antigen-specificity, using micromanipulation [102], laser capture microdissection [103] and FACS [90], [104], [105], or in an antigen-selective way, with antigen-coated magnetic beads [106], haemolytic plaque assay [107], fluorochrome-labelled antigen via multi-parameter FACS [108]–[110] and fluorescent foci method [111]. Furthermore, high-throughput screening methods have been developed for rapid and efficient identification of single cells producing mAbs with the desired specificity and reactivity profile. These include cell-based microarray chip systems [112], [113], microengraving techniques [112], [114] and immunospot array assay on a chip (ISAAC method) [113]. FACS technologies are particularly advantageous for the isolation of B cells, as they can exploit the expression pattern of specific surface markers to determinate their stage of development and differentiation. For example, Ig class-switched memory B cells and ASCs exhibit hypersomatic mutations on the B cell receptors (BCRs) that increase their affinity for a given antigen, making them optimal candidates for mAbs retrieval [101]. Before isolating single B cells, it is necessary to define the degree of antigen-specific immune response in the donor for an efficient mAbs recovery. This is achieved through ASCs titration in peripheral blood through ELISPOT [90], [115];

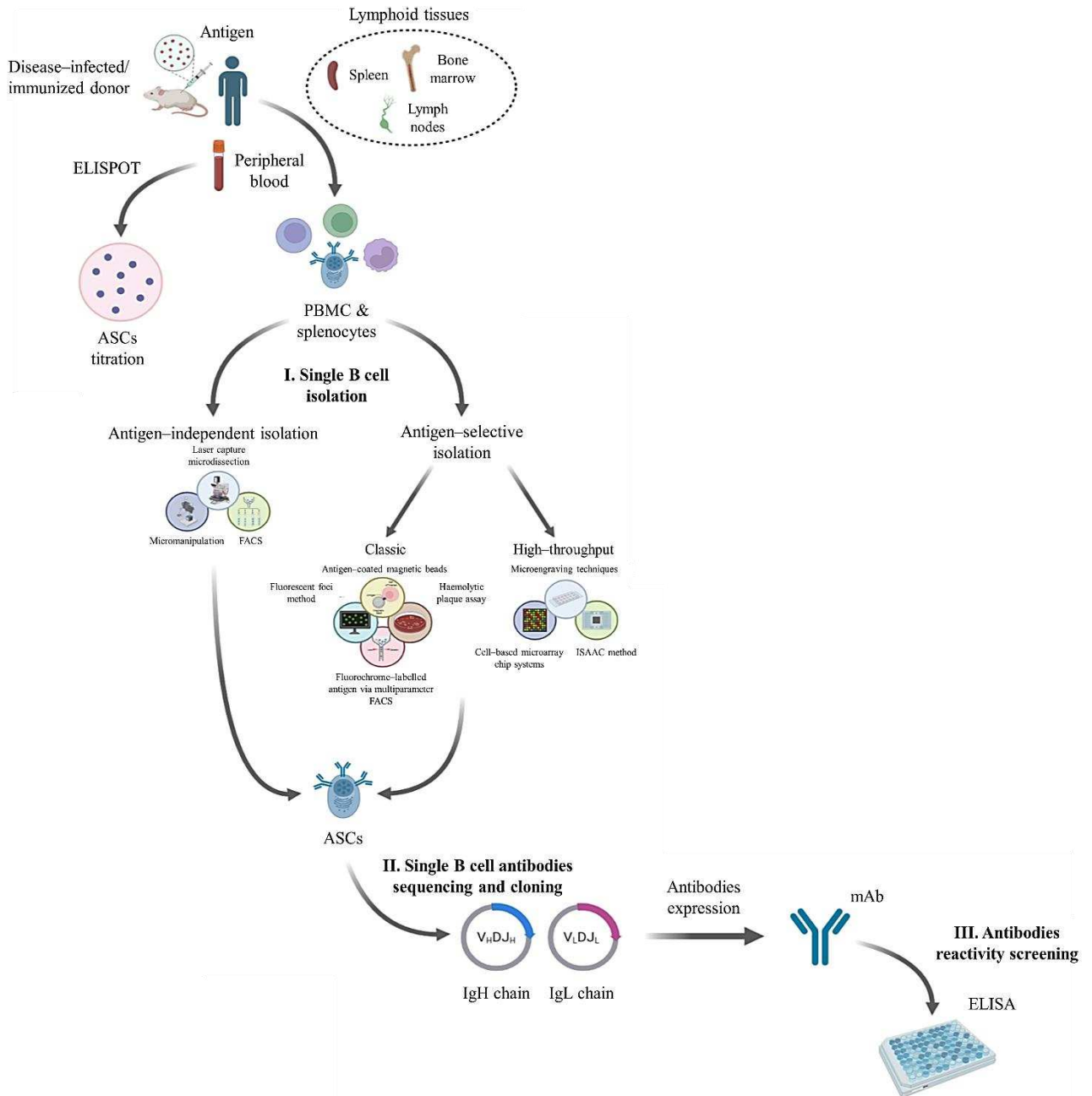


Figure 2.7: Schematic depiction of the single B cell technology main stages: **I.** Single B cells isolation; **II.** Single B cell antibodies sequencing and cloning; **III.** Antibodies reactivity screening.

II. Single B cell antibodies sequencing and cloning: through the reverse transcription of single B cell mRNA into cDNA, it is possible to have an unbiased and simultaneous approach analysis of the expressed IgH and IgL chain genes [116], [117]. Full length IgH and IgL gene mRNAs are normally amplified by nested or semi-nested RT-PCR. During the first round of PCR, where reverse transcription can be performed as a one-step reaction, the leader regions of the V_H and V_L genes

and the constant regions are amplified using forward primer mixes and a sequence-specific reverse primer, respectively [105], [118]–[120]. In case the B cells are isolated independently of their isotype, amplification of heavy chains with different constant regions can be performed with reverse primer mixes. During the second round of PCR, in which the sensitivity and specificity of the encoded antibody is increased using nested primer or primer mixes, it is possible to introduce restriction sites into the rearranged IgH and IgL chain genes for the subsequent cloning stage, or linear expression cassettes to make them directly transfectable in mammalian cells for *in vitro* expression [121]. Strategies have also been developed for the combination of IgH and IgL chain genes, for example through a single cell multiplex RT-PCR with an overlap extension step and a subsequent cloning in a plasmid expression vector [89]. An alternative to single cell RT-PCR approaches, restricted to the functional V_H and V_L chain genes amplification by the limitations in forward primer mixes used, is the 5' rapid amplification of cDNA ends – 5'-RACE method. This technology, which allows the amplification of 50 unknown 5'-ends of mRNA, normally is not suitable for the reverse transcription by single cell. However, the high levels of Ig-specific transcripts found in B cells make this approach appropriate for their isolation [122]. Once amplified, the IgH and IgL chain genes are sequenced in order to retrieve information relating the antibody specificity and to evaluate the presence of mutations, insertions and deletions introduced by somatic hypermutation of the V, D and J gene segments [123], [124] using specific databases (e.g., IgBLAST). To minimize the risk of cross contamination and facilitate handling of numerous samples, cDNA synthesis is typically performed in the original device used for cell deposition and lysis (e.g., 96-well plate). The type of B cells used for the amplification step influences the amount of specific Ig gene transcripts available, making some cells (e.g., ASCs) more suitable for its reverse transcription;

III. Antibodies reactivity screening: In order to evaluate the biophysical and reactivity profiles of antibodies encoded by previously isolated Ig genes, it is essential to insert them in an *in vitro* expression system to have a large-scale production. The most commonly used expression systems are bacterial systems (e.g., *Escherichia coli*), in which the antibody is typically expressed as Fab, and stable or transient mammalian cell systems (e.g., CHO, HEK293 cells), where its expression can be in full Ig format.

If the single B cells had been isolated by cell-based microarray chip systems, the reactivity screening of the corresponding antibodies could be conducted even before the cloning step.

Through these innovative technologies it is therefore possible to isolate mAbs from single B cells avoiding the inefficient fusion step of the hybridoma, which allows to isolate even infrequent antibodies with desired specificity and reactivity characteristics thanks to an efficient mining of the immune B cell repertoire.

Unlike display technologies, these methodologies maintain the natural IgH and IgL chains pairing throughout the antibody cloning stage, and this feature favours the generation of recombinant antibodies with high affinity, specificity, stability and developability profiles.

This approach can also be used for the isolation of mAbs from human immune donors, through peripheral blood recovery of ASCs from vaccinated subject which can be followed up 6 to 14 days post-immunization. It is imperative that their recovery occurs at the peak of the immune response against the antigen of interest, as the abundance of these cells in the blood stream rapidly decreases due to their maturation to long-lived plasma cells in the bone marrow for the maintenance of a specific humoral memory in the absence of persistent antigenic stimulation for the individual lifetime [125]. Alternatively, antigen-specific memory B cells can be recovered from peripheral blood of naturally infected or vaccinated subjects even months to years after exposure. In order to identify appropriate memory B cell donors, it is very useful to define the serum antigen-specific antibody titer, although the correlation with the frequency of these cells in human is not yet clear [101].

2.11 Antibodies against structurally complex membrane proteins

To date, antibody development has mainly focused on addressing molecular targets as largely soluble proteins and cell surface receptors, the latter often investigated as single transmembrane α -helix (bitopic or mono-pass) proteins with a large extracellular ligand-binding domain, such as tyrosine kinase receptor. Membrane proteins are one of the most important class of targets in term of drug development. Approximately the 26% of the human protein-coding genes encodes for membrane proteins [126] and include an immense structural and functional variety of proteins involved in important homeostatic and physiological processes, both in health and disease contexts [127].

In addition to these integral membrane proteins, there is also great interest in structurally–complex membrane proteins, characterized by multiple transmembrane α –helix domains (polytopic or multi–pass proteins). They comprise a wide range of protein families, including G protein–coupled receptors (GPCRs), ion channels and transporters, which can be associated with an equally extensive assortment of physio–pathological conditions [128]–[130]. These protein families are also numerous; in fact, it is currently estimated the existence of approximately 350 non olfactory GPCRs, 400 ion channels and 1.500 transporters in the human genome [128], [131], [132].

Small molecules are commonly used for an effective pharmacological targeting of these integral membrane proteins, especially for GPCRs and ion channels, that represent the first (33%) and third (18%) largest classes of marketed drugs, respectively [133]. However, their progression towards the clinical application can be severely limited by off–targets effects due to their lack of target selectivity or to *in vivo* toxicity, making these structurally–complex membrane proteins understudied opportunities for biomedical research and clinical development [134].

Therefore, the use of antibodies appears to be a much more suitable and advantageous choice for interfacing with structurally complex membrane proteins. In addition to providing the target–selectivity that is lacking in small molecule drugs, mAbs are also characterized by a high binding specificity and a longer duration of action, due to a long half–life in blood stream (11 to 30 days) [135]. Another factor antibodies benefits of, especially when it comes to modulating the activity of GPCRs that bind peptides, is their size more consistent with the ligand–receptor binding interface, which could be very limiting for small molecule drugs.

The great efficacy of antibodies in the therapeutic field is closely linked to the extensive typology of mechanisms that they can implement specifically to the target they bind. For example, they can act as direct agonist or antagonist towards cell surface proteins with receptor function or bind the specific signal mediators of these membrane proteins, thus activating or inhibiting the downstream cell signalling pathways. Moreover, through their binding to specific allosteric sites, they can be used for a pharmacological modulation and stabilization of different conformational states of these integral membrane proteins. Thanks to the recognition of the Fc domain, antibodies are also able to activate components of the immune system such as the complement cascade or immune–effector cells (e.g., macrophages, NK cells), to induce the lysis of the cells that exhibit their specific binding

target [136]. Particularly interesting in this context is the use of recombinant mAbs with customized Fc domains for the induction of cellular exhaustion through the recruitment and activation of effector functions [137].

All these functional advantages resulted in recent years in a strong push towards the development of preclinical and clinical pipelines of mAbs against structurally complex membrane proteins. Despite this, currently there are only two clinically authorized mAbs specific for GPCRs [138], [139] and no antibody therapy that targets ion channels or transport proteins has yet been approved, making their applicational potential against these target classes still largely ignored.

2.12 Challenges for structurally complex membrane proteins antibody discovery

Although there is a great interest in the development of mAbs against structurally complex membrane proteins, this goal presents several technical problems.

The main limitation in antibody discovery and their functional profile screening lies in the difficulties encountered in the expression of polytopic membrane proteins and in their purification from the phospholipid bilayer for the generation of a stable and conformationally relevant antigen. Generally, there are low levels of native expression for integral membrane proteins on the cell surface, and their heterologous expression requires the optimization of different systems to reach sufficiently high levels, due to their conformational flexibility, lipophilicity, and low stability [140]–[142]. The development of heterologous overexpression systems, such as bacterial [143], [144], yeast [145], [146], insect [147], [148], and mammalian cells systems [149], [150], are commonly used as a source for protein extraction and purification. The formats used for antibodies isolation range from soluble portions of the antigen, such as extracellular domains or synthetic peptides [151], to full-length proteins purified through the use of detergents (e.g., calixarenes [152], maltose–neopentyl glycols [153]), discoid lipid nanoparticles (e.g., nanodiscs [154], saposin–lipoproteins – Salipro [155], styrene–maleic acid lipid particles, SMALPs [156], peptidiscs [157]) and complex membranous systems (e.g., virus–like particles, VLPs [158], proteoliposomes [159], paramagnetic proteoliposomes [160]), up to whole cells. Moreover, antigen preparations strategies must be adaptable to the high structural and functional diversity of the target proteins. For example, large extracellular domains, which will be more

easily recognized as antigenic determinants during antibody development, can be expressed and isolated as correctly folded functional units. On the other hand, the smaller extracellular domains, although still reachable by antibodies, do not present particular advantages in practical terms.

The heterologous expression systems can also provide a stable cellular model for antigen native presentation useful for both *in vitro* or *in vivo* antibody identification and for preparation of functional screening analyses, such as electrophysiology, radioactive ion uptake, radioactive ligand binding, and reporter assays [161]. However, it is very important to underline that high levels of expression are not always indicative of the presence of a correctly folded and functional protein, so it is still essential to check its quality preparation [162].

3 Aims and scope of the thesis

Taking into account what has been detailed so far, the aim of this PhD project therefore is to define a reliable and robust method for the production of recombinant chimeric monoclonal antibodies as tools to address structurally–complex transmembrane proteins, in order to facilitate the development of potential diagnostics and therapeutics towards hardly targetable antigens.

As a model to address this problem, it was selected a human multi–pass membrane protein, here called TLS2 for confidentiality issues, with a molecular weight of approximately 70kDa and a particularly complicated conformation, composed of 12 transmembrane α –helix domains and 6 predicted extracellular loops of various sizes (Figure 3.1). This protein performs the function of amino acids transporter and is mainly expressed in small intestine and kidney proximal tubule epithelium, where it mediates their absorption and reabsorption, respectively. It is also known that mutations affecting this protein can lead to the onset of different metabolic pathologies, all linked to amino acids malabsorption. The choice of this protein for the establishment of our methodology was guided not only by its complex structure but also by the absence of antibodies capable to recognize the conformationally folded protein expressed on the cell surface. In this way, the obtainment of a conformational mAb specifically recognizing TLS2, in addition to validate our method, could also be the starting point for both a more in–depth characterization of this amino acid transporter and the development of an engineered antibody with possible diagnostic or therapeutic applications.

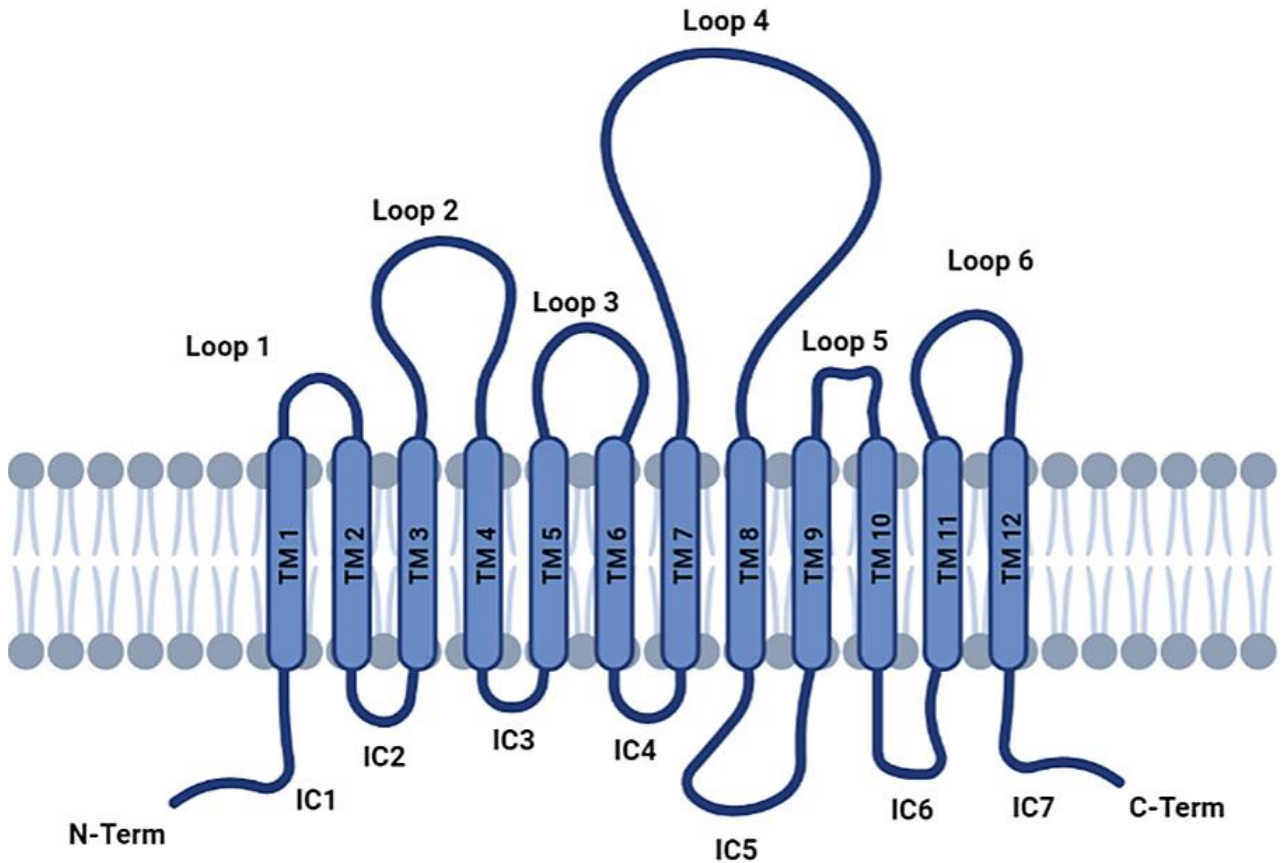


Figure 3.1: Schematic depiction of human TLS2 amino acid transporter in plasma membrane. This human multi-pass membrane protein with a molar weight of approximately 70kDa is composed of 12 transmembrane α -helix domains (TM1–12) and 6 predicted extracellular loops of various sizes (Loop1–6).

As a starting material for the identification and isolation of monoclonal antibodies it was chosen to purify CD138⁺ plasma cells from murine bone marrow after the induction of a suitable TLS2-specific antibody titre in BALB/c mice by an appropriate immunization strategy. The choice to focus on plasma cells for the recovery of Ig-specific genes, although they represent less than 1% of lymphoid cells, was based on evidence that these cells are responsible for the secretion of the vast majority of IgG present in the serum [125], [163]–[165]. Unlike memory B cells which require a process of differentiation into effector cells before being able to secrete immunoglobulins, plasma cells readily secrete large amounts of antibodies and can be used directly after purification to evaluate their antigen specificity in functional assays. Another advantage over memory B cells is that plasma cells exhibit higher Ig-specific mRNA transcriptional level [120], [165], [166], which allows an easier retrieval of corresponding genes from single isolated cells. For the generation of recombinant mAbs it was chosen to investigate a new protocol to combine the recovery of the Ig heavy and light

chains variable regions by RT-PCR with their insertion into a human antibody framework through Transcriptionally Active PCR (TAP), in order to generate linear minigenes that are directly transfectable into mammalian cells for the production of recombinant chimeric mAbs. After the identification of antibodies with a good binding specificity against the antigen of interest, their V_H and V_L corresponding sequences will be inserted into appropriate expression vectors, in order to obtain a large-scale production of the chimeric antibodies, thus increasing the reproducibility of subsequent functional analyses for further characterization.

4 Materials and Methods

4.1 Recombinant plasmids creation

4.1.1 Synthetic plasmids design

4 synthetic plasmids (TLS2polyP–HuIgFc, TLS2Full, pcDNA3.4–6His, pAAV.CMV.Luc.IRES.EGFP.SV40) were designed and ordered to GeneArt Gene Synthesis (*Invitrogen*). The characteristics of each construct are listed below:

- TLS2polyP–HuIgFc: synthetic plasmid containing the DNA sequence coding a poly–epitope derived from TLS2 extracellular loops intercalated by (G₄S)₃ linkers and fused to human IgG constant region (HuIgFc);
- TLS2Full: synthetic plasmid containing the DNA sequence coding the full–length amino acid transporter TLS2;
- pcDNA3.4–6His: synthetic plasmid developed by inserting a 6His–TAG inside a pcDNATM 3.4 TOPOTM backbone;
- pAAV.CMV.Luc.IRES.EGFP.SV40: synthetic plasmid containing an Internal Ribosome Entry Site (IRES) sequence cloned upstream a EGFP cassette (Addgene plasmid #105533; <http://n2t.net/addgene:105533>; RRID: Addgene_105533);

Each freeze–dried synthetic plasmid was rehydrated with 50μL of TE Buffer (10mM Tris–HCl, 1mM EDTA, pH 8.0) to reach a final concentration of 100ng/μL.

A pcDNA5–FRT–EGFP recombinant plasmid, obtained cloning pEGFP–N1 (*Clontech*, #6085–1) HindIII+NotI digested cassette in a pcDNATM5/FRT Mammalian Expression Vector (*Invitrogen*, #V601020), and a pcDNATM 3.4 TOPOTM plasmid with a customized multiple cloning site (GeneArt Gene Synthesis, *Invitrogen*) were already available in laboratory.

4.1.2 Synthetic DNA strings design

3 synthetic DNA strings (TLS2Loop4, TLS2stopcodon–IRES–BstXI, cMyc–AP2,) were designed and ordered to GeneArt Gene Synthesis (*Invitrogen*). The characteristics of each construct are listed below:

- TLS2Loop4: synthetic DNA string containing the coding sequence for a TLS2 recombinant fragment derived from the largest loop4;
- TLS2stopcodon–IRES–BstXI: synthetic DNA string containing the TLS2 stop codon fused upstream of an IRES sequence;
- cMyc–AP2: synthetic DNA string containing the auxiliary protein AP2–encoding sequence, cloned downstream of a cMyc–TAG.

Each freeze–dried synthetic DNA string was rehydrated with 50 μ L of TE Buffer (10mM Tris–HCl, 1mM EDTA, pH 8.0) to reach a final concentration of 100ng/ μ L.

4.1.3 Plasmid DNA amplification (heat–shock bacterial transformation)

All synthetic and recombinant plasmids were amplified in *E. coli* Subcloning Efficiency™ DH5 α Competent Cells (*Invitrogen*, #18265017) through heat–shock transformation, as per manufacturers' instructions.

For each transformation, 50 μ L of chemically competent cells were thawed on ice and aliquoted into a 1,5mL microcentrifuge tube containing 10ng of DNA (1 μ l of plasmid diluted 1:10 in TE Buffer). Each tube was incubated on ice for 30min and then heat–shocked, using a MB–5A Heating Circulator with Open Bath (*Julabo*, #9142305) at 42°C for 30sec. The tubes were placed again on ice for 2 minutes. Afterwards, 950 μ l of pre–warmed sterilized Luria–Bertani (LB) Broth (*Sigma–Aldrich*, #L3522) medium were added to each tube and they were incubated at 37°C for 1h in the Multitron Standard (*Infors HT*) incubator shaker for bacterial cultures at 250rpm. Then, 100 μ L and 900 μ L of each transformation cell culture were seeded on pre–warmed selective plates Lennox LB Broth with agar (*Sigma–Aldrich*, #L2897) + 100 μ g/mL Ampicillin (*Millipore*, #171254) and incubated at 37°C O/N. The following day a single colony was spotted, added to 6mL of LB+100 μ g/mL ampicillin medium and incubated at 37°C O/N at 250rpm. 5mL of the culture recovered the next day were submitted to the plasmid DNA purification, while the remaining 1mL was used to create a working seed with the addition of 25% glycerol and kept at –80°C.

4.1.4 Plasmid DNA purification

All plasmids transformed into DH5 α cells were extracted using QIAprep Spin Miniprep Kit (*Qiagen*, #27106), as per manufacturers' instructions.

Briefly, 5mL of the bacterial cultures were centrifuged at 4,000rpm for 10min, after which the resulting pellets were resuspended in 250 μ L of Resuspension Buffer P1. The bacterial cells were lysed by adding 250 μ L of Lysis Buffer P2, mixed gently by rotation and inversion of the tube, and incubated for 3–5min at room temperature. Then, 350 μ L of Neutralization/Binding Buffer N3 were added to stop the cell lysis: this determined the formation of precipitates with a gelatinous consistency that contains both cellular debris and genomic DNA. The suspensions thus obtained were centrifuged at 13,000rpm for 10min. The supernatants were transferred into a QIAprep spin column and centrifuged at 8,000rpm for 1min, in order to retain the plasmid DNA in the silica membrane. The columns were washed by adding first 500 μ L of Wash Buffer PB and then 750 μ L of Wash Buffer PE, centrifuging each time at 13,000rpm for 1min. They were centrifuged an additional time at 13,000rpm for 2min, in order to remove any residual ethanol traces of Wash Buffer PE from the silica membranes. The plasmids were finally eluted in 50 μ L of Elution Buffer EB and recovered by centrifugation at 13,000rpm for 2min.

For DNA quantification and purity evaluation, the absorbances were measured at 260 and 280nm with NanoVueTM 4282 V1.7 Spectrophotometer (*GE Healthcare*). Only purified plasmids with a A_{260}/A_{280} ratio between 1.75 and 2.00 were kept and used for the subsequent steps.

4.1.5 Synthetic DNA strings amplification (PCR)

All synthetic DNA strings were amplified through polymerase chain reaction (PCR), using specific primers which allow the introduction of cutting sites for their correct cloning within the corresponding expression vectors. The DNA templates were diluted in TE Buffer to a final concentration of 10ng/ μ L and then 1 μ L was added to the PCR Mix (Table 4.1):

Table 4.1: PCR Mix used for the amplification of *TLS2Loop4–6His*, *TLS2stopcodon–IRES–BstXI* and *cMyc–AP2* synthetic DNA strings.

PCR Mix	1×	Final concentration
UltraPure™ DNase/RNase–Free Distilled H ₂ O (<i>Invitrogen</i> , #10977035)	17,3μL	
10× Taq DNA Polymerase PCR Buffer (<i>Invitrogen</i> , #18067017)	2,5μL	1×
2,5mM each dNTP Mix (<i>Invitrogen</i> , #R72501)	2,5μL	0,25mM each
25mM MgCl ₂ (<i>Thermo Scientific</i> , #AB0359)	1μL	1mM
100μM Primer Forward (<i>Eurofins Genomics</i>)	0,1μL	0,4μM
100μM Primer Reverse (<i>Eurofins Genomics</i>)	0,1μL	0,4μM
1U/μL KOD Hot Start DNA Polymerase (<i>Sigma–Aldrich</i> , #71086)	0,3μL	0,012U/μL
5U/μL Taq DNA Polymerase, recombinant (<i>Invitrogen</i> , #10342046)	0,2μL	0,04U/μL
Final volume/sample	24μL	

PCR was conducted using a MiniAmp™ Plus Thermal Cycler (*Applied Biosystems*, #A37835), with the following amplification profile (Table 4.2):

Table 4.2: Amplification profile used for *TLS2Loop4–6His*, *TLS2stopcodon–IRES–BstXI* and *cMyc–AP2* synthetic DNA strings.

Step	Temperature	Time	Cycle
Initial denaturation	95°C	3min	1
Denaturation	95°C	30sec	35
Annealing	55°C	30sec	
Extension	72°C	1min	
Final extension	72°C	10min	1
Maintenance	4°C	∞	–

Due to overlaps with specific sequences of TLS2 and AP2 proteins, the primer sequences used for synthetic DNA strings amplification cannot be reported for confidentiality reasons. The quality of the amplified sequences was evaluated by run on an electrophoresis 1% agarose (*Sigma–Aldrich*, #A9539) gel with 1×TAE Buffer (40mM Tris–HCl, 1mM EDTA, pH 8.5), using 5μL of 1Kb Plus DNA Ladder (*Invitrogen*, #10787018) for DNA sizing.

4.1.6 PCR products purification

For higher purity of all PCR products, previously amplified synthetic DNA strings were purified using QIAquick Gel Extraction Kit (*Qiagen*, #28706), as per manufacturers' instructions. Amplification products were run on electrophoresis 1% agarose gel with 1×TAE Buffer, using 5µL of 1Kb Plus DNA Ladder for DNA sizing. Gel bands corresponding to the amplified DNA fragments of interest were excised from the gel and weighed, to which Buffer QG was subsequently added with a 1:1 w/v ratio. The gel slices were incubated at 50°C and mixed by vortexing the tubes every 2min, until it was completely dissolved. 1 gel volume of isopropanol was then added to the samples, which were loaded on QIAquick column and centrifuged at 8,000rpm for 10min, in order to retain the DNA in the silica membranes. Subsequently, the columns were washed by adding first 500µL of Buffer QG and then 750µL of Buffer PE, centrifuging each time at 13,000rpm for 1min. They were centrifuged an additional time at 13,000rpm for 2min, to remove any residual ethanol traces of Buffer PE from the silica membranes. The DNA fragments were finally eluted in 50µL of Buffer EB, recovered by centrifugation at 13,000rpm for 2min and quantified with NanoVue™ 4282 V1.7 Spectrophotometer. Only purified amplification products with a A_{260}/A_{280} ratio between 1.75 and 2.00 were kept and used for the subsequent steps.

4.1.7 Production of pcDNA3.4_TLS2Loop4–6His recombinant plasmid

The recombinant plasmids used for the transient expression of TLS2 extracellular loop4 recombinant fragment in ExpiCHO–S™ cells were obtained through a ligase–dependent cloning strategy.

For pcDN3.4_TLS2Loop4–6His, both amplified TLS2Loop4 DNA string and pcDNA3.4–6His synthetic plasmid were subjected to digest reaction with HindIII (*NEB*, #R0104) and BamHI (*NEB*, #R0136) restriction enzymes for 1h at 37°C. During this enzymatic cutting step, pcDNA3.4–6His was also dephosphorylated at the 5'–ends adding FastAP Thermosensitive Alkaline Phosphatase (*Thermo Scientific*, #EF0651) at the last 10min of the incubation at 37°C, in order to prevent vector recircularization during the ligation step. At the end of the restriction digestion, TLS2Loop4_HindIII+BamHI insert and dephosphorylated pcDNA3.4–6His_HindIII+BamHI vector were purified through agarose gel electrophoresis using QIAquick Gel Extraction Kit, as previously described (see in

Section 4.1.6). These were then used to set up the ligase step with T4 DNA Ligase (*Invitrogen*, #15224017) with a 5:1 insert:vector molar ratio, incubating the reaction O/N at room temperature.

The next day, the ligase mixture was used for the heat–shock transformation of chemically competent DH5 α , selecting the transfected cells on LB+100 μ g/mL ampicillin plates (see in Section 4.1.3). The colonies present on the plate the following day were expanded in 100 μ L of LB+100 μ g/mL ampicillin medium for 3h at 37°C in the incubator shaker for bacterial cultures at 250rpm, and screened through colony PCR with specific primers to evaluate the effective presence of TLS2Loop4 insert (sequences not shown, confidential) in the plasmid contained within them. 1 μ L of the bacterial cultures was directly added to the Colony PCR Mix (Table 4.3):

Table 4.3: Colony PCR Mix.

Colony PCR Mix	1 \times	Final concentration
UltraPure™ DNase/RNase–Free Distilled H ₂ O (<i>Invitrogen</i> , #10977035)	5,6 μ L	
10 \times Taq DNA Polymerase PCR Buffer (<i>Invitrogen</i> , #18067017)	1 μ L	1 \times
2,5mM each dNTP Mix (<i>Invitrogen</i> , #R72501)	1 μ L	0,25mM each
50mM MgCl ₂ (<i>Invitrogen</i>)	1 μ L	5mM
100 μ M Primer Forward (<i>Eurofins Genomics</i>)	0,1 μ L	1 μ M
100 μ M Primer Reverse (<i>Eurofins Genomics</i>)	0,1 μ L	1 μ M
5U/ μ L Taq DNA Polymerase, recombinant (<i>Invitrogen</i> , #10342046)	0,2 μ L	0,1U/ μ L
Final volume/sample	9 μ L	

PCR was conducted using a MiniAmp™ Plus Thermal Cycler, with the following amplification profile (Table 4.4):

Table 4.4: Amplification profile used for colony PCR.

Step	Temperature	Time	Cycle
Initial denaturation	95°C	3min	1
Denaturation	95°C	30sec	40
Annealing	55°C	30sec	
Extension	72°C	1min	
Final extension	72°C	10min	1
Maintenance	4°C	∞	–

The quality of the amplified sequences was evaluated by run on an electrophoresis 1% agarose gel with 1×TAE Buffer, using 1Kb Plus DNA Ladder for DNA sizing.

If successful, the positive colonies were expanded into LB+100µg/mL ampicillin medium, to amplify and subsequently purify pcDNA3.4_TLS2Loop4–6His recombinant plasmid using QIAprep Spin Miniprep Kit (see in Section 4.1.4). Quantification of DNA and its purity were established by measuring the absorbance at 260 and 280nm with NanoVue™ 4282 V1.7 Spectrophotometer.

4.1.8 Production of pcDNA5_TLS2–EGFP recombinant plasmid

The recombinant plasmid used for the stable/transient expression of TLS2–EGFP protein in Flp–In™–293 cells was obtained through a ligase–dependent cloning strategy.

For pcDNA5_TLS2–EGFP, pcDNA5–FRT–EGFP recombinant plasmid was amplified through PCR, using specific primers (sequences not shown, confidential) that allowed the correct cloning of the TLS2Full insert in frame with the EGFP cassette. The DNA template was diluted in TE Buffer to a final concentration of 10ng/µL and then 1µL was added to the PCR Mix (Table 4.5):

Table 4.5: PCR Mix used for the amplification of pcDNA5–FRT–EGFP recombinant plasmid.

PCR Mix	1×	Final concentration
UltraPure™ DNase/RNase–Free Distilled H ₂ O (<i>Invitrogen</i> , #10977035)	17,3µL	
10× Taq DNA Polymerase PCR Buffer (<i>Invitrogen</i> , #18067017)	2,5µL	1×
2,5mM each dNTP Mix (<i>Invitrogen</i> , #R72501)	2,5µL	0,25mM each
25mM MgCl ₂ (<i>Thermo Scientific</i> , #AB0359)	1µL	1mM
100µM Primer Forward (<i>Eurofins Genomics</i>)	0,1µL	0,4µM
100µM Primer Reverse (<i>Eurofins Genomics</i>)	0,1µL	0,4µM
1U/µL KOD Hot Start DNA Polymerase (<i>Sigma–Aldrich</i> , #71086)	0,3µL	0,012U/µL
5U/µL Taq DNA Polymerase, recombinant (<i>Invitrogen</i> , #10342046)	0,2µL	0,04U/µL
Final volume/sample	24µL	

PCR was conducted using a MiniAmp™ Plus Thermal Cycler, with the following amplification profile (Table 4.6):

Table 4.6: Amplification profile used for pcDNA5–FRT–EGFP recombinant plasmid.

Step	Temperature	Time	Cycle
Initial denaturation	95°C	3min	1
Denaturation	95°C	30sec	35
Annealing	55°C	1min	
Extension	72°C	5min	
Final extension	72°C	10min	1
Maintenance	4°C	∞	–

The quality of the amplified sequence was evaluated by run on an electrophoresis 1% agarose gel with 1×TAE Buffer, using 1Kb Plus DNA Ladder for DNA sizing. Gel band corresponding to the amplified vector of interest was recovered and purified using QIAquick Gel Extraction Kit, as previously described (see in Section 4.1.6).

At this point, both TLS2Full synthetic plasmid and pcDNA5–FRT–EGFP amplified vector were subjected to digest reaction with HindIII and BamHI restriction enzymes for 1h at 37°C. During this enzymatic cutting step, amplified pcDNA5–FRT–EGFP was also dephosphorylated at the 5'-ends adding FastAP Thermosensitive Alkaline Phosphatase at the last 10min of the incubation at 37°C, in order to prevent vector recircularization during the ligation step.

At the end of the restriction digestion, TLS2Full_HindIII+BamHI insert and dephosphorylated pcDNA5–FRT–EGFP_HindIII+BamHI vector were purified through agarose gel electrophoresis using QIAquick Gel Extraction Kit, as previously described (see in Section 4.1.6). These were then used to set up two ligase reaction with T4 DNA Ligase with different insert:vector molar ratio (2:1 and 5:1), which were incubated O/N at room temperature.

The next day, the ligase mixtures were used for the heat–shock transformation of chemically competent DH5α, selecting the transfected cells on LB+100μg/mL ampicillin plates (see in Section 4.1.3). Each colony present on the plate the following day was expanded in 100μL of LB+100μg/mL ampicillin medium for 3h at 37°C in the incubator shaker for bacterial cultures at 250rpm, and screened through colony PCR (see in Section 4.1.7) with specific primers to evaluate the effective presence of TLS2Full insert (sequences not shown, confidential) in the plasmid contained within them.

If successful, the positive colonies were expanded into LB+100µg/mL ampicillin medium, to amplify and subsequently purify pcDNA5_TLS2-EGFP recombinant plasmid using QIAprep Spin Miniprep Kit (see in Section 4.1.4). Quantification of DNA and its purity were established by measuring the absorbance at 260 and 280nm with NanoVue™ 4282 V1.7 Spectrophotometer.

4.1.9 Production of pcDNA5_TLS2-IRES-EGFP recombinant plasmid

The recombinant plasmid used for the creation of a TLS2-IRES-EGFP stable line in Flp-In™-CHO cells was obtained through a ligase-dependent cloning strategy.

For pcDNA5_TLS2-IRES-EGFP, in order to separate the TLS2-encoding sequence and EGFP cassette by introducing an IRES between them, both pAAV.CMV.Luc.IRES.EGFP.SV40 synthetic and pcDNA5_TLS2-EGFP recombinant plasmid were subjected to digestion with BamHI and NotI (*NEB*, #R0189) restriction enzymes for 1h at 37°C. pcDNA5_TLS2-EGFP vector was dephosphorylated with FastAP Thermosensitive Alkaline Phosphatase in the last 10min of the incubation at 37°C, to prevent the vector recircularization. At the end of the restriction digestion, both pIRES-EGFP_BamHI+NotI insert and dephosphorylated pcDNA5_TLS2-EGFP_BamHI+NotI vector were purified through agarose gel electrophoresis using QIAquick Gel Extraction Kit, as previously described (see in Section 4.1.6). These were then used to set up the ligase step with T4 DNA Ligase with a 5:1 insert:vector molar ratio, incubating the reaction O/N at room temperature. The ligase mixture was used for the transformation of DH5α, selecting the transformed cells on LB+100µg/mL ampicillin plates (see in Section 4.1.3). The colonies present on the plate the following day were screened by digestion with HindIII restriction enzyme, for the purpose of verifying the identity of the plasmid contained within them. pcDNA5_TLS2nostop-IRES-EGFP recombinant plasmid was then recovered from the positive colonies, expanded into LB+100µg/mL ampicillin medium and purified using QIAprep Spin Miniprep Kit (see in Section 4.1.4).

Subsequently, the stop codon of TLS2-encoding sequence was restored by inserting amplified TLS2stopcodon-IRES-BstXI synthetic DNA string into pcDNA5_TLS2nostop-IRES-EGFP recombinant plasmid. They were both subjected to digest reaction with BstXI (*NEB*, #R0113) restriction enzymes for 1h at 37°C, dephosphorylating pcDNA5_TLS2nostop-IRES-EGFP recombinant plasmid at the 5'-ends with FastAP

Thermosensitive Alkaline Phosphatase, added at the last 10min of the incubation at 37°C, in order to prevent vector recircularization during the ligation step.

At the end of the restriction digestion, TLS2stopcodon–IRES–BstXI_BstXI insert and dephosphorylated pcDNA5_TLS2nostop–IRES–EGFP_BstXI vector were purified through agarose gel electrophoresis using QIAquick Gel Extraction Kit, as previously described (see in Section 4.1.6). These were then used to set up the ligase step using T4 DNA Ligase with a 5:1 insert:vector molar ratio, incubating the reaction O/N at room temperature. The ligase mixture was then transformed into DH5α cells, as previously described (see in Section 4.1.3), and the ampicillin–resistant colonies were screened by digestion with XhoI restriction enzyme. If successful, they were expanded into LB+100μg/mL ampicillin medium and pcDNA5_TLS2–IRES–EGFP recombinant plasmid was purified using QIAprep Spin Miniprep Kit (see in Section 4.1.4). Quantification of DNA and its purity were established by measuring the absorbance at 260 and 280nm with NanoVue™ 4282 V1.7 Spectrophotometer.

4.1.10 Production of pcDNA3.4_cMyc–AP2 recombinant plasmid

The recombinant plasmid used for the creation of a TLS2–IRES–EGFP/AP2 stable line in Flp–In™–CHO cells was obtained through a ligase–dependent cloning strategy.

For pcDNA3.4_cMyc–AP2, both amplified cMyc–AP2 synthetic DNA string and customized pcDNA3.4 plasmid were subjected to digest reaction with HindIII and NotI restriction enzymes for 1h at 37°C, with a dephosphorylation step of pcDNA3.4 with FastAP Thermosensitive Alkaline Phosphatase in the last 10min of the incubation. cMyc–AP2_HindIII+NotI insert and dephosphorylated pcDNA3.4_HindIII+NotI vector were purified through agarose gel electrophoresis using QIAquick Gel Extraction Kit (see in Section 4.1.6) and used to set up the ligase reaction with T4 DNA Ligase (5:1 insert:vector ratio). The ligase mixture was then transformed into DH5α and selected on LB+100μg/mL ampicillin plates, as previously described (see in Section 4.1.3). The resulting colonies were screened through digestion with XbaI (*NEB*, #R0145) and NotI restriction enzymes, and pcDNA3.4_cMyc–AP2 recombinant plasmid was then recovered from the positive ones expanded into LB+100μg/mL ampicillin medium and purified using QIAprep Spin Miniprep Kit (see in Section 4.1.4). Quantification of DNA and its purity were established by

measuring the absorbance at 260 and 280nm with NanoVue™ 4282 V1.7 Spectrophotometer.

4.1.11 Recombinant plasmids sequencing

The identity of the recombinant plasmids thus obtained was confirmed by sequencing, using the LightRun Tube Barcodes (*Eurofins*) service. Briefly, 5µL of 100ng/µL purified recombinant DNA were added to 5µL of specific primer diluted to a final concentration of 5pmol/µL in a 1,5mL DNA LoBind™ tube (*Eppendorf*, #0030108418). Due to overlaps with specific sequences of TLS2 and AP2 proteins, the primer sequences used for recombinant plasmids sequencing cannot be reported for confidentiality reasons. The LightRun Tube Barcodes were attached to the tubes, and they were brought to the GATC Collection Point at Le Scotte Hospital in Siena. Once the results of the sequencing were received via email, they were analysed through CLC Main Workbench software (*Qiagen*).

4.2 TLS2polyP–HuIgFc poly–epitope and TLS2Loop4–6His recombinant fragment expression

4.2.1 Cell cultures

- Expi293F™ Cells (*Gibco*, #A14527) were cultured in Expi293™ Expression Medium (*Gibco*, #A143510). This suspension cell line was maintained in Nalgene™ Single–Use PETG Erlenmeyer Flask at 125rpm (*Thermo Scientific*, #4115), or in Deepwell Plate 96/2mL (*Eppendorf*, #0030502302) at 1,000rpm with MixMate™ Shaker (*Eppendorf*), at 37°C in a shaker with a humidified atmosphere of 8% CO₂;
- ExpiCHO–S™ Cells (*Gibco*, #A29127) were cultured in ExpiCHO™ Expression Medium (*Gibco*, #A291000). This suspension cell line was maintained in Nalgene™ Single–Use PETG Erlenmeyer Flask at 37°C in a shaker with a humidified atmosphere of 8% CO₂ at 125rpm.

All the cell lines were tested for mycoplasma contamination through PCR analysis [167], [168].

4.2.2 Expi293F™ cells transient transfection

TLS2polyP–HuIgFc synthetic plasmid was transiently transfected into Expi293F™ cells using ExpiFectamine™ 293 Transfection Kit (*Gibco*, #A14525) as per manufacturers' instructions.

On the day before transfection, Expi293F™ cells were seeded in Nalgene™ Single–Use PETG Erlenmeyer Flask at a density of 8×10^5 viable cells/mL in 25mL of Expi293™ Expression Medium and maintained O/N at 37°C and 8% CO₂ in a shaker at 125rpm, so that cell density reached $2,5 \times 10^6$ cells/mL at the time of transfection.

On the day of transfection, $2,5 \times 10^7$ cells were recovered and diluted in 22,1mL of fresh, pre–warmed medium to a final density of approximately $1,13 \times 10^6$ viable cells/mL.

Plasmid DNA and ExpiFectamine dilutions were prepared in microtubes as described below:

- Plasmid DNA: 26µg of TLS2polyP–HuIgFc synthetic plasmid were diluted in OptiMEM™ I Reduced Serum Medium (*Gibco*, #319850) to a final volume of 1,3mL;
- ExpiFectamine: 70,2µL of ExpiFectamine™ 293 Reagent were diluted in OptiMEM™ I Reduced Serum Medium to a final volume of 1,3mL.

The plasmid DNA dilution was mixed with the diluted ExpiFectamine to a final volume of 2,6mL and incubated for 5min at room temperature. The DNA–ExpiFectamine solution was then added dropwise to the shaker flask and the Expi293F™ cells were incubated at 37°C in a shaker with a humidified atmosphere of 8% CO₂ at 125rpm.

On the day after transfection (18 to 22 hours post–transfection), 130µL of ExpiFectamine™ 293 Transfection Enhancer 1 and 1,3mL of ExpiFectamine™ 293 Transfection Enhancer 2 were added to the transfected cell culture.

At this point, the flask was incubated for 2 days before the supernatants were harvested by centrifugation at 1,800rpm for 5min, filtered with 0,22µm syringe filters and kept at +4°C for further characterization, while pellet was resuspended with fresh medium and placed in incubation again. A second recovery of the supernatants were made at 5–days post–transfection (dpt).

4.2.3 Immunoaffinity chromatography

The HuIgFc-tagged TLS2polyP-HuIgFc poly-epitope, secreted in the transfected Expi293F™ cells' supernatant, was purified through immunoaffinity chromatography. For this purpose, HiTrap™ Protein G HP 1mL column (*Cytiva*, #17040401) was used through the help of the ÄKTA start (*Cytiva*).

The column was conditioned with 10mL of Wash/Binding Buffer at 1mL/min, then the sample was applied by pumping it onto the column and recovering the flowthrough. The column was washed with 3mL of Wash/Binding Buffer A (dH₂O + 20mM sodium phosphate, pH 7.0) at 1mL/min for 5 times, to remove any non-specifically adsorbed protein. Finally, the protein was eluted with 3mL of Elution Buffer B (dH₂O + 0,1M glycine-HCl, pH 2.7) at 1mL/min for 5 times, so as to be able to weak the binding affinity between the HuIgFc-tagged protein and the G protein present in the resin of the column. To prevent the acid environment from damaging the TLS2polyP-HuIgFc poly-epitope, each fraction was immediately adjusted to neutral pH, adding 300µL of Equilibration Buffer C (1M Tris-HCl, pH 9.0).

4.2.4 ExpiCHO-S™ cells transient transfection

TLS2Loop4-6His recombinant plasmid was transiently transfected into ExpiCHO-S™ cells using ExpiFectamine™ CHO Transfection Kit (*Gibco*, #A29129) as per manufacturers' instructions.

On the day before transfection, ExpiCHO-S™ cells were seeded in Nalgene™ Single-Use PETG Erlenmeyer Flask at a density of $4-6 \times 10^6$ viable cells/mL in 25mL of ExpiCHO™ Expression Medium and maintained O/N at 37°C and 8% CO₂ in a shaker at 125rpm, so that cell density reached 7×10^6 cells/mL at the time of transfection.

On the day of transfection, $1,5 \times 10^8$ cells were recovered and diluted in 25mL of fresh, pre-warmed medium to a final density of 6×10^6 viable cells/mL.

Plasmid DNA and ExpiFectamine dilutions were prepared in microtubes as described below:

- Plasmid DNA: 20µg of TLS2Loop4-6His recombinant plasmid were diluted in OptiPRO™ SFM (*Gibco*, #12309019) to a final volume of 1mL;
- ExpiFectamine: 80µL of ExpiFectamine™ CHO Reagent were diluted in OptiPRO™ SFM to a final volume of 1mL.

The plasmid DNA dilution was mixed with the diluted ExpiFectamine to a final volume of 2mL and incubated for 5min at room temperature. The DNA–ExpiFectamine solution was then added dropwise to the shaker flask and the ExpiCHO–S™ cells were incubated at 37°C in a shaker with a humidified atmosphere of 8% CO₂ at 125rpm.

On the day after transfection (18 to 22 hours post–transfection), 150µL of ExpiFectamine™ CHO Enhancer and 6mL of ExpiCHO™ Feed were added to the transfected cell culture.

At this point, the flask was incubated for 9 days before the supernatants were harvested by centrifugation at 1,800rpm for 15min, filtered with 0,22µm syringe filters and kept at +4°C for further characterization.

4.2.5 Immobilized Metal Affinity Chromatography (IMAC)

The 6His–tagged TLS2Loop4–6His recombinant fragment, secreted in the transfected ExpiCHO–S™ cells' supernatant, was purified through Immobilized Metal Affinity Chromatography (IMAC). For this purpose, HisTrap™ FF 1mL column (*Cytiva*, #11000458) was used through the help of the ÄKTA start (*Cytiva*).

The column was conditioned with 10mL of Wash/Binding Buffer A (dH₂O + 20mM sodium phosphate, 500mM NaCl, 10mM imidazole, pH 7.4) at 1mL/min, then the sample was applied by pumping it onto the column and recovering the flowthrough. The column was washed with 3mL of Wash/Binding Buffer A at 1mL/min for 5 times, to remove any non–specifically adsorbed proteins. Finally, the protein was recovered through competitive elution with 3mL of Elution Buffer B (dH₂O + 20mM sodium phosphate, 500mM NaCl, 500mM imidazole, pH 7.4) at 1mL/min for 5 times, so as to be able to disrupt the protein binding with the Ni²⁺ ions present in the resin of the column.

4.2.6 Purification control (SDS–PAGE)

To verify the correct purification of TLS2polyP–HuIgFc poly–epitope and TLS2Loop4–6His recombinant fragment, each fraction was analysed with Sodium Dodecyl Sulfate–Polyacrylamide Gel Electrophoresis (SDS–PAGE).

For the sample preparation, 30µL of each fraction (supernatant, flowthrough, wash and elution fractions) was added to 10µL of NuPAGE™ LDS Sample Buffer 4× (*Invitrogen*, #NP0007) and boiled for 10min at 96°C.

20µL of each sample were loaded onto NuPAGE™ 4 to 12%, Bis–Tris, 1.0mm, Mini Protein Gel, 12–well (*Invitrogen*, #NP0322), using as reference 5µL of SeeBlue™ Plus2 Pre–stained Protein Standard (*Invitrogen*, #LC5925) for protein sizing. Then, the gels were run for 1h at 150V in SDS Running Buffer, prepared by diluting 50mL of NuPAGE™ MOPS SDS Running Buffer 20× (*Invitrogen*, #NP0001) or NuPAGE™ MES SDS Running Buffer 20× (*Invitrogen*, #NP0002) in 950mL of dH₂O, respectively for TLS2polyP–HuIgFc poly–epitope and TLS2Loop4–6His recombinant fragment, and loaded into the XCell *SureLock*™ Mini–Cell (*Invitrogen*, #EI0001) electrophoresis system.

At the end of the run, the gels were stained by incubation with SimplyBlue™ SafeStain (*Invitrogen*, #LC6060) for 1h at room temperature under agitation. Subsequently, the staining solution was removed, and the gels were rinsed with dH₂O under agitation until they became clear again. Images of the gel were obtained by ImageQuant LAS4000 (*Cytiva*).

4.2.7 Desalting and protein quantification

Once verified through the SDS–PAGE the quality of purified TLS2polyP–HuIgFc poly–epitope and TLS2Loop4–6His fragment, the fractions containing the recombinant proteins of interest were desalted using PD–10 Desalting Columns (*Cytiva*, #17085101). The PD–10 columns, containing Sephadex G–25 resin, were equilibrated by filling them with 5mL of 1× DPBS (*Gibco*, #14190) for 5 times and letting the equilibration buffer to enter the packed bed completely. Subsequently, the elutions were loaded onto the columns and eluted in 3,5mL of Desalting Buffer D (1× DPBS).

To quantify recombinant proteins present in each elution, the desalted fractions were analysed with Pierce™ BCA Protein Assay Kit (*Thermo Scientific*, #23225), following manufacturer's instructions. 25µL of each desalted sample were added to 200µL of Working Solution, prepared by diluting Pierce™ BCA Protein Assay Reagent A (*Thermo Scientific*, #23222) and Pierce™ BCA Protein Assay Reagent B (*Thermo Scientific*, #23224) with a 50:1 v:v ratio, and left to incubate at 37°C for 30min to allow the development of colorimetric reactions. The absorbances were measured at 562nm with Spectramax M2 Microplates Reader (*Molecular Devices*), using dilutions of Albumin – BSA at known concentrations (2mg/mL, 1mg/mL, 500µg/mL, 250µg/mL, 125µg/mL, 76,5µg/mL) to define a standard curve.

4.2.8 Digestion with IdeZ protease

A portion of the purified TLS2polyP–HuIgFc poly–epitope was subjected to enzymatic digestion with IdeZ Protease (*Promega*, #V8341), capable of recognizing and cleaving a unique site below the IgG hinge region, in order to generate the TLS2polyP fragment which will be used during the plasma cells screening step.

After having reconstituted the lyophilized protease with 100 μ L of dH₂O, to reach a final concentration of 50U/ μ L, the recombinant protein digestion was carried out by adding 1 unit of IdeZ per 1 μ g of TLS2polyP–HuIgFc. Samples were incubated at 37°C for 1h, after which the 6His–tagged enzyme was removed using Dynabeads™ His–Tag Isolation and Pulldown (*Invitrogen*, #10104D), with a ratio of 1mg of magnetic beads (40mg beads/mL) per 40 μ g of IdeZ protease. The purification mixtures were left to incubate on a roller for 30min at room temperature and then the IdeZ–beads complexes were removed through the application of a magnetic field.

Subsequently, the HuIgFc–TAG was removed using Pierce™ Protein G Magnetic Beads (*Thermo Scientific*, #88848), with a ratio of 1mg of magnetic beads (10mg beads/mL) per 60 μ g of HuIgFc fragment. The purification mixtures were left to incubate on a roller for 1h at room temperature and then the HuIgFc–beads complexes were removed through the application of a magnetic field. The purity of the TLS2polyP fragment thus recovered was verified through SDS–PAGE, as previously described.

4.3 TLS2–EGFP and TLS2–IRES–EGFP/AP2 stable lines generation

4.3.1 Cell cultures

- Flp–In™–293 Cell Line (*Invitrogen*, #R75007) was cultured in DMEM, high glucose (*Gibco*, #41965) supplemented with 10% (v/v) heat–inactivated Fetal Bovine Serum FBS (*Gibco*, #10082147), 2mM (v/v) GlutaMAX™ Supplement (*Thermo Scientific*, #350500) and 1% (v/v) Penicillin–Streptomycin P/S (*Gibco*, #15140122). This adherent cell line was maintained in sterile, tissue culture multiwell plates, dishes or flasks (*Corning*) at 37°C in an environment with a humidified atmosphere of 5% CO₂;
- Flp–In™–CHO Cell Line (*Invitrogen*, #R75807) was cultured in Ham’s F12 Nutrient Mix (*Gibco*, #11765054) supplemented with 10% (v/v) heat–inactivated Fetal

Bovine Serum FBS, 2mM (v/v) GlutaMAX™ Supplement and 1% (v/v) Penicillin–Streptomycin P/S. This adherent cell line was maintained in sterile, tissue culture multiwell plates, dishes or flasks (*Corning*) at 37°C in an environment with a humidified atmosphere of 5% CO₂.

All the cell lines were tested for mycoplasma contamination through PCR analysis.

4.3.2 Flp–In™ cell lines stable transfection

pcDNA5_TLS2–EGFP and pcDNA5_TLS2–IRES–EGFP recombinant plasmids were stably transfected into Flp–In™–293 and Flp–In™–CHO cells, respectively, using Lipofectamine™ 2000 Transfection Reagent (*Invitrogen*, #11668) as per manufacturers' instructions.

On the day before transfection, 1×10^6 viable cells were seeded into p100 tissue culture dish in 6,5mL of complete medium and allowed to adhere in incubation O/N at 37°C and 5% CO₂.

On the day of transfection, plasmid DNA and Lipofectamine were prepared in microtubes as described below:

- Plasmid DNA: 20µg of DNA, with a proportion of 10% of pcDNA5_TLS2–EGFP/pcDNA5_TLS2–IRES–EGFP plasmid and 90% of pOG44 Flp–Recombinase plasmid (already available in laboratory), and 70µL of PLUS™ Reagent were diluted in Opti–MEM™ I Reduced Serum Medium, GlutaMAX™ Supplement (*Gibco*, #519850) to a final volume of 750µL;
- Lipofectamine: 60µL of Lipofectamine™ 2000 Reagent were diluted in Opti–MEM™ I Reduced Serum Medium to a final volume of 750µL.

The plasmid DNA dilutions were mixed with the diluted Lipofectamine to a final volume of 1,5mL and incubated for 5min at room temperature. The DNA–Lipofectamine solutions were then added dropwise to the dishes and the cells were incubated at 37°C in an environment with a humidified atmosphere of 5% CO₂. After 48h of incubation, the transfection medium was replaced with fresh one supplemented with Hygromycin B (*Gibco*, #10687010) at a final concentration of 200µg/mL for Flp–In™–293 cells or 400µg/mL for Flp–In™–CHO cells. Every 2 days of selection, the medium was replaced and the transfected Flp–In™–293/Flp–In™–CHO cells were monitored with inverted microscope, to evaluate cell viability, and with fluorescence microscope, comparing the EGFP emission

with the expression of TLS2–EGFP and TLS2–IRES–EGFP recombinant plasmids. After 12 to 14 days of antibiotic selection, drug-resistant and well-isolated colonies were removed from the dish and seeded in 24-well plates, with a limited dilution of 0,3 cells/well, in order to selectively expand only the clones of interest. Once the Flp–InTM–293 clones have reached the confluence, they will then be tested to evaluate the expression of the TLS2 proteins by confocal microscopy. The HEK293_TLS2–EGFP clones tested positive for this analysis, and the CHO_TLS2–IRES–EGFP clones that maintained the fluorescence given by the expression of the reporter protein were brought to confluence, expanded in p100 tissue culture dish and frozen in –80°C.

To enhance TLS2 trafficking to the plasma membrane, CHO_TLS2–IRES–EGFP clones were used to generate stable lines expressing the auxiliary protein AP2. For this transfection, the LipofectamineTM 2000 Transfection Reagent protocol was maintained as previously described, however pOG44 plasmid was not required and the selection step was carried out with GeneticinTM Selective Antibiotic (*Gibco*, #101310) at a final concentration of 600µg/mL. Once the Flp–InTM–CHO clones have reached the confluence, they will then be tested to evaluate the expression of the AP2 and TLS2 proteins by flow cytometric and Western Blot analysis, respectively. Only the clones positive for both testes were kept, expanded in p100 tissue culture dish and frozen in –80°C until their use.

4.3.3 Confocal microscopy

The TLS2 protein expression in HEK293_TLS2–EGFP stable lines was verified through confocal analysis.

Once the TLS2–EGFP transfected Flp–InTM–293 clones have reached the confluence in a 24-well plate, they were collected by centrifugation at 1,800rpm for 5min and washed with 1× DPBS to remove the remaining culture medium. For each sample, including a negative control with Flp–InTM–293 wild type, 5×10⁴ viable cells were diluted in 500µL of complete DMEM Medium + 200µg/mL Hygromycin B and seeded on sterile FisherbrandTM Cover Glasses: Circles (*Fisher Scientific*, #22–293–232P), previously placed into the wells of a 24-well plate. After an O/N incubation at 37°C in an environment with a humidified atmosphere of 5% CO₂, to allow the cells to adhere on the coverslips, they were washed with 500µL of 1× DPBS and fixed with 200µL of 4% PFA in 1× DPBS for 10min at room temperature. The cells were washed again with 500µL of 1× DPBS and permeabilized with 500µL of

Permeabilization Buffer (0,25% TritonX–100 in 1× DPBS) for 5min at room temperature. After this step, the cells were washed 3 times with 500µL of 1× DPBS and incubated with 500µL of Blocking Buffer (3% BSA + 0,05% TritonX–100 in 1× DPBS), in order to reduce the noise originating from nonspecific protein–protein interactions. At this point, the fixed and permeabilized cells were labelled with Concanavalin A, Tetramethylrhodamine Conjugate (*Invitrogen*, #C860) diluted 1:100 (50µg/mL) in Ab Dilution Buffer (1%BSA in 1× DPBS) and incubated for 1h at room temperature. This will be followed by 3 more washes with 500µL of 1× DPBS and 5min incubation at room temperature with Hoechst 33342, Trihydrochloride, Trihydrate (*Invitrogen*, #H3570) diluted 1:3,000 (approximately 3,3µg/mL) in 1× DPBS for the nuclear counterstaining. After this last incubation, the cells were washed again with 500µL of 1× DPBS and the coverslips were placed overturned on glass slides, on which were previously deposited a drop of ProLong™ Gold Antifade Mountant (*Invitrogen*, #P36934). The mounting medium was then left to dry O/N at room temperature in the dark and the following day the glass slides were acquired using Leica TCS SP5 Confocal Laser Scanning Microscope (*Leica Microsystems*) and Leica Application Suite Advanced Fluorescence – LAS AF, version 2.7.3–9723 software (*Leica Microsystems*).

4.3.4 Flow cytometry

The cMyc–tagged AP2 protein expression in CHO_TLS2–IRES–EGFP/AP2 stable line was verified through flow cytometric (Fluorescent–Activated Cell Sorter, FACS) analysis. Once the AP2 transfected TLS2–IRES–EGFP stable line clones have reached the confluence in a 24–well plate, they were collected by centrifugation at 1,800rpm for 5min and washed with 1× DPBS to remove the remaining culture medium. For each sample, including a negative control with Flp–In™–CHO wild type, 5×10^4 viable cells were incubated with a c–Myc Monoclonal Antibody 9E10 (*Invitrogen*, #MA1980) diluted 1:100 in 1× DPBS + 5% FBS for 1h at 4°C. At the end of the incubation, the cell pellets were washed twice with 1× DPBS + 5% FBS and incubated with an Alexa Fluor™ 647 F(ab')₂ fragment of goat anti–mouse IgG (H+L) antibody (*Invitrogen*, #A21237) diluted 1:200 (1µg/mL) in 1× DPBS + 5% FBS for 1h at 4°C. The samples were washed again and resuspended in 200µL of 1× DPBS + 5% FBS. The fluorescence signal from the stained cells was acquired on the BD FACSCanto II (*BD*), through BD FACSDiva™ Software (*BD*).

4.3.5 Western Blot

The TLS2 protein expression in CHO_TLS2-IRES-EGFP and CHO_TLS2-IRES-EGFP/AP2 stable lines was verified through Western Blot analysis.

For the samples' preparation, 1×10^6 viable Flp-InTM-CHO wild type, CHO_TLS2-IRES-EGFP and CHO_TLS2-IRES-EGFP/AP2 cells were collected by centrifugation at 1,800rpm for 5min and washed twice with cold $1 \times$ DPBS to remove the remaining culture medium. These cells were then lysed using RIPA Lysis and Extraction Buffer (*Thermo Scientific*; #89900), in order to extract their total protein content. The cell pellets were resuspended in 600 μ L of lysis buffer and incubated for 15min at 4°C under agitation. Subsequently, the mixtures were centrifugated at 13,000rpm for 15min at 4°C to pellet the cell debris and recover the proteins present in the supernatants.

To quantify the protein content in each sample, the cell lysates were analysed with PierceTM BCA Protein Assay Kit, as previously described (see in Section 4.2.7).

For each cell line, 20 μ g of lysate was added to an appropriate volume of NuPAGETM LDS Sample Buffer 4 \times and boiled for 10min at 96°C. The samples were loaded onto NuPAGETM 4 to 12%, Bis-Tris, 1.0mm, Mini Protein Gel, 12-well, using as reference 5 μ L of SeeBlueTM Plus2 Pre-stained Protein Standard for protein sizing. Then, the gel was run for 1h at 150V in SDS Running Buffer, prepared by diluting 50mL of NuPAGETM MOPS SDS Running Buffer 20 \times in 950mL of dH₂O and loaded into the XCell SureLockTM Mini-Cell electrophoresis system.

At the end of the run, the proteins in the polyacrylamide gel were dry-electroblotted in a Polyvinylidene Difluoride (PVDF) membrane using iBlotTM Transfer Stack, PVDF (*Invitrogen*, #IB4010). through iBlotTM Gel Transfer System (*Invitrogen*, #2033731).

Finished the transfer, the PDVF membrane was incubated with 10% Skim Milk in $1 \times$ TBS-T (20mM Tris, 150mM NaCl, 0,1% Tween-20) for 1h, in order to block free binding surface of the membrane and to avoid non-specific binding of the primary antibody. The membrane was then incubated with a commercial, rabbit-polyclonal anti-TLS2 antibody (reference number not shown, for confidentiality) diluted 1:1,000 in 1% Skim Milk in $1 \times$ TBS-T O/N at 4°C in a shaker at 15rpm. At the end of the incubation, the PDVF membrane was washed 3 times with $1 \times$ TBS-T and incubated with a Goat Anti-Rabbit IgG (H+L) HorseRadish Peroxidase (HRP)-conjugated antibody (*Bio-Rad*, #1706515) diluted 1:5,000 in 1% Skim

Milk in 1× TBS–T for 1h at 4°C in a shaker at 15rpm. The membrane was washed again 3 times with 1× TBS–T and the proteins were detected using Pierce™ ECL Western Blotting Substrate (*Thermo Scientific*, #32209), with an incubation in ECL Substrate (dilution 1:1 Detection Reagent 1 Peroxide Solution + Detection Reagent 2 Luminol Enhancer Solution) of 2–5min. Images of the PDVF membrane were obtained by ImageQuant LAS4000, in chemiluminescence condition for the proteins or in fluorescence condition (Cy5) for the SeeBlue™ Plus2 Pre–stained Protein Standard acquisition.

4.4 TLS2 antibodies production

4.4.1 BALB/c mice immunization

For the production of murine TLS2–specific CD138⁺ plasma cells, 3 immunization groups were set up, each consisting of 5 Female BALB/c mice (*Charles River*) 4 weeks old, to which CHO_TLS2–IRES–EGFP/AP2 stable line cells or TLS2polyP–HuIgFc/TLS2Loop4–6His recombinant proteins were respectively administered. Each mouse was immunized through 3 intra–peritoneal injections every 14 days with 1×10⁷ CHO_TLS2–IRES–EGFP/AP2 cells or 20µg of purified TLS2polyP–HuIgFc/TLS2Loop4–6His protein with 1µL 200mM Dithiothreitol DTT (*Invitrogen*, #P2325) in a total volume of 100µL 1× DPBS, added to and 100µL of Complete Freund’s Adjuvant CFA (*Invitrogen*, #F5506) or Incomplete Freund’s Adjuvant IFA (*Invitrogen*, #F5881). CFA was used only for the first dose and IFA for the subsequent boosts. Blood for sera analyses was taken 7 days after the 3rd immunization to evaluate the antibody titer through ELISA test. The CHO_TLS2–IRES–EGFP/AP2 stable line–immunized group underwent 2 further boosts, following which antibody titration was carried out again.

Completed the immunization protocols, the mice were anesthetized with IsoFlo (*Zoetis*, #50019100) and, once the terminal blood sample was collected, they were euthanized by cervical dislocation. Subsequently, the mice bone marrow and spleen were recovered and used for the isolation of TLS2–specific single CD138⁺ plasma cells, or cryopreserved at –80°C.

4.4.2 Antibody titration

Anti-TLS2 antibody titer developed in sera of mice immunized with CHO_TLS2-IRES-EGFP/AP2 stable line cells or TLS2polyP-HuIgFc/TLS2Loop4-6His recombinant proteins were assessed through Enzyme-linked Immunosorbent Assay (ELISA).

Purified TLS2polyP or TLS2Loop4-6His fragments were coated onto SpectraPlate-384 High Binding plates (*PerkinElmer*, #6007500) at 10µg/mL in a total volume of 12µL 1× DPBS /well, and incubated overnight at 4°C. The following day the plates were washed with 0,05% Tween 20-1× DPBS and then blocked with 35µL Blocking Buffer (1× DPBS + 1% BSA, 1% FBS)/well for 1 hour at 37°C. Subsequently, the plates were washed again with 0,05% Tween 20-1× DPBS and then mice sera were applied at various dilutions in Blocking Buffer (20µL/well) for 1 hour at 37°C. Then, the plates were washed 5 times with 0,05% Tween 20-1× DPBS and incubated with a Goat Anti-Mouse IgG (H+L) HRP-conjugated antibody (*Bio-Rad*, #170-6516) diluted 1:5,000 in Blocking Buffer (20µL/well) for 1 hour at 37°C. After 6 washes with 0,05% Tween 20-1× DPBS, the plates were incubated with 20µL 1-Step™ Ultra TMB (3,3',5,5'-Tetramethylbenzidine)-ELISA Substrate Solution (*Thermo Scientific*, #34028)/well for 30 minutes at RT and then the reaction was halted with 0.5M HCl (20µL/well). The absorbances were measured at 450nm with Spectramax M2 Microplates Reader.

To evaluate the antibody titer developed in mice immunized with TLS2polyP-HuIgFc against the full-length, membrane TLS2 protein, a flow cytometric analysis (see in Section 4.3.4) was performed on Flp-In™-293 cells transiently transfected with pcDNA5_TLS2-EGFP using Lipofectamine™ 2000 Transfection Reagent but omitting the use of pOG44 plasmid. (see in Section 4.3.2). For the immunostaining, the serum of mice immunized with the poly-epitope and a pre-immune serum as a negative control were used as primary antibodies, and a Goat Anti-Mouse IgG (H+L) DyLight™ 650-conjugated antibody (*Invitrogen*, #84545) diluted 1:200 in 1× DPBS + 5% FBS as secondary antibody. The fluorescence signal from the stained cells was acquired on the BD FACSCanto II, through BD FACSDiva™ Software.

To evaluate the antibody titer developed in mice immunized with TLS2Loop4-6His against the full-length TLS2 protein, Western Blot analysis was performed using Flp-In™-CHO wild type and CHO_TLS2-IRES-EGFP/AP2 stable line cell lysates, obtained using RIPA Lysis and Extraction Buffer, and TLS2Loop-6His recombinant fragment (see in Section

4.3.5). For the immunostaining, the serum of a mouse from both immunization groups and a pre-immune serum as a negative control diluted 1:1,000 in 1% Skim Milk in 1× TBS-T were used as primary antibodies, and a Goat Anti-Mouse IgG (H+L)-HRP conjugated antibody (*Bio-Rad*, #1706516) diluted 1:5,000 in 1% Skim Milk in 1× TBS-T as secondary antibody. The detection step was carried out using PierceTM ECL Western Blotting Substrate, and the images of PDVF membranes were obtained by ImageQuant LAS4000, in chemiluminescence condition for the proteins or in fluorescence condition (Cy5) for the SeeBlueTM Plus2 Pre-stained Protein Standard acquisition.

4.5 Selection and identification of new TLS2 mAbs

4.5.1 Identification and isolation of TLS2-specific single ASCs

The enrichment of antigen-specific CD138⁺ plasma cells from bone marrow samples of mice immunized with CHO_TLS2-IRES-EGFP/AP2 stable line cells or TLS2Loop4-6His recombinant fragment was performed using the CD138⁺ Plasma Cell Isolation Kit (*Miltenyi Biotec*, #130092530), following the manufacturer's instructions.

The bone marrow samples were washed with 1× DPBS and transferred into sterile 35mm culture dishes containing 1mL of Dissociation Buffer (1× DPBS + 0,5% FBS, 2mM EDTA), where they were mechanically minced with the flat end of a syringe plunger. The supernatants were then passed through FalconTM 100µm Cell Strainers (*Falcon*, # 352360), in turn washed with 2mL of Dissociation Buffer. The cell suspensions were centrifuged at 1,500rpm for 5min, and the pellets thus obtained were resuspended in 50µL of Dissociation Buffer. The CD138⁺ plasma cells were magnetically labelled with 10µL of CD138 Micro Beads, mouse (*Miltenyi Biotec*, #130098257)/10⁷ total cells and incubated for 15min on ice. At the end of the incubation, the cells were washed by adding 2mL of Dissociation Buffer, centrifuged at 1,500rpm for 5min and resuspended in 500µL of Dissociation Buffer. The cell suspensions were then passed through a LS Columns (*Miltenyi Biotec*, #130042401) placed in the magnetic field of a MidiMACSTM Separator (*Miltenyi Biotec*, #130042302) and washed 3 times with 3mL of Dissociation Buffer, in order to collect the unlabelled cells in negative selections. Subsequently, the LS Columns were removed from the MidiMACSTM Separator and washed again 3 times with 3mL of Dissociation Buffer, this time to recover the fraction with magnetically labelled cells.

The enriched CD138⁺ plasma cells were resuspended in Antibodies Expression Medium (RPMI1640 + 10% FBS, 1× NeAA, 10ng/mL recombinant mouse IL-6, 25% filtered supernatant of day3 M210B4 cell culture, 10μM β-mercaptoethanol) and plated with a distribution of 50 cells per well in a final volume of 25μL in Corning™ Low Volume 384-well TC-treated Microplates (*Corning*, #3542). After 24h of incubation at 37°C with a humidified atmosphere of 5% CO₂, the supernatant of each well was used to set up an ELISA assay on SpectraPlate-384 High Binding plates previously coated with TLS2Loop4-6His recombinant fragment at 10μg/mL (see in Section 4.4.2). For this analysis it was prepared a negative control, only Antibodies Expression Medium, and a positive control, using the serum of immunized mice diluted 1:100 in Antibodies Expression Medium. The cells inside the positive wells, containing the antibodies against TLS2, were resuspended in Antibodies Expression Medium and replated with a limiting distribution of 0,3 cells per well in news Corning™ Low Volume 384-well TC-treated Microplates. The next day, the ELISA assay was repeated to identify the single TLS2-specific plasma cells. The plasma cells inside the positive wells were washed with 1× DPBS and moved to 8-tubes PCR-strips containing 4μl of Lysis Buffer (Table 4.7), in sterile conditions, and used for the Reverse Transcriptase-Polymerase Chain Reaction (RT-PCR), or cryopreserved at -80°C.

Table 4.7: TLS2-specific single CD138⁺ plasma cells Lysis Buffer.

Lysis Buffer	1×	Final concentration
UltraPure™ DNase/RNase-Free Distilled H ₂ O (<i>Invitrogen</i> , #10977035)	3,31μL	
10× sterile PBS	0,25μL	0,625×
0,1M DL-DTT (<i>Promega</i> , #P1171)	0,14μL	3,5mM
40U/μL RNasin™ Plus RNase Inhibitor (<i>Promega</i> , #N2611)	0,3μL	3U
Final volume/sample	4μL	

4.5.2 Recovery of V_H and V_L coding sequences from single antigen-specific ASC and “minigenes” assembly

The TLS2-specific single CD138⁺ plasma cell lysates were reverse-transcribed to cDNA, using SuperScriptTM IV Reverse Transcriptase (*Invitrogen*, #18090050) primed with Oligo(dT)₁₂₋₁₈ Primer (*Invitrogen*, #18418012) and Custom LNA Oligonucleotide Template-Switching Oligos – TSO (*Qiagen*, #339407) [AAGCAGTGGTATCAACGCAGAGTACATrGrG+G] [169]. For this amplification step, EppendorfTM ep Dualfilter T.I.P.STM (Eppendorf, #EP0030078500/#0030078535/#0030078551/#0030078578) PCR clean and sterile were used, and all subsequent mixes were prepared in a DNA/RNA-free hood.

Single CD138⁺ plasma cell lysates were thawed on ice for 5min and centrifugated at 400g for 30sec at 4°C. To each sample was then added 4μL of RT-PCR Mix I (Table 4.8) in a circular motion along the edges of the tube:

Table 4.8: RT-PCR Mix I.

RT-PCR Mix I	1×	Final concentration
UltraPure TM DNase/RNase-Free Distilled H ₂ O (<i>Invitrogen</i> , #10977035)	3μL	
25mM each dNTPs Mix (<i>Thermo Scientific</i> , #R1121)	0,8μL	1mM each
100μM Oligo(dT) ₁₂₋₁₈ Primer (<i>Invitrogen</i> , #18418012)	0,2μL	1μM
Final volume/sample	4μL	

Subsequently, they were centrifuged at 400g for 1min at 4°C and incubated for 3min at 72°C in pre-heated MiniAmpTM Plus Thermal Cycler. After the incubation, samples were placed on ice for 1–5min, during which time the RT-PCR Mix II was prepared as shown below (Table 4.9):

Table 4.9: RT-PCR Mix II.

RT-PCR Mix II	1×	Final concentration
5× First Strand Buffer (<i>Invitrogen</i> , 180910)	4μL	1×
50mM Betaine (<i>Merck</i>)	2,9μL	7,25mM
50mM MgCl ₂ (<i>Invitrogen</i>)	2,4μL	6mM
100μM DL-DTT (<i>Promega</i> , #P1171)	1μL	5μM
100μM Custom LNA Oligonucleotide TSO (<i>Qiagen</i> , #339407)	0,2μL	1μM
40U/μL RNasin™ Plus RNase Inhibitor (<i>Promega</i> , #N2611)	0,5μL	1U/μL
200U/μL SuperScript™ IV Reverse Transcriptase (<i>Invitrogen</i> , #18090050)	1μL	10U/μL
Final volume/sample	12μL	

12μL of RT-PCR Mix II were added to each sample in a circular motion along the edges of the tube, then they were centrifugated at 400g for 1 min at 4°C and incubated in a MiniAmp™ Plus Thermal Cycler with the following amplification profile (Table 4.10):

Table 4.10: Amplification profile of RT-PCR.

Temperature	Time
42°C	10min
25°C	10min
50°C	1h
94°C	5min
4°C	∞

The complementary DNAs double strands thus obtained were then pre-amplified with Terra™ PCR Direct Polymerase (*Takara Bio*, #639270), in order to increase the total amount of genetic material while maintaining reduced amplification bias [170], and IS-PCR primers [AAGCAGTGGTATCAACGCAGAGT] (*Eurofins Genomics*).

10μL of each cDNA sample diluted 1:2 with UltraPure™ DNase/RNase-Free Distilled H₂O was added to 15μL of preAmp-PCR Mix, previously prepared as shown below (Table 4.11):

Table 4.11: *preAmp-PCR Mix.*

preAmp-PCR Mix	1×	Final concentration
UltraPure™ DNase/RNase-Free Distilled H ₂ O (<i>Invitrogen</i> , #10977035)	1,95μL	
2× Terra PCR Direct Buffer (<i>Takara Bio</i> , #639270)	12,5μL	1×
10μM IS-PCR primers (<i>Eurofins Genomics</i>)	0,05μL	20nM
1,25U/μL Terra PCR Direct Polymerase Mix (<i>Takara Bio</i> , #639270)	0,5μL	0,025U/μL
Final volume/sample	15μL	

cDNA pre-amplification was conducted using a MiniAmp™ Plus Thermal Cycler, with the following amplification profile (Table 4.12):

Table 4.12: *Amplification profile used for cDNA pre-amplification.*

Step	Temperature	Time	Cycle
Initial denaturation	98°C	3min	1
Denaturation	98°C	15sec	18
Annealing	65°C	30sec	
Extension	68°C	4min	
Final extension	72°C	10min	1
Maintenance	4°C	∞	–

At this point, both cDNAs and pre-amplified DNAs were amplified through 3 rounds of antibody-specific PCR, using KOD DNA Polymerase and Taq DNA Polymerase primed with Ig-specific primers [105], to amplify heavy- and light-chain variable region (V_H and V_L) genes and insert them into a human antibody framework. Through this approach it is possible to generate two linear Transcriptionally Active PCR (TAP) products directly transfectable into mammalian cells to produce recombinant chimeric mAbs, without the need of cloning into expression vectors or purification steps.

Primers used in each amplification step were resuspended with UltraPure™ DNase/RNase-Free Distilled H₂O at 100pmol/μL and putted together in specific primer mixes. Subsequently, 0,1μL of each primer mix was added to the corresponding PCR mix.

Every PCR product was verified through electrophoresis on 1.5% agarose gel with 1Kb Plus DNA Ladder for DNA sizing and used as a template for subsequent amplification step.

The amplification protocols used are the followings:

- For the primary PCR (PCR I), it was set up a touchdown PCR in order to increase the specificity of the amplification reaction. As template, 3 μ L of the cDNA obtained through the RT-PCR step or 3 μ L of pre-amplified DNA diluted 1:10 with UltraPure™ DNase/RNase-Free Distilled H₂O were added to 22 μ L of PCR I/II Mix (Table 4.13):

Table 4.13: PCR I/II Mix.

PCR I Mix	1\times	Final Concentration
UltraPure™ DNase/RNase-Free Distilled H ₂ O (<i>Invitrogen</i> , #10977035)	15,5 μ L	
10 \times Taq DNA Polymerase PCR Buffer (<i>Invitrogen</i> , #18067017)	2,5 μ L	1 \times
2,5mM each dNTP Mix (<i>Invitrogen</i> , #R72501)	2,5 μ L	0,25mM each
25mM MgCl ₂ (<i>Thermo Scientific</i> , #AB0359)	1 μ L	1mM
100 μ M Primer Forward (<i>Eurofins Genomics</i>)	0,1 μ L	0,4 μ M
100 μ M Primer Reverse (<i>Eurofins Genomics</i>)	0,1 μ L	0,4 μ M
1U/ μ L KOD Hot Start DNA Polymerase (<i>Sigma-Aldrich</i> , #71086)	0,2 μ L	0,008U/ μ L
5U/ μ L Taq DNA Polymerase, recombinant (<i>Invitrogen</i> , #10342046)	0,1 μ L	0,02U/ μ L
Final volume/sample	22 μ L	

The primer mixes used for V_H and V_L PCR I step were (Table 4.14):

Table 4.14: V_H and V_L PCR I primers.

Chain	Primer	Sequence
V_H	F–MsVHE	GGGAATTCGAGGTGCAGCTGCAGGAGTCTGG
	R–C–M outer	AGGGGGCTCTCGCAGGAGACGAGG
	R–C–gamma1 outer	GGAAGGTGTGCACACCGCTGGAC
	R–C–gamma2c outer	GGAAGGTGTGCACACCACTGGAC
	R–C–gamma2b outer	GGAAGGTGTGCACACTGCTGGAC
	R–C–gamma3 outer	AGACTGTGCGCACACCGCTGGAC
	R–Calpha outer	GAAAGTTCACGGTGGTTATATCC
V_L	F–L–Vk_3	TGCTGCTGCTCTGGTTCCAG
	F–L–Vk_4	ATTWTCAGCTTCCTGCTAATC
	F–L–Vk_5	TTTTGCTTTTCTGGATTYCAC
	F–L–Vk_6	TCGTGTTKCTSTGGTTGTCTG
	F–L–Vk_6_8_9	ATGGAATCACAGRCYCWGGT
	F–L–Vk_14	TCTTGTTGCTCTGGTTYCCAG
	F–L–Vk_19	CAGTTCCTGGGGCTCTTGTTGTTC
	F–L–Vk_20	TCACTAGCTCTTCTCCTC
	R–mCK	GATGGTGGGAAGATGGATACAGTT

PCR I was conducted using a MiniAmp™ Plus Thermal Cycler, with the following amplification profile for both V_H and V_L genes (Table 4.15):

Table 4.15: Amplification profile used for PCR I.

Step	Temperature	Time	Cycle
Initial denaturation	94°C	3min	1
Denaturation	94°C	30sec	15
Annealing	65→50°C (–1°C per cycle)	30ses	
Extension	72°C	55sec	
Denaturation	94°C	30sec	50
Annealing	50°C	30sec	
Extension	72°C	55sec	
Final extension	72°C	10min	1
Maintenance	4°C	∞	–

- As template for the secondary PCR (PCR II), 3μL of the touchdown PCR I products were added to 23μL of PCR I/II Mix (see in Table 4.13).

The primer mixes used for V_H and V_L PCR II step were (Table 4.16):

Table 4.16: PCR II primers.

Chain	Primer	Sequence
V _H	F-AgeI P-mVH01	CTGCAACCGGTGTACATTCCCAGGTGCAGCTGCAGCAGCCTGG
	F-AgeI P-mVH02	CTGCAACCGGTGTACATTCCCAGGTGCAGCTGCAGCAGTCTGG
	F-AgeI P-mVH03	CTGCAACCGGTGTACATTCCCAGGTGCAGCTGAAGCAGTCTGG
	F-AgeI P-mVH04	CTGCAACCGGTGTACATTCCCAGGTGCAGCTGAAGGAGTCTGG
	F-AgeI P-mVH05	CTGCAACCGGTGTACATTCCGAGGTGAAGCTGGAGGAGTCTGG
	F-AgeI P-mVH06	CTGCAACCGGTGTACATTCCGAGGTGCAGCTGGTGGAGTCTGG
	F-AgeI P-mVH07	CTGCAACCGGTGTACATTCCGAAGTGCAGCTGTTGGAGACTGG
	F-AgeI P-mVH08	CTGCAACCGGTGTACATTCCGAGGTGCAGCTGCAGCAGTCTGG
	F-AgeI P-mVH09	CTGCAACCGGTGTACATTCCGAGGTGCAGCTGCAGGAGTCTGG
	F-AgeI P-mVH10	CTGCAACCGGTGTACATTCCGAGGTGCAGCTGCAGCAGTCTGTG
	F-AgeI P-mVH11	CTGCAACCGGTGTACATTCCGAGGTGAAGCTGGTGGAGTCTGG
	F-AgeI P-mVH12	CTGCAACCGGTGTACATTCCCAGATCCAGCTGCAGCAGTCTGG
	F-AgeI P-mVH13	CTGCAACCGGTGTACATTCCCAGTTCAGCTGCAACAGTCTGA
	F-AgeI P-mVH14	CTGCAACCGGTGTACATTCCGAGTTCAGCTGCAGCAGTCTGG
	F-AgeI P-mVH15	CTGCAACCGGTGTACATTCCGATGTACAGCTTCAGGAGTCAGG
	F-AgeI P-mVH16	CTGCAACCGGTGTACATTCCGAGGTGCAGCTTGTGAGTCTGGTGGAG
	F-AgeI P-mVH17	CTGCAACCGGTGTACATTCCCAGCGTGAGCTGCAGCAGTCTGG
	F-AgeI P-mVH18	CTGCAACCGGTGTACATTCCGACGTGAAGCTGGTGGAGTCTGG
	F-AgeI P-mVH19	CTGCAACCGGTGTACATTCCGAAGTGATGCTGGTGGAGTCTGG
	F-AgeI P-mVH20	CTGCAACCGGTGTACATTCCCAGGTGCAGCTTGTAGAGACCGG
	F-AgeI P-mVH21	CTGCAACCGGTGTACATTCCCAGATGCAGCTTCAGGAGTCAGG
	F-AgeI P-mVH22	CTGCAACCGGTGTACATTCCCAGGCTTATCTACAGCAGTCTGG
	F-AgeI P-mVH23	CTGCAACCGGTGTACATTCCGAGTTCAGCTGCAGCAGTCTGG
V _H	R-SalI P-mJH01	GCTTGGGCCCTTGGTCGAAGCTGAGGAGACGGTGACCGTGG
	R-SalI P-mJH02	GCTTGGGCCCTTGGTCGAAGCTGAGGAGACTGTGAGAGTGG
	R-SalI P-mJH03	GCTTGGGCCCTTGGTCGAAGCTGCAGAGACAGTGACCAGAG
	R-SalI P-mJH04	GCTTGGGCCCTTGGTCGAAGCTGAGGAGACGGTGACTGAGG
V _L	F-AgeI P-mVK01	CTGCAACCGGTGTACATTCCAACATTATGATGACACAGTCGCCA
	F-AgeI P-mVK02	CTGCAACCGGTGTACATTCCAACATTGTGCTGACCCAATCTCCA
	F-AgeI P-mVK03	CTGCAACCGGTGTACATTCCCAAATTGTTCTCACCAGTCTCCA
	F-AgeI P-mVK04	CTGCAACCGGTGTACATTCCCAAATTGTTCTCTCCAGTCTCCA
	F-AgeI P-mVK05	CTGCAACCGGTGTACATTCCGAAAATGTTCTCACCAGTCTCCA
	F-AgeI P-mVK06	CTGCAACCGGTGTACATTCCGAAACAATGTTGACCCAGTCTCCA

V _L	F-AgeI P-mVK07	CTGCAACCGGTGTACATTCCGAAATTGTGCTCACTCAGTCTCCA
	F-AgeI P-mVK08	CTGCAACCGGTGTACATTCCGACATCAAGATGACCCAGTCTCCA
	F-AgeI P-mVK09	CTGCAACCGGTGTACATTCCGACATCCAGATGAACCAGTCTCCA
	F-AgeI P-mVK10	CTGCAACCGGTGTACATTCCGACATCCAGATGACTCAGTCTCCA
	F-AgeI P-mVK11	CTGCAACCGGTGTACATTCCGACATTGTGATGACTCAGTCTC
	F-AgeI P-mVK12	CTGCAACCGGTGTACATTCCGACATTGTGATGTACACAGTCTCCA
	F-AgeI P-mVK13	CTGCAACCGGTGTACATTCCGACATTGTGCTGACCCAATCTCCA
	F-AgeI P-mVK14	CTGCAACCGGTGTACATTCCGATATCCAGATGACACAGACTACA
	F-AgeI P-mVK15	CTGCAACCGGTGTACATTCCGATGTTGTGATGACCCAACTCCA
	F-AgeI P-mVK16	CTGCAACCGGTGTACATTCCGAAATCCAGATGACCCAGTCTCCA
	F-AgeI P-mVK17	CTGCAACCGGTGTACATTCCGACATCCAGATGACACAATCTTCA
	F-AgeI P-mVK18	CTGCAACCGGTGTACATTCCGACATCCAGATGACCCAGTCTCCA
	F-AgeI P-mVK19	CTGCAACCGGTGTACATTCCGACATCCTGATGACCCAATCTCCA
	F-AgeI P-mVK20	CTGCAACCGGTGTACATTCCGACATTGTGCTACCCAATCTCC
	F-AgeI P-mVK21	CTGCAACCGGTGTACATTCCGATGTTGTGGTGACTCAAACCTCCA
	F-AgeI P-mVK22	CTGCAACCGGTGTACATTCCAACATTGTAATGACCCAATCTCCC
	F-AgeI P-mVK23	CTGCAACCGGTGTACATTCCGATGTTTTGATGACCCAACTCCA
	F-AgeI P-mVK24	CTGCAACCGGTGTACATTCCGATATTGTGATGACTCAGGCTGCA
	F-AgeI P-mVK25	CTGCAACCGGTGTACATTCCGACATCCAGATGATTCAGTCTCCA
	F-AgeI P-mVK26	CTGCAACCGGTGTACATTCCGACATCTTGCTGACTCAGTCTCCA
	F-AgeI P-mVK27	CTGCAACCGGTGTACATTCCGATGTCCAGATGATTCAGTCTCCA
	F-AgeI P-mVK28	CTGCAACCGGTGTACATTCCGATGTCCAGATAACCCAGTCTCCA
	R-BsiWI P-mJK01	CAGATGGTGCAGCCACGGTACGTTTTGATTTCCAGCTTGGTG
	R-BsiWI P-mJK02	CAGATGGTGCAGCCACGGTACGTTTTATTTCAGCTTGGTC
	R-BsiWI P-mJK03	CAGATGGTGCAGCCACGGTACGTTTTATTTCAACTTTGTC
	R-BsiWI P-mJK04	CAGATGGTGCAGCCACGGTACGTTTCAGCTCCAGCTTGGTC

PCR II was conducted using a MiniAmp™ Plus Thermal Cycler, with different amplification profiles for V_H and V_L genes (Table 4.17):

Table 4.17: Amplification profiles used for PCR II.

Step	Temperature		Time	Cycle
Initial denaturation	94°C		3min	1
Denaturation	94°C		30sec	50
Annealing	60°C (V _H)	45°C (V _L)	30sec	
Extension	72°C		45sec	
Final extension	72°C		10min	1
Maintenance	4°C		∞	–

- For the tertiary PCR (TAP), the V_H and V_L genes previously amplified were merged with a strong human cytomegalovirus promoter (pCMV) and a human constant region fragment containing a Bovine Growth Hormone – BGH polyadenylation signal (C_H/C_κ–polyA), in order to generate two separate linear minigenes directly transfectable into mammalian cells for the production of the resulting recombinant chimeric mAbs.

As templates to obtain pCMV and C_H/C_κ–polyA constant region fragments, it was used AbVec2.0–IGHG1 (Addgene plasmid #80795; <http://n2t.net/addgene:80795>; RRID:Addgene_80795) and AbVec1.1–IGKC (Addgene plasmid #80796; <http://n2t.net/addgene:80796>; RRID:Addgene_80796), two recombinant plasmids encoding respectively immunoglobulin heavy and light chains with constant region (IgG1 and kappa isotype) of a human antibody [171].

1μL of AbVec2.0–IGHG1/AbVec1.1–IGKC plasmids, previously diluted with UltraPure™ DNase/RNase–Free Distilled H₂O to a final concentration of 10ng/μL, were added to 24μL of V_H/V_L Vector PCR Mix (Table 4.18):

Table 4.18: V_H/V_L Vector PCR Mix.

V_H/V_L Vector PCR Mix	1×	Final Concentration
UltraPure™ DNase/RNase-Free Distilled H ₂ O (<i>Invitrogen</i> , #10977035)	17,5μL	
10× Taq DNA Polymerase PCR Buffer (<i>Invitrogen</i> , #18067017)	2,5μL	1×
2,5mM each dNTP Mix (<i>Invitrogen</i> , #R72501)	2,5μL	0,25mM each
25mM MgCl ₂ (<i>Thermo Scientific</i> , #AB0359)	1μL	1mM
100μM Primer Forward (<i>Eurofins Genomics</i>)	0,1μL	0,4μM
100μM Primer Reverse (<i>Eurofins Genomics</i>)	0,1μL	0,4μM
1U/μL KOD Hot Start DNA Polymerase (<i>Sigma-Aldrich</i> , #71086)	0,2μL	0,008U/μL
5U/μL Taq DNA Polymerase, recombinant (<i>Invitrogen</i> , #10342046)	0,1μL	0,02U/μL
Final volume/sample	24μL	

Primers used for the V_H and V_L vectors PCR step were (Table 4.19):

Table 4.19: V_H and V_L vectors PCR primers.

Vector	Primer	Sequence
V_{et_H} pCMV	CMV-WA-F	CGCCCGACATTGATTATTGACTAG
	Ig-Age-PCRvC-R	GGAATGTACACCGGTTGCAGTTGCTACTAG
V_{et_H} C _H -polyA	Kim-IgG-vect-F	GCTTCGACCAAGGGCCCAAGCGTC
	SV40epA2-R	GATCCAGACATGATAAGATACATTG
V_{et_L} pCMV-Gaussia + C _K -polyA	Kim-IgK-vect-F	ACCGTGGCTGCACCATCTG
	Ig-Age-PCRvC-R	GGAATGTACACCGGTTGCAGTTGCTACTAG

V_H and V_L vectors PCR was conducted using a MiniAmp™ Plus Thermal Cycler, with different amplification profiles (Table 4.20):

Table 4.20: Amplification profile used for V_H and V_L vectors PCR.

Sample	Step	Temperature	Time	Cycle
AbVec2.0–IGHG1	Initial denaturation	95°C	3min	1
	Denaturation	95°C	30sec	35
	Annealing	55°C	30sec	
	Extension	72°C	1min	
	Final extension	72°C	10min	1
	Maintenance	4°C	∞	–
AbVec1.1–IGKC	Initial denaturation	95°C	3min	1
	Denaturation	95°C	30sec	15
	Annealing	65→50°C (–1°C per cycle)	30sec	
	Extension	72°C	5min	
	Denaturation	95°C	30sec	30
	Annealing	55°C	30sec	
	Extension	72°C	5min	
	Final extension	72°C	10min	1
	Maintenance	4°C	∞	–

Subsequently, 2 μ L of heavy and light–variable genes obtained for the PCR II, if necessary diluted according to their actual quantities observed through electrophoretic run controls, were mixed with 1 μ L of V_{eH} pCMV and V_{eH} C_H –polyA or V_{eL} pCMV–Gaussia + C_K –polyA, respectively, and added to the TAP Mix (Table 4.21).

Table 4.21: TAP Mix.

TAP PCR Mix	1×		Final concentration
UltraPure™ DNase/RNase–Free Distilled H ₂ O (<i>Invitrogen</i> , #10977035)	14,5 μ L (V_H)	15,5 μ L (V_L)	
10× Taq DNA Polymerase PCR Buffer (<i>Invitrogen</i> , #18067017)	2,5 μ L		1×
2,5mM each dNTP Mix (<i>Invitrogen</i> , #R72501)	2,5 μ L		0,2mM each
25mM MgCl ₂ (<i>Thermo Scientific</i> , #AB0359)	1 μ L		1mM
100 μ M Primer Forward (<i>Eurofins Genomics</i>)	0,1 μ L		0,4 μ M
100 μ M Primer Reverse (<i>Eurofins Genomics</i>)	0,1 μ L		0,4 μ M
1U/ μ L KOD Hot Start DNA Polymerase (<i>Sigma–Aldrich</i> , #71086)	0,2 μ L		0,008U/ μ L
5U/ μ L Taq DNA Polymerase, recombinant (<i>Invitrogen</i> , #10342046)	0,1 μ L		0,02U/ μ L
Final volume/sample	21 μ L (V_H)	22 μ L (V_L)	

Primers used for the TAP step were CMV–WA–F (CGCCCGACATTGATTATTGACTAG) and SV40epA2–R (GATCCAGACATGATAAGATACATTG).

TAP was conducted using a MiniAmp™ Plus Thermal Cycler, with different amplification profiles for heavy and light chain (Table 4.22):

Table 4.22: Amplification profiles used for TAP.

Step	Temperature		Time	Cycle
Initial denaturation	95°C		3min	1
Denaturation	95°C		30sec	35
Annealing	64°C (V _H)	55°C (V _L)	30sec	
Extension	72°C		1min	
Final extension	72°C		10min	1
Maintenance	4°C		∞	–

4.5.3 Expi293F™ cells transient transfection into Deepwell plates

The minigenes obtained through TAP, encoding for recombinant chimeric TLS2 mAbs, were transiently transfected into Expi293F™ cells using ExpiFectamine™ 293 Transfection Kit, as per manufacturers' instructions and scaling down the protocol to Deepwell Plate 96/2mL. On the day before transfection, Expi293F™ cells were seeded in 125mL shaker flasks at a density of $1\text{--}2 \times 10^6$ viable cells/mL in 25mL of Expi293™ Expression Medium and maintained O/N at 37°C and 8% CO₂ in a shaker at 125rpm.

On the day of transfection, 7×10^7 cells were recovered and diluted in 49mL of fresh, pre-warmed medium to a final density of approximately $1,43 \times 10^6$ viable cells/mL. Then, 700μL of cells dilution was aliquoted in the 60 internal wells of the 96–deepwell plate, as a precaution to obtain a better well–to–well consistency avoiding greater evaporation of the samples, in order to seed 1×10^6 viable cells/well.

TAP minigenes and ExpiFectamine dilutions were prepared in microtubes as described below:

- TAP minigenes: for each well, 400ng of DNA, with a proportion of 30% heavy chain–encoding minigenes and 70% light chain–encoding minigenes, were diluted in OptiMEM™ I Reduced Serum Medium to a final volume of 35μL;

- ExpiFectamine: for each well, 1,08µL of ExpiFectamine™ 293 Reagent were diluted in OptiMEM™ I Reduced Serum Medium to a final volume of 35µL and incubated at RT for 5min.

The DNA dilutions was mixed with the diluted ExpiFectamine to a final volume of 70µL and incubated for 20min at room temperature. The DNA–ExpiFectamine solutions were then added dropwise to the wells and the Expi293F™ cells were incubated at 37°C in an environment with a humidified atmosphere of 8% CO₂ at 1,000rpm with MixMate™ Shaker. On the day after transfection (18 to 22 hours post–transfection), 2µL of ExpiFectamine™ 293 Transfection Enhancer 1 and 20µL of ExpiFectamine™ 293 Transfection Enhancer 2 were added to each transfection well.

The 96–deepwell plate was incubated for 2 days before the supernatants were harvested by centrifugation at 1,800rpm for 15min and used to evaluate binding capacity against TLS2Loop4–6His recombinant fragment and their expression levels.

4.5.4 mAbs quantification and binding activity validation

TLS2 antibodies binding activity and concentration in the supernatant of TAP minigenes–transfected Expi293F™ cells were assessed through qualitative and quantitative ELISA, respectively.

For the qualitative ELISA, SpectraPlate–384 High Binding plates were coated with TLS2Loop4–6His recombinant fragment at 10µg/mL, while for the quantitative ELISA they were coated with a Goat Anti–Human IgG Fc antibody (*Invitrogen*, #A18819) at 1µg/mL. After an O/N incubation at 4°C, both the immunological assays proceed with a wash in 0,05% Tween 20–1× DPBS, a blocking step with Blocking Buffer (1× DPBS + 1% BSA, 1% FBS) for 1 hour at 37°C and a further washing of the plates. The supernatants were applied non diluted in the qualitative ELISA plates and at various dilutions (1:5, 1:50, 1:500) in the quantitative ELISA, using dilutions of Cetuximab (*Merck*) at known concentration (100ng/mL, 50ng/mL, 25ng/mL, 12,5ng/mL, 6,25ng/mL, 3,12ng/mL, 1,56ng/mL, 781,25pg/mL, 390,62pg/mL, 195,31pg/mL, 97,65pg/mL, 48,82pg/mL) to define a standard curve, for 1h at 37°C. The plates were washed 5 times with 0.05% Tween 20–1× DPBS and incubated with a Goat Anti–Human IgG (H+L) HRP–conjugated antibody (*Invitrogen*, #H10307) diluted 1:5,000 in Blocking Buffer for 1 hour at 37°C. After 6 washes with 0,05%

Tween 20–1× DPBS, the secondary antibodies detection was performed using 1–Step™ Ultra TMB–ELISA Substrate Solution, as previously described.

The absorbances were measured at 450nm with Spectramax M2 Microplates Reader.

Once there were identified supernatants positive for the presence of TLS2–specific antibodies at a relevant concentration, they were used to further assess reactivity against the target antigen by Western Blot (see in Section 4.3.5) and flow cytometric analysis (see in Section 4.3.4), as previously described.

Western Blot test was performed using Flp–In™–CHO wild type, CHO_TLS2–IRES–EGFP and CHO_TLS2–IRES–EGFP/AP2 stable lines cell lysates, obtained using RIPA Lysis and Extraction Buffer, and TLS2Loop–6His recombinant fragment. For the immunostaining, different supernatant containing TLS2–specific chimeric mAbs were used at the highest possible concentration as primary antibody, and a Goat anti–Human IgG Fc–HRP conjugated antibody (*DIESSE – diagnostica senese*) diluted 1:5,000 in 1% Skim Milk in 1× TBS–T as secondary antibody. The detection step was carried out using Pierce™ ECL Western Blotting Substrate, and the images of PDVF membranes were obtained by ImageQuant LAS4000, in chemiluminescence condition for the mAbs or in fluorescence condition (Cy5) for the SeeBlue™ Plus2 Pre–stained Protein Standard acquisition.

For the flow cytometry test, supernatants were used to evaluate the chimeric mAbs binding activity against the conformationally folded antigen presented by both the CHO_TLS2–IRES–EGFP and CHO_TLS2–IRES–EGFP/AP2 stable lines, using Flp–In™–CHO wild type as a negative control and a Goat Anti–Human IgG Fc Cross–Adsorbed DyLight™ 650–conjugated antibody (*Invitrogen*, #SAS–10137) diluted 1:200 in 1× DPBS + 5% FBS as secondary antibody. The fluorescence signal from the stained cells was acquired on the BD FACSCanto II, through BD FACSDiva™ Software.

4.6 Production and characterization of TLS2 recombinant chimeric mAbs

4.6.1 Cell cultures

- HEL 92.1.7 Cell Line (*ATCC*, #TIB-180) was cultured in RPMI 1640 Medium (*Gibco*, #A1049101) supplemented with 10% (v/v) heat-inactivated Fetal Bovine Serum FBS and 1% (v/v) Penicillin–Streptomycin P/S. This suspension cell line was maintained in sterile, tissue culture flasks at 37°C in an environment with a humidified atmosphere of 5% CO₂.

All the cell lines were tested for mycoplasma contamination through PCR analysis.

4.6.2 V_H and V_L sequences cloning into expression vectors

After having established the binding activity of the chimeric mAbs, the coding sequence of the corresponding heavy and light variable regions genes were inserted into AbVec2.0–IGHG1 and AbVec1.1–IGKC recombinant plasmids, which will act as expression systems for their large-scale production. This cloning step was performed through a ligase-independent, restriction enzymes-free strategy based on the amplification of V_H/V_L genes and respective IgH/IgL plasmids through Polymerase Incomplete Primer Extension PCR (PIPE-PCR), in order to generate mixtures of incomplete extended products with short, overlapping sequences, that can anneal and produce hybrid insert-vector combinations.

To do this, 1μL of V_H/V_L PCR II products and respective AbVec2.0–IGHG1/AbVec1.1–IGKC recombinant plasmids diluted to a final concentration of 10ng/μL were added to 24μL of PIPE-PCR Mix (Table 4.23):

Table 4.23: PIPE–PCR Mix.

PIPE–PCR Mix	1×	Final Concentration
UltraPure™ DNase/RNase–Free Distilled H ₂ O (<i>Invitrogen</i> , #10977035)	17,3μL	
10× Taq DNA Polymerase PCR Buffer (<i>Invitrogen</i> , #18067017)	2,5μL	1×
2,5mM each dNTP Mix (<i>Invitrogen</i> , #R72501)	2,5μL	0,25mM each
25mM MgCl ₂ (<i>Thermo Scientific</i> , #AB0359)	1μL	1mM
100μM Primer Forward (<i>Eurofins Genomics</i>)	0,1μL	0,4μM
100μM Primer Reverse (<i>Eurofins Genomics</i>)	0,1μL	0,4μM
1U/μL KOD Hot Start DNA Polymerase (<i>Sigma–Aldrich</i> , #71086)	0,3μL	0,012U/μL
5U/μL Taq DNA Polymerase, recombinant (<i>Invitrogen</i> , #10342046)	0,2μL	0,04U/μL
Final volume/sample	24μL	

The primers used for V_H/V_L inserts and AbVec2.0–IGHG1/AbVec1.1–IGKC vectors PIPE–PCR step were (Table 4.24):

Table 4.24: V_H/V_L inserts and AbVec2.0–IGHG1/AbVec1.1–IGKC vectors PIPE–PCR primers.

Insert	Vector	Primer	Sequence
mAb_V _H	AbVec2.0–IGHG1	Kim–IgG–vect–F	GCTtcgaccaagggcccaagcgtc
		Ig–Age–PCRvC–R	GGAATGTACaccggttcagttgctactag
mAb_V _L	AbVec1.1–IGKC	Kim–IgK–vect–F	Accgtggctgcaccatctg
		Ig–Age–PCRvC–R	GGAATGTACaccggttcagttgctactag

PIPE–PCR was conducted using a MiniAmp™ Plus Thermal Cycler, with the following amplification profile (Table 4.25):

Table 4.25: Amplification profile used for PIPE–PCR.

Sample	Step	Temperature		Time	Cycle
mAb_V _H / mAb_V _L	Initial denaturation	95°C		3min	1
	Denaturation	95°C		30sec	35
	Annealing	60°C (V _H)	45°C (V _L)	30sec	
	Extension	72°C		45sec	
	Maintenance	4°C		∞	–
AbVec2.0–IGHG1/ AbVec1.1–IGKC	Initial denaturation	95°C		3min	1
	Denaturation	95°C		30sec	35
	Annealing	55°C (AbVec2.0–IGHG1)	62°C (AbVec1.1–IGKC)	30sec	
	Extension	72°C		5min	
	Maintenance	4°C		∞	–

At the end of the PIPE–PCR, AbVec2.0–IGHG1/AbVec1.1–IGKC vectors were dephosphorylated with FastAP Thermosensitive Alkaline Phosphatase for 10min at 37°C, to prevent their recircularization during the transformation step. The quality of the amplified sequences was evaluated by run on an electrophoresis 1% agarose gel with 1×TAE Buffer, using 5µL of 1Kb Plus DNA Ladder for DNA sizing. Subsequently, both amplified inserts and vectors were purified through agarose gel electrophoresis using QIAquick Gel Extraction Kit, as previously described (see in Section 4.1.6).

The amplified mAb_V_H/V_L inserts and the corresponding dephosphorylated AbVec2.0–IGHG1/AbVec1.1–IGKC vectors thus obtained were co–transformed into MultiShot™ StripWell Mach1™ T1 Phage–Resistant Chemically Competent *E. coli* (Invitrogen, #C869601), using the same heat–shock transformation protocol previously used for the DH5α cells and selecting the transformed cells on LB+100µg/mL ampicillin plates (see in Section 4.1.3). The colonies present on the plates the following day were screened by digestion with EcoRI and HindIII restriction enzymes, for the purpose of verifying the identity of the plasmid contained within them.

mAbH and mAbL recombinant plasmids were then recovered from the positive colonies, expanded into 5mL of LB+100µg/mL ampicillin medium and purified using QIAprep Spin Miniprep Kit (see in Section 4.1.4). Quantification of DNA and its purity were established by measuring the absorbance at 260 and 280nm with NanoVue™ 4282 V1.7 Spectrophotometer.

4.6.3 Scale up of production and purification for selected TLS2 mAbs

mAbH and mAbL recombinant plasmids were transiently cotransfected, with a proportion of 70% and 30% between the heavy and light chain–encoding plasmids respectively, into Expi293F™ cells using ExpiFectamine™ 293 Transfection Kit (*Gibco*, #A14525) as per manufacturers' instructions, for a large–scale production of the chimeric mAbs, in order to increase the reproducibility of subsequent functional analyses (see in Section 4.2.2).

The TLS2 chimeric mAbs, secreted in the transfected cells' supernatant, were purified through affinity chromatography, using HiTrap™ Protein G HP 1mL columns and with the help of the ÄKTA start system, as previously described (see in Section 4.2.3).

Once their correct purification has been verified and the fractions containing the mAbs of interest have been identified through SDS–PAGE (see in Section 4.2.6), these were buffer exchanged using PD–10 Desalting Columns and quantified with Pierce™ BCA Protein Assay Kit, as previously described (see in Section 4.2.7).

4.6.4 Characterization of TLS2 chimeric mAbs

To evaluate the binding efficiency of TLS2 recombinant mAbs against the antigen of interest, the purified chimeric antibodies were through various functional assays, such as Western Blot (see in Section 4.3.5), confocal analysis (see in Section 4.3.3), and flow cytometry (see in Section 4.3.4).

Western Blot was performed using Flp–In™–CHO wild type and CHO__TLS2–IRES–EGFP/AP2 stable lines cell lysates, obtained using RIPA Lysis and Extraction Buffer, and TLS2Loop–6His recombinant fragment. For the immunostaining, purified TLS2 chimeric mAbs diluted in 1% Skim Milk in 1× TBS–T to a final concentration of 20µg/mL were used as primary antibody, and a Goat anti–Human IgG Fc–HRP conjugated antibody (*DIESSE – diagnostica senese*) diluted 1:5,000 in 1% Skim Milk in 1× TBS–T as secondary antibody. The detection step was carried out using Pierce™ ECL Western Blotting Substrate, and the images of PDVF membranes were obtained by ImageQuant LAS4000, in chemiluminescence condition for the mAbs or in fluorescence condition (Cy5) for the SeeBlue™ Plus2 Pre–stained Protein Standard acquisition.

In the confocal analysis, both CHO__TLS2–IRES–EGFP and CHO__TLS2–IRES–EGFP/AP2 stable lines, together with Flp–In™–CHO wild type as a negative control, were fixed with 4% PFA in 1× DPBS, permeabilized with Permeabilization Buffer (0,25% TritonX–100 in

1× DPBS) and incubated with Blocking Buffer (3% BSA + 0,05% TritonX-100 in 1× DPBS), as previously described. After these steps, the fixed and permeabilized cells were labelled with purified TLS2 chimeric mAbs diluted to a final concentration of 30µg/mL in Ab Dilution Buffer (1%BSA in 1× DPBS) and incubated for 1h at room temperature. Subsequently, the cells were washed 3 times with 500µL of 1× DPBS and incubated with Goat Anti-Human IgG Fc Cross-Adsorbed DyLight™ 650-conjugated antibody (*Invitrogen*, #SAS-10137) diluted 1:1,000 in Ab Dilution Buffer for 1h at room temperature. After this incubation, the protocol will continue as previously described with the nuclear counterstaining with Hoechst 33342, Trihydrochloride, Trihydrate and the mounting of the coverslips on the glass slides using ProLong™ Gold Antifade Mountant. The glass slides were acquired using Leica TCS SP5 Confocal Laser Scanning Microscope and Leica Application Suite Advanced Fluorescence – LAS AF, version 2.7.3-9723 software.

For the flow cytometric test, the recombinant mAbs binding activity was evaluated against the conformationally folded antigen presented by both CHO_TLS2-IRES-EGFP and CHO_TLS2-IRES-EGFP/AP2 stable lines, using Flp-In™-CHO wild type as a negative control, and by HEL 92.1.7 Cell Line (*ATCC*, #TIB-180), for which the expression of TLS2 genes was confirmed through mRNA level analysis. Different concentration of purified TLS2 chimeric mAbs ranging from 30 to 0,03µg/mL in 1× DPBS + 5% FBS were used as primary antibody, and a Goat Anti-Human IgG Fc Cross-Adsorbed DyLight™ 650-conjugated antibody (*Invitrogen*, #SAS-10137) diluted 1:200 in 1× DPBS + 5% FBS as secondary antibody. The fluorescence signal from the stained cells was acquired on the BD FACSCanto II, through BD FACSDiva™ Software.

5 Results

5.1 Generation of a poly-epitope antigen and a stable cell line to raise and screen antibody against TLS2

Several approaches were followed during the development of an experimental process for the production of TLS2-specific mAbs. The first one, illustrated in Figure 5.1, employs an immunization protocol with a recombinant poly-epitope containing the TLS2 extracellular loops intercalated by (G₄S)₃ linkers, to provide flexibility to the structure and facilitate its folding, fused to the human immunoglobulin constant region (HuIgFc) to promote its solubility (TLS2polyP-HuIgFc). This recombinant protein, deprived of the HuIgFc purification tag, was used for the titration of the antibodies generated in mice following immunization.

As screening method for the isolation of TLS2-specific conformational antibodies, this approach involves the creation of a stable cell line overexpressing the full-length TLS2 on its surface. In order to easily evaluate its expression and cellular localization through a fluorescence signal, TLS2 was fused to EGFP reporter protein (TLS2-EGFP).

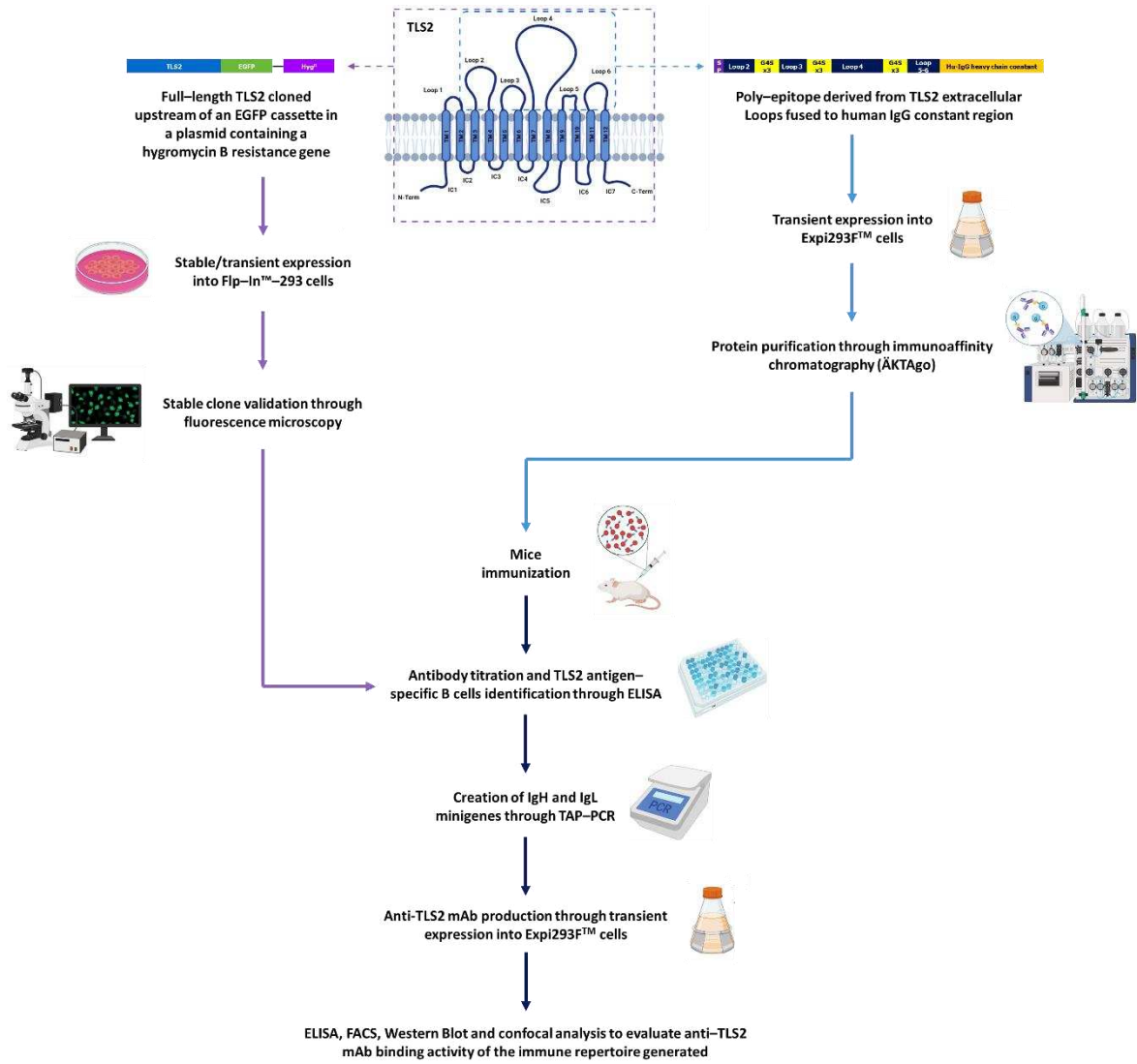


Figure 5.1: Schematic depiction of TLS2-EGFP and TLS2 poly-epitope strategy experimental workflow.

5.1.1 Design and production of TLS2polyP–HuIgFc plasmid

For the first immunization approach, TLS2polyP–HuIgFc synthetic plasmid (Figure 5.2) was designed and ordered to GeneArt Gene Synthesis service. It was generated using the pcDNA™ 3.4 TOPO™ backbone, a constitutive mammalian expression vector designed to achieve high levels of protein expression.

This synthetic plasmid contains the DNA sequence coding for a poly–epitope derived from the TLS2 extracellular loops intercalated by (G₄S)₃ linkers. The TLS2–encoding sequence was placed downstream of a signal peptide (SP), in order to induce the secretion of the recombinant protein in the culture medium, and fused with a HuIgFc–TAG, to facilitate its purification.

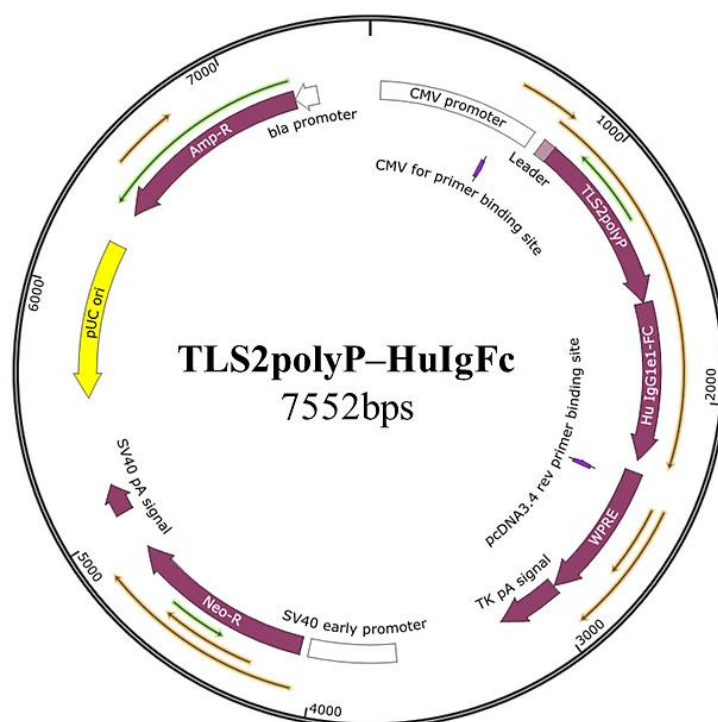


Figure 5.2: Schematic depiction of TLS2polyP–HuIgFc synthetic plasmid.

TLS2polyP–HuIgFc synthetic plasmid was introduced into DH5 α cells through heat–shock transformation. The transformed colonies were selected in LB+100 μ g/mL ampicillin plates and grown in LB+100 μ g/mL ampicillin medium. The amplified plasmid was purified from the culture using QIAprep Spin Miniprep Kit. Quantification of DNA and its purity were established by measuring the absorbance at 260 and 280nm with NanoVue™ 4282 V1.7 Spectrophotometer.

5.1.2 TLS2polyP–HuIgFc protein expression and purification

TLS2polyP–HuIgFc synthetic plasmid was transfected into Expi293F™ cells using ExpiFectamine™ 293 Transfection Kit for transient expression of the poly–epitope derived from the TLS2 extracellular loops fused to human IgG constant region. The HuIgFc–tagged protein present in the culture medium, recovered at 3– and 5–dpt, was purified by immunoaffinity chromatography, using HiTrap™ Protein G HP 1mL columns. Following the purification protocol designed (see in Section 3.2.3), the sample was loaded onto the column (previously equilibrated in Wash/Binding Buffer A) and washed to constant baseline, removing all proteins with non–specific interactions. Elution was performed using Elution Buffer B, resulting in a single peak containing the protein (Figure 5.3–A, red square). To prevent the acid environment from damaging the TLS2polyP–HuIgFc poly–epitope, each elution fraction was immediately adjusted to neutral pH with the addition of Equilibration Buffer C.

The elution peak fractions were analysed through SDS–PAGE and stained with SimplyBlue™ SafeStain (Figure 5.3–B), in order to verify the correct purification of TLS2polyP–HuIgFc protein.

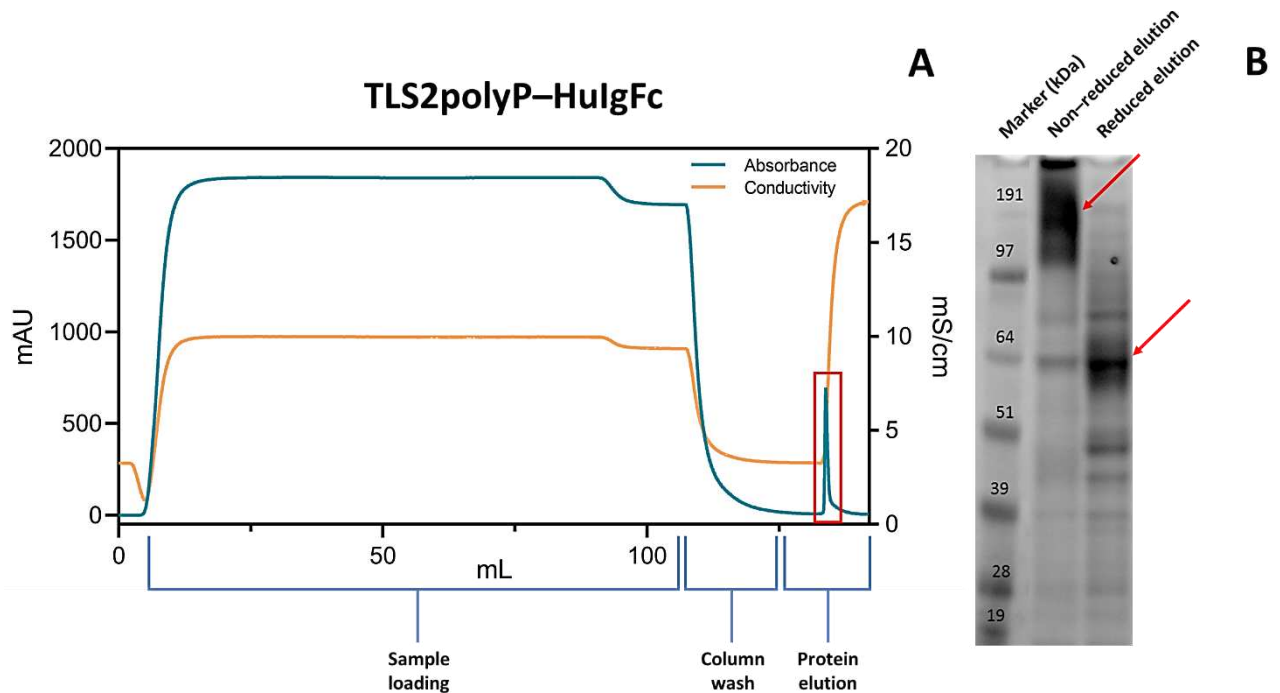


Figure 5.3: Elution profile of TLS2polyP-HuIgFc. The red square indicates the single elution peak containing the poly-epitope (A); Purification control of TLS2polyP-HuIgFc. The red arrows indicate the presence of the poly-epitope in multimeric forms in the non-reduced fraction and in monomeric form in the reduced fraction (with an expected molecular weight of approximately 63kDa) (B).

The red arrows in Figure 5.3–B indicate the presence of TLS2polyP-HuIgFc poly-epitope in multimeric forms in the non-reduced fraction and in monomeric form in the reduced fraction. It therefore appears that the purified recombinant protein, despite the HuIgFc-TAG fused at its C-terminus to increase its solubility, still tends to form aggregates.

Once verified through the SDS-PAGE the purity and the quality of the TLS2polyP-HuIgFc, the elution fraction containing the protein of interest was desalted in Desalting Buffer D using PD-10 Desalting Columns. Subsequently, the TLS2polyP-HuIgFc recombinant protein was quantified with Pierce™ BCA Protein Assay Kit and used as whole molecule as to prepare the antigen for mice immunization and to generate through enzymatic cleavage the TLS2polyP fragment deprived of the HuIgFc-TAG for the quantification of the antibody titer in the immunized animals.

5.1.3 HuIgFc–TAG removal and TLS2polyP purification

To remove the HuIgFc–TAG, TLS2polyP–HuIgFc poly–epitope was subjected to enzymatic digestion with IdeZ, an IgG–specific protease evolved by *Streptococcus equi* subspecies *zooepidemicus* as a defence mechanism to interfere with the immune response triggered by the host during infection, capable of recognizing and cleaving a unique site below the hinge region of the antibodies. After IdeZ and HuIgFc–TAG removal using respectively Dynabeads™ His–Tag and Pierce™ Protein G Magnetic Beads, the purity of the recovered TLS2polyP fragment was verified through SDS–PAGE and stained with SimplyBlue™ SafeStain. Figure 5.4 lane 4 shows that it was possible to recover the pure TLS2polyP fragment after enzymatic digestion.

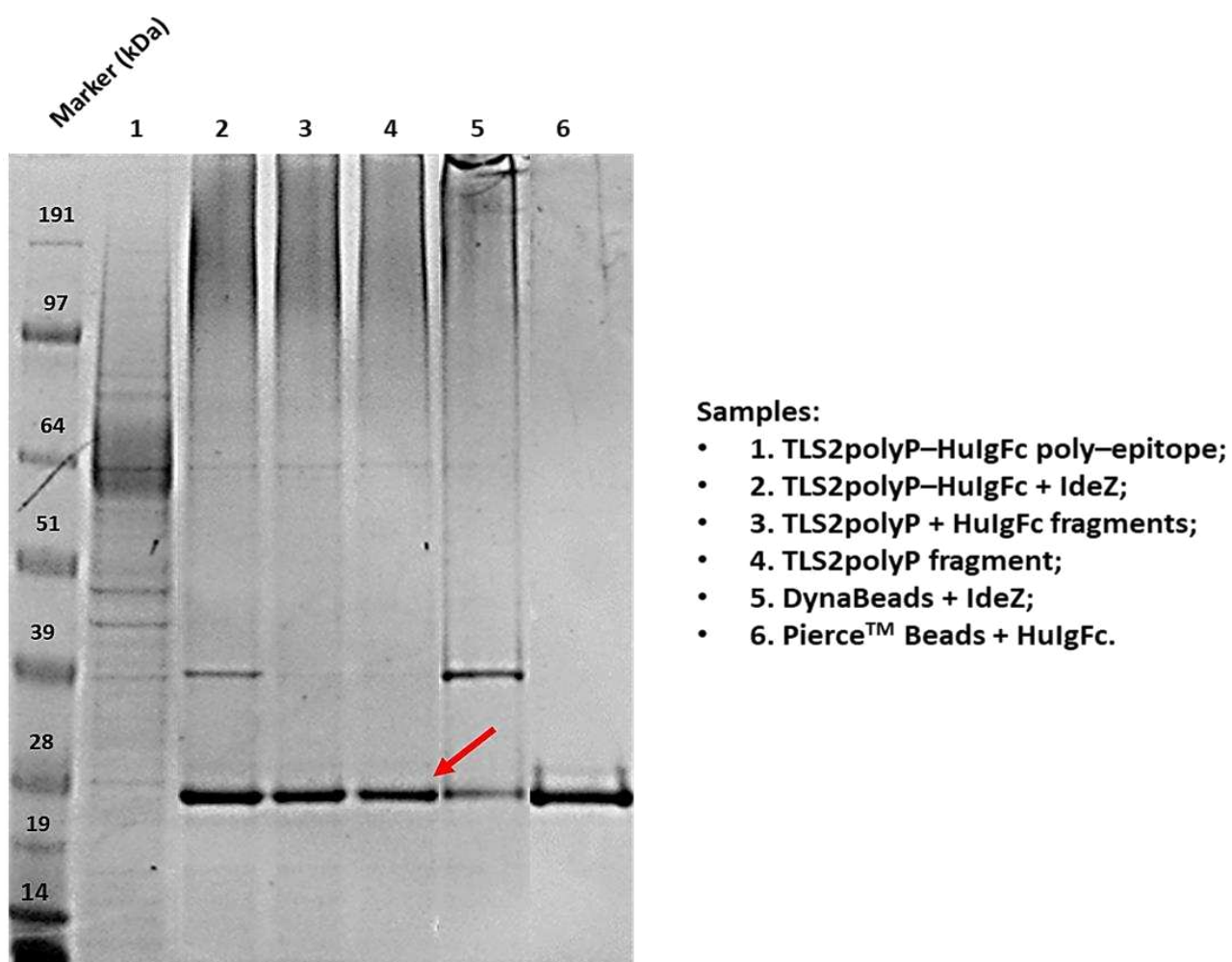


Figure 5.4: SDS–PAGE of TLS2polyP fragment after the removal of HuIgFc–TAG. The red arrow indicates the TLS2poly fragment (with an expected molecular weight of approximately 25kDa).

The protein fragment thus purified (Figure 5.4, red arrow) was coated onto SpectraPlate–384 High Binding plates, then used for the antibody titration through ELISA test of the serum samples recovered for mice immunized with the whole TLS2polyP–HuIgFc poly–epitope.

5.1.4 Design and production of pcDNA5_TLS2–EGFP recombinant plasmid

For the development of a screening system that allows to evaluate the generation of antibodies specifically recognizing TLS2 expressed on the cell surface in response to the immunization with TLS2polyP–HuIgFc poly–epitope, the full coding sequence for TLS2 (Figure 5.5–A) was designed and ordered to GeneArt Gene Synthesis service. It contains the DNA sequence coding the full–length TLS2 protein, which were inserted into pcDNA5–FRT–EGFP recombinant plasmid, already available in laboratory (Figure 5.5–B). The TLS2 insert was cloned upstream of an EGFP reporter cassette, in order to generate a fusion protein (TLS2–EGFP) that could be easily monitored through the emitted fluorescence signal. The expression vector contains also a Flp Recombination Target (FRT) site, which allows for its stable integration in Flp–In™–293 cells genome through Flp–In™ system (see in Section 5.1.5).

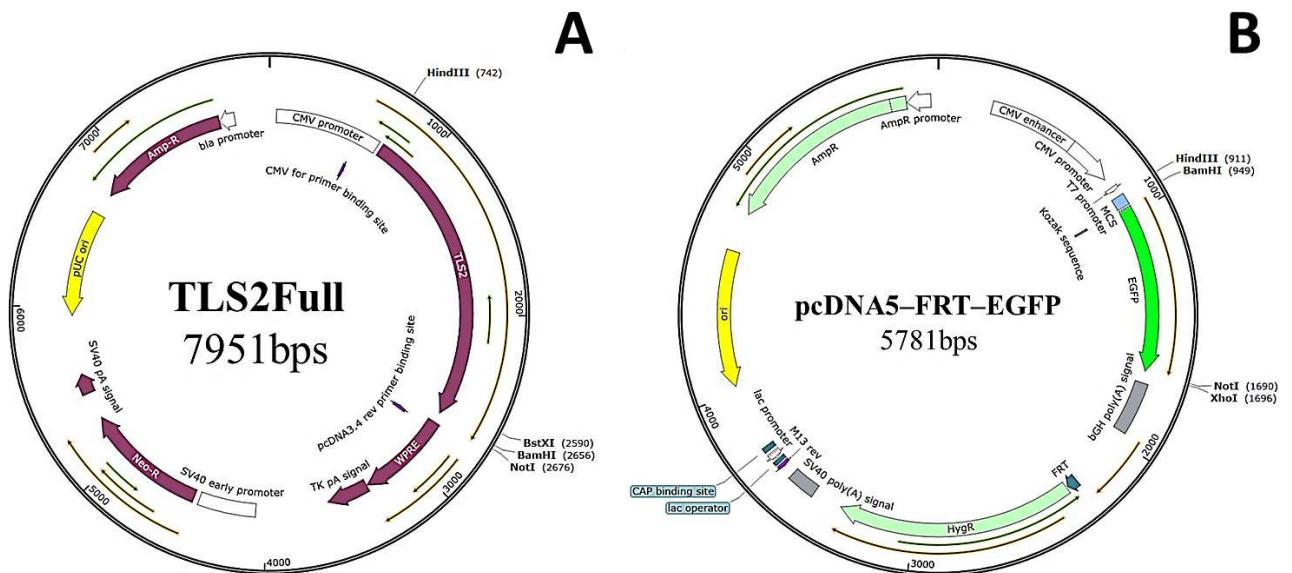


Figure 5.5: Schematic depiction of TLS2Full synthetic plasmid (A) and pcDNA5–FRT–EGFP recombinant plasmid (B).

The aim is therefore to generate a recombinant plasmid for the stable/transient expression of TLS2–EGFP fusion protein on the plasma membrane of Flp–In™–293 cells. To do this, pcDNA5–FRT–EGFP recombinant plasmid was amplified through PCR, using specific primers that allowed the correct cloning of the TLS2Full insert in frame with the EGFP cassette (Figure 5.6).

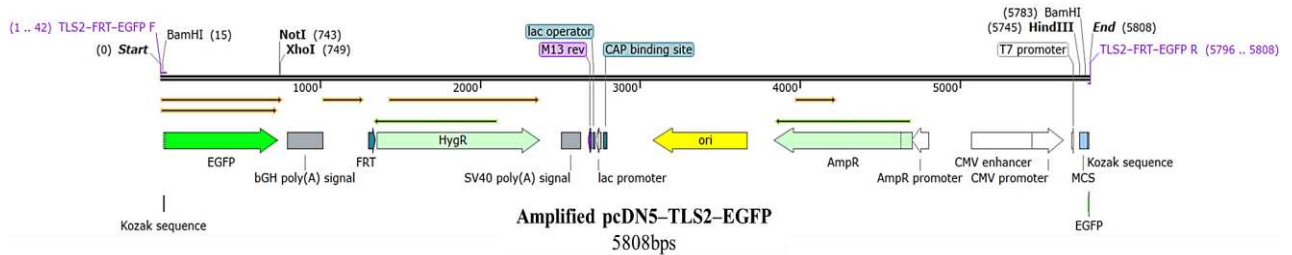


Figure 5.6: Schematic depiction of *pcDNA–FRT–EGFP* plasmid amplification product.

The quality of the amplified sequence was evaluated by electrophoretic run on agarose gel (see in Figure A–1), and the band corresponding to the vector of interest was purified through QIAquick Gel Extraction Kit.

At this point, a restriction enzyme digestion was performed to recover the TLS2–encoding insert from the synthetic plasmid TLS2Full, then cloned into the pcDNA5–FRT–EGFP vector via ligase reaction. The restriction enzymes used in this step were selected to insert the TLS2–encoding DNA sequence upstream of the EGFP cassette contained within the amplified vector, so as to express single fused protein (Figure 5.7).

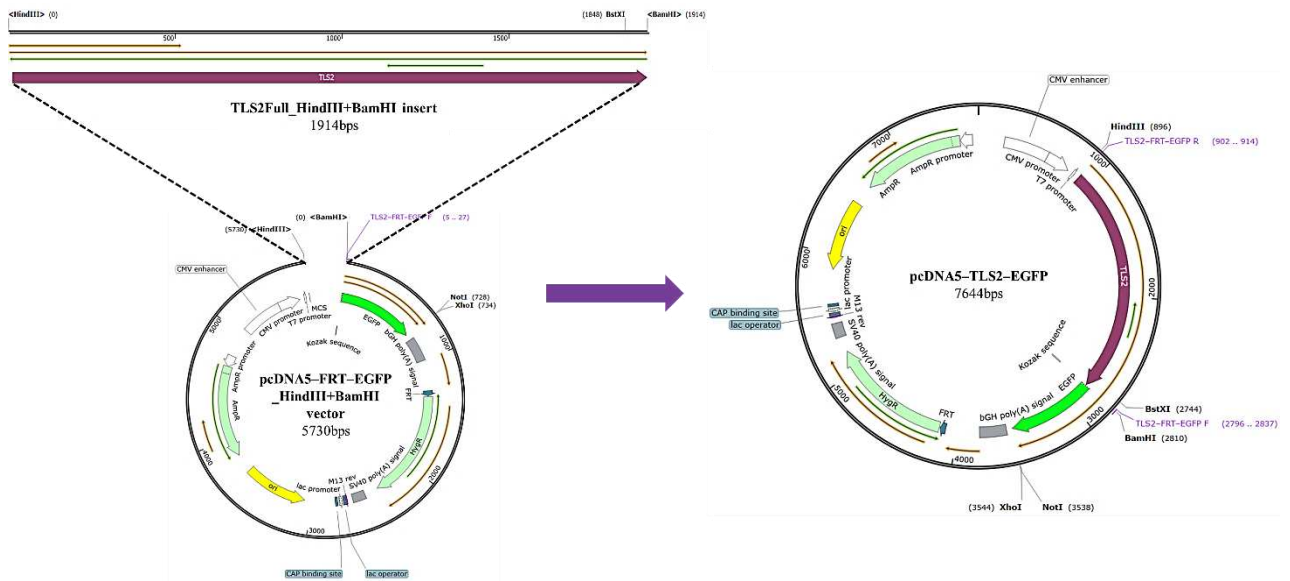


Figure 5.7: Schematic depiction of the ligation reaction between *TLS2Full_HindIII+BamHI* insert and *pcDNA5-FRT-EGFP_HindIII+BamHI* vector.

Both *TLS2Full* plasmid, previously expanded in *DH5α* cells through heat-shock transformation, and *pcDNA5-FRT-EGFP* amplified vector were subjected to digest reaction with *HindIII* and *BamHI* restriction enzymes. In order to prevent a possible recirculation of the vector during the ligation reaction, the 5'-ends of *pcDNA5-FRT-EGFP* vector were dephosphorylated with *FastAP* Thermosensitive Alkaline Phosphatase (see in Table A-1). The quality of the enzymatic digestions was confirmed by electrophoretic run on agarose gel (see in Figure A-2), and the bands with the correct dimensions were purified through *QIAquick* Gel Extraction Kit.

TLS2Full_HindIII+BamHI insert and dephosphorylated *pcDNA5-FRT-EGFP_HindIII+BamHI* vector thus obtained were used to set up two ligation reactions at different molar ratio insert:vector (2:1 and 5:1) to generate *pcDNA5_TLS2-EGFP* recombinant plasmid.

The different ligation products were then used for the heat-shock transformation of *DH5α* cells. Some of the bacterial colonies that grew in the *LB+100μg/mL* ampicillin plates, selective for the transformed cells containing the resistance cassette of the *pcDNA5-FRT-EGFP* vector, were spotted and then screened through colony PCR. The primers used in this step were selected to evaluate the actual presence of *TLS2Full* within the recombinant plasmid, thus avoiding the recovery of any recircularized *pcDNA5-EGFP* vectors without the insert of interest. It was possible to identify several colonies presenting the recombinant

plasmid which contains the TLS2Full insert (see in Figure A-3), from both the ligase reactions used for DH5 α cells transformation. Colonies that tested positive at screening were then amplified in LB+100 μ g/mL ampicillin medium, and the pcDNA5_TLS2-EGFP recombinant plasmid was purified using QIAprep Spin Miniprep Kit. Quantification of DNA and its purity were established by measuring the absorbance at 260 and 280nm with NanoVue™ 4282 V1.7 Spectrophotometer.

5.1.5 Generation and validation of a cell line stably expressing TLS2-EGFP

The pcDNA5_TLS2-EGFP plasmid, previously made, was used for the generation of a stable cell line overexpressing the TLS2-EGFP fusion protein.

To do this, pcDNA5_TLS2-EGFP was transfected into Flp-In™-293 cells using Lipofectamine™ 2000 Transfection Reagent and exploiting the Flp-In™ system, which allow the integration of the DNA sequence of interest in a specific genomic location involving the Flp recombinase expressed by the poG44 plasmid and the Flp Recombination Target (FRT) site present in both mammalian cells genome and expression vector [172]. Through the homologous recombination process the hygromycin resistance cassette of the expression vector is inserted in frames with the SV40 promoter and the ATG start codon, already present in the host cell line for the regulation of the lacZ-Zeo reporter gene, allowing the isolation of clones expressing TLS2-EGFP using a selective medium containing hygromycin (Figure 5.8). The selection process of single antibiotic-resistant colonies was monitored under fluorescence microscope, in order to directly compare the signal emitted by EGFP with the expression of full-length TLS2 amino acid transporter.

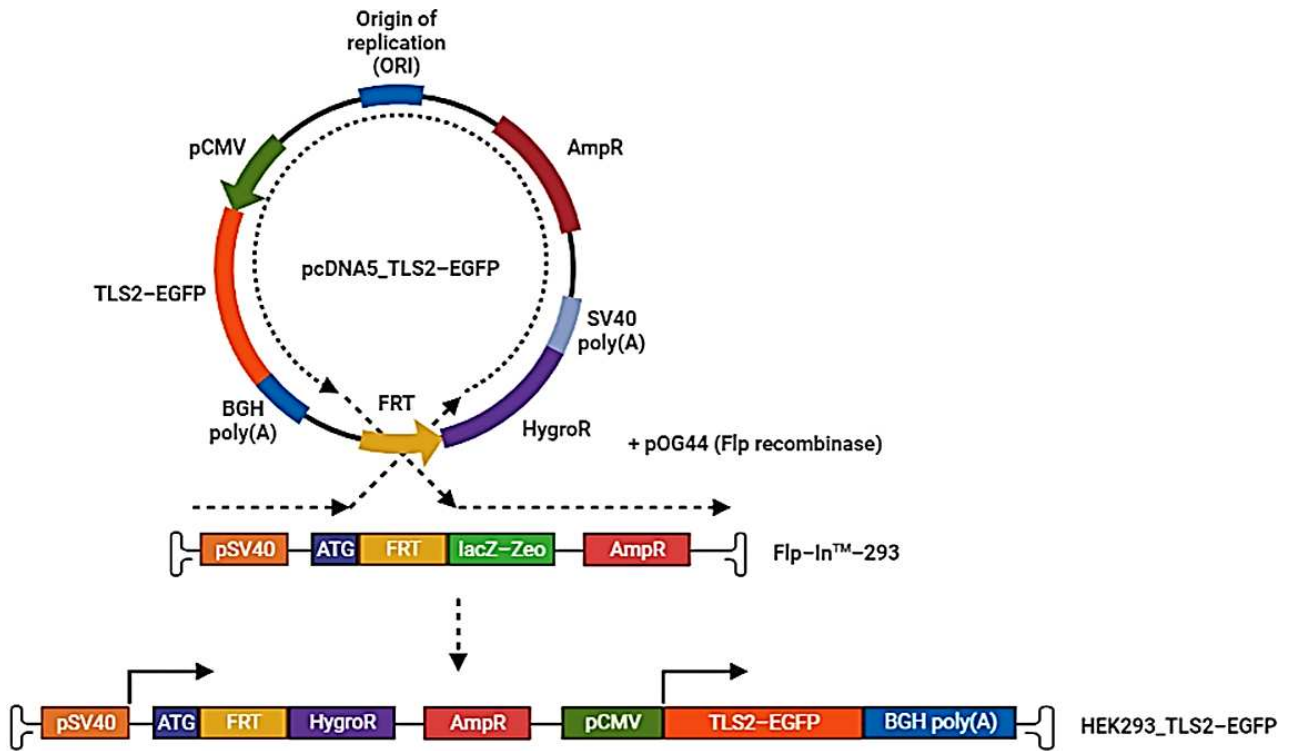


Figure 5.8: Schematic depiction of FRT recombination between Flp-In™-293 genome and pcDNA5_TLS2-EGFP recombinant plasmid and generation of HEK293_TLS2-EGFP stable line.

To validate the association of the TLS2 protein with the plasma membrane, EGFP-fluorescent and hygromycin-resistant HEK293 stable clones were analysed by confocal microscopy, using Concanavalin A-Tetramethylrhodamine conjugate (Con A-TRITC) as cell surface marker. In Figure 5.9 is possible to appreciate colocalization of the EGFP and TRITC signals indicating the association of TLS2-EGFP with the plasma membrane.

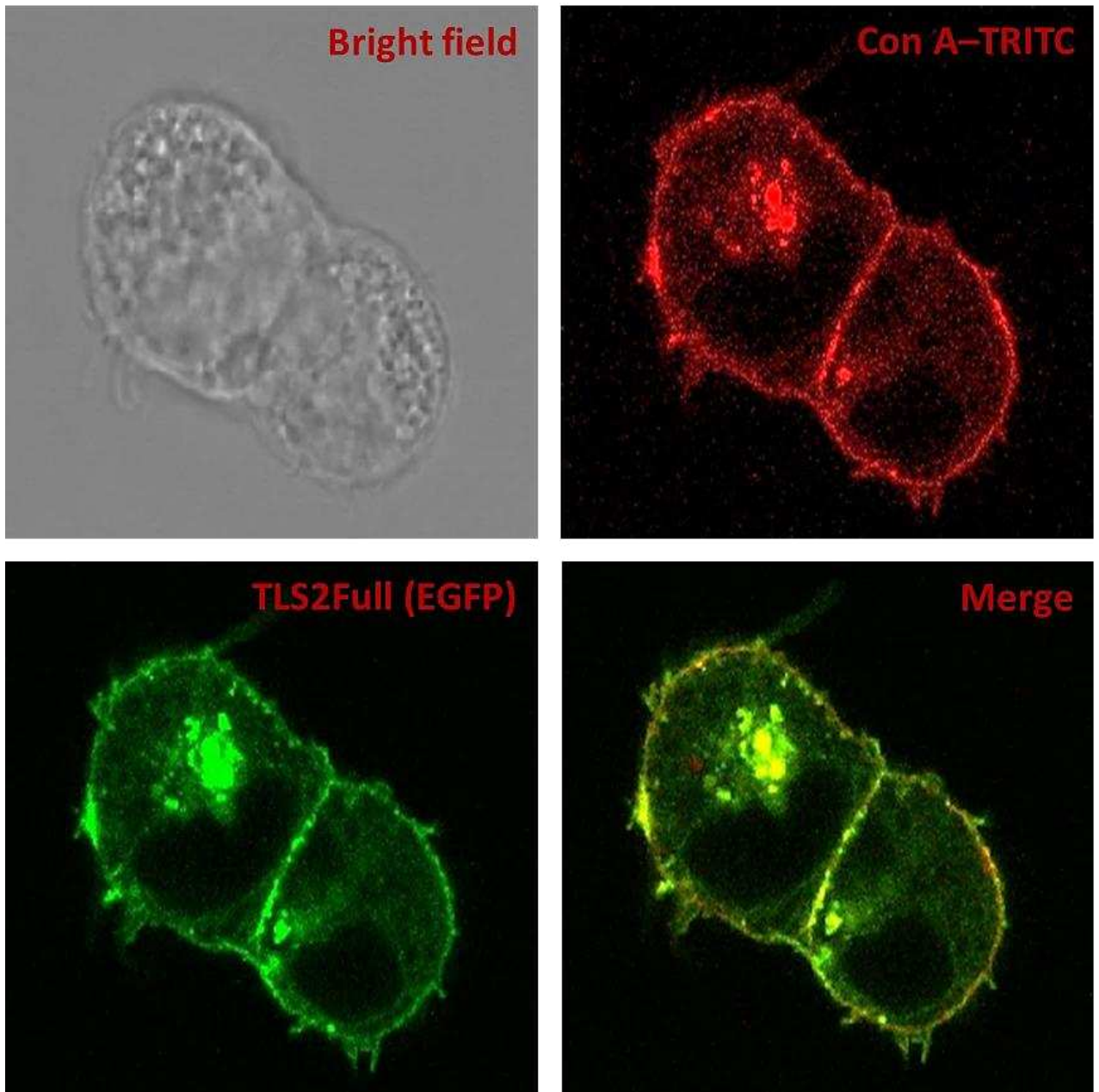


Figure 5.9: The TLS2-EGFP associate with the cell membrane in HEK293 stable line. The association was visualized by the colocalization of the EGFP fluorescence with a plasma membrane marker labelled with TRITC in confocal microscopy.

5.1.6 Mice immunization and antibody titer evaluation

For the development of a murine TLS2-specific antibody repertoire, 5 Female BALB/c mice 4 weeks old were immunized with 20 μ g purified TLS2polyP-HuIgFc poly-epitope every 14 days for 3 times, as shown in the following timeline (Figure 5.10).

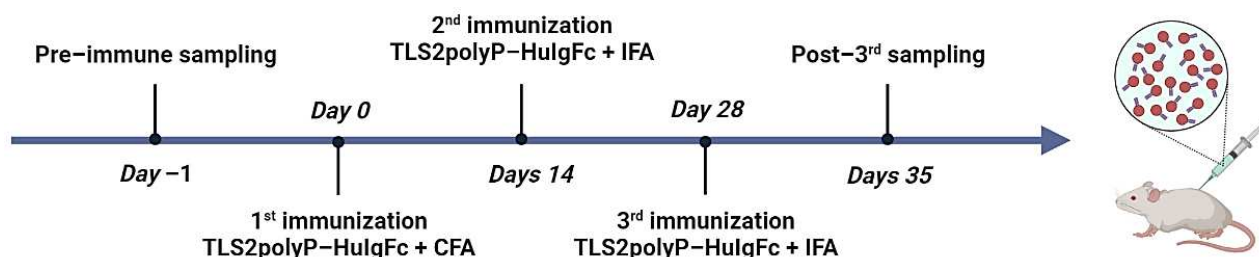


Figure 5.10: Immunization and sampling timeline for TLS2polyP-HuIgFc.

In order to evaluate the specific immune response developed following immunization with TLS2polyP-HuIgFc, the sera recovered one week after the 3rd dose were used in an ELISA assay, using SpectraPlate-384 High Binding plates coated with the TLS2polyP fragment to assess the abundance of only the TLS2-specific antibodies. The pre-immune serum recovered the day before of the immunization protocol starting was used as a negative control (Figure 5.11).

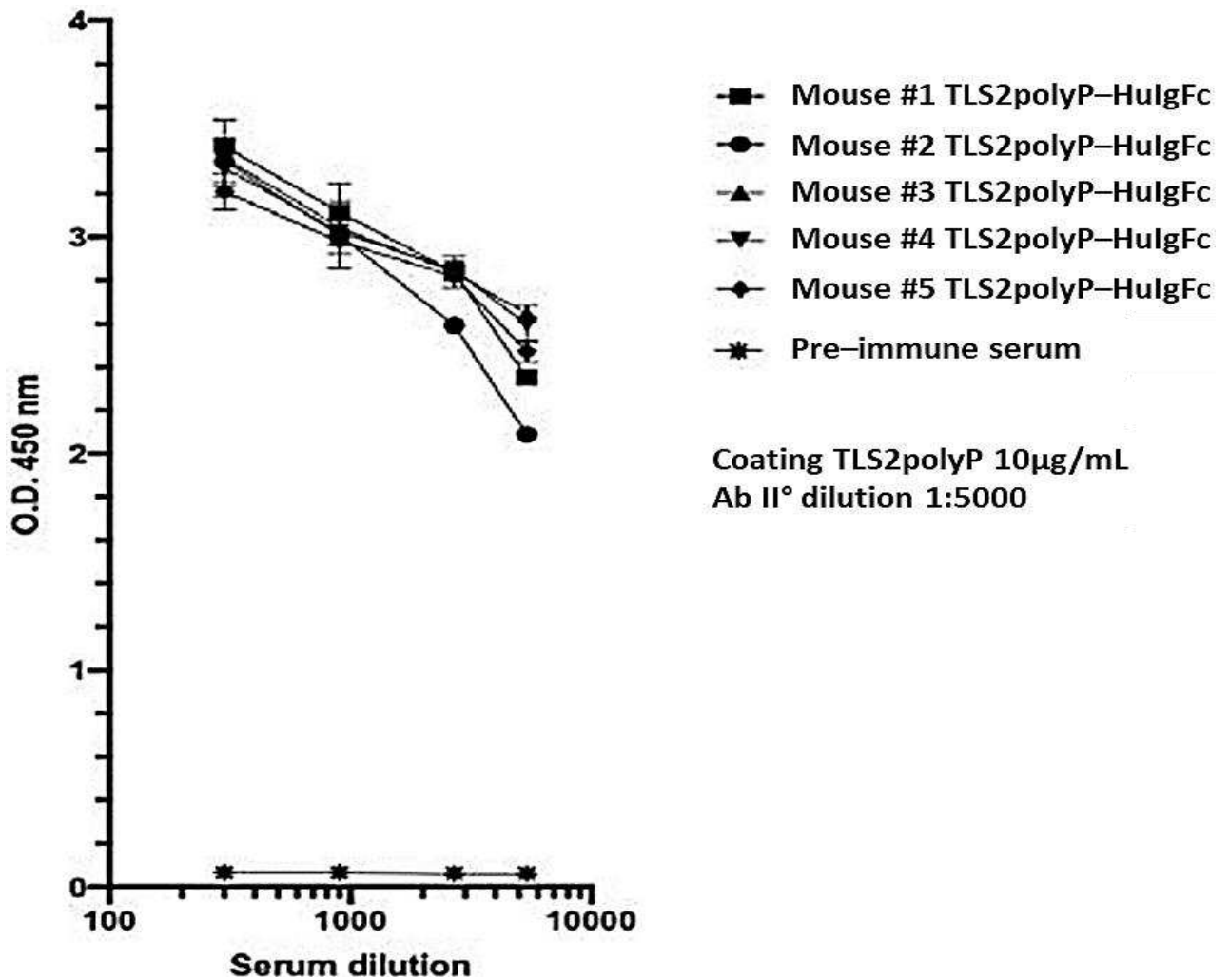


Figure 5.11: Immunization of mice with TLS2polyP–HuIgFc poly–epitope induced a good antibody titer against the TLS2polyP fragment. The antigen–specific antibodies were revealed in an ELISA assay.

As can be seen from Figure 5.11, all mice immunized with TLS2polyP–HuIgFc poly–epitope developed a good antibody titer, with absorbance value that remained high for a good range of dilutions examined.

A flow cytometry assay was used to assess whether the antibodies developed following the immunization with TLS2polyP–HuIgFc show also specificity towards TLS2–epitopes exposed on cell surface. For this assay, it was decided to use Flp–In™–293 cells transiently transfected with the recombinant pcDNA5_TLS2–EGFP plasmid, in order to evaluate a possible cross–reactivity against wild–type cells in a mixed population. The expression of the full–length TLS2 protein was evaluated through the fluorescence signal emitted by the EGFP fused at its C–terminus, while the presence of anti–TLS2 antibodies was detected using a Goat Anti–Mouse IgG (H+L) DyLight™ 650–conjugated antibody (Figure 5.12).

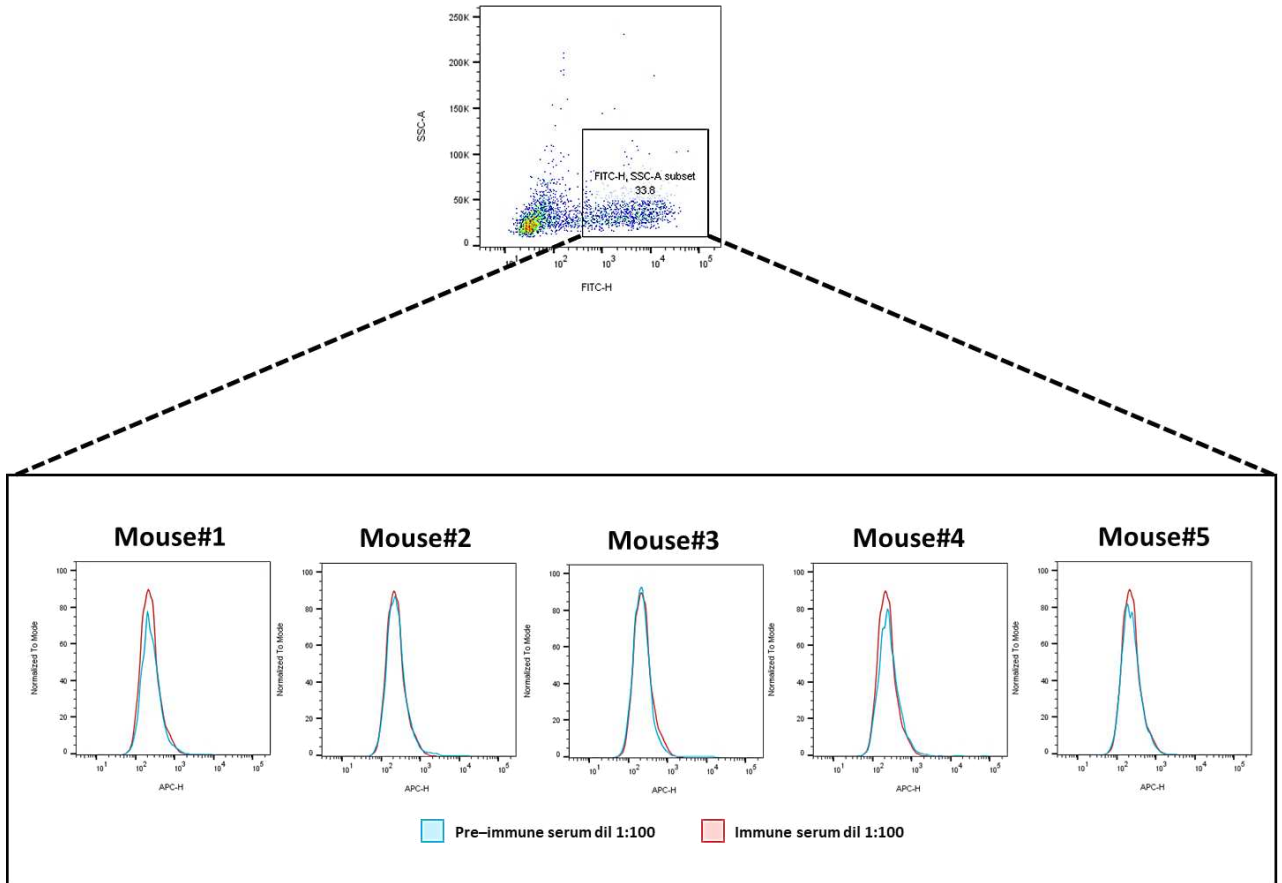


Figure 5.12: Flow cytometry recognition of the full-length TLS2 protein transiently expressed in HEK293 cells with individual mouse serum of mice immunized with TLS2polyP–HuIgFc poly–epitope.

Surprisingly, the data shown in Figure 5.12 indicate that the sera of mice immunized with TLS2polyP–HuIgFc poly–epitope are unable to recognize the population of HEK293 cells expressing the recombinant TLS2–EGFP fusion protein.

To assess whether these results were due to an alteration in the correct exposure of the protein on the plasma membrane, the experiment was repeated with the addition of TritonX–100 to permeabilize the HEK293 cells transiently expressing TLS2–EGFP (Figure 5.13).

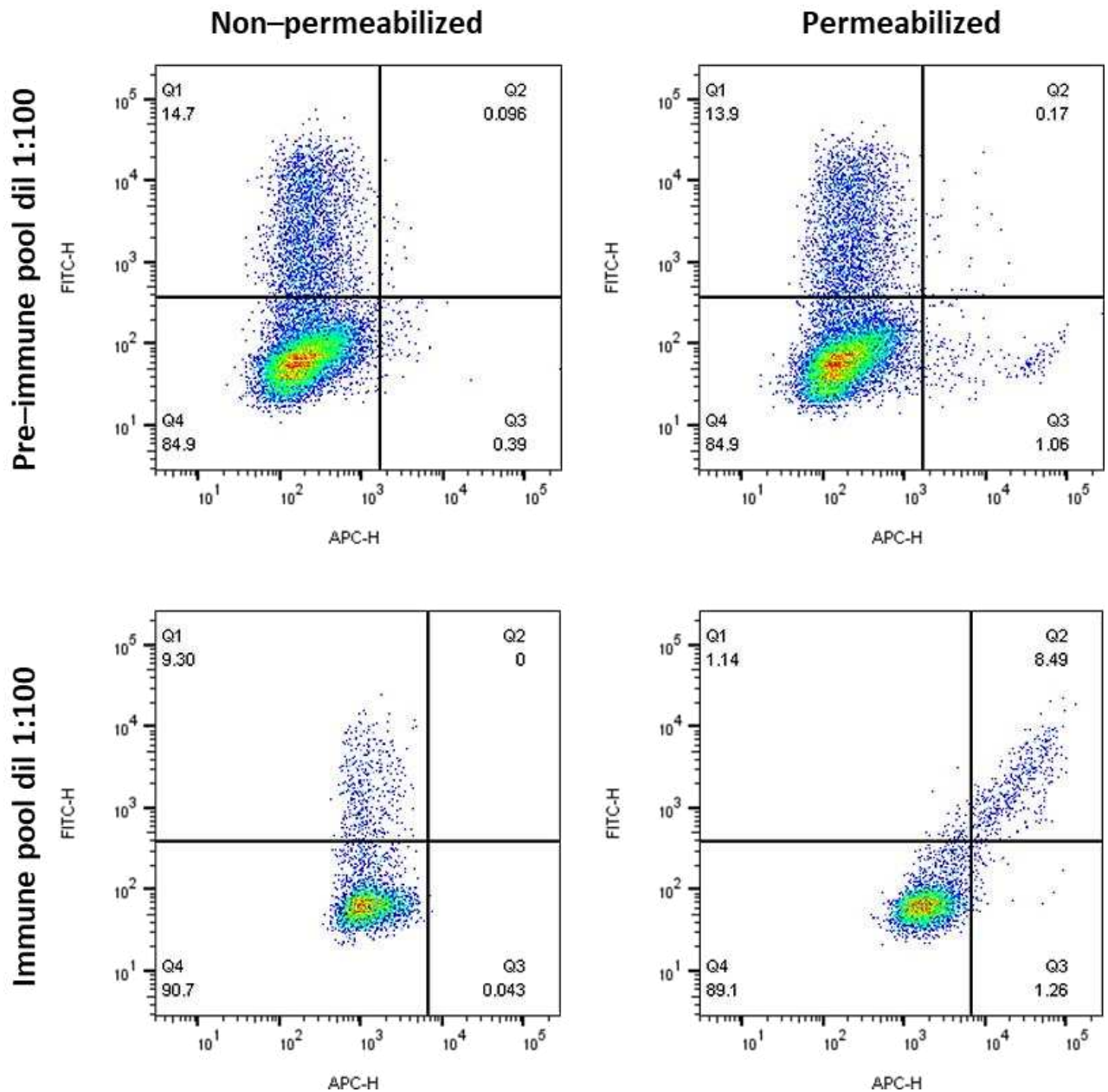


Figure 5.13: Evaluation of the correct exposure of full-length TLS2 protein through flow cytometry test.

As can be seen from Figure 5.13, the sera of mice immunized with TLS2polyP-HuIgFc poly-epitope are able to recognize the transiently expressed full-length TLS2 protein in HEK293 cells only after cell permeabilization. This therefore demonstrates that the protein expressed by the recombinant plasmid, although it can be transported on the plasma membrane, does not expose its predicted extracellular loops on the cell surface, thus invalidating the use of the stable cell line as a screening system for conformational antibodies specifically recognizing the extracellular domains of TLS2.

5.1.7 Open questions and mitigation approaches

The results obtained in the first part of the project asked for a reconsideration of the approach undertaken so far. First, it was tried to understand how to improve the immunization step, since the previously used TLS2polyP–HuIgFc poly–epitope may not be able to induce adequate TLS2–specific conformational antibody titer due to its predisposition to form multimeric aggregates that were observed during TLS2polyP–HuIgFc poly–epitope purification.

This problem has been handled by developing two different correction approaches, which provide (1) for a simplification of the poly–epitope excessive complexity (2) for a more natural representation of the TLS2 extracellular epitopes correctly folded. For the first issue it was decided to produce a shorter fragment of TLS2 in the attempt to reduce the protein complexity, reducing it to the largest extracellular domain (Loop4). Although the recombinant fragment thus generated does not consider potential epitopes present on the other extracellular loops and does not ensure a representative conformation of the full–length TLS2 protein, it still provides a simplified approach, with a more convincing native structure than the TLS2polyP–HuIgFc poly–epitope. Thus, the larger extracellular loop of TLS2 was chosen for the production of a simpler recombinant protein maximizing the probability to find a conformational epitope while reducing the complexity (Figure 5.14).

For the second issue, to mitigate the hazard that the immune response induced using recombinant polypeptides is not appropriate to generate conformational antibodies against structurally–complex antigens, it was decided to add an immunization protocol with ‘native’ TLS2 complexes derived from a cell line stably overexpressing TLS2. This approach has the disadvantage, compared to the use of purified recombinant proteins, to induce an immune response against a plethora of other unwanted cell proteins. However, it provides a more accurate representation of the correctly folded protein of interest. A second important point, was to correct the altered exposure of the TLS2 protein on the cell membrane of the stable cell line to be used in the immunization step and for the characterization of the antibodies developed following immunization. A possible explanation for this problem is that the EGFP reporter protein fused at the TLS2 C–terminus could hamper the correct folding and/or the cellular localization of the amino acid transporter. Based on this hypothesis, it was decided to generate a recombinant plasmid in which TLS2 and EGFP coding sequences are separated by an Internal Ribosome Entry Site (IRES), which allow their expression as separate proteins

from the same mRNA. In this way it would still be possible to evaluate the expression of the TLS2 protein, through the signal emitted by the fluorescent reporter, without altering its natural sequence. Another factor possibly causing the abnormal presentation of TLS2 could be the necessity of specific proteins responsible for its correct localization and function. Through research on the literature available for this amino acid transporter, it emerged that there are two alternative transmembrane glycoproteins, AP1 and AP2, fundamental for TLS2 trafficking and catalytic activation. To explore this possibility, it was decided to generate a stable cell line expressing both the TLS2–IRES–EGFP construct and one of the auxiliary proteins. Although both AP1 and AP2 proteins have the same chaperone function, AP1 has a particularly bulky extracellular domain, which could create an inconvenient space footprint for TLS2 antibody recognition. For this reason, it was decided to use the AP2 auxiliary protein, which has a shorter extracellular domain with less chance of hiding the amino acid transporter and therefore of biasing the binding efficiency of TLS2–specific antibodies.

5.2 Revised approach to generate monoclonal antibodies recognizing conformational extracellular epitopes of TLS2

This second approach, illustrated in Figure 5.14, employs two immunization protocols: the first with a recombinant TLS2Loop4 recombinant fragment to maximize the probability to find a conformational epitope while reducing the complexity, and second with a cell line stably overexpressing TLS2 in a native as possible 3D structure.

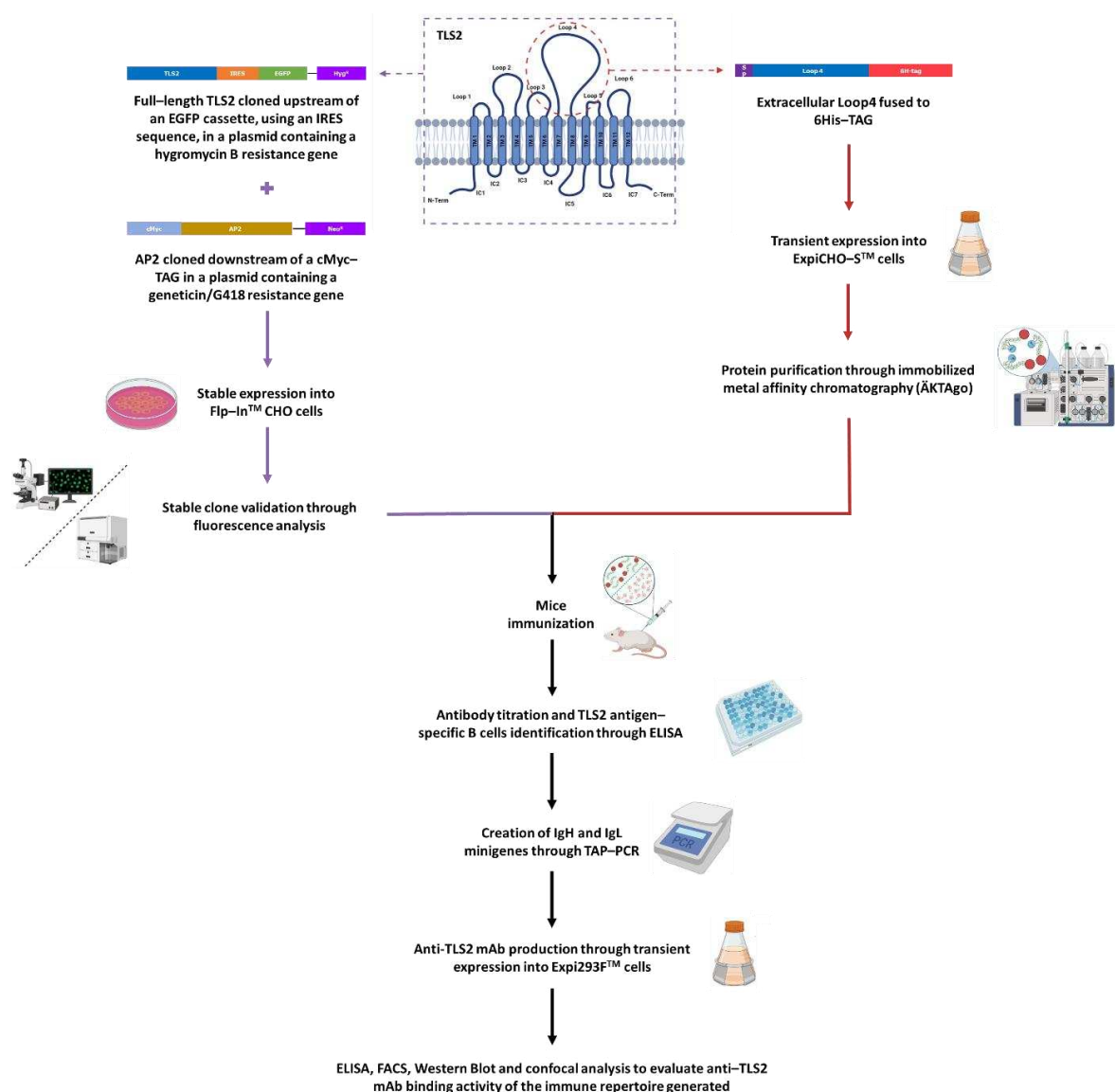


Figure 5.14: Schematic depiction of TLS2-IRES-EGFP+AP2 and TLS2Loop4 recombinant fragment strategy experimental workflow.

5.2.1 Design and production of pcDNA3.4_TLS2Loop4-6His recombinant plasmid

For the immunization approach with recombinant protein fragment, synthetic TLS2Loop4 DNA string and pcDNA3.4-6His plasmid were designed and ordered to GeneArt Gene Synthesis service. The aim was to generate a recombinant plasmid for the transient production of TLS2Loop4-6His protein in ExpiCHO-S™ cells.

The synthetic DNA string contains the coding sequence for a recombinant fragment derived from the TLS2 largest Loop4, was placed downstream of a SP to induce its secretion in the culture medium (Figure 5.15-A). The TLS2-Loop4-encoding sequence was recovered from the DNA string and cloned into pcDNA3.4-6His synthetic plasmid (Figure 5.15-B), upstream of a 6His-TAG to facilitate its purification and increase its solubility.

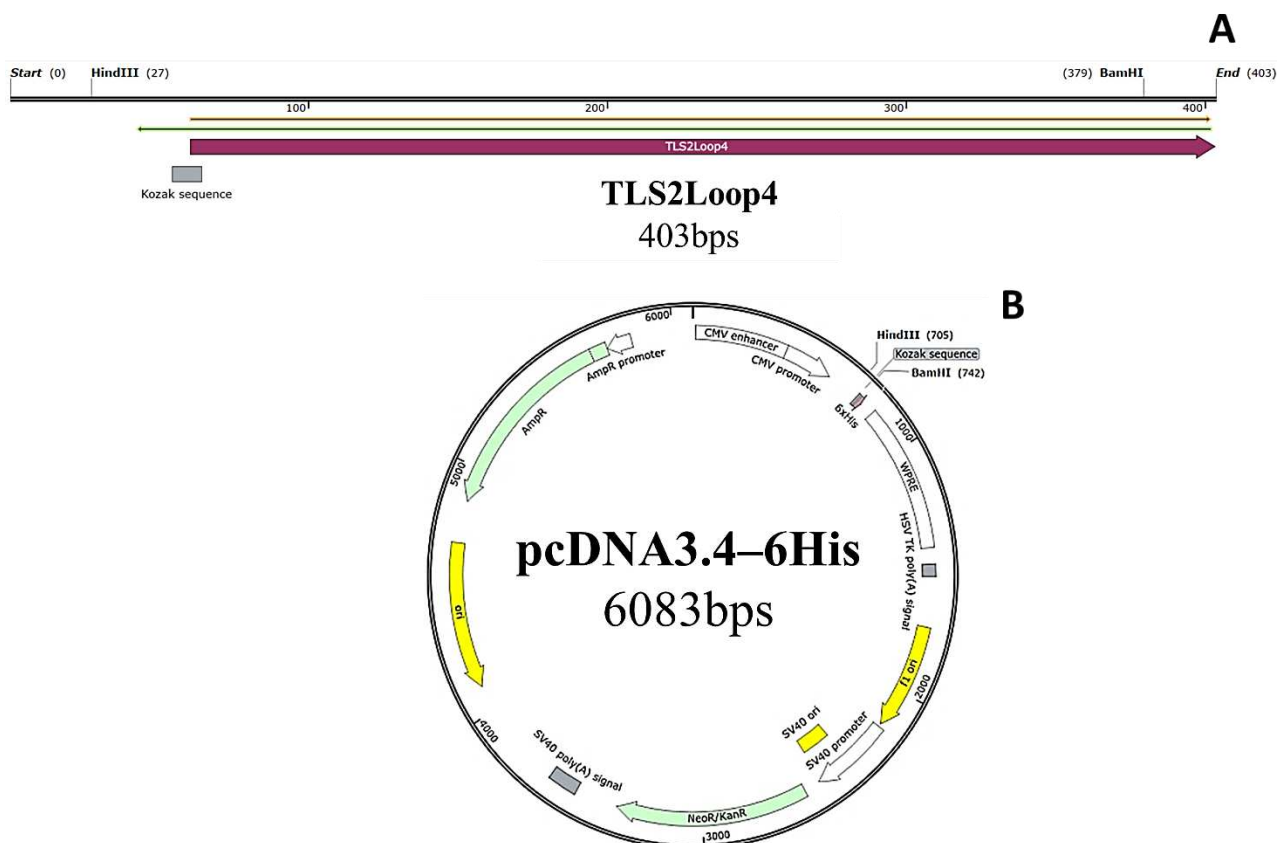


Figure 5.15: Schematic depiction of synthetic TLS2Loop4 DNA string (A) and pcDNA3.4-6His plasmid (B).

To do this, TLS2Loop4 synthetic DNA string was amplified through PCR, using specific primers which allow the introduction of cutting sites for its correct cloning within the corresponding expression vector. The quality of the amplified sequence was evaluated by

electrophoretic run on agarose gel and the band related to the PCR products of interest (see in Figure B–1) was purified through QIAquick Gel Extraction Kit.

Subsequently, the TLS2Loop4–encoding sequence was extracted through restriction enzyme digestion approach and inserted into the pcDNA3.4–6His vector via ligase reaction (Figure 5.16).

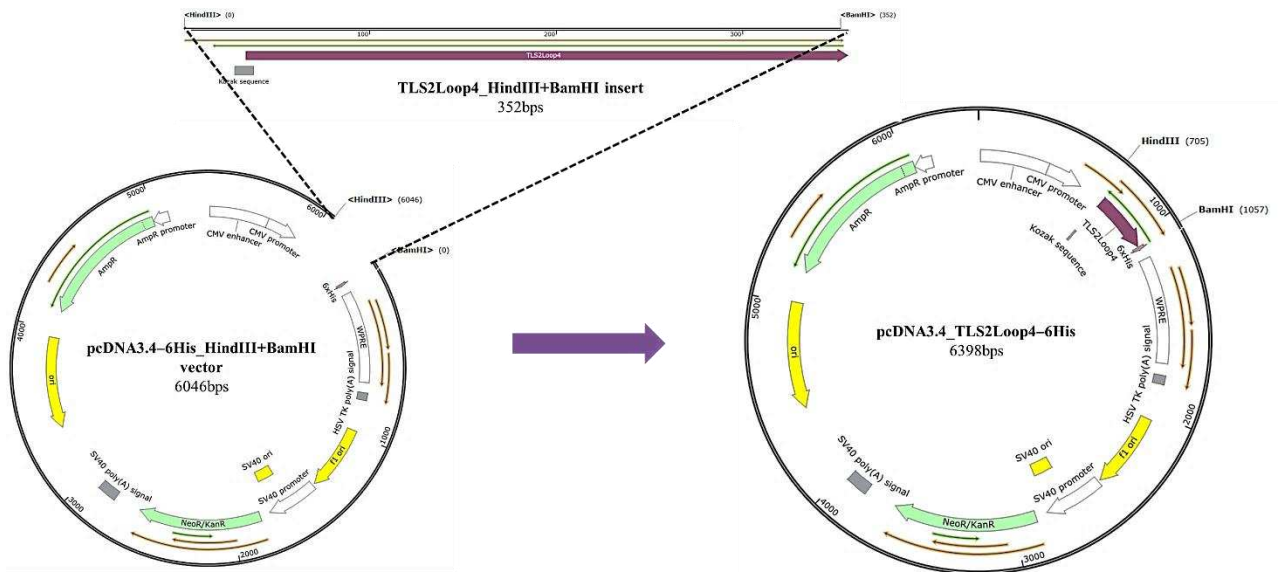


Figure 5.16: Schematic depiction of the ligase reaction between *TLS2Loop4_HindIII+BamHI* insert and *pcDNA3.4-6His_HindIII+BamHI* vector.

Both amplified TLS2Loop4 insert and pcDNA3.4–6His synthetic plasmid, previously expanded in DH5 α cells through heat–shock transformation, were subjected to digest reaction with HindIII and BamHI restriction enzymes. In order to prevent a possible recirculation of the vector during the ligase reaction, the 5’–ends of pcDNA3.4–6His were dephosphorylated with FastAP Thermosensitive Alkaline Phosphatase (see in Table B–1). The quality of the enzymatic digestions was confirmed by electrophoretic run on agarose gel (see in Figure B–2), and the bands with the correct dimensions were purified through QIAquick Gel Extraction Kit.

TLS2Loop4_HindIII+BamHI insert and dephosphorylated pcDNA3.4–6His_HindIII+BamHI vector thus obtained were used to set up a ligase reaction with an insert:vector ratio set to 5:1 to generate pcDNA3.4_TLS2Loop4–6His recombinant plasmid. The ligase reaction was used for the transformation of DH5 α cells through heat–shock transformation. Some of the bacterial colonies that grew in the LB+100 μ g/mL ampicillin

plates, selective for the transformed cells containing the resistance cassette of the pcDNA3.4–6His vector, were spotted and screened through colony PCR. The primers used in this step were selected to evaluate the actual presence of TLS2Loop4 within the recombinant plasmid, thus avoiding the recovery of any recircularized pcDNA3.4–6His vectors without the insert of interest. It was possible to identify several colonies presenting the recombinant plasmid which contains the TLS2Loop4 insert (see in Figure B–3). Colonies that tested positive at screening were then amplified in LB+100µg/mL ampicillin medium, and the pcDNA3.4_TLS2Loop4–6His recombinant plasmid was purified using QIAprep Spin Miniprep Kit.

5.2.2 TLS2Loop4–6His protein expression and purification

The pcDNA3.4_TLS2Loop4–6His plasmid, previously made, was transfected into ExpiCHO–S™ cells using ExpiFectamine™ CHO Transfection Kit for transient expression of the recombinant fragment derived from TLS2 extracellular Loop 4 fused to 6His–TAG. The 6His–tagged protein present in the culture medium recovered at 10–dpt was purified by IMAC, using HisTrap™ FF 1mL columns.

Following the purification protocol designed (see in Section 3.2.5), the sample was loaded onto the column (previously equilibrated in Wash/Binding Buffer A) and washed to constant baseline, removing all proteins with non–specific interactions. Elution was performed using Elution Buffer B, resulting in a single peak containing the protein (Figure 5.17–A, red square).

The elution peak fractions were analysed through SDS–PAGE and stained with SimplyBlue™ SafeStain (Figure 5.17–B), in order to verify the correct purification of TLS2Loop4–6His recombinant fragment.

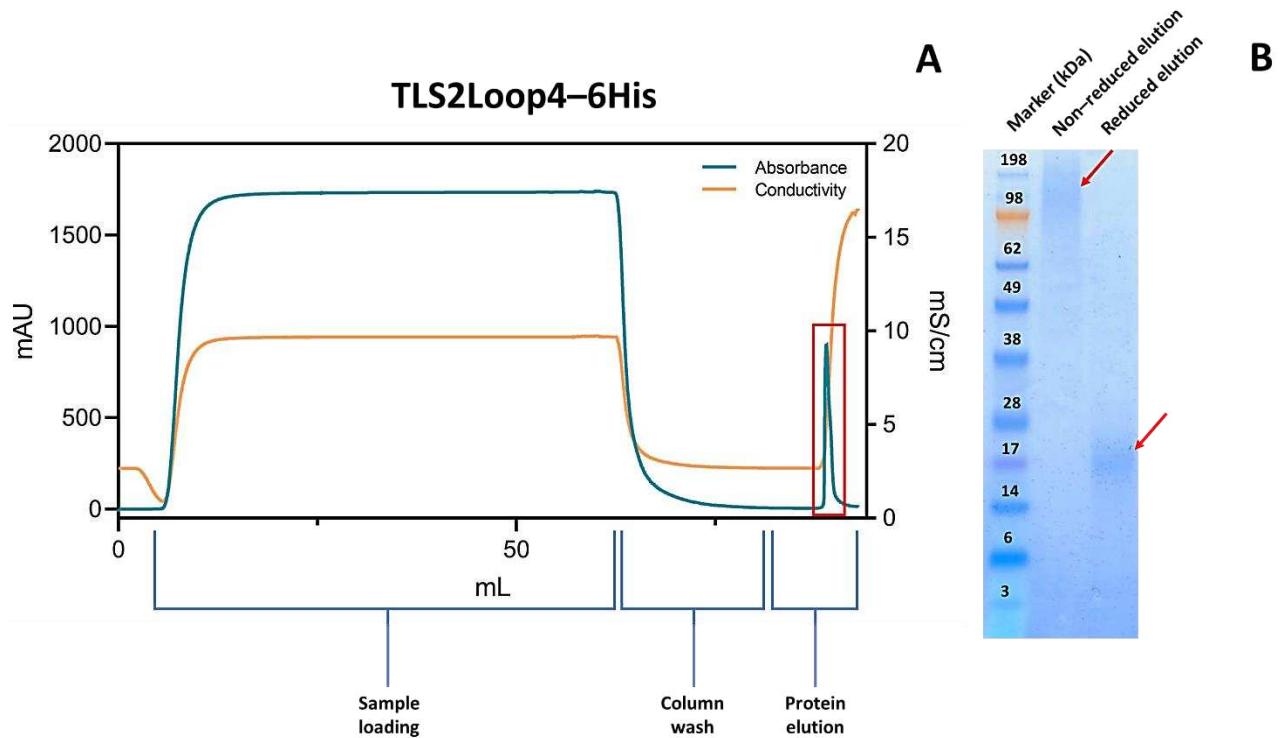


Figure 5.17: Elution profile of TLS2Loop4-6His. The red square indicates the single elution peak containing the recombinant fragment (A); Purification control of TLS2Loop4-6His. The red arrows indicate the presence of the recombinant fragment in multimeric forms in the non-reduced fraction and in monomeric form in the reduced fraction (with an expected molecular weight of approximately 18kDa) (B).

The red arrows in Figure 5.17-B indicate the presence of TLS2Loop4-6His fragment in multimeric forms in the non-reduced fraction or in monomeric form in the reduced fraction. Just as previously observed for TLS2polyP-HuIgFc poly-epitope, despite the presence of the 6His-TAG fused to its C-terminus, the recombinant protein still tends to form aggregates. Once verified through the SDS-PAGE the purity and the quality of the TLS2Loop4-6His, the elution fraction containing the protein of interest was desalted in Desalting Buffer C using PD-10 Desalting Columns. Subsequently, the TLS2Loop4-6His fragment was quantified with Pierce™ BCA Protein Assay Kit and used both to prepare the antigen for mice immunization protocol and as the coating of SpectraPlate-384 High Binding plates for the quantification of the antibody response in the immunized animals.

5.2.3 Design and production of a recombinant plasmid allowing the separate expression of TLS2 and EGFP from the same transcript (pcDNA5_TLS2-IRES-EGFP)

For the immunization approach with stable TLS2-overexpressing cell line, it was needed to generate a plasmid that allows the separated expression of TLS2 from EGFP reporter protein. The pAAV.CMV.Luc.IRES.EGFP.SV40 synthetic plasmid, designed and ordered to GeneArt Gene Synthesis service, contains an IRES sequence placed upstream of an EGFP cassette, which were cloned downstream of the TLS2-encoding DNA into pcDNA5_TLS2-EGFP recombinant plasmid (Figure 5.18). In this way, it was generated a construct in which the TLS2 and EGFP-encoding sequences were separated but kept under the control of the same promoter.

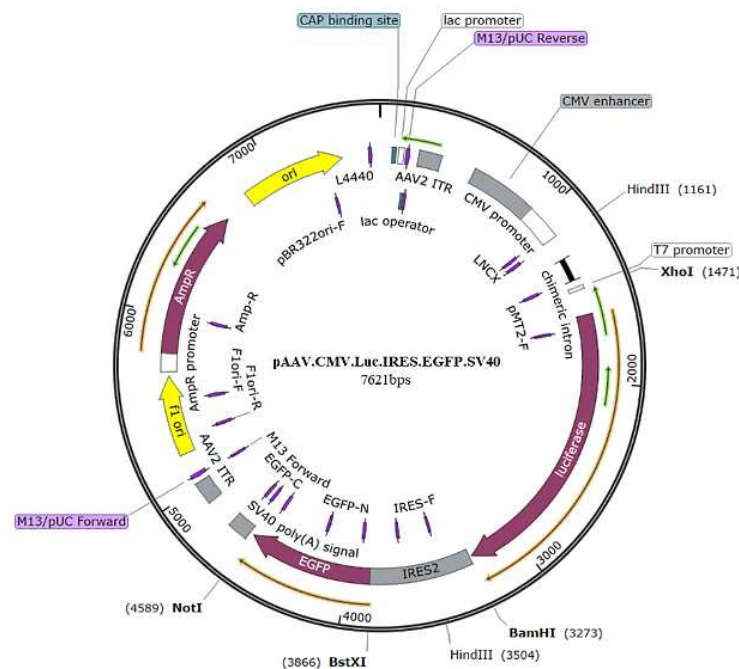


Figure 5.18: Schematic depiction of pAAV.CMV.Luc.IRES.EGFP.SV40 synthetic plasmid.

To do this, a restriction enzyme digestion approach was followed to recover the IRES and EGFP sequences from the plasmid pAAV.CMV.Luc.IRES.EGFP.SV40, which were then cloned into the recombinant pcDNA5_TLS2-EGFP vector via ligase reaction (Figure 5.19).

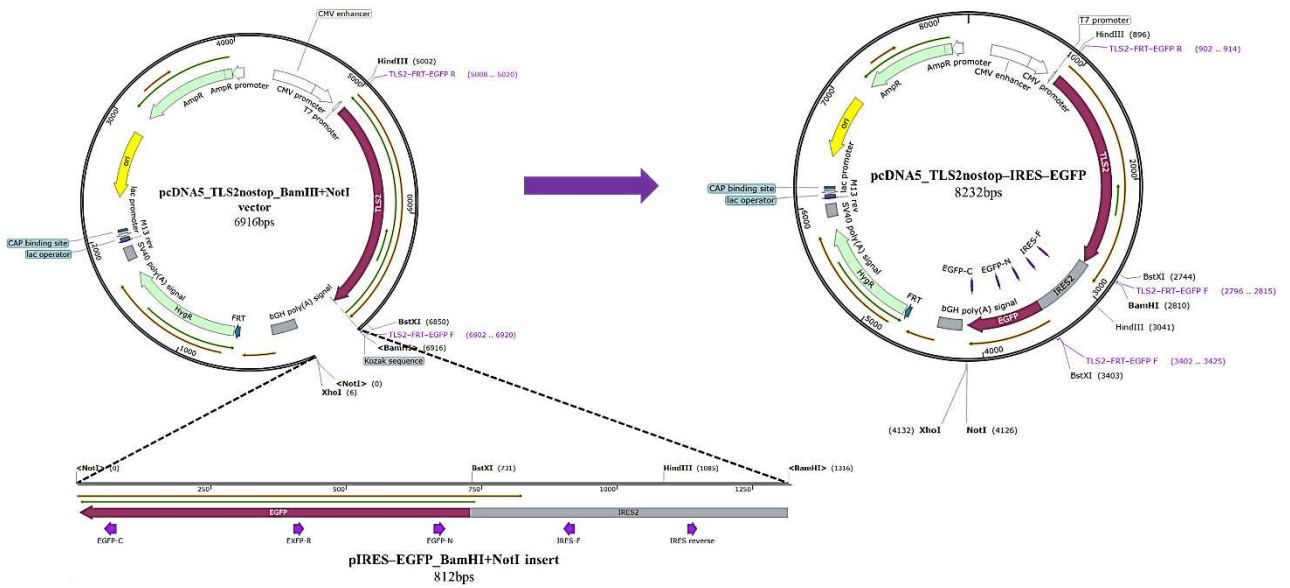


Figure 5.19: Schematic depiction of the ligase reaction between *pIRES-EGFP_BamHI+NotI* insert and *pcDNA5_TLS2nostop_BamHI+NotI*.

Both pAAV.CMV.Luc.IRES.EGFP.SV40 synthetic plasmid, previously expanded in DH5 α cells through heat–shock transformation, and *pcDNA5_TLS2-EGFP* recombinant plasmid were subjected to digest reaction with *BamHI* and *NotI* restriction enzymes. In order to prevent a possible recirculation of the vector during the ligase reaction, the 5’–ends of *pcDNA5_TLS2-EGFP* were dephosphorylated with FastAP Thermosensitive Alkaline Phosphatase at the last 10min of the incubation at 37°C (see in Table B–2). The quality of the enzymatic digestions was confirmed by electrophoretic run on agarose gel (see in Figure B–4), and the bands with the correct dimensions were purified through QIAquick Gel Extraction Kit.

pIRES-EGFP_BamHI+NotI insert and dephosphorylated *pcDNA5_TLS2nostop_BamHI+NotI* vector thus obtained were used to set up a ligase reaction with an insert:vector ratio set to 5:1 to generate *pcDNA5_TLS2nostop-IRES-EGFP* recombinant plasmid.

The ligase reaction was then used for the transformation of DH5 α cells through heat–shock transformation. Some of the bacterial colonies that grew in the LB+100 μ g/mL ampicillin plates, selective for the transformed cells containing the resistance cassette of the *pcDNA5_TLS2-EGFP* vector, were spotted and amplified in LB+100 μ g/mL ampicillin medium. The different recombinant plasmids were then purified using QIAprep Spin Miniprep Kit and tested through control digestion with *HindIII* restriction enzyme, to

evaluate the correct insertion of the pIRES–EGFP insert and avoid the recovery of any recircularized vectors without the insert of interest (see in Table B–3). It was possible to identify several colonies presenting the banding pattern indicative of the pIRES–EGFP insert correct cloning into the recombinant plasmid (see in Figure B–5).

However, the pcDNA5_TLS2nostop–IRES–EGFP recombinant plasmid thus obtained shows an alteration in the TLS2 stop codon, which would compromise the normal expression of the protein. To restore its original sequence, the terminal portion of TLS2–encoding DNA was reintroduced using TLS2stopcodon–IRES–BstXI synthetic string (Figure 5.20), containing the TLS2 stop codon cloned upstream of an IRES sequence. The TLS2stopcodon–IRES–BstXI synthetic DNA string was designed and ordered to GeneArt Gene Synthesis service.

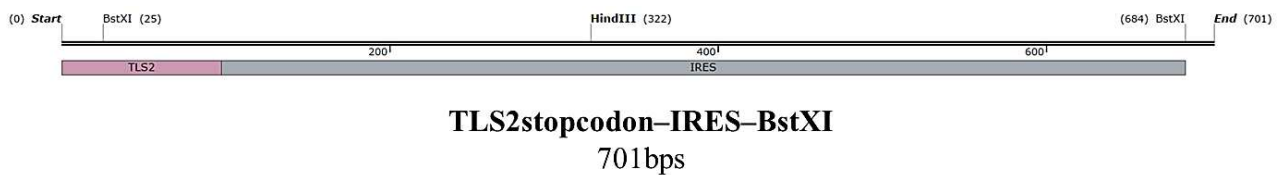


Figure 5.20: Schematic depiction of TLS2stopcodon–IRES–BstXI synthetic DNA string.

The aim is therefore to generate a recombinant plasmid in which the full–length TLS–encoding sequence is separated from that of EGFP but maintained within the same ORF. This was then used for the generation of a stable line in Flp–In™–CHO cells, in which their expression will occur as distinct proteins from a single mRNA.

To do this, TLS2stopcodon–IRES–BstXI synthetic DNA string was amplified through PCR, using specific primers which allow the introduction of cutting sites for its correct cloning within the corresponding expression vector. The quality of the amplified sequence was evaluated by electrophoretic run on agarose gel and the band related to the PCR product of interest (see in Figure B–6) was purified through QIAquick Gel Extraction Kit.

Subsequently, the TLS2stopcodon–IRES–encoding sequence was extracted through restriction enzyme digestion approach and inserted into the pcDNA5_TLS2nostop–IRES–EGFP vector via ligase reaction (Figure 5.21).

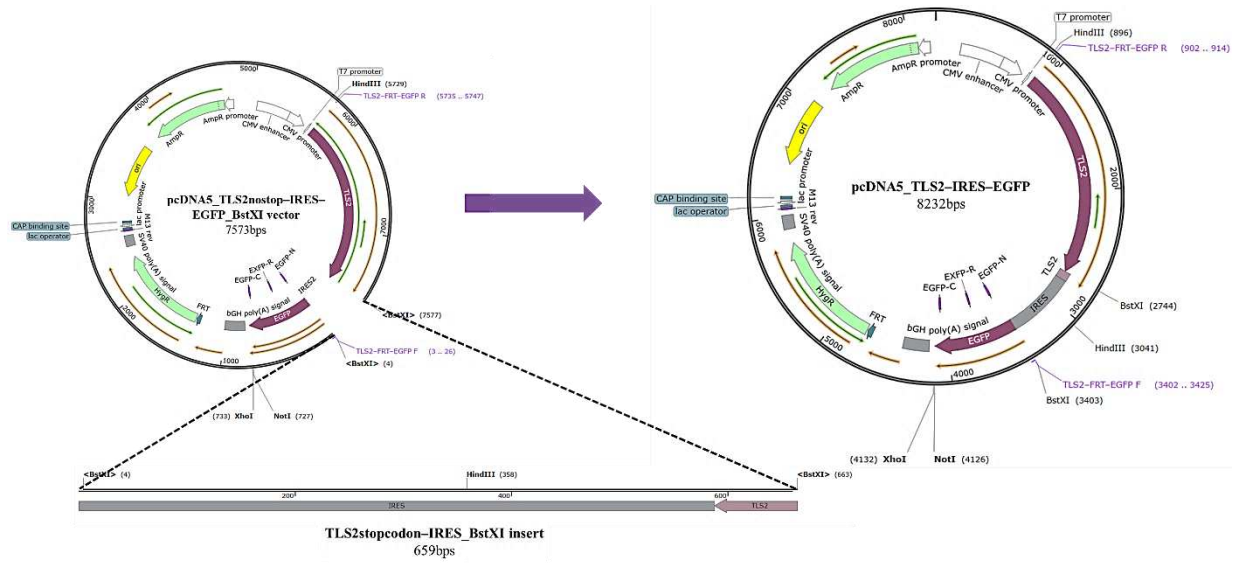


Figure 5.21: Schematic depiction of the ligase reaction between *TLS2stopcodon-IRES_BstXI* insert and *pcDNA5_TLS2nostop-IRES-EGFP_BstXI* vector.

Both amplified *TLS2stopcodon-IRES-BstXI* synthetic DNA string and *pcDNA5_TLS2nostop-IRES-EGFP* recombinant plasmid were subjected to digest reaction with *BstXI* restriction enzyme. In order to prevent a possible recirculation of the vector during the ligase reaction, the 5'-ends of *pcDNA5_TLS2nostop-IRES-EGFP* were dephosphorylated with FastAP Thermosensitive Alkaline Phosphatase at the last 10min of the incubation at 37°C (see in Table B-4). The quality of the enzymatic digestions was confirmed by electrophoretic run on agarose gel (see in Figure B-7), and the bands with the correct dimensions were purified through QIAquick Gel Extraction Kit.

TLS2stopcodon-IRES_BstXI insert and dephosphorylated *pcDNA5_TLS2nostop-IRES-EGFP_BstXI* vector thus obtained were used to set up a ligase reaction with an insert:vector ratio set to 5:1 to generate *pcDNA5_TLS2-IRES-EGFP* recombinant plasmid.

The ligase reaction was used for the transformation of DH5 α cells through heat-shock transformation. Some of the bacterial colonies that grew in the LB+100 μ g/mL ampicillin plates, selective for the transformed cells containing the resistance cassette of the *pcDNA5_TLS2nostop-IRES-EGFP* vector, were spotted and amplified in LB+100 μ g/mL ampicillin medium. The different recombinant plasmids were then purified using QIAprep Spin Miniprep Kit and tested through control digestion with *XhoI* restriction enzyme, to evaluate the correct insertion of the *TLS2stopcodon-IRES* insert and avoid the recovery of any recircularized vectors without the insert of interest (see in Table B-5). It was possible

to identify two colonies presenting the banding pattern indicative of the TLS2stopcodon–IRES insert correct cloning into the pcDNA5_TLS2–IRES–EGFP recombinant plasmid (see in Figure B–8).

5.2.4 Design and production of pcDNA3.4_cMyc–AP2 recombinant plasmid

To facilitate the trafficking and the correct folding of the TLS2 protein on the cell plasma membrane in CHO_TLS2–IRES–EGFP stable line, cMyc–AP2 synthetic DNA string (Figure 5.22–A) was designed and ordered to GeneArt Gene Synthesis service. It contains the sequence coding the auxiliary protein AP2, a molecular chaperone of the amino acid transporter of interest, fused downstream of a cMyc–TAG, to easily evaluate its expression and cellular localization through flow cytometric analysis (see in Section 5.2.5).

This was recovered and inserted into a customized pcDNA3.4 plasmid, already available in laboratory (Figure 5.22–B), used as expression vector for the production of AP2 in CHO_TLS2–IRES–EGFP cell lines.

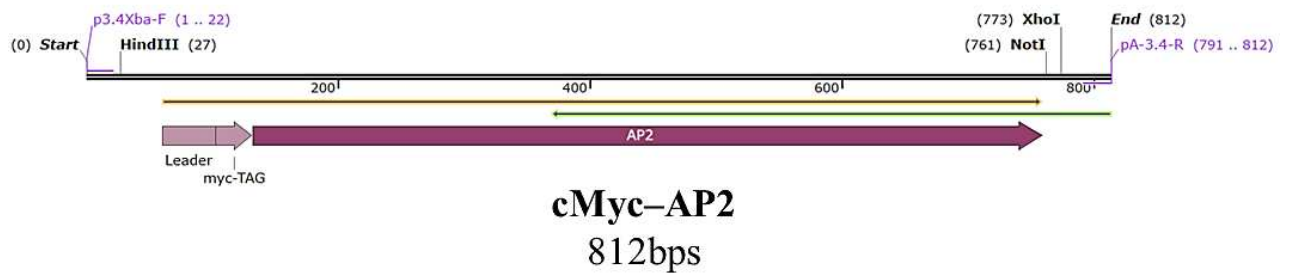
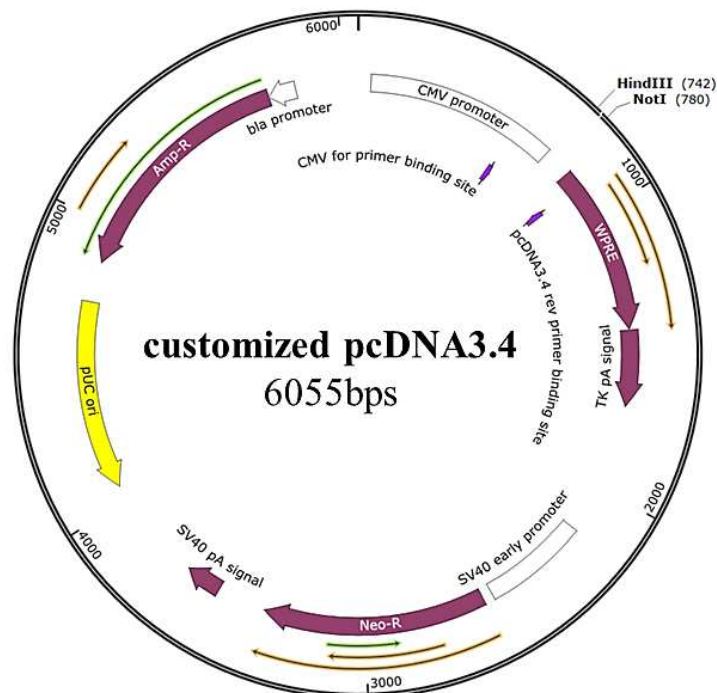
A**B**

Figure 5.22: Schematic depiction of *cMyc-AP2* synthetic DNA string (A) and customized *pcDNA3.4* plasmid (B).

The aim is therefore to generate a recombinant plasmid for the stable expression of AP2 auxiliary protein in CHO_TLS2-IRES-EGFP cell line, in order to facilitate the correct exposure of TLS2 amino acid transporter on the cell surface.

To do this, *cMyc-AP2* synthetic DNA string was amplified through PCR, using specific primers which allow the introduction of cutting sites for its correct cloning within the corresponding expression vector. The quality of the amplified sequence was evaluated by electrophoretic run on agarose gel and the band related to the PCR product of interest (see in Figure B-9) was purified through QIAquick Gel Extraction Kit.

Subsequently, the AP2-encoding sequence was extracted through restriction enzyme digestion approach and inserted into the customized pcDNA3.4 vector via ligase reaction (Figure 5.23).

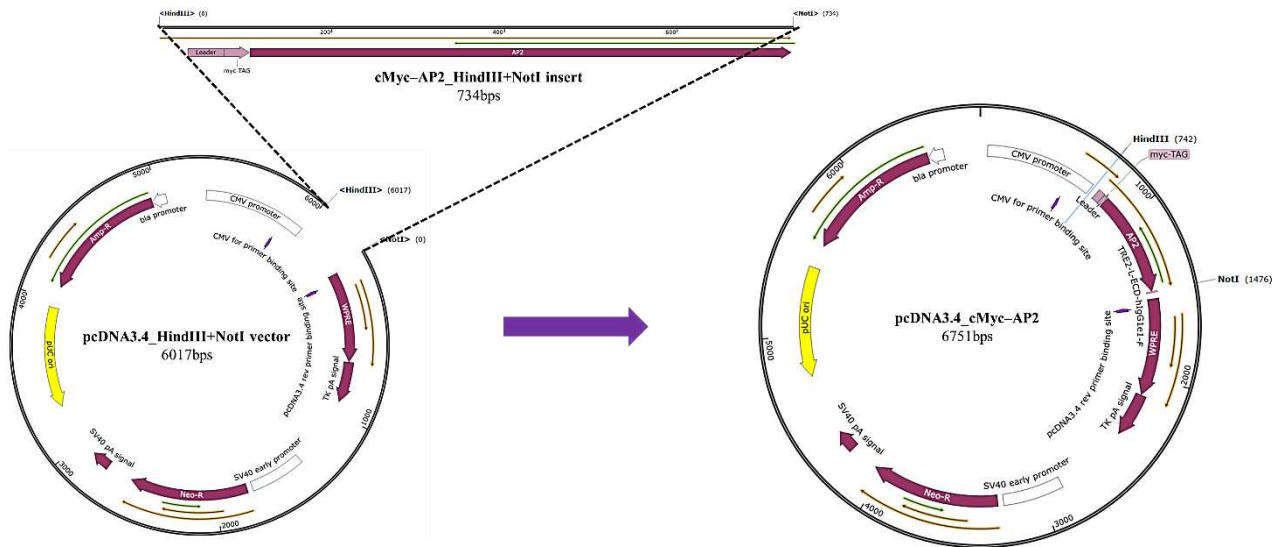


Figure 5.23: Schematic depiction of the ligase reaction between *cMyc-AP2_HindIII+NotI* insert and *pcDNA3.4_HindIII+NotI* vector.

Both amplified cMyc-AP2 synthetic DNA string and customized pcDNA3.4 plasmid, previously expanded in DH5 α cells through heat-shock transformation, were subjected to digest reaction with HindIII and NotI restriction enzymes. In order to prevent a possible recirculation of the vector during the ligase reaction, the 5'-ends of pcDNA3.4 were dephosphorylated with FastAP Thermosensitive Alkaline Phosphatase at the last 10min of the incubation at 37°C (see in Table B-6). The quality of the enzymatic digestions was confirmed by electrophoretic run on agarose gel (see in Figure B-10), and the bands with the correct dimensions were purified through QIAquick Gel Extraction Kit. The cMyc-AP2_HindIII+NotI insert and the dephosphorylated pcDNA3.4_HindIII+NotI vector thus obtained were used to set up a ligase reaction with an insert:vector ratio set to 5:1 to generate pcDNA3.4_cMyc-AP2 recombinant plasmid.

The ligase reaction was used for the transformation of DH5 α cells through heat-shock transformation. Some of the bacterial colonies that grew in the LB+100 μ g/mL ampicillin plates, selective for the transformed cells containing the resistance cassette of the pcDNA3.4 vector, were spotted and amplified in LB+100 μ g/mL ampicillin medium. The different recombinant plasmids were then purified using QIAprep Spin Miniprep Kit and tested

through control digestion with XbaI and NotI restriction enzymes, to evaluate the correct insertion of the cMyc-AP2 insert and avoid the recovery of any recircularized vectors without the insert of interest (see in Table B-7). It was possible to identify several colonies presenting the banding pattern indicative of the cMyc-AP2 insert correct cloning into the pcDNA3.4_cMyc-AP2 recombinant plasmid (see in Figure B-11).

5.2.5 Generation and validation of a cell line stably expressing TLS2-IRES-EGFP and AP2

The pcDNA5_TLS2-IRES-EGFP and pcDNA3.4_cMyc-AP2 plasmids, previously made, were used for the generation of a stable cell line expressing the full-length TLS2 amino acid transporter on the plasma membrane, assisted by the molecular chaperone function of the auxiliary protein AP2.

To do this, pcDNA5_TLS2-IRES-EGFP was transfected into Flp-In™-CHO cells using Lipofectamine™ 2000 Transfection Reagent and exploiting the Flp-In™ system, as previously described (see in Section 5.1.5), isolating also in this case the clones expressing TLS2-IRES-EGFP by using a selective medium containing hygromycin (Figure 5.24).

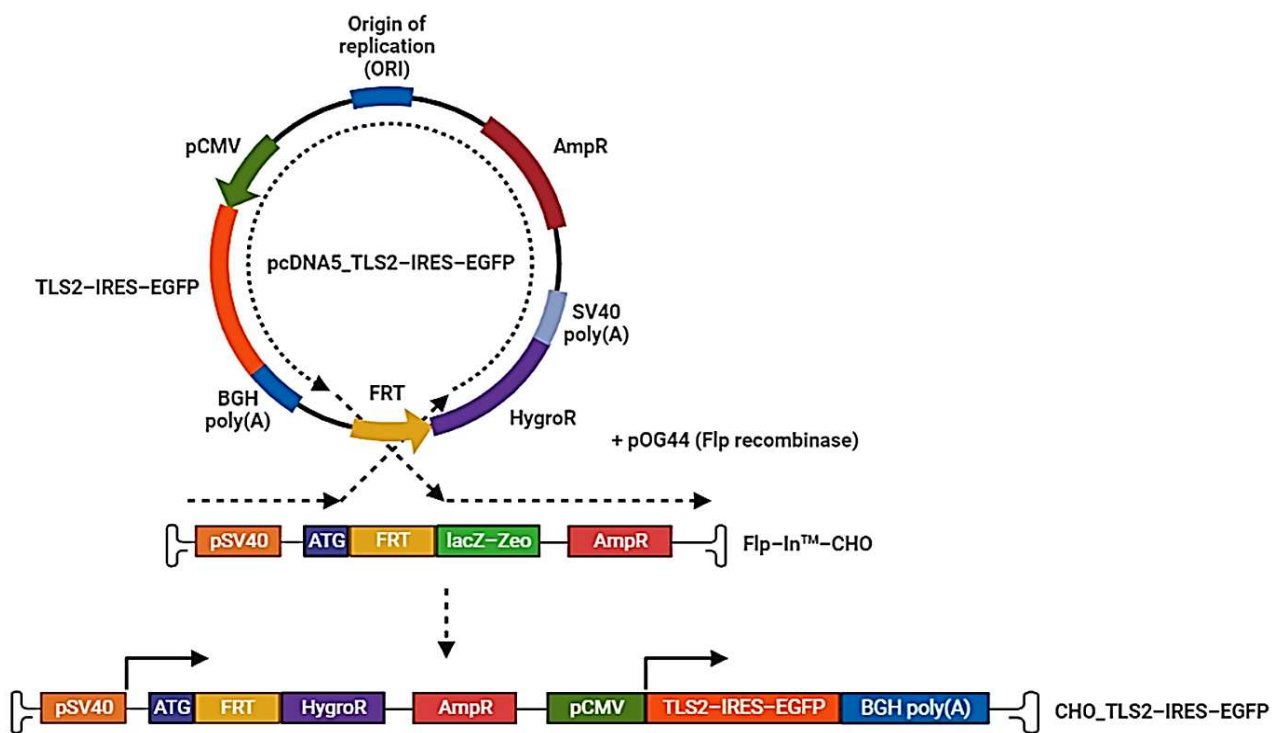


Figure 5.24: Schematic depiction of FRT recombination between Flp-In™-CHO genome and pcDNA5_TLS2-IRES-EGFP recombinant plasmid and generation of CHO_TLS2-IRES-EGFP stable line.

The selection process of single antibiotic-resistant colonies was monitored under fluorescence microscope, in order to indirectly compare the signal emitted by EGFP with the expression of full-length TLS2 amino acid transporter (Figure 5.25).

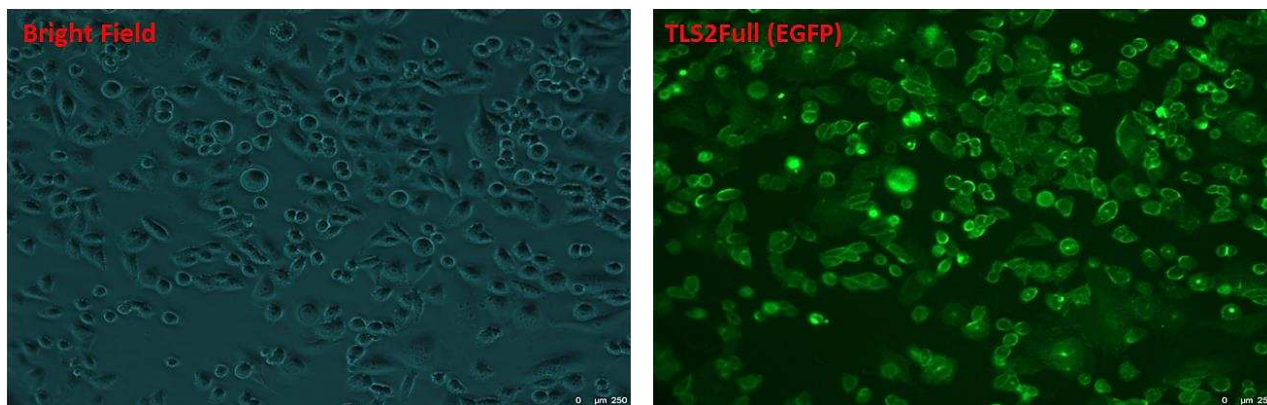


Figure 5.25: *pcDNA5_TLS2-IRES-EGFP* expression validation in Flp-In™-CHO stable line through fluorescence microscopy (B).

The CHO_TLS2-IRES-EGFP stable cell line was stably transfected with the recombinant plasmid pcDNA3.4_cMyc-AP2, again using Lipofectamine™ 2000 Transfection Reagent but without the Flp-In system, so as not to alter the expression of hygromycin resistance cassette. The AP2-expressing clones were selected using a selective culture medium containing geneticin, an antibiotic for which the cells obtain resistance thanks to the NeoR/KanR cassette present in the customized pcDNA3.4 vector.

To validate the association of the cMyc-tagged AP2 protein with the plasma membrane, the geneticin-resistant CHO_TLS2-IRES-EGFP stable clones were analysed through flow cytometric analysis, using an anti-cMyc mAb as primary antibody (Figure 5.26).

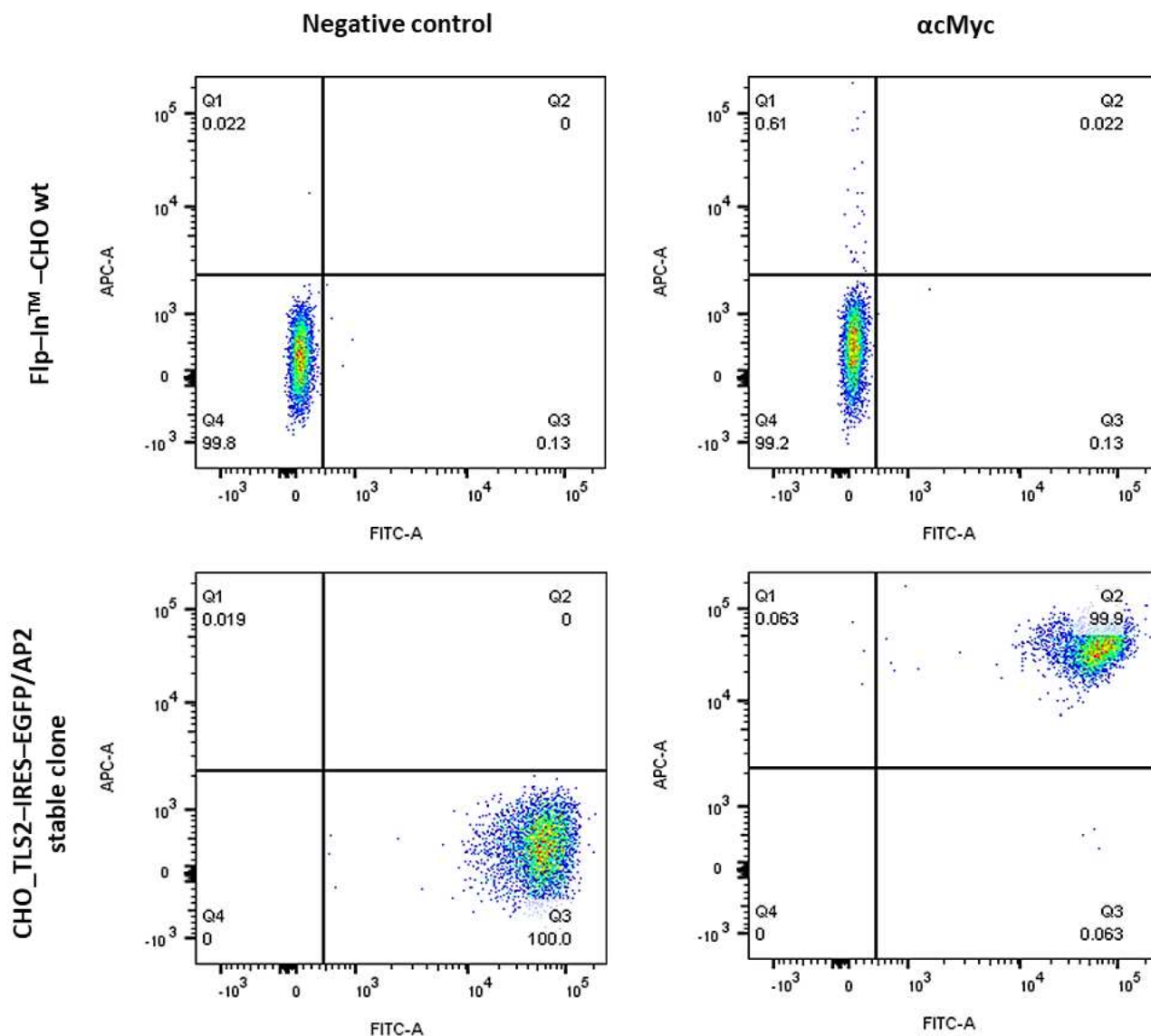
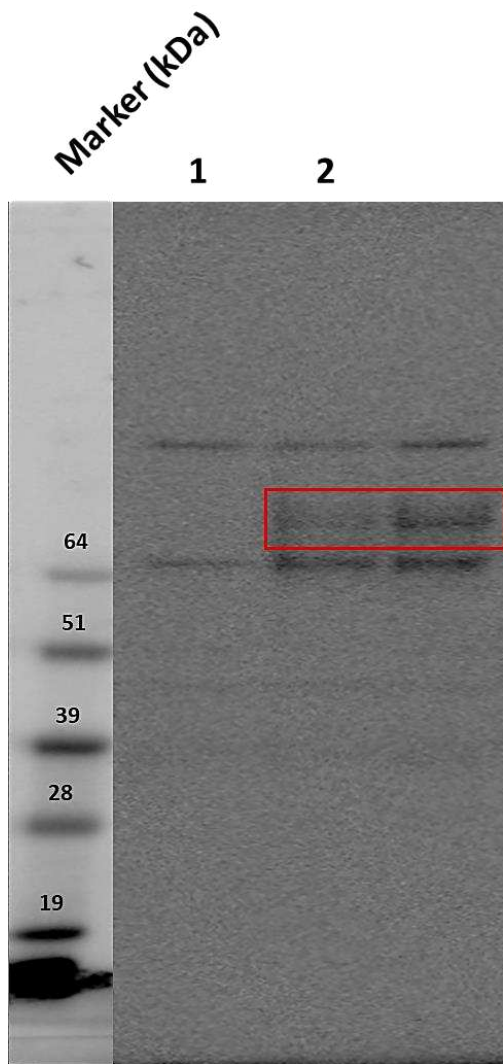


Figure 5.26: Flow cytometry recognition of the cMyc-tagged AP2 protein stably expressed in CHO_TLS2-IRES-EGFP cells with anti-cMyc mAb (Ab I°) and F(ab')₂-Goat anti-Mouse IgG (H+L) Cross-Adsorbed-Alexa Fluor™ 647 conjugated (Ab II°). The division into quadrants allows to identify the cMyc-AP2-expressing cells (top-right).

As reported in these dot plots in Figure 5.26, the fluorescence signal in APC is much higher in the isolated stable clone than in the wild-type Flp-In™-CHO wild type cells, indicating a successful cMyc-AP2 expression.

To demonstrate the effective production of the TLS2 amino acid transporter by TLS2-IRES-EGFP and TLS2-IRES-EGFP/AP2 stable lines, they were analysed as cell lysates through Western Blot, using the commercial TLS2Loop4 pAb as primary antibody (Figure 5.27).



Samples:

- 1. 20µg Flp-In™ CHO wt cell lysate;
- 2. 20µg CHO_TLS2-IRES-EGFP cell lysate;
- 3. 20µg CHO_TLS2-IRES-EGFP/AP2 cell lysate.

Ab I°:

- Commercial polyclonal αTLS2loop4 (rabbit) dil 1:1000.

Ab II°:

- Goat anti-rabbit IgG (H+L)-HRP conjugated dil 1:5000.

Figure 5.27: Western Blot recognition of TLS2 protein stably expressed in both CHO_TLS2-IRES-EGFP and CHO_TLS2-IRES-EGFP/AP2 cell lines. The red square indicates the presence of a band at the expected molecular weight for the TLS2 protein (approximately 70kDa).

As can be seen from the immunostained PDVF membrane in Figure 5.27, both the cell lysates of CHO_TLS2-IRES-EGFP and CHO_TLS2-IRES-EGFP/AP2 stable lines show a band at the expected molecular weight for the TLS2 protein (red square).

5.2.6 Mice immunization and antibody titer evaluation

For the development of a murine TLS2-specific antibody repertoire, two distinct immunization groups were set up, each consisting of 5 Female BALB/c mice 4 weeks old. The mice of the first group (Group A) were immunized with 1×10^7 CHO_TLS2-IRES-EGFP/AP2 stable line cells, while the second group (Group B) was immunized with 20 μ g of purified TLS2Loop4-6His recombinant fragment. The different antigen administration was repeated every 14 days for 5 or 3 times, respectively, as shown in the following timelines (Figure 5.28).

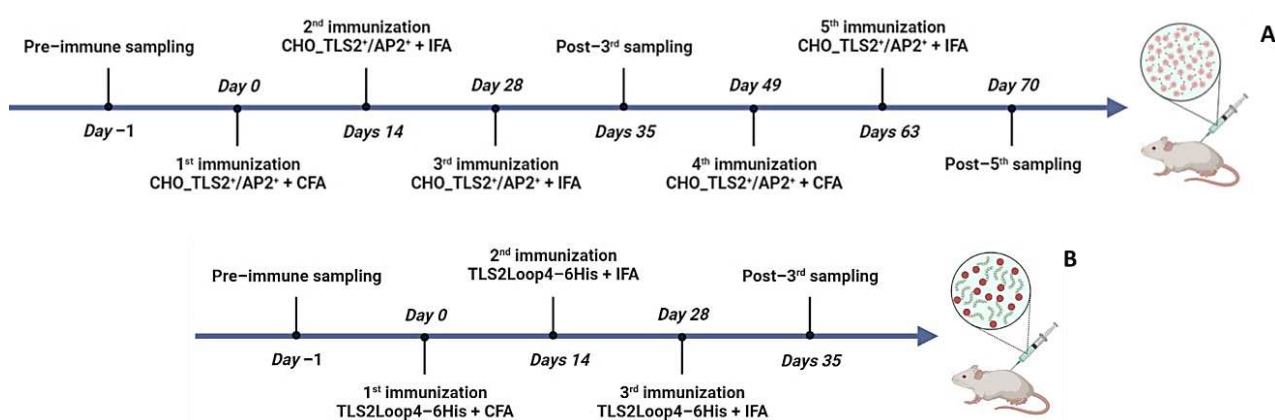


Figure 5.28: Immunization and sampling timeline for Group A (CHO_TLS2-IRES-EGFP/AP2 stable line cells) (A) and Group B (TLS2Loop4-6His recombinant fragment) (B).

In order to evaluate the specific immune response developed following immunization with CHO_TLS2-IRES-EGFP/AP2 or TLS2Loop4-6His, the sera recovered one week after the 3rd and the 5th dose were used in an ELISA assay, using SpectraPlate-384 High Binding plates coated with the TLS2Loop4-6His recombinant fragment to assess the abundance of TLS2 largest extracellular domain-specific antibodies. The pre-immune serum recovered the day before of the immunization protocol starting was used as a negative control (Figure 5.29).

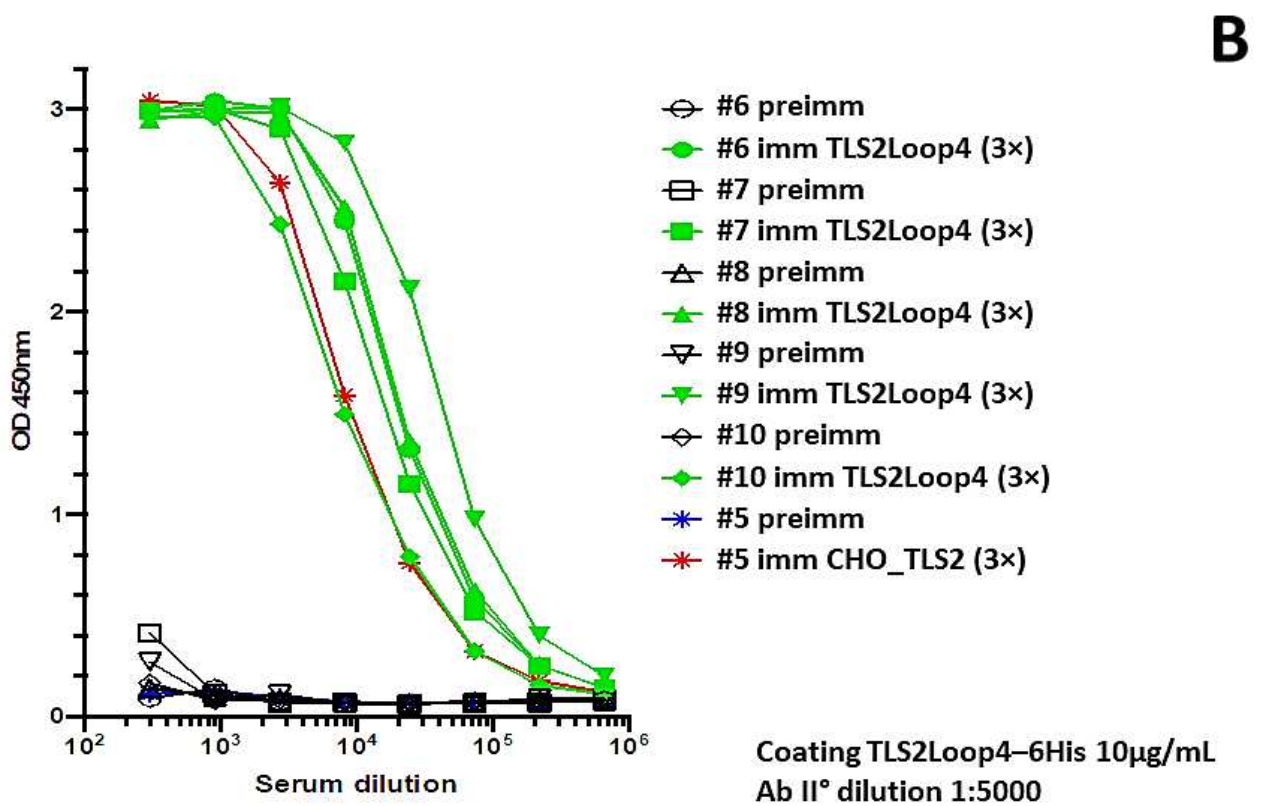
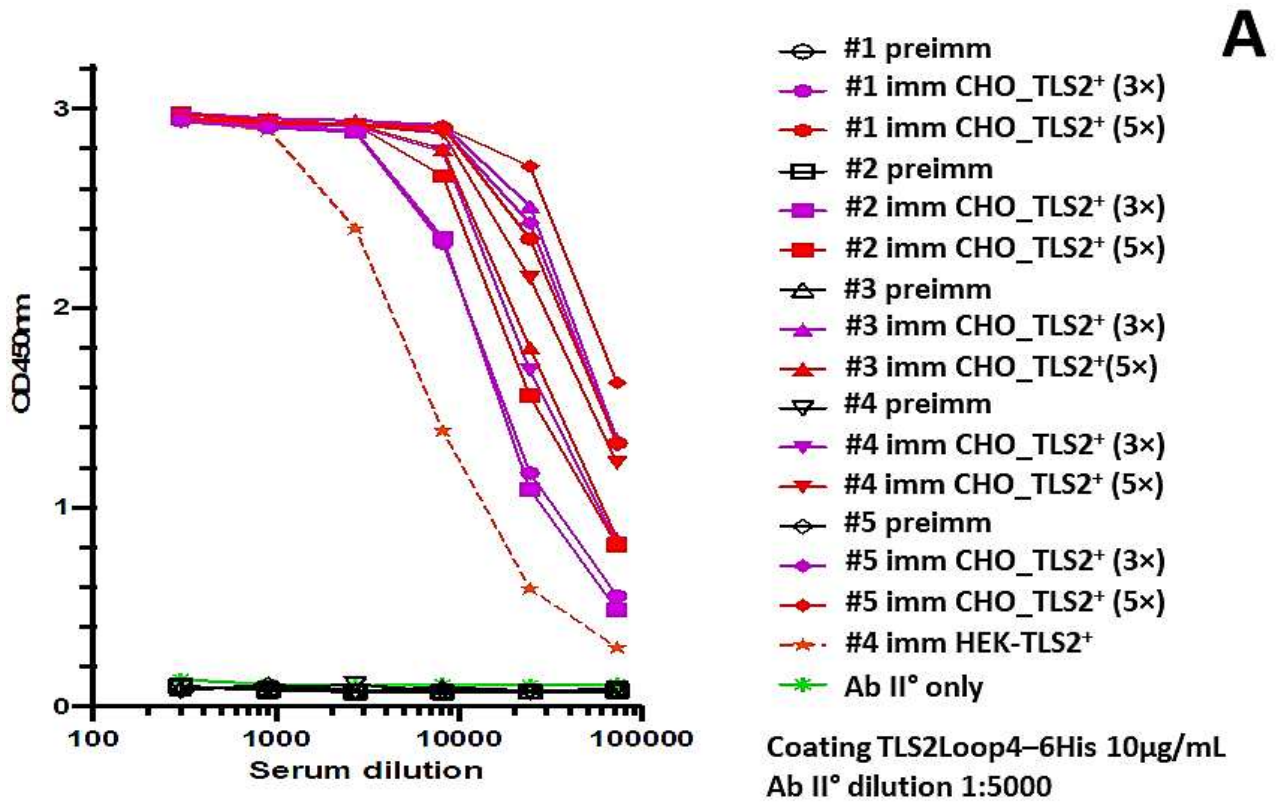


Figure 5.29: Immunization of mice with CHO_TLS2–IRES–EGFP/AP2 stable line (Group A) (A) or with TLS2Loop4–6His recombinant fragment (Group B) (B) induced a good antibody titer against TLS2Loop4–6His. The antigen-specific antibodies were revealed in an ELISA assay.

As can be seen from Figure 5.29, both mice immunized with CHO_TLS2-IRES-EGFP/AP2 cells and mice immunized with TLS2Loop4-6His protein developed a good antibody titer against the recombinant fragment, with absorbance value that remained high for a good range of dilutions examined.

A Western Blot assay was used to assess whether the antibodies developed following the immunization with the TLS2Loop4-6His recombinant fragment show also specificity toward the full-length TLS2 epitopes. For this assay, it was decided to use the serum of a mouse from both immunization group for the staining of Flp-InTM-CHO wild type and CHO_TLS2-IRES-EGFP/AP2 cell lysates, and a pre-immune serum as a negative control (Figure 5.30).

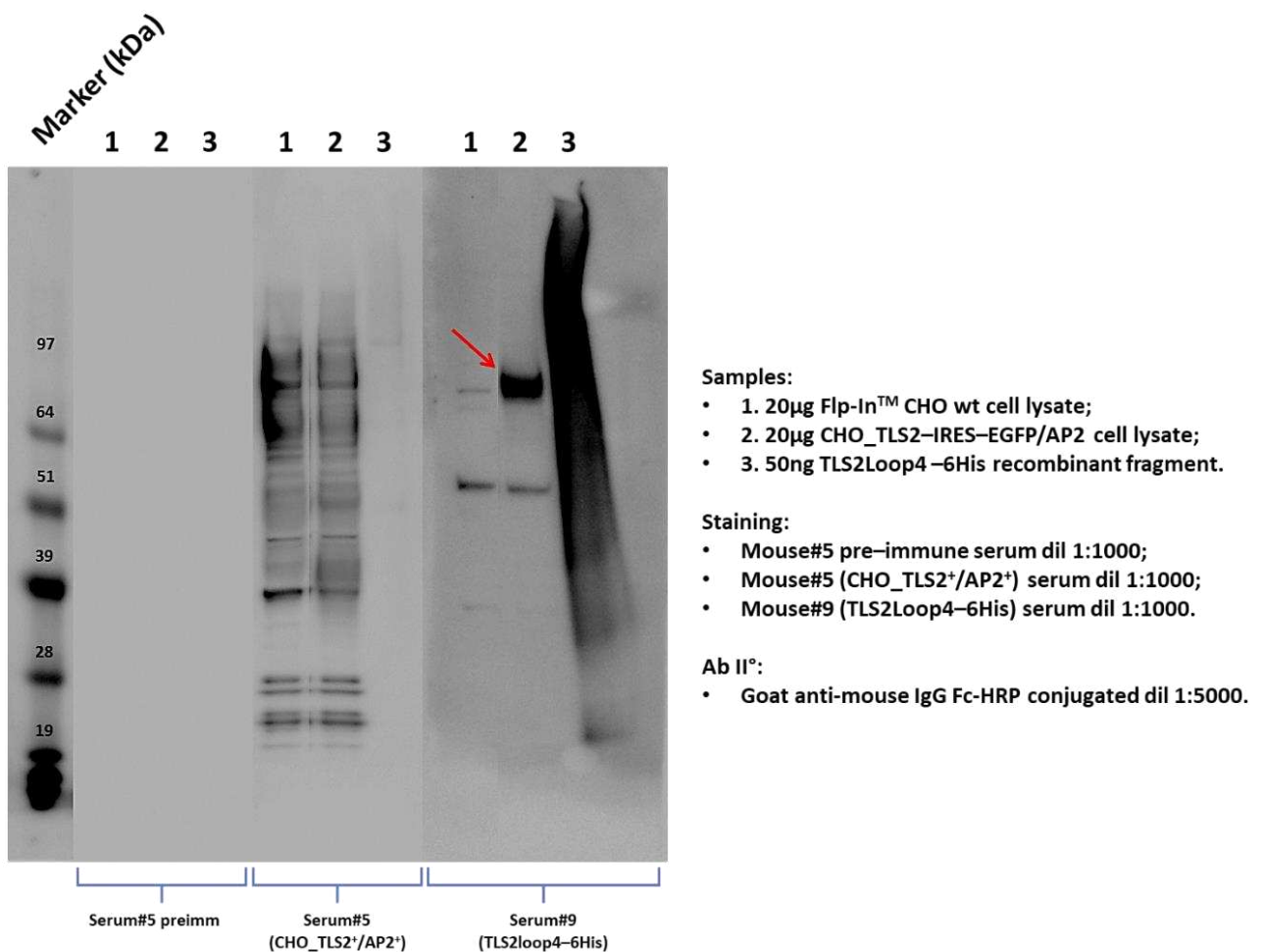


Figure 5.30: Immunization of mice with TLS2Loop4-6His recombinant fragment (Group B) induced a good antibody titer against full-length TLS2 protein expressed in CHO_TLS2-IRES-EGFP/AP2 stable line. The antigen-specific antibodies were revealed in a Western Blot assay. The red arrow indicates the presence of a band at the expected molecular weight for the TLS2 protein (approximately 70kDa).

As reported in the immunostained PDVF membrane in Figure 5.30, the serum of the mouse immunized with the recombinant fragment relating to the only extracellular Loop4 is able to recognize a protein in the cell lysate of the stable line CHO_TLS2-IRES-EGFP/AP2 with a molecular weight equal to that expected for the full-length TLS2 protein (red arrow).

5.2.7 Identification and isolation of TLS2-specific single ASCs

Once confirmed the presence of TLS2-specific antibody repertoire, the bone marrow of mice with an appropriate Ig titer was processed as the main lymphoid tissue for the isolation of plasma cells, which are responsible for the secretion of the vast majority of IgG present in the serum [125], [163]–[165]. As previously mentioned, the choice to use plasma cells for the recovery of Ig-specific genes, rather the memory B cells, is due to the fact that they allow both an immediate evaluation of secreted antibodies and an easier recovery of the variable region coding sequences from the isolated single cells, due to a high transcriptional level of immunoglobulin mRNA [120], [165], [166].

The identification and isolation of TLS2-specific single ASCs was performed according to the scheme showed in Figure 5.31. To optimize the recovery of the single plasma cells from the bone marrow samples, the cell suspension was prepared immediately after the mouse sacrifice. Their enrichment was performed using the CD138⁺ Plasma Cell Isolation Kit, taking advantage of the fact that this cellular biomarker is highly expressed upon differentiation into plasmablast and plasma cells. The plasma cells were directly labelled with magnetic CD138 Micro Beads and isolated as positive selection from the pre-enriched cell fraction through separation over a LS Columns placed in the magnetic field of a MidiMACS™ Separator. Subsequently, the enriched samples have been plated in 384-well microplates with a distribution of 50 cells per well concentrated in a small volume, using a medium in which were added factors capable to stimulate the antibody secretion in the culture supernatant. After 24 hours of incubation, it was possible to evaluate the presence of TLS2-specific antibodies through ELISA assay, in which the supernatant of each well was tested for antibodies binding the TLS2Loop4 recombinant fragment. The cells inside the wells that tested positive were replated with a limiting dilution of 0,3 cells per well, in order to isolate single plasma cells with a second screening round.

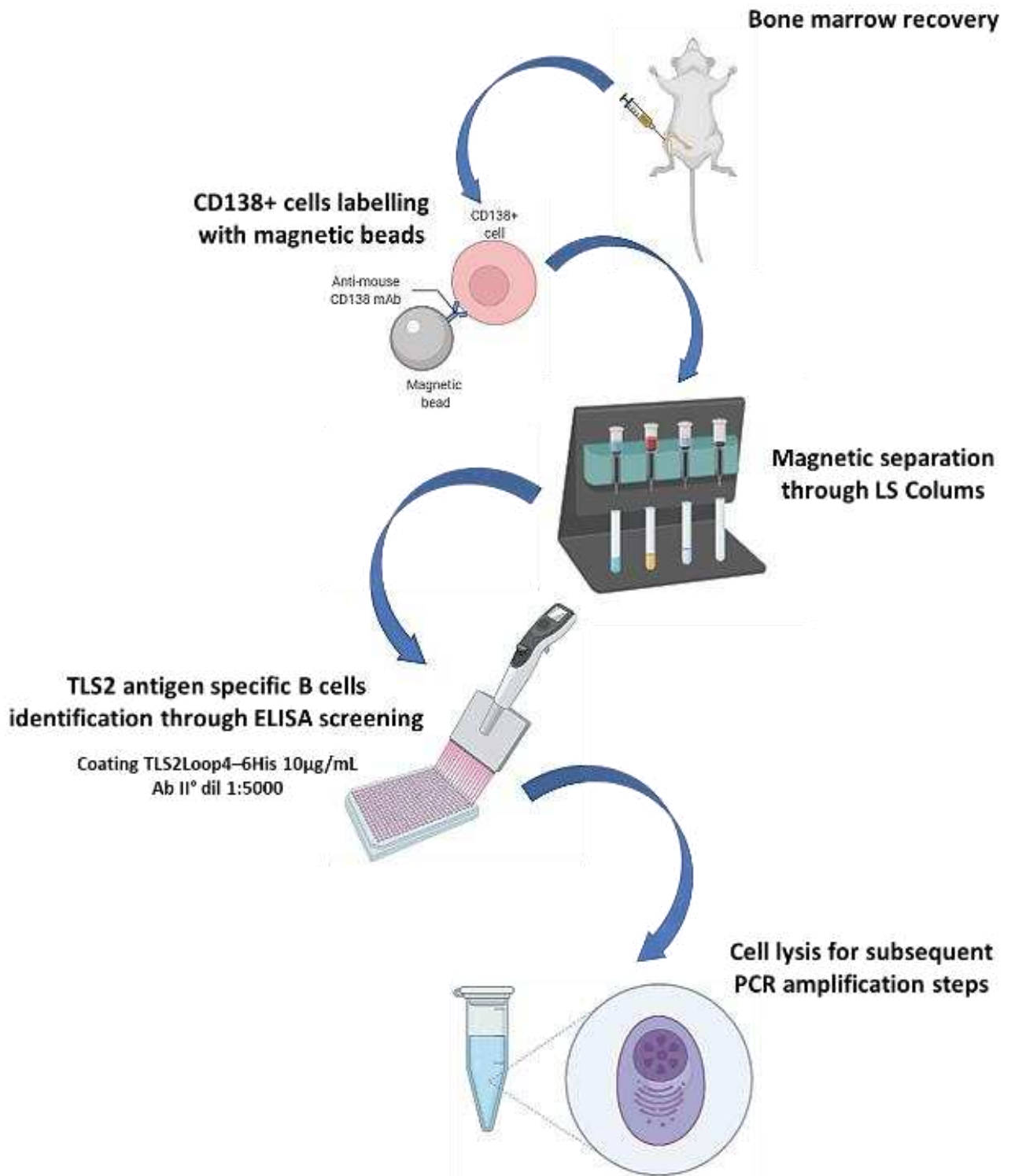


Figure 5.31: Schematic depiction of the method used to isolate single antigen-specific CD138⁺ plasma cells.

As shown in Table 5.1 using this approach it was possible to identify and isolate more than hundred single TLS2-specific antibody secreting plasma cells either from the bone marrow of mice immunized with the Flp-InTM-CHO stable cell line expressing TLS2-IRES-

EGFP/AP2 or from the mice immunized with the TLS2Loop4 recombinant fragment. These plasma cells were then transferred in 8-tubes PCR-strips containing 4µl of Lysis Buffer, in order to prepare the samples for the next step of reverse transcription.

Table 5.1: Summary of TLS2 antigen-specific plasma cells isolation from bone marrow of mice immunized with CHO_TLS2-IRES-EGFP/AP2 stable line and TLS2Loop4 recombinant fragment.

Immunization	#Mouse	Cells in bone marrow ($\times 10^7$ cells)	Purified plasma cells ($\times 10^5$ cells)	Screened plasma cells ($\times 10^4$ cells)	Single plasma cells	
Group A (CHO_TLS2-IRES-EGFP/AP2)	#1	0,01	0,1	1 (100%)	4	35
	#2	2,12	6,6	8 (12,1%)	0	
	#3	1,91	5,4	12 (22,3%)	12	
	#4	2,13	6,8	8 (11,8%)	5	
	#5	2,36	16,5	12 (7,3%)	14	
Group B (TLS2Loop4-6His)	#6	16,4	8	8 (10%)	8	79
	#7	2,39	3	8 (26,6)	13	
	#8	2,25	3	0 (0%)	0	
	#9	2,2	1,05	10 (100%)	36	
	#10	1,89	2	8 (40%)	22	

5.2.8 Recovery of V_H and V_L coding sequences from single antigen-specific ASCs and “minigenes” assembly

The TLS2-specific single CD138⁺ plasma cell lysates were reverse-transcribed and pre-amplified to cDNA, which were subjected to 3 rounds of antibody-specific PCR to amplify the cognate pairs of V_H and V_L genes and insert them into a human framework by Transcriptionally Active PCR (TAP) to generate chimeric minigenes. Figure 5.32 schematically describes this process. Through this rapid methodology it is possible to generate linear minigenes that upon direct transfection into mammalian cells induce the production of recombinant chimeric antibodies straight from the amplified heavy and light chain variable regions, without the need of cloning into expression vectors or purification steps [173].

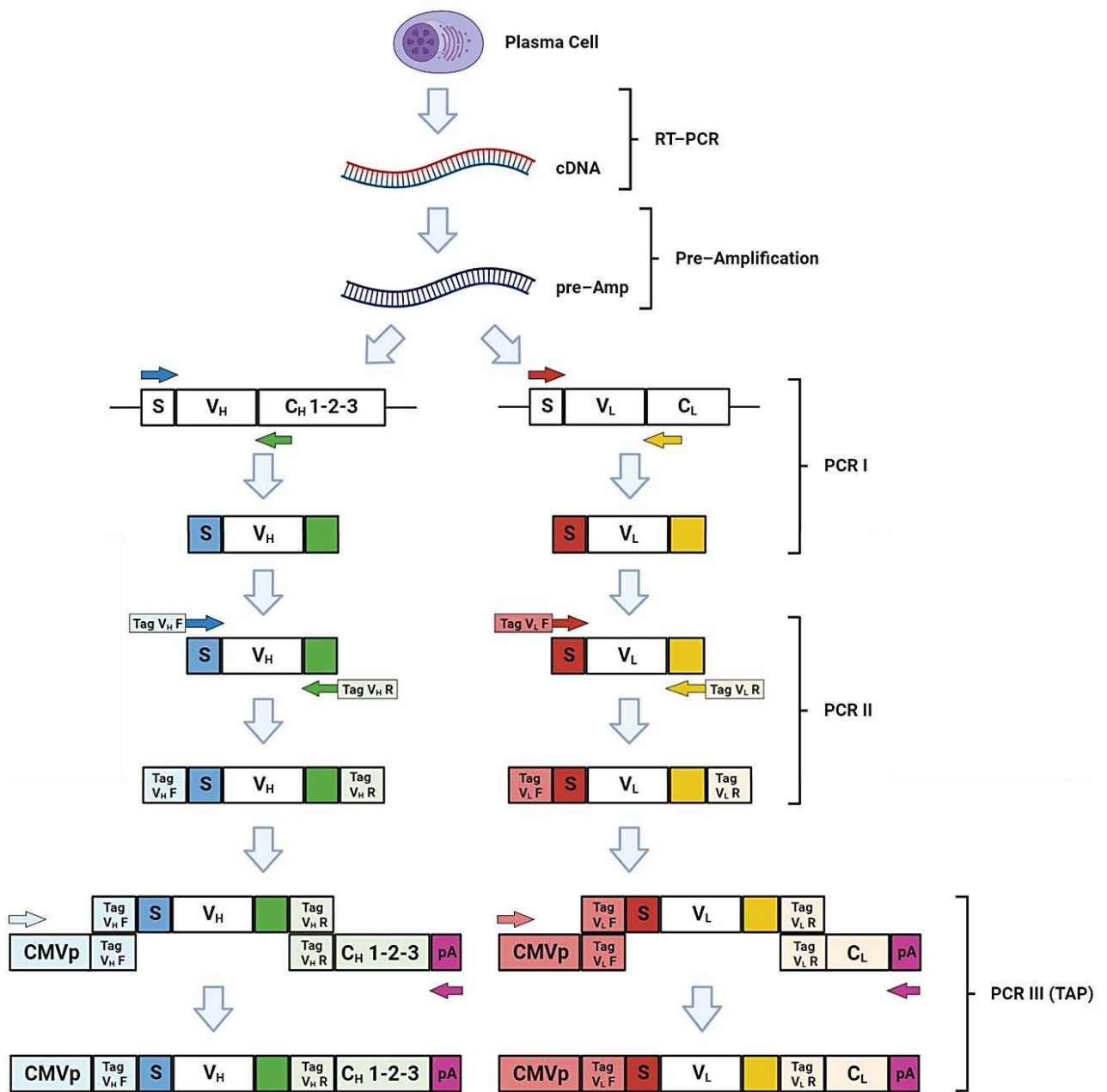


Figure 5.32: Schematic depiction of the Transcriptionally Active PCR (TAP) minigenes assembly.

During the primary PCR (PCR I), specific primer mixes were used for the amplification of the heavy and light variable region sequences. These oligonucleotides anneal at leader sequence 5' end, upstream of framework 1 region (FWR1) of the mature V_H and V_L sequences, and at the 3' end of the respective $C_H 1$ (heavy) or C_L (light) regions. In the secondary nested PCR (PCR II), the primer mixes used anneal with the FWR1 at the 5' end and with the J region at the 3' end, where they add the specific isotype for the heavy variable regions. These oligonucleotides allow the introduction of approximately 25bps

overlapping regions at both ends of the PCR I products, which serve for the minigenes assembly during the tertiary PCR (PCR III – TAP). During this last round of amplification, a human cytomegalovirus promoter (pCMV) and a human heavy or light chain constant region fragment fused to a BGH–polyadenylation signal (C_H/C_κ–polyA) are added to the 5’ end and 3’ end, respectively, of the V_H and V_L regions. These regulatory regions were previously amplified from AbVec2.0–IGHG1 and AbVec1.1–IGKC plasmids shown in Figure 5.33. In this way, the two linear TAP products were finally obtained, which can then be transiently expressed in mammalian cells for the production of TLS2–specific chimeric mAbs.

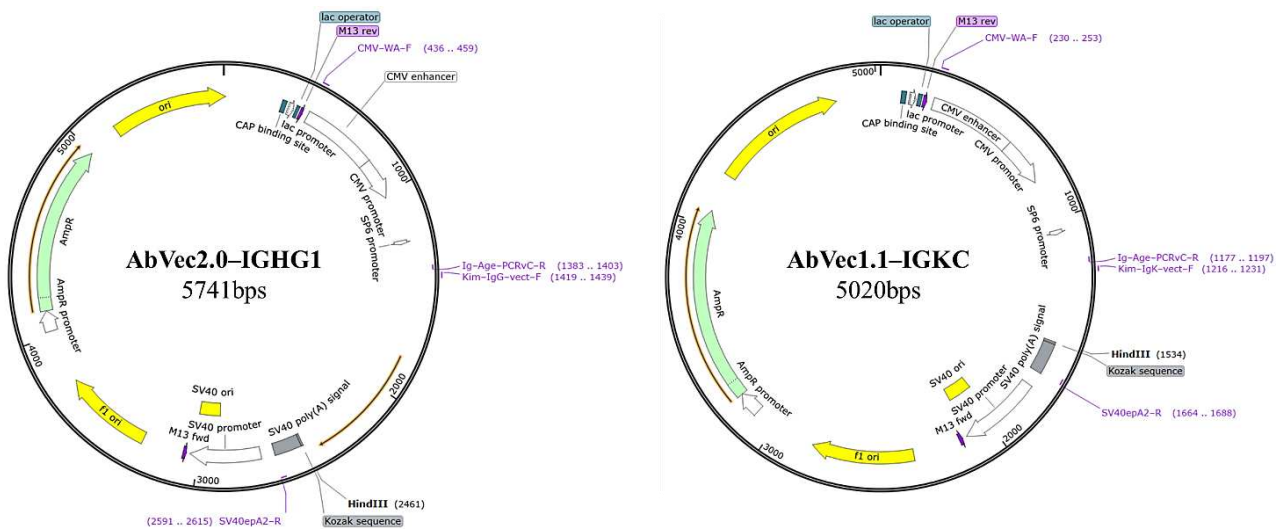


Figure 5.33: Schematic depiction of *AbVec2.0-IGHG1* and *AbVec1.1-IGKC* plasmid.

The quality of each PCR amplification product was confirmed by electrophoretic run on agarose gel (see in Figure B–12) and the final TAP minigenes were quantified by measuring absorbance at 260 and 280nm with NanoVue™ 4282 V1.7 Spectrophotometer.

5.2.9 Transient mAbs production, quantification and binding activity validation

The TAP products encoding for recombinant TLS2 mAbs heavy and light chains were transiently cotransfected, with a proportion of 70% and 30% between the heavy and light chain-encoding chimeric minigenes respectively, into Expi293FTM cells using ExpiFectamineTM 293 Transfection Kit and scaling down the protocol to Deepwell Plate 96/2mL. Supernatants harvested at 3dpt were used to evaluate TLS2 specific binding activity and immunoglobulin concentration through qualitative and quantitative ELISA assays, respectively.

For the qualitative analysis, SpectraPlate-384 High Binding plates were coated with the TLS2Loop4-6His recombinant fragment, while for the quantitative analysis the plates coated with a goat anti-human IgG Fc antibody. In both the ELISA tests, a positive and negative control were set up, using a pool of sera from TLS2 immunized mice and a mock transfected Expi293FTM cell supernatant, respectively. For the quantification of the antibodies present in the culture medium, a standard curve was developed using dilutions of Cetuximab at defined concentrations.

Once supernatants of Expi293FTM transient transfected cells were identified positive in ELISA assays for the presence of TLS2-specific antibodies at a relevant concentration, they were used to further assess reactivity against the target antigen by Western Blot and flow cytometric analysis. Western Blot test was performed using both the cell lysates of the CHO_TLS2-IRES-EGFP and CHO_TLS2-IRES-EGFP/AP2 stable lines and the TLS2Loop recombinant fragment. For the flow cytometry test, supernatants were used to evaluate the binding activity against both the stable lines expressing TLS2 (CHO_TLS2-IRES-EGFP and CHO_TLS2-IRES-EGFP/AP2) compared to the parental cell line (Flp-InTM-CHO).

Table 5.2: Summary of TLS2 antigen-specific plasma cells isolation, recovery of TAP minigenes and reactivity of chimeric mAbs.

Immunization	ELISA screening single plasma cells	#Mouse	#Ab	Ig concentration in supernatant (ng/mL)	ELISA	WB		FACS
						TLS2Loop4-6His	CHO_TLS2/AP2	CHO_TLS2/AP2
Group A (CHO_TLS2-IRES-EGFP/AP2)	35	#8	#51	70	++	ND	ND	POSITIVE
			#54	30000	++	ND	ND	NEGATIVE
		#10	#46	85	+++	ND	ND	NEGATIVE
			#44	<0,5	+	ND	ND	NEGATIVE
			#47	<0,5	+	ND	ND	NEGATIVE
Group B (TLS2Loop4-6His)	79	#16	#55	3000	+++	POSITIVE	NEGATIVE	NEGATIVE
			#56	6500	+++	POSITIVE	POSITIVE	NEGATIVE
		#19	#2	<0,5	+	ND	ND	NEGATIVE
			#5	<0,5	+	ND	ND	NEGATIVE
			#11	<0,5	+++	ND	ND	NEGATIVE
			#12	20	+++	ND	ND	NEGATIVE
			#21	860	+++	POSITIVE	NEGATIVE	NEGATIVE
			#25	1000	+++	POSITIVE	NEGATIVE	NEGATIVE
			#26	12000	+++	POSITIVE	POSITIVE	NEGATIVE
			#35	140	+++	NEGATIVE	NEGATIVE	NEGATIVE
		#20	#60	140	+	ND	ND	NEGATIVE
			#62	1000	+++	NEGATIVE	NEGATIVE	NEGATIVE
			#69	140	+	ND	ND	NEGATIVE
	#72	1000	+++	NEGATIVE	NEGATIVE	NEGATIVE		

qELISA screening: $OD_{450} < 0.9 = +$; $0.9 \leq OD_{450} \leq 1.9 = ++$; $OD_{450} > 1.9 = +++$

Through these functional assays it was possible to identify 19 recombinant monoclonal antibodies recognizing the TLS2Loop4 recombinant protein in ELISA. Among them, two chimeric mAbs expressed at very high concentration in the transient supernatants were found reactive in Western Blot against the full-length TLS2 protein expressed in the stable cell lines lysates.

Due to the nature of the primary and secondary ELISA screening with the recombinant protein is not surprising that most of the selected the recombinant antibodies derive from the group immunized with the TLS2Loop4. However, it was also possible with this screening to retrieve antibodies from the group immunized with cells expressing TLS2. Noteworthy it was possible to identify by flow cytometric analysis one recombinant mAb capable to recognize the TLS2 antigen expressed on the cell surface of the stable cell line from the group immunized with cells expressing TLS2.

5.2.10 V_H and V_L sequences cloning into expression vectors

After having established the binding activity of the chimeric mAbs, mAb#51 and mAb#56 were selected for the preparation of stably coding plasmids for subsequent functional analyses. To this aim, the coding sequence of the corresponding heavy and light variable regions were recovered and inserted into AbVec2.0–IGHG1 and AbVec1.1–IGKC recombinant plasmids, respectively coding for human immunoglobulin heavy (IgG1 isotype) and light (kappa constant region) chain.

To do this, both the V_H/V_L PCR II products and the respective AbVec2.0–IGHG1/AbVec1.1–IGKC recombinant plasmids were amplified through Polymerase Incomplete Primer Extension PCR (PIPE–PCR), to generate mixtures of incomplete extension products with short overlapping sequences at their ends, which allow mutual annealing between complementary strands. This makes possible to adopt a ligase–independent and restriction enzyme–free cloning strategy, directly transforming the recipient cells with hybrid insert–vector mixes, without the need of post–PCR enzymatic manipulation (Figure 5.34).

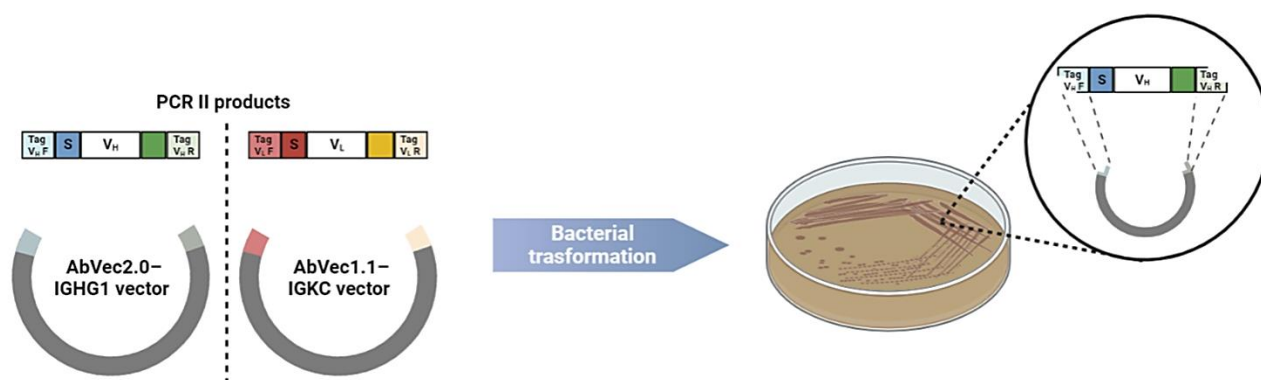


Figure 5.34: Schematic depiction of the Polymerase Incomplete Primer Extension PCR (PIPE–PCR) method.

The quality of the amplified sequences was evaluated by electrophoretic run on agarose gel (see in Figure B–13), and the bands with dimension expected for the vector of interest were purified through QIAquick Gel Extraction Kit.

PIPE amplified mAb#51/#56_V_H/V_L inserts and linear AbVec2.0–IGHG1/AbVec1.1–IGKC vectors were mixed and heat–shock transformed into MultiShot™ StripWell Mach1™ T1 Phage–Resistant Chemically Competent *E. coli*, with an insert:vector ratio set to 5:1. Some of the bacterial colonies that grew in the LB+100μg/mL ampicillin plates,

selective for the transformed cells containing the resistance cassette of the AbVec2.0–IGHG1/AbVec1.1–IGKC vectors, were spotted and then screened through colony PCR and control digestion with EcoRI and HindIII restriction enzymes. Both primers and restriction enzymes used in this step were selected to evaluate the actual presence of V_H/V_L within the recombinant plasmid, thus avoiding the recovery of any recircularized AbVec2.0–IGHG1/AbVec1.1–IGKC vectors without the insert of interest. It was possible to identify several colonies presenting the recombinant plasmids which contain the mAb#51/#56_V_H/V_L inserts (see in Figure B–14).

Colonies that tested positive at screening were then amplified in LB+100µg/mL ampicillin medium, and the recombinant plasmids thus obtained, named respectively mAb#51H/L and mAb#56H/L, were purified using QIAprep Spin Miniprep Kit. Quantification of DNA and its purity were established by measuring the absorbance at 260 and 280nm with NanoVue™ 4282 V1.7 Spectrophotometer.

5.2.11 Scale up of production and purification for selected TLS2 mAbs

The mAb#51H/L and mAb#56H/L recombinant plasmids were transiently cotransfected, with a proportion of 70% and 30% between the heavy and light chain–encoding plasmids respectively, into Expi293F™ cells using ExpiFectamine™ 293 Transfection Kit in 125mL flasks. The immunoglobulins present in the culture media recovered at 3– and 5–dpt were purified by immunoaffinity chromatography, using HiTrap™ Protein G HP 1mL columns. Following the purification protocol designed (see in Section 3.6.3), the samples are loaded onto the columns (previously equilibrated in Wash/Binding Buffer A) and washed to constant baseline, removing all proteins with non–specific interactions. Elution is performed using Elution Buffer B, resulting in single peaks containing the mAbs (Figure 5.35–A/C, red squares). To prevent the acid environment from damaging the immunoglobulins, each elution fraction was immediately adjusted to neutral pH with the addition of Equilibration Buffer C.

The elution peak fractions were analysed through SDS–PAGE and stained with SimplyBlue™ SafeStain (Figure 5.35–B/D), in order to verify the quality of mAb#51 and mAb#56 after purification.

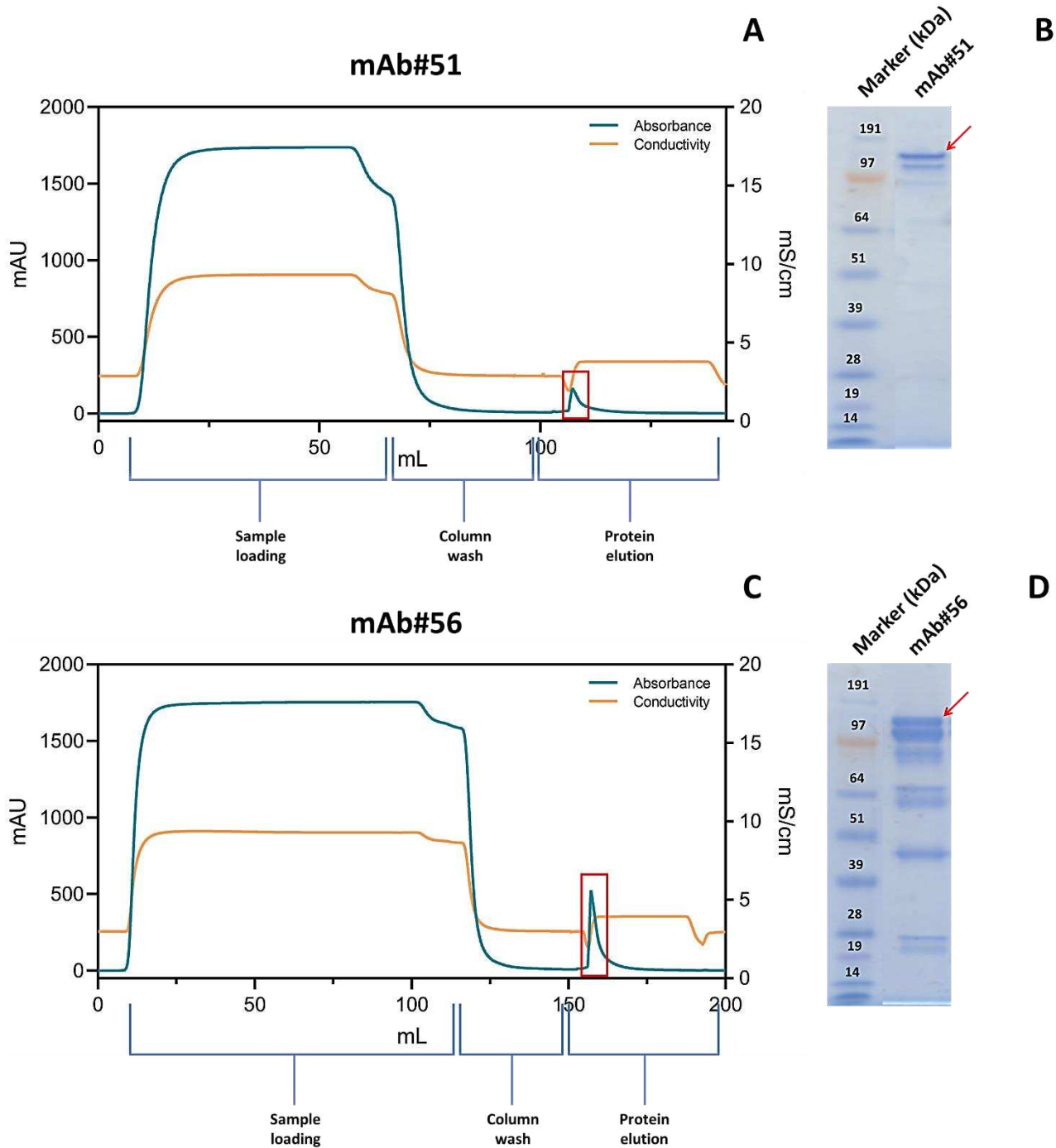


Figure 5.35: Elution profile of TLS2 mAb#51 and mAb#56. The red squares indicate the single elution peaks containing the monoclonal antibodies (A/C); Purification control of TLS2 mAb#51 and mAb#56. The red arrows indicate the presence of the monoclonal antibodies (with an expected molecular weight of approximately 150kDa) (B/D).

The red arrows in Figure 5.35–B/D indicate the presence of both the recombinant mAb#51 and mAb#56 in the fractions analysed. Once verified through the SDS–PAGE the purity and the quality of the antibodies, the corresponding elution fractions were desalted in Desalting

Buffer D using PD-10 Desalting Columns. Subsequently, the mAb#51 and mAb#56 were quantified with Pierce™ BCA Protein Assay Kit.

5.2.12 Characterization of the selected monoclonal antibodies

To proceed further with the characterization of the selected recombinant mAbs, the purified chimeric antibodies were tested in various assays, such as Western Blot, confocal analysis, and flow cytometry. Western Blot analysis was performed against the TLS2Loop4 recombinant fragment and the cell lysates of the parental Flp-In™-CHO and CHO_TLS2-IRES-EGFP/AP2 stable lines.

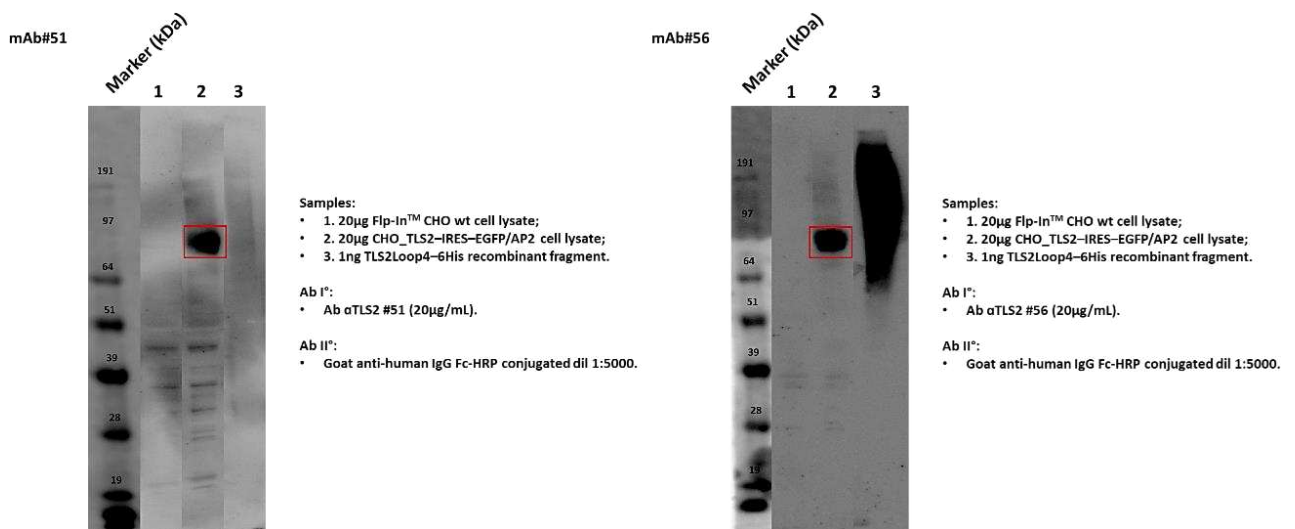


Figure 5.36: TLS2 mAb#51 and mAb#56 binding activity characterization against CHO_TLS2-IRES-EGFP/AP2 stable line and TLS2Loop4-6His recombinant fragment through Western Blot. The red squares indicate the presence of bands at the expected molecular weight for the TLS2 protein (approximately 70kDa).

Figure 5.36 shows that both the mAb#51 and mAb#56 are able to recognize a band of a molecular weight corresponding to the full-length TLS2 protein expressed in the CHO_TLS2-IRES-EGFP/AP2 stable line in denature conditions (red squares) while not staining the parental cell line. A high chemiluminescence signal is noted for the mAb#56 against the TLS2Loop4-6His recombinant fragment, which is consistent with the fact that it is the same protein used for the immunization of the mouse that generated this antibody. Interestingly mAb#51 shows very limited binding against the recombinant and aggregated protein indicating that its binding might be specific for a TLS2 conformational epitope.

For confocal analysis, the recombinant antibodies were used to assess their binding activity against parental Flp-In™ CHO cell line and both CHO_TLS2-IRES-EGFP and CHO_TLS2-IRES-EGFP/AP2 stable lines, fixed with PFA 4% and permeabilized with TritonX-100 Buffer.

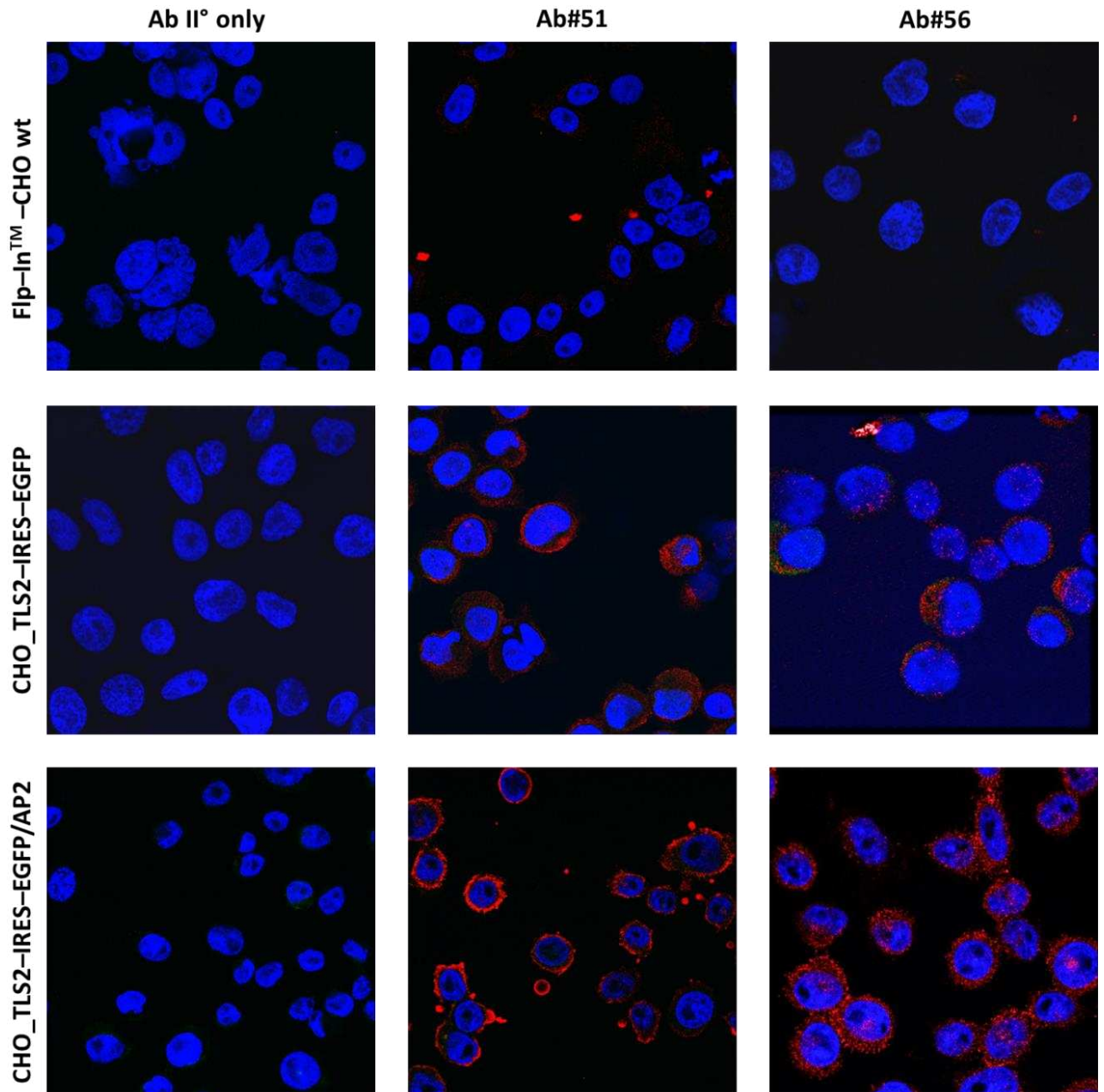


Figure 5.37: TLS2 mAb#51 and mAb#56 binding activity characterization against CHO_TLS2-IRES-EGFP and CHO_TLS2-IRES-EGFP/AP2 stable lines through confocal analysis.

Figure 5.37 shows that both mAb#51 and mAb#56 specifically stain both the CHO_TLS2–IRES–EGFP and CHO_TLS2–IRES–EGFP/AP2 stable lines while no specific binding is associated to the parental cell line. It can also be seen that the fluorescent signal associated to mAb#56 is predominantly at cytoplasmic level in both cell lines, while the fluorescence signal for mAb#51 in CHO_TLS2–IRES–EGFP/AP2 cell line is mostly located on the surface.

To evaluate the actual binding capacity of these recombinant antibodies against the TLS2 protein exposed on the cell surface, in correctly folded form, the two mAbs were subjected to flow cytometric analysis. Different concentrations of mAb#51 and mAb#56 ranging from 30 to 0,03 μ g/mL were tested to define a dose–response curve.

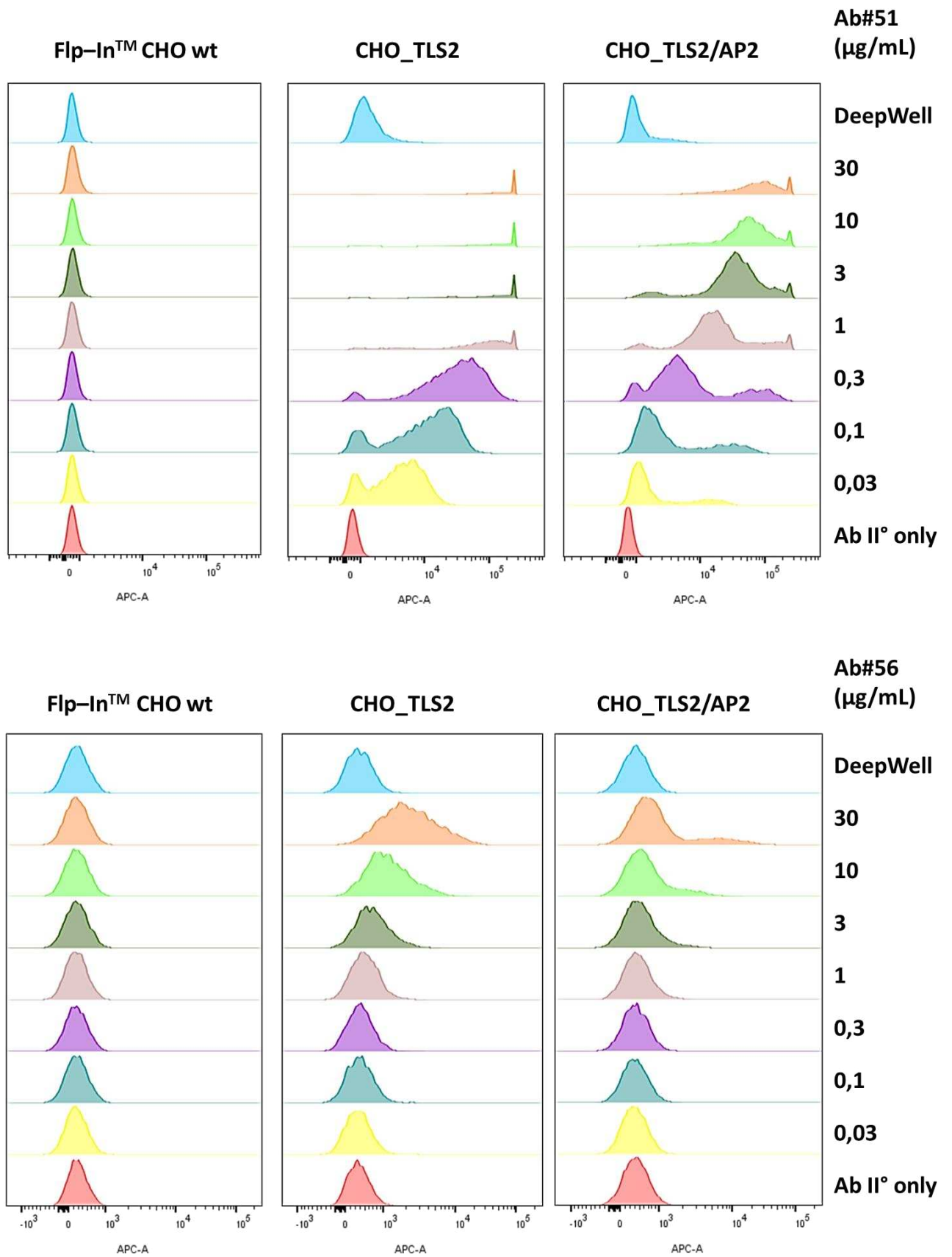


Figure 5.38: TLS2 mAb#51 and mAb#56 binding activity characterization against CHO_TLS2-IRES-EGFP and CHO_TLS2-IRES-EGFP/AP2 stable lines through flow cytometry.

The results of this analysis shown in Figure 5.38 indicate that mAb#51 recognizes the TLS2 protein on the cell membrane of both the CHO_TLS2-IRES-EGFP and CHO_TLS2-IRES-EGFP/AP2 cell lines in a dose dependent manner and still active at low nanomolar-picomolar range, while the mAb#56 has a low binding activity at the higher concentrations tested. This might suggest that the alteration in the TLS2 exposure in the previous HEK293_TLS2-EGFP line was due more to its association with the EGFP protein than to the absence of an auxiliary protein. The fact that mAb#56 did not give any recognition of TLS2 protein expressed in both the CHO_TLS2-IRES-EGFP and CHO_TLS2-IRES-EGFP/AP2 stable lines during the first reactivity tests could therefore be due to its lower binding capacity against the conformational protein, in addition to a generic lower yield of antibodies not still purified from the culture medium.

To confirm the binding specificity against the TLS2 protein in a context other than the stable lines generated for its overexpression, a non-engineered cell line was sought. By consulting gene expression profiles in public databases, it was possible to discover some TLS2 gene expression in HEL human erythroleukemia cell line at the mRNA level. This human cell line was thus used to assess the binding of mAb#51 and mAb#56 by flow cytometry. Figure 5.39 shows that in accordance with what was observed in CHO_TLS2-IRES-EGFP and CHO_TLS2-IRES-EGFP/AP2 stable lines, both chimeric mAb#51 and mAb#56 stain HEL cells in a dose-dependent manner, although with proportionally lower intensity respect to that observed in the TLS2-overexpressing lines. It is also confirmed the greater binding capacity of mAb#51 making this recombinant antibody a potential tool for an in-depth characterization of its target antigen.

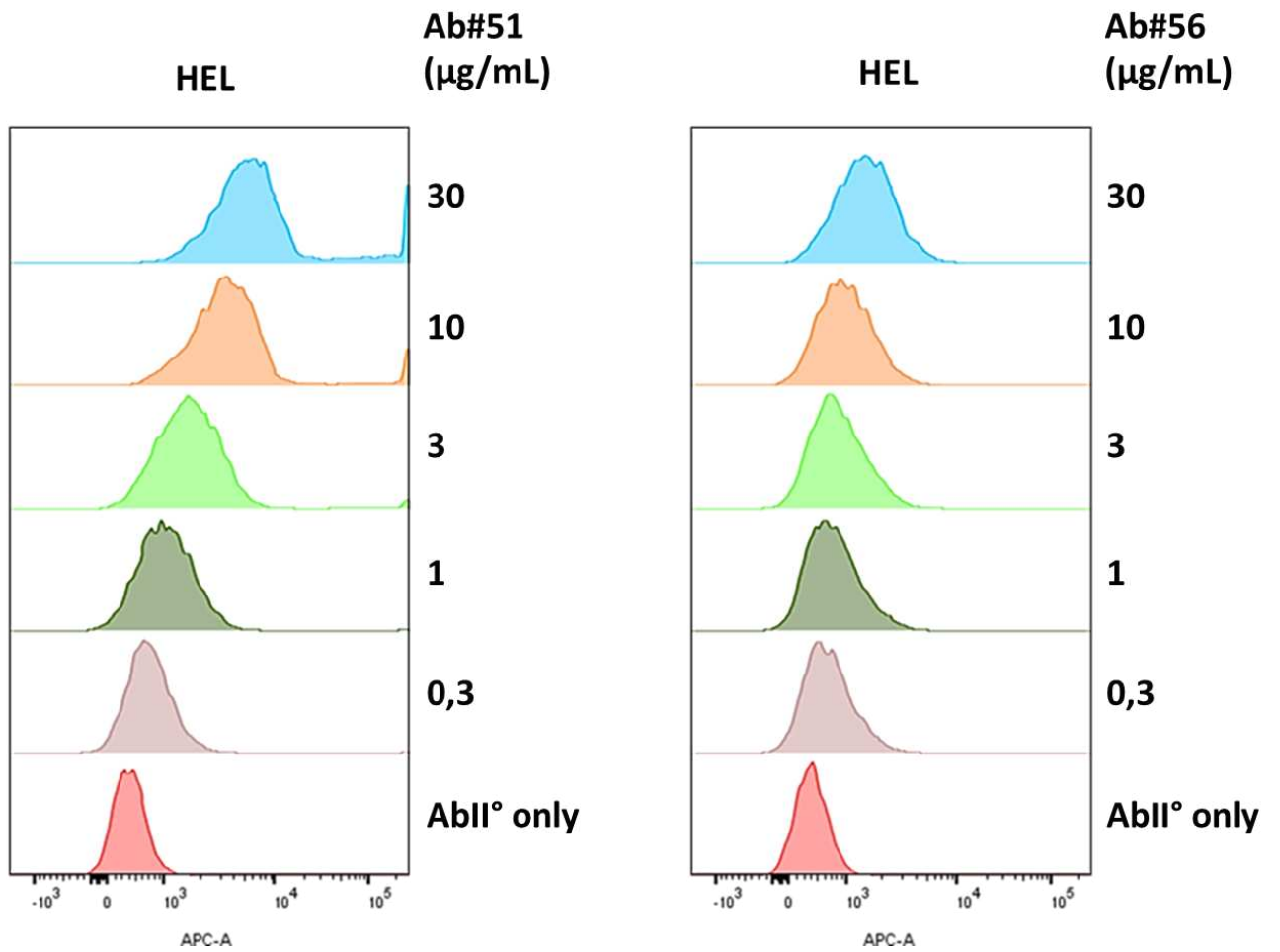


Figure 5.39: TLS2 mAb#51 and mAb#56 binding activity characterization against HEL cell lines through flow cytometry.

6 Discussion

Although structurally–complex transmembrane proteins such as GPCRs, ion channels and solute carrier (SLC) membrane transporters are intriguing targets for drug discovery, as they are active in many important cellular processes and also involved in different pathological conditions, the technical difficulties encountered in the development of specific mAbs that could modulate their functions, hinder the exploitation of these targets.

One of the main problems encountered in the generation of antibodies against these membrane proteins is the availability of a correctly folded antigen for the immunization and screening processes. Many of these structurally–complex multi–spanning membrane proteins have also short extracellular stretches exposed on the cell membrane. Therefore, the choice of the antigen to be used in the immunization step is a critical point to face in the development of mAbs against these proteins.

To develop and isolate stereospecific mAbs recognizing conformational structures against complex multi-spanning membrane proteins, based on the literature available on the topic, a so far poorly characterized amino acid carrier was selected (TLS2) and a strategy was conceived that envisaged the evaluation of different antigenic formats. The first antigen was designed as a fusion polypeptide comprising all amino acid stretches predicted in the extracellular loops separated by spacer linkers to allow proper folding (TLS2polyP–HuIgFc). The second recombinant antigen was made of a single peptide corresponding to the major extracellular loop (TLS2Loop4–6His). Finally, the last immunization strategy involved the use of whole cells engineered for overexpression of the correctly folded protein in the native context, the cell surface (CHO_TLS2–IRES–EGFP/AP2).

The results obtained in the first part of this study in which a EGFP tag was fused to TLS2 indicate that the use of fusion–tags could alter the natural insertion in the plasma membrane and/or the correct folding of structurally–complex transmembrane proteins.

Among the various antigenic formats, recombinant peptides are certainly the simplest, easiest to product at low cost, and are particularly suitable to tackle membrane proteins that have a large extracellular domain (e.g., TLS2Loop4) [174]. These peptides can also be stabilized through the use of linkers like (G₄S)₃, or circularized, to allow them to mimic the native folded structure of the original protein [175]. Some examples of membrane proteins

for which this antigenic format has successfully led to the development of antibodies are GPCRs C–C chemokine receptor–4 (CCR4) [138] and C–X–C chemokine receptor–2 (CXCR2) [176].

The use of engineered cell lines able to express at high levels the correctly folded membrane protein of interest, with proper post translational modifications, has also proved to be a valid immunization strategy for the isolation of mAbs with potential therapeutic applications towards GPCRs such as the leucine–rich repeat–containing G–protein coupled receptor 5 (LGR5) [177] or ion channel such as the ligand–gated ion channel P2X7 [178] and the calcium release–activated calcium channel protein 1 (Orai–1) [179].

Another potential obstacle for the advancement of antibodies towards the preclinical development stage is the access to innovative technologies for their generation and recovery. In fact, these imply tools and expertise necessary both to produce and maintain different source of antibodies and methods for their functionality–based isolation [174]. The definition of an effective antibody discovery approach is therefore essential for the retrieval of rare mAbs capable of binding difficult–to–target antigen such as structurally–complex transmembrane proteins.

The use of mice as a source of antibodies targeting difficult membrane proteins has been successful for the isolation of numerous mAbs, both through the use of wild type mice as in the case of EDD 7H9, an antibody blocking the sphingosine–1–phosphate receptor 3 (S1P3) [180], or the use of Hu–Ig transgenic mice, through which it was possible to isolate fully–human monoclonal GPCR–targeting antibodies such as Erenumab [139] and REMD–477 [181]. However, this approach often relies on developing hybridomas as a stable source for mAbs generation which, as explained above, is a very inefficient method limiting the potential diversity of the antibody repertoire generated following immunization and highly time/material consuming.

By contrast, the strategy followed in the generation of TLS2 mAbs was based on single B cell technology, through a FACS sorting–free approach for the isolation of CD138⁺ plasma cells that does not require expensive equipment and specific expertise. The isolated plasma cells were then profiled individually for their reactivity against the antigen of interest and the corresponding V_H and V_L–specific genes were cloned into a human framework for the generation of chimeric antibodies. The usage of the human constant regions adopted in this

method is the first step towards the complete humanization process that the murine monoclonal antibodies have to undergo to be used in therapeutic applications.

The results obtained from the initial characterization of the recombinant antibodies obtained through the Ig-specific genes cloning of single CD138⁺ plasma cells isolated from mice immunized either with a stable cell line overexpressing the full-length protein of interest (CHO_TLS2-IRES-EGFP/AP2) or with a recombinant peptide (TLS2Loop4-6His), show that it was possible to isolate chimeric monoclonal antibodies from both immunization schemes. Moreover, mA#b51 exhibit a remarkable reactivity towards a conformationally folded region expressed on the cell surface.

This data suggests that, for the generation of conformational antibodies against structurally-complex transmembrane proteins, the use of cell lines overexpressing the protein of interest in native conformation can prove to be a more successful strategy, as they give a more realistic and natural conformation of the antigen than recombinant peptides.

These results therefore allowed to validate the conceived strategy for the development of recombinant chimeric mAbs against hardly targetable antigens such as structurally-complex transmembrane proteins. It is also important to underline that the actual output of this process can be easily converted into a high-throughput system using instruments that allow a faster evaluation of the functional activity of antibodies secreted by single plasma cells (e.g., CellCelectorTM – Sartorius, Cyto-MineTM – Sphere Fluidics).

The binding specificity of chimeric mAb#51 against conformationally folded TLS2 amino acid transporter was also confirmed in a non-engineered human erythroleukemia cell line (HEL). To date, there is no evidence in the literature of existing antibodies capable of specifically recognizing the selected target protein in its conformational form. This new molecular tool will be very useful for a in-depth functional characterization of TLS2 involved in several diseases; a tool that could be eventually further developed for diagnostic and therapeutic applications.

7 References

- [1] G Köhler and C Milstein, “Continuous cultures of fused cells secreting antibody of predefined specificity”, *Nature*, vol. 256, no. 5517, pp. 495–7, Aug. 1975, doi: 10.1038/256495a0.
- [2] P. Nelson, S. Fletcher, D. Macdonald, D. Goodall, and R. Jefferis, “Assay restriction profiles of three monoclonal antibodies recognizing the G3m(u) allotype. Development of an allotype specific assay”, *J Immunol Methods*, vol. 138, pp. 57–64, Mar. 1991, doi: 10.1016/0022-1759(91)90064-m.
- [3] P. Hornbeck, S. Winston, and S. Fuller, “Enzyme-Linked Immunosorbent Assays”, *Curr Protoc Mol Biol*, pp. 11.2.1-11.2.22, May 2001, doi: 10.1002/0471142727.mb1102s15.
- [4] D. Klinman and T. Nutman, “ELISPOT assay to detect cytokine-secreting murine and human cells”, *Curr Protoc Immunol*, pp. 6.19.1-6.19.8, May 2001, doi: 10.1002/0471142735.im0619s10.
- [5] D. Ni, P. Xu, and S. Gallagher, “Immunoblotting and Immunodetection”, *Curr Protoc Cell Biol*, pp. 74:6.2.1–6.2.37, Mar. 2017, doi: 10.1002/cpcb.18.
- [6] J. Bonifacino and E. Dell’Angelica, “Immunoprecipitation”, *Curr Protoc Cell Biol*, pp. 7.2.1-7.2.21, 1998.
- [7] Y. Zhou, J. H. Morais-Cabral, A. Kaufman, and R. MacKinnon, “Chemistry of ion coordination and hydration revealed by a K⁺ channel-Fab complex at 2.0 Å resolution”, *Nature*, vol. 414, no. 6859, pp. 43–8, 2001, doi: 10.1038/35102009.
- [8] G. A. Michaud *et al.*, “Analyzing antibody specificity with whole proteome microarrays”, *Nat Biotechnol*, vol. 21, no. 12, pp. 1509–1512, Dec. 2003, doi: 10.1038/nbt910.
- [9] U. B. Nielsen and B. H. Geierstanger, “Multiplexed sandwich assays in microarray format”, *Journal of Immunological Methods*, vol. 290, no. 1–2. pp. 107–120, Jul. 2004. doi: 10.1016/j.jim.2004.04.012.
- [10] E. Harlow and D. Lane, “Using Antibodies: A Laboratory Manual”, *Journal of Antimicrobial Chemotherapy*, vol. 45, p. 413, 2000.
- [11] A. L. Givan, “Flow Cytometry: First Principles”, *New York: Wiley-Liss, Inc*, 2001.
- [12] P. K. E. Börjesson *et al.*, “Radioimmunodetection and radioimmunotherapy of head and neck cancer”, *Oral Oncol*, vol. 40, no. 8, pp. 761–772, Sep. 2004, doi: 10.1016/j.oraloncology.2003.11.009.
- [13] T. Springer, “Immunoaffinity chromatography”, *Curr Protoc Mol Biol*, p. 10.11.A, 2001, doi: 10.1002/0471142727.mb1011as36.
- [14] S. Miltenyi, W. Muller, W. Weichel, and A. Radbruch, “High gradient magnetic cell separation with MACS”, *Wiley-Liss, Inc*, 1990. doi: 10.1002/cyto.990110203.

- [15] D. Hollenbaugh, A. Aruffo, B. Jones, and P. Linsley, "Use of monoclonal antibodies for expression cloning", *Curr Protoc Immunol*, p. 10.18, 2001, doi: 10.1002/0471142735.im1018s31.
- [16] B. DeSilva, G. Orosz, K. Egodage, R. Carlson, R. Schowen, and G. Wilson, "Catalytic antibodies for complex reactions: hapten design and the importance of screening for catalysis in the generation of catalytic antibodies for the NDA/CN reaction", *Appl Biochem Biotechnol*, vol. 83, no. 1–3, pp. 195–206, 2000, doi: 10.1385/abab:83:1-3:195.
- [17] J. Mond and M. Brunswick, "Proliferative assays for B cell function", *Curr Protoc Immunol*, p. 3.10, 2003, doi: 10.1002/0471142735.im0310s57.
- [18] J. J. Buza *et al.*, "Neutralization of interleukin-10 significantly enhances gamma interferon expression in peripheral blood by stimulation with Johnin purified protein derivative and by infection with Mycobacterium avium subsp. paratuberculosis in experimentally infected cattle with paratuberculosis". *Infect Immun*, vol. 72, no. 4, pp. 2425–2428, Apr. 2004, doi: 10.1128/IAI.72.4.2425-2428.2004.
- [19] M. Visintin, G. A. Meli, I. Cannistraci, and A. Cattaneo, "Intracellular antibodies for proteomics", *J Immunol Methods*, vol. 290, no. 1–2, pp. 135–153, Jul. 2004, doi: 10.1016/j.jim.2004.04.014.
- [20] P. L. Mottram, L. J. Murray-Segal, W. Han, J. Maguire, and A. N. Stein-Oakley, "Remission and pancreas isograft survival in recent onset diabetic NOD mice after treatment with low-dose anti-CD3 monoclonal antibodies", *Transpl Immunol*, vol. 10, pp. 63–72, 2002, doi: 10.1016/s0966-3274(02)00050-3.
- [21] I. Kirman, R. L. Whelan, and O. H. Nielsen, "Infliximab: mechanism of action beyond TNF- α neutralization in inflammatory bowel disease", *Eur J Gastroenterol Hepatol*, vol. 16, no. 7, pp. 639–641, Jul. 2004, doi: 10.1097/01.meg.0000108345.41221.c2.
- [22] F. Winau, O. Westphal, and R. Winau, "Paul Ehrlich--in search of the magic bullet", *Microbes and Infection*, vol. 6, no. 8. Elsevier Masson SAS, pp. 786–789, 2004. doi: 10.1016/j.micinf.2004.04.003.
- [23] H. Kaplon, A. Chenoweth, S. Crescioli, and J. M. Reichert, "Antibodies to watch in 2022", *MAbs*, vol. 14, no. 1, 2022, doi: 10.1080/19420862.2021.2014296.
- [24] The Antibody Society. In: Antibody Therapeutics Approved or in regulatory review in the EU or US. <https://www.antibodysociety.org/>.
- [25] R.-M. Lu *et al.*, "Development of therapeutic antibodies for the treatment of diseases", *Journal of Biomedical Science*, vol. 27, no. 1. BioMed Central Ltd., Jan. 02, 2020. doi: 10.1186/s12929-019-0592-z.
- [26] A. L. Grilo and A. Mantalaris, "The Increasingly Human and Profitable Monoclonal Antibody Market", *Trends Biotechnol*, vol. 37, no. 1, pp. 9–16, Jan. 2019, doi: 10.1016/j.tibtech.2018.05.014.

- [27] F. Helling *et al.*, “GM2-KLH conjugate vaccine increased immunogenicity in melanoma patients after administration with immunological adjuvant QS-21”, *Cancer Res*, vol. 55, no. 13, pp. 2783–8, 1995.
- [28] M. Cragg, R. French, and M. Glennie, “Signaling antibodies in cancer therapy”, *Curr Opin Immunol*, vol. 11, no. 5, pp. 541–7, Oct. 1999, doi: 10.1016/s0952-7915(99)00010-2.
- [29] P. Vieira and K. Rajewsky, “The half-lives of serum immunoglobulins in adult mice”, *Eur. J. Immunol*, vol. 18, no. 2, pp. 313–316, 1988, doi: 10.1002/eji.1830180221.
- [30] M. F. W. Festing, *Inbred Strains in Biomedical Research*. Macmillan Education UK, 1979. doi: 10.1007/978-1-349-03816-9.
- [31] T. Raybould and M. Takahashi, “Production of stable rabbit-mouse hybridomas that secrete rabbit mAb of defined specificity”, *Science (1979)*, vol. 240, no. 4860, pp. 1788–90, 1988, doi: 10.1126/science.3289119.
- [32] Y. Kishiro, M. Kagawa, I. Naito, and Y. Sado, “A novel method of preparing rat-mono-clonal antibody-producing hybridomas by using rat medial iliac lymph node cells”, *Cell Struct Funct*, vol. 20, no. 2, pp. 151–6, Apr. 1995, doi: 10.1247/csf.20.151.
- [33] D. Kim, G. Noh, K. Ham, K. Lee, and O. Kwon, “Antibody response of mouse splenocytes using mixture of supernatants of thymocytes, adherent and non-adherent splenocytes: in-vitro immunization-II”, *J Korean Med Sci.*, vol. 5, no. 1, pp. 25–31, 1990, doi: 10.3346/jkms.1990.5.1.25.
- [34] R. W. Steubing, S. Cheng, W. H. Wright, Y. Numajiri, and M. W. Berns, “Laser induced cell fusion in combination with optical tweezers: the laser cell fusion trap”, *Cytometry*, vol. 12, no. 6, pp. 505–10, 1991, doi: 10.1002/cyto.990120607.
- [35] J. Yang and M. H. Shen, “Polyethylene glycol-mediated cell fusion”, *Methods Mol Biol*, vol. 325, pp. 59–66, 2006, doi: 10.1385/1-59745-005-7:59.
- [36] M. Tomita and T. Y. Tsong, “Selective production of hybridoma cells: antigenic-based pre-selection of B lymphocytes for electrofusion with myeloma cells”, *Biochim Biophys Acta*, pp. 199–206, Dec. 1990, doi: 10.1016/0167-4889(90)90033-a.
- [37] W. B. M. de Lau, A. E. van Loon, K. Heije, D. Valerio, and B. J. E. G. Bast, “Production of hybrid hybridomas based on HATS-neomycin r double mutants”, *J Immunol Methods*, vol. 117, pp. 1–8, Feb. 1989, doi: 10.1016/0022-1759(89)90111-7.
- [38] P. Nelson, G. Reynolds, E. Waldron, E. Ward, K. Giannopoulos, and P. Murray, “Monoclonal antibodies”, *J Clin Pathol: Mol Pathol*, vol. 53, pp. 111–117, 2000, doi: 10.1136/mp.53.3.111.

- [39] J. Schlom, D. Wunderlich, and Y. A. Teramoto, "Generation of human monoclonal antibodies reactive with human mammary carcinoma cells", *Medical Sciences*, vol. 77, no. 11, pp. 6841–6845, 1980, doi: 10.1073/pnas.77.11.6841.
- [40] J. C. Howard, G. W. Butcher, D. R. Licence, G. Galfre, B. Wright, and C. Milstein, "Isolation of six monoclonal alloantibodies against rat histocompatibility antigens: clonal competition", *Immunology*, vol. 41, no. 1, pp. 131–41, Sep. 1980.
- [41] R. Jefferis *et al.*, "Evaluation of monoclonal antibodies having specificity for human IgG sub-classes: results of an IUIS/WHO collaborative study", *Immunol Lett*, vol. 10, pp. 223–252, 1985, doi: 10.1016/0165-2478(85)90082-3.
- [42] G. A. Molinaro, W. C. Eby, and C. Reimer, "A monoclonal antibody may show cross-reactivities in Ouchterlony assays but not in other assays", *J Immunol Methods*, vol. 96, pp. 219–224, Feb. 1987, doi: 10.1016/0022-1759(87)90317-6.
- [43] H. Bull *et al.*, "Reactivity and assay restriction profiles of monoclonal and polyclonal antibodies to acid phosphatases: a preliminary study", *Immunol Lett*, vol. 70, no. 3, pp. 143–149, Dec. 1999, doi: 10.1016/s0165-2478(99)00154-6.
- [44] P. N. Nelson, O. Mwestwood, R. Jefferis, M. Goodall, and F. C. Hay, "Characterisation of anti-IgG monoclonal antibody A57H by epitope mapping", *Biochem Soc Trans*, vol. 25, p. 373, May 1997, doi: 10.1042/bst025373s.
- [45] P. A. Edwards, "Some properties and applications of monoclonal antibodies", *Biochem. J*, vol. 200, no. 1, pp. 1–10, Oct. 1981, doi: 10.1042/bj2000001.
- [46] X. Yu, P. A. McGraw, F. S. House, and J. E. J. Crowe, "An optimized electrofusion-based protocol for generating virus-specific human monoclonal antibodies", *J Immunol Methods*, vol. 336, no. 2, pp. 142–151, Jul. 2008, doi: 10.1016/j.jim.2008.04.008.
- [47] R. J. Ober, C. G. Radu, V. Ghetie, and E. S. Ward, "Differences in promiscuity for antibody-FcRn interactions across species: implications for therapeutic antibodies", *Int Immunol*, vol. 13, no. 12, pp. 1551–1559, Dec. 2001, doi: 10.1093/intimm/13.12.1551.
- [48] N. A. P. S. Buss, S. J. Henderson, M. McFarlane, J. M. Shenton, and L. de Haan, "Monoclonal antibody therapeutics: history and future", *Curr Opin Pharmacol*, vol. 12, no. 5, pp. 615–622, Oct. 2012, doi: 10.1016/j.coph.2012.08.001.
- [49] M. Stern and R. Herrmann, "Overview of monoclonal antibodies in cancer therapy: present and promise", *Crit Rev Oncol Hematol*, vol. 54, no. 1, pp. 11–29, Apr. 2005, doi: 10.1016/j.critrevonc.2004.10.011.
- [50] W. Y. K. Hwang and J. Foote, "Immunogenicity of engineered antibodies", *Methods*, vol. 36, no. 1, pp. 3–10, May 2005, doi: 10.1016/j.ymeth.2005.01.001.
- [51] S. L. Morrison, M. J. Johnson, L. A. Herzenberg, and V. T. Oi, "Chimeric human antibody molecules: Mouse antigen-binding domains with human constant region

- domains”, *Proc. Natl. Acad. Sci. USA*, vol. 81, no. 21, pp. 6851–6855, Nov. 1984, doi: 10.1073/pnas.81.21.6851.
- [52] O. W. Press *et al.*, “Monoclonal Antibody 1F5 (Anti-CD20) Serotherapy of Human B Cell Lymphomas”, *Blood*, vol. 69, no. 2, pp. 584–59, Feb. 1987.
- [53] P. Jones, P. Dear, J. Foote, M. Neuberger, and G. Winter, “Replacing the complementarity-determining regions in a human antibody with those from a mouse”, *Nature*, vol. 321, no. 6069, pp. 522–5, 1986, doi: 10.1038/321522a0.
- [54] H. Watier and J. M. Reichert, “Evolution of Antibody Therapeutics”, *Protein Therapeutics*, pp. 25–49, 2017.
- [55] J. McCafferty, A. Griffiths, G. Winter, and D. Chiswell, “Phage antibodies: filamentous phage displaying antibody variable domains”, *Nature*, vol. 348, no. 6301, pp. 552–4, Dec. 1990, doi: 10.1038/348552a0.
- [56] J. Glanville *et al.*, “Precise determination of the diversity of a combinatorial antibody library gives insight into the human immunoglobulin repertoire”, *Proc Natl Acad Sci U S A*, vol. 106, no. 48, pp. 20216–21, Dec. 2009, doi: 10.1073/pnas.0909775106.
- [57] A. Persson, “Twenty years of combinatorial antibody libraries, but how well do they mimic the immunoglobulin repertoire?”, *Proc Natl Acad Sci U S A*, vol. 106, no. 48, pp. 20137–8, Dec. 2009, doi: 10.1073/pnas.0912118106.
- [58] R. R. Beerli and C. Rader, “Mining human antibody repertoires”, *MAbs*, vol. 2, no. 4, pp. 365–378, 2010, doi: 10.4161/mabs.12187.
- [59] C. F. Barbas 3rd, A. S. Kang, R. A. Lerner, and S. J. Benkovic, “Assembly of combinatorial antibody libraries on phage surfaces: the gene III site”, *Proc Natl Acad Sci USA*, vol. 88, no. 18, pp. 7978–7982, 1991, doi: 10.1073/pnas.88.18.7978.
- [60] H. Orum *et al.*, “Efficient method for constructing comprehensive murine Fab antibody libraries displayed on phage”, *Nucleic Acids Res*, vol. 21, no. 19, pp. 4491–4498, Sep. 1993, doi: 10.1093/nar/21.19.4491.
- [61] I. Benhar, “Design of synthetic antibody libraries”, *Expert Opin Biol Ther*, vol. 7, no. 5, pp. 763–779, May 2007, doi: 10.1517/14712598.7.5.763.
- [62] H. R. Hoogenboom and G. Winter, “By-passing immunisation. Human antibodies from synthetic repertoires of germline VH gene segments rearranged in vitro”, *J Mol Biol*, vol. 227, no. 2, pp. 381–8, Sep. 1992, doi: 10.1016/0022-2836(92)90894-p.
- [63] W. G. T. Willats, “Phage display: practicalities and prospects”, *Plant Mol Biol*, vol. 50, no. 6, pp. 837–854, 2002, doi: 10.1023/a:1021215516430.
- [64] N. H. Hairul Bahara, G. J. Tye, Y. S. Choong, E. B. B. Ong, A. Ismail, and T. S. Lim, “Phage display antibodies for diagnostic applications”, *Biologicals*, vol. 41, no. 4, pp. 209–216, Jul. 2013. doi: 10.1016/j.biologicals.2013.04.001.

- [65] D. Ponsel, J. Neugebauer, K. Ladetzki-Baehs, and K. Tissot, “High affinity, developability and functional size: The holy grail of combinatorial antibody library generation”, *Molecules*, vol. 16, no. 5, pp. 3675–3700, May 2011, doi: 10.3390/molecules16053675.
- [66] B. N. Lim, G. J. Tye, Y. S. Choong, E. B. B. Ong, A. Ismail, and T. S. Lim, “Principles and application of antibody libraries for infectious diseases”, *Biotechnol Lett*, vol. 36, no. 12, pp. 2381–2392, Dec. 2014, doi: 10.1007/s10529-014-1635-x.
- [67] A. C. W. Ch’ng, Y. S. Choong, and T. S. Lim, “Phage Display-Derived Antibodies: Application of Recombinant Antibodies for Diagnostics”, in *Proof and Concepts in Rapid Diagnostic Tests and Technologies*, InTech, 2016, pp. 107–135. doi: 10.5772/63927.
- [68] J. Hanes, L. Jermutus, S. Weber-Bornhauser, H. R. Bosshard, and A. P. Plückthun, “Ribosome display efficiently selects and evolves high-affinity antibodies in vitro from immune libraries”, *Proc Natl Acad Sci USA*, vol. 95, no. 24, pp. 14130–14135, Nov. 1998, doi: 10.1073/pnas.95.24.14130.
- [69] E. T. Boder and K. D. Wittrup, “Yeast surface display for screening combinatorial polypeptide libraries”, *Nat Biotechnol*, vol. 15, no. 6, pp. 553–7, Jun. 1997, doi: 10.1038/nbt0697-553.
- [70] P. S. Daugherty, M. J. Olsen, B. L. Iverson, and G. Georgiou, “Development of an optimized expression system for the screening of antibody libraries displayed on the Escherichia coli surface”, *Protein Engineering vol*, vol. 12, no. 7, pp. 613–621, 1999, doi: 10.1093/protein/12.7.613.
- [71] R. R. Beerli *et al.*, “Isolation of human monoclonal antibodies by mammalian cell display”, *Proc Natl Acad Sci U S A*, vol. 105, no. 38, pp. 14336–41, Sep. 2008, doi: 10.1073/pnas.0805942105.
- [72] M. R. Tohidkia, J. Barar, F. Asadi, and Y. Omid, “Molecular considerations for development of phage antibody libraries”, *J Drug Target*, vol. 20, no. 3, pp. 195–208, Apr. 2012, doi: 10.3109/1061186X.2011.611517.
- [73] W. R. Strohl, “Current progress in innovative engineered antibodies”, *Protein Cell*, vol. 9, no. 1, pp. 86–120, Jan. 2018, doi: 10.1007/s13238-017-0457-8.
- [74] G. P. Smith and V. A. Petrenko, “Phage Display”, *Chem Rev*, vol. 97, no. 2, pp. 391–410, Apr. 1997, doi: 10.1021/cr960065d.
- [75] J. W. Kehoe and B. K. Kay, “Filamentous phage display in the new millennium”, *Chem Rev*, vol. 105, no. 11, pp. 4056–4072, Nov. 2005, doi: 10.1021/cr000261r.
- [76] G. Garufi, O. Minenkova, C. lo Passo, I. Pernice, and F. Felici, “Display libraries on bacteriophage lambda capsid”, *Biotechnology Annual Review*, vol. 11, no. SUPPL. pp. 153–190, Sep. 28, 2005. doi: 10.1016/S1387-2656(05)11005-9.

- [77] N. Malys, D. Y. Chang, R. G. Baumann, D. Xie, and L. W. Black, “A bipartite bacteriophage T4 SOC and HOC randomized peptide display library: detection and analysis of phage T4 terminase (gp17) and late sigma factor (gp55) interaction”, *J Mol Biol*, vol. 319, no. 2, pp. 289–304, May 2002, doi: 10.1016/S0022-2836(02)00298-X.
- [78] Z. Kalniņa *et al.*, “Evaluation of T7 and lambda phage display systems for survey of autoantibody profiles in cancer patients”, *J Immunol Methods*, vol. 334, no. 1–2, pp. 37–50, May 2008, doi: 10.1016/j.jim.2008.01.022.
- [79] D. O’connell, B. Becerril, A. Roy-Burman, M. Daws, and J. D. Marks, “Phage versus phagemid libraries for generation of human monoclonal antibodies”, *J Mol Biol*, vol. 321, no. 1, pp. 49–56, Aug. 2002, doi: 10.1016/S0022-2836(02)00561-2.
- [80] L. Chasteen, J. Ayriss, P. Pavlik, and A. R. M. Bradbury, “Eliminating helper phage from phage display”, *Nucleic Acids Res*, vol. 34, no. 21, Dec. 2006, doi: 10.1093/nar/gkl772.
- [81] M. Baca, L. G. Presta, S. J. O’connor, and J. A. Wells, “Antibody humanization using monovalent phage display”, *J Biol Chem*, vol. 272(16), pp. 10678–84, Apr. 1997, doi: 10.1074/jbc.272.16.10678.
- [82] A. S. Kang, C. F. Barbas, K. D. Janda, S. J. Benkovic, and R. A. Lerner, “Linkage of recognition and replication functions by assembling combinatorial antibody Fab libraries along phage surfaces”, *Proc. Natl. Acad. Sci. USA*, vol. 88, no. 10, pp. 4363–4366, May 1991, doi: 10.1073/pnas.88.10.4363.
- [83] L. Shi *et al.*, “De novo selection of high-affinity antibodies from synthetic Fab libraries displayed on phage as pIX fusion proteins”, *J Mol Biol*, vol. 397, no. 2, pp. 385–396, Mar. 2010, doi: 10.1016/j.jmb.2010.01.034.
- [84] C.-H. Wu, I.-J. Liu, R.-M. Lu, and H.-C. Wu, “Advancement and applications of peptide phage display technology in biomedical science”, *J Biomed Sci*, vol. 23:8, Jan. 2016, doi: 10.1186/s12929-016-0223-x.
- [85] Z. Konthur, J. Wilde, and T. S. Lim, “Semi-automated Magnetic Bead-Based Antibody Selection from Phage Display Libraries”, in *Antibody Engineering*, vol. 1, Springer Berlin Heidelberg, 2010, pp. 267–287. doi: 10.1007/978-3-642-01144-3_18.
- [86] W. Noppe, F. Plieva, I. Y. Galaev, H. Pottel, H. Deckmyn, and B. Mattiasson, “Chromato-panning: An efficient new mode of identifying suitable ligands from phage display libraries”, *BMC Biotechnol*, vol. 9:21, Mar. 2009, doi: 10.1186/1472-6750-9-21.
- [87] M. Lunder, T. Bratkovič, U. Urleb, S. Kreft, and B. Štrukelj, “Ultrasound in phage display: A new approach to nonspecific elution”, *Biotechniques*, vol. 44, no. 7, pp. 893–900, Jun. 2008, doi: 10.2144/000112759.

- [88] J. Osbourn, L. Jeremius, and A. Duncan, “Current methods for the generation of human antibodies for the treatment of autoimmune diseases”, *Drug Discov Today*, vol. 8, no. 18, pp. 845–51, Sep. 2003, doi: 10.1016/s1359-6446(03)02803-4.
- [89] P. J. Meijer *et al.*, “Isolation of human antibody repertoires with preservation of the natural heavy and light chain pairing”, *J Mol Biol*, vol. 358, no. 3, pp. 764–772, May 2006, doi: 10.1016/j.jmb.2006.02.040.
- [90] K. Smith *et al.*, “Corrigendum: rapid generation of fully human monoclonal antibodies specific to a vaccinating antigen”, *Nat Protoc*, vol. 9, no. 12, p. 2903, Oct. 2014, doi: 10.1038/nprot1214-2903a.
- [91] N. Lonberg *et al.*, “Antigen-specific human antibodies from mice comprising four distinct genetic modifications”, *Nature*, vol. 368, no. 6474, pp. 856–859, Apr. 1994, doi: 10.1038/368856a0.
- [92] M. Mendez *et al.*, “Functional transplant of megabase human immunoglobulin loci recapitulates human antibody response in mice”, *Nat Genet*, vol. 15, no. 2, pp. 146–156, Feb. 1997, doi: 10.1038/ng0297-146.
- [93] T. S. Christopher, “Mice with a human touch”, *Nat Biotechnol*, vol. 25, no. 10, pp. 1075–7, Oct. 2007, doi: 10.1038/nbt1007-1075.
- [94] S. M. Mompó and Á. González-Fernández, “Antigen-Specific Human Monoclonal Antibodies from Transgenic Mice”, *Methods in Molecular Biology*, vol. 1904, pp. 253–291, 2019, doi: 10.1007/978-1-62703-586-6_13.
- [95] M. Brüggemann *et al.*, “Human antibody production in transgenic animals”, *Arch Immunol Ther Exp (Warsz)*, vol. 63, no. 2, pp. 101–108, Apr. 2015, doi: 10.1007/s00005-014-0322-x.
- [96] I. Ishida, K. Tomizuka, H. Yoshida, and Y. Kuroiwa, “Transchromo mouseTM”, *Biotechnol Genet Eng Rev*, vol. 19, no. 1, pp. 73–83, Nov. 2002, doi: 10.1080/02648725.2002.10648023.
- [97] A. Jakobovits, R. G. Amado, X. Yang, L. Roskos, and G. Schwab, “From Xenomouse technology to panitumumab, the first fully human antibody product from transgenic mice”, *Nat Biotechnol*, vol. 25, no. 10, pp. 1134–1143, Oct. 2007, doi: 10.1038/nbt1337.
- [98] D. Ribatti, “From the discovery of monoclonal antibodies to their therapeutic application: an historical reappraisal”, *Immunol Lett*, vol. 161, no. 1, pp. 96–99, Sep. 2014, doi: 10.1016/j.imlet.2014.05.010.
- [99] C. A. K. Borrebaeck, A.-C. Malmberg, and M. Ohlin, “Does endogenous glycosylation prevent the use of mouse monoclonal antibodies as cancer therapeutics?”, *Immunol Today*, vol. 14, no. 10, pp. 477–9, Oct. 1993, doi: 10.1016/0167-5699(93)90259-n.

- [100] J. F. Scheid *et al.*, “Broad diversity of neutralizing antibodies isolated from memory B cells in HIV-infected individuals”, *Nature*, vol. 458, no. 7238, pp. 636–640, Apr. 2009, doi: 10.1038/nature07930.
- [101] T. Tiller, “Single B cell antibody technologies”, *N Biotechnol*, vol. 28, no. 5, pp. 453–457, Sep. 2011, doi: 10.1016/j.nbt.2011.03.014.
- [102] R. Kuppers, M. Zhao, M. L. Hansmann, and K. Rajewsky, “Tracing B cell development in human germinal centres by molecular analysis of single cells picked from histological sections”, *EMBO Journal*, vol. 12, no. 13, pp. 4955–4967, Dec. 1993, doi: 10.1002/j.1460-2075.1993.tb06189.x.
- [103] H. Obiakor, D. Sehgal, J. F. Dasso, R. F. Bonner, A. Malekafzali, and R. G. Mage, “A comparison of hydraulic and laser capture microdissection methods for collection of single B cells, PCR, and sequencing of antibody VDJ”, *Anal Biochem*, vol. 306, no. 1, pp. 55–62, Jul. 2002, doi: 10.1006/abio.2002.5671.
- [104] H. Wardemann, S. Yurasov, A. Schaefer, J. W. Young, E. Meffre, and M. C. Nussenzweig, “Predominant autoantibody production by early human B cell precursors”, *Science (1979)*, vol. 301, no. 5638, pp. 1374–1377, Sep. 2003, doi: 10.1126/science.1086907.
- [105] T. Tiller, E. Meffre, S. Yurasov, M. Tsuiji, M. C. Nussenzweig, and H. Wardemann, “Efficient generation of monoclonal antibodies from single human B cells by single cell RT-PCR and expression vector cloning”, *J Immunol Methods*, vol. 329, no. 1–2, pp. 112–124, Jan. 2008, doi: 10.1016/j.jim.2007.09.017.
- [106] A. Lagerkvist, C. Furebring, and C. Borrebaeck, “Single, antigen-specific B cells used to generate Fab fragments using CD40-mediated amplification or direct PCR cloning”, *Biotechniques*, vol. 18, no. 5, pp. 862–9, May 1995.
- [107] J. S. Babcook, K. B. Leslie, O. A. Olsen, R. A. Salmon, and J. W. Schrader, “A novel strategy for generating monoclonal antibodies from single, isolated lymphocytes producing antibodies of defined specificities”, *Proc Natl Acad Sci U S A*, vol. 93, no. 15, pp. 7843–7848, Jul. 1996, doi: 10.1073/pnas.93.15.7843.
- [108] F. L. Battye, A. Light, and D. M. Tarlinton, “Single cell sorting and cloning”, *J Immunol Methods*, vol. 243, no. 1–2, pp. 25–32, Sep. 2000, doi: 10.1016/s0022-1759(00)00225-8.
- [109] L. A. Herzenberg, D. Parks, B. Sahaf, O. Perez, M. Roederer, and L. A. Herzenberg, “The history and future of the fluorescence activated cell sorter and flow cytometry: a view from Stanford”, *Clin Chem*, vol. 48, no. 10, pp. 1819–1827, Oct. 2002.
- [110] J. F. Scheid *et al.*, “A method for identification of HIV gp140 binding memory B cells in human blood”, *J Immunol Methods*, vol. 343, no. 2, pp. 65–67, Apr. 2009, doi: 10.1016/j.jim.2008.11.012.

- [111] S. Tickle, R. Adams, D. Brown, M. Griffiths, D. Lightwood, and A. Lawson, “High-Throughput Screening for High Affinity Antibodies”, *J Lab Autom*, vol. 14, no. 5, pp. 303–307, 2009, doi: 10.1016/j.jala.2009.05.004.
- [112] J. C. Love, J. L. Ronan, G. M. Grotenbreg, A. G. van der Veen, and H. L. Ploegh, “A microengraving method for rapid selection of single cells producing antigen-specific antibodies”, *Nat Biotechnol*, vol. 24, no. 6, pp. 703–707, Jun. 2006, doi: 10.1038/nbt1210.
- [113] A. Jin *et al.*, “A rapid and efficient single-cell manipulation method for screening antigen-specific antibody-secreting cells from human peripheral blood”, *Nat Med*, vol. 15, no. 9, pp. 1088–1092, Sep. 2009, doi: 10.1038/nm.1966.
- [114] A. O. Ogunniyi, C. M. Story, E. Papa, E. Guillen, and J. C. Love, “Screening individual hybridomas by microengraving to discover monoclonal antibodies”, *Nat Protoc*, vol. 4, no. 5, pp. 767–782, 2009, doi: 10.1038/nprot.2009.40.
- [115] J. Wrammert *et al.*, “Rapid cloning of high-affinity human monoclonal antibodies against influenza virus”, *Nature*, vol. 453, no. 7195, pp. 667–671, May 2008, doi: 10.1038/nature06890.
- [116] A. Kantor, C. Merrill, L. Herzenberg, and J. Hillson, “An unbiased analysis of V(H)-D-J(H) sequences from B-1a, B-1b, and conventional B cells”, *J Immunol*, vol. 158, no. 3, pp. 1175–86, Feb. 1997.
- [117] A. Kantor *et al.*, “Construction of cDNA from single unstimulated mouse B lymphocytes: method and application to the study of expressed antibody repertoires in FACS-sorted murine B cell subsets”, *Handbook of Experimental Immunology*, vol. 13, pp. 1–6, 1998.
- [118] J. D. Marks, M. Tristem, A. Karpas, and G. Winte, “Oligonucleotide primers for polymerase chain reaction amplification of human immunoglobulin variable genes and design of family-specific oligonucleotide probes”, *Eur. J. Immunol*, vol. 21, pp. 985–991, Apr. 1991, doi: 10.1002/eji.1830210419.
- [119] X. Wang and B. David Stollar, “Human immunoglobulin variable region gene analysis by single cell RT-PCR”, *J Immunol Methods*, vol. 244, pp. 217–225, Oct. 2000, doi: 10.1016/s0022-1759(00)00260-x.
- [120] J. A. Coronella, P. Telleman, T. D. Truong, F. Ylera, and R. P. Junghans, “Amplification of IgG VH and VL (Fab) from single human plasma cells and B cells”, *Nucleic Acids Res*, vol. 28, no. 20, p. E85, Oct. 2000, doi: 10.1093/nar/28.20.e85.
- [121] H. X. Liao *et al.*, “High-throughput isolation of immunoglobulin genes from single human B cells and expression as monoclonal antibodies”, *J Virol Methods*, vol. 158, no. 1–2, pp. 171–179, Jun. 2009, doi: 10.1016/j.jviromet.2009.02.014.
- [122] M. J. Embleton, G. Gorochov, P. T. Jones, and G. Winter, “In-cell PCR from mRNA: amplifying and linking the rearranged immunoglobulin heavy and light

- chain V-genes within single cells”, *Nucleic Acids Res*, vol. 20, no. 15, pp. 3831–3837, Aug. 1992, doi: 10.1093/nar/20.15.3831.
- [123] P. C. Wilson *et al.*, “Somatic hypermutation introduces insertions and deletions into immunoglobulin V genes”, *J. Exp. Med*, vol. 187, no. 1, pp. 59–70, Jan. 1998, doi: 10.1084/jem.187.1.59.
- [124] R. M. T de Wildt, W. J. van Venrooij, G. Winter, R. M. A Hoet, and I. M. Tomlinson, “Somatic insertions and deletions shape the human antibody repertoire”, *J. Mol. Biol.*, vol. 294, no. 3, pp. 701–710, Dec. 1999, doi: 10.1006/jmbi.1999.3289.
- [125] R. A. Manz, A. E. Hauser, F. Hiepe, and A. Radbruch, “Maintenance of serum antibody levels”, *Annu Rev Immunol*, vol. 23, pp. 367–386, 2005, doi: 10.1146/annurev.immunol.23.021704.115723.
- [126] L. Fagerberg, K. Jonasson, G. von Heijne, M. Uhlén, and L. Berglund, “Prediction of the human membrane proteome”, *Proteomics*, vol. 10, no. 6, pp. 1141–1149, Mar. 2010, doi: 10.1002/pmic.200900258.
- [127] T. M. Bakheet and A. J. Doig, “Properties and identification of human protein drug targets”, *Bioinformatics*, vol. 25, no. 4, pp. 451–457, Feb. 2009, doi: 10.1093/bioinformatics/btp002.
- [128] C. Hutchings, M. Koglin, W. Olson, and F. Marshall, “Opportunities for therapeutic antibodies directed at G-protein-coupled receptors”, *Nat Rev Drug Discov*, vol. 16, no. 9, pp. 787–810, Sep. 2017, doi: 10.1038/nrd.2017.91.
- [129] C. J. Hutchings, P. Colussi, and T. G. Clark, “Ion channels as therapeutic antibody targets”, *MAbs*, vol. 11, no. 2, pp. 265–296, Feb. 2019, doi: 10.1080/19420862.2018.1548232.
- [130] Q. Yan, “Membrane transporters and drug development: relevance to pharmacogenomics, nutrigenomics, epigenetics, and systems biology”, *Methods Mol Biol*, vol. 637, pp. 1–21, 2010, doi: 10.1007/978-1-60761-700-6_1.
- [131] D. E. Grigoriadis, S. R. J. Hoare, S. M. Lechner, D. H. Slee, and J. A. Williams, “Drugability of extracellular targets: Discovery of small molecule drugs targeting allosteric, functional, and subunit-selective sites on GPCRs and ion channels”, *Neuropsychopharmacology*, vol. 34, no. 1, pp. 106–125, Jan. 2009, doi: 10.1038/npp.2008.149.
- [132] A. Y. Ye, Q. R. Liu, C. Y. Li, M. Zhao, and H. Qu, “Human transporter database: comprehensive knowledge and discovery tools in the human transporter genes”, *PLoS One*, vol. 9, no. 2, Feb. 2014, doi: 10.1371/journal.pone.0088883.
- [133] R. Santos *et al.*, “A comprehensive map of molecular drug targets”, *Nat Rev Drug Discov*, vol. 16, no. 1, pp. 19–34, Jan. 2017, doi: 10.1038/nrd.2016.230.
- [134] T. I. Oprea *et al.*, “Unexplored therapeutic opportunities in the human genome”, *Nat Rev Drug Discov*, vol. 17, no. 5, pp. 317–332, May 2018, doi: 10.1038/nrd.2018.14.

- [135] M. Ovacik and K. Lin, “Tutorial on Monoclonal Antibody Pharmacokinetics and Its Considerations in Early Development”, *Clin Transl Sci*, vol. 11, no. 6, pp. 540–552, Nov. 2018, doi: 10.1111/cts.12567.
- [136] I. Zafir-Lavie, Y. Michaeli, and Y. Reiter, “Novel antibodies as anticancer agents”, *Oncogene*, vol. 26, no. 25, pp. 3714–3733, May 2007, doi: 10.1038/sj.onc.1210372.
- [137] B. V. Ayyar, S. Arora, and R. O’Kennedy, “Coming-of-Age of Antibodies in Cancer Therapeutics”, *Trends Pharmacol Sci*, vol. 37, no. 12, pp. 1009–1028, Dec. 2016, doi: 10.1016/j.tips.2016.09.005.
- [138] R. Niwa *et al.*, “Defucosylated chimeric anti-CC chemokine receptor 4 IgG1 with enhanced antibody-dependent cellular cytotoxicity shows potent therapeutic activity to T-cell leukemia and lymphoma”, *Cancer Res*, vol. 64, no. 6, pp. 2127–2133, Mar. 2004, doi: 10.1158/0008-5472.can-03-2068.
- [139] L. Shi *et al.*, “Pharmacologic Characterization of AMG 334, a Potent and Selective Human Monoclonal Antibody against the Calcitonin Gene-Related Peptide Receptor”, *J Pharmacol Exp Ther*, vol. 356, no. 1, pp. 223–231, Jan. 2016, doi: 10.1124/jpet.115.227793.
- [140] D. N. Wiseman *et al.*, “Expression and purification of recombinant G protein-coupled receptors: A review”, *Protein Expr Purif*, vol. 167, p. 105524, Mar. 2020, doi: 10.1016/j.pep.2019.105524.
- [141] M. Haffke, M. Duckely, C. Bergsdorf, V. P. Jaakola, and B. Shrestha, “Development of a biochemical and biophysical suite for integral membrane protein targets: A review”, *Protein Expr Purif*, vol. 167, p. 105545, Mar. 2020, doi: 10.1016/j.pep.2019.105545.
- [142] J. C. Errey and C. Fiez-Vandal, “Production of membrane proteins in industry: The example of GPCRs”, *Protein Expr Purif*, vol. 169, p. 105569, May 2020, doi: 10.1016/j.pep.2020.105569.
- [143] C. A. Sarkar *et al.*, “Directed evolution of a G protein-coupled receptor for expression, stability, and binding selectivity”, *Proc Natl Acad Sci U S A*, vol. 105, no. 39, pp. 14808–13, 2008, doi: 10.1073/pnas.0803103105.
- [144] S. Mallipeddi, N. Zvonok, and A. Makriyannis, “Expression, Purification and Characterization of the Human Cannabinoid 1 Receptor”, *Sci Rep*, vol. 8, no. 1, p. 2935, Feb. 2018, doi: 10.1038/s41598-018-19749-5.
- [145] B. Byrne, “*Pichia pastoris* as an expression host for membrane protein structural biology”, *Curr Opin Struct Biol*, vol. 32, pp. 9–17, Jun. 2015, doi: 10.1016/j.sbi.2015.01.005.
- [146] S. J. Routledge *et al.*, “The synthesis of recombinant membrane proteins in yeast for structural studies”, *Methods*, vol. 95, pp. 26–37, Feb. 2016, doi: 10.1016/j.ymeth.2015.09.027.

- [147] A. L. Aloia, R. v. Glatz, E. J. McMurchie, and W. R. Leifert, “GPCR expression using baculovirus-infected Sf9 cells”, *Methods Mol Biol*, vol. 552, pp. 115–129, 2009, doi: 10.1007/978-1-60327-317-6_8.
- [148] J. A. Lyons, A. Shahsavari, P. A. Paulsen, B. P. Pedersen, and P. Nissen, “Expression strategies for structural studies of eukaryotic membrane proteins”, *Curr Opin Struct Biol*, vol. 38, pp. 137–144, Jun. 2016, doi: 10.1016/j.sbi.2016.06.011.
- [149] A. Ooi, A. Wong, L. Esau, F. Lemtiri-Chlieh, and C. Gehring, “A Guide to Transient Expression of Membrane Proteins in HEK-293 Cells for Functional Characterization”, *Front Physiol*, vol. 7, no. JUL, p. 300, Jul. 2016, doi: 10.3389/fphys.2016.00300.
- [150] N. Tandon, K. N. Thakkar, E. L. LaGory, Y. Liu, and A. J. Giaccia, “Generation of Stable Expression Mammalian Cell Lines Using Lentivirus”, *Bio Protoc*, vol. 8, no. 21, Nov. 2018, doi: 10.21769/bioprotoc.3073.
- [151] B. S. Lee, J. S. Huang, L. P. Jayathilaka, J. Lee, and S. Gupta, “Antibody production with synthetic peptides”, *Methods in Molecular Biology*, vol. 1474, pp. 25–47, 2016, doi: 10.1007/978-1-4939-6352-2_2.
- [152] R. Matar-Merheb *et al.*, “Structuring detergents for extracting and stabilizing functional membrane proteins”, *PLoS One*, vol. 6, no. 3, 2011, doi: 10.1371/journal.pone.0018036.
- [153] P. S. Chae *et al.*, “Maltose-neopentyl glycol (MNG) amphiphiles for solubilization, stabilization and crystallization of membrane proteins”, *Nat Methods*, vol. 7, no. 12, pp. 1003–1008, Dec. 2010, doi: 10.1038/nmeth.1526.
- [154] I. G. Denisov, Y. v. Grinkova, A. A. Lazarides, and S. G. Sligar, “Directed self-assembly of monodisperse phospholipid bilayer Nanodiscs with controlled size”, *J Am Chem Soc*, vol. 126, no. 11, pp. 3477–3487, Mar. 2004, doi: 10.1021/ja0393574.
- [155] J. Frauenfeld *et al.*, “A saposin-lipoprotein nanoparticle system for membrane proteins”, *Nat Methods*, vol. 13, no. 4, pp. 345–351, Apr. 2016, doi: 10.1038/nmeth.3801.
- [156] S. C. Lee *et al.*, “A method for detergent-free isolation of membrane proteins in their local lipid environment”, *Nat Protoc*, vol. 11, no. 7, pp. 1149–1162, Jul. 2016, doi: 10.1038/nprot.2016.070.
- [157] M. L. Carlson *et al.*, “The Peptidisc, a simple method for stabilizing membrane proteins in detergent-free solution”, *Elife*, vol. 7, Aug. 2018, doi: 10.7554/eLife.34085.001.
- [158] M. Delchambre *et al.*, “The GAG precursor of simian immunodeficiency virus assembles into virus-like particles”, *EMBO Journal*, vol. 8, no. 9, pp. 2653–2660, 1989, doi: 10.1002/j.1460-2075.1989.tb08405.x.

- [159] A. A. Kondrashin, Kh. Mikel'saar, E. G. Semenova, and B. P. Skulachev, "Role of phospholipids in the generation of membrane potentials by proteoliposomes", *Biokhimiia*, vol. 40, no. 5, pp. 1071–80, 1975.
- [160] T. Mirzabekov, H. Kontos, M. Farzan, W. Marasco, and J. Sodroski, "Paramagnetic proteoliposomes containing a pure, native, and oriented seven-transmembrane segment protein, CCR5", *Nat Biotechnol*, vol. 18(6), pp. 649–54, 2000, doi: 10.1038/76501.
- [161] C. S. Colley, E. England, J. E. Linley, and T. C. I. Wilkinson, "Screening Strategies for the Discovery of Ion Channel Monoclonal Antibodies", *Curr Protoc Pharmacol*, vol. 82, no. 1, Sep. 2018, doi: 10.1002/cpph.44.
- [162] J. Andréll and C. G. Tate, "Overexpression of membrane proteins in mammalian cells for structural studies.", *Mol Membr Biol*, vol. 30, no. 1, pp. 52–63, Feb. 2013, doi: 10.3109/09687688.2012.703703.
- [163] R. McMillan, R. Longmire, R. Yelenosky, J. Lang, V. Heath, and C. Craddock, "Immunoglobulin synthesis by human lymphoid tissues normal bone marrow as a major site of IgG production", *J Immunol*, vol. 109, no. 6, pp. 1386–1394, Dec. 1972.
- [164] M. Slifka and R. Ahmed, "Long-lived plasma cells: a mechanism for maintaining persistent antibody production", *Curr Opin Immunol*, vol. 10, no. 3, pp. 252–258, Jun. 1998, doi: 10.1016/s0952-7915(98)80162-3.
- [165] M. Shapiro-Shelef and K. C. Calame, "Regulation of plasma-cell development", *Nat Rev Immunol*, vol. 5, no. 3, pp. 230–242, Mar. 2005, doi: 10.1038/nri1572.
- [166] U. Chen-Bettecken, E. Wecker, and A. Schimpl, "Transcriptional control of μ - and κ -Gene expression in resting and bacterial lipopolysaccharide-activated normal B cells", *Immunobiology*, vol. 174, no. 2, pp. 162–176, Mar. 1987, doi: 10.1016/S0171-2985(87)80036-0.
- [167] C. C. Uphoff and H. G. Drexler, "Comparative PCR Analysis for detection of mycoplasma infections in continuous cell lines", *In Vitro Cellular & Development Biology. Animal*, vol. 38, no. 2, pp. 79–85, Feb. 2002, doi: 10.1290/1071-2690(2002)038<0079:CPAFDO>2.0.CO;2.
- [168] C. C. Uphoff and H. G. Drexler, "Detecting Mycoplasma Contamination in Cell Cultures by Polymerase Chain Reaction", *Methods Mol Med*, vol. 88, pp. 319–326, 2004, doi: 10.1385/1-59259-406-9:319.
- [169] A. J. Tarashansky, Y. Xue, P. Li, S. R. Quake, and B. Wang, "Self-assembling manifolds in single-cell RNA sequencing data", *Elife*, vol. 8, Sep. 2019, doi: 10.7554/eLife.48994.
- [170] J. W. Bagnoli *et al.*, "Sensitive and powerful single-cell RNA sequencing using mcSCRIB-seq", *Nat Commun*, vol. 9, no. 1, p. 2937, Jul. 2018, doi: 10.1038/s41467-018-05347-6.

- [171] T. Tiller, C. E. Busse, and H. Wardemann, “Cloning and expression of murine Ig genes from single B cells”, *J Immunol Methods*, vol. 350, no. 1–2, pp. 183–193, Oct. 2009, doi: 10.1016/j.jim.2009.08.009.
- [172] S. O’Gorman, D. Fox, and G. Wahl, “Recombinase-mediated gene activation and site-specific integration in mammalian cells”, *Science (1979)*, vol. 251, no. 4999, pp. 1351–1355, Mar. 1991, doi: 10.1126/science.1900642.
- [173] X. Liang *et al.*, “Transcriptionally active polymerase chain reaction (TAP): high throughput gene expression using genome sequence data”, *Journal of Biological Chemistry*, vol. 277, no. 5, pp. 3593–3598, Feb. 2002, doi: 10.1074/jbc.M110652200.
- [174] G. To’a Salazar, Z. Huang, N. Zhang, X. G. Zhang, and Z. An, “Antibody Therapies Targeting Complex Membrane Proteins”, *Engineering*, vol. 7, no. 11, pp. 1541–1551, Nov. 2021, doi: 10.1016/j.eng.2020.11.013.
- [175] Y. Zhang *et al.*, “Selection of active ScFv to G-protein-coupled receptor CCR5 using surface antigen-mimicking peptides”, *Biochemistry*, vol. 43, no. 39, pp. 12575–12584, Oct. 2004, doi: 10.1021/bi0492152.
- [176] R. S. Boshuizen *et al.*, “A combination of in vitro techniques for efficient discovery of functional monoclonal antibodies against human CXC chemokine receptor-2 (CXCR2)”, *MAbs*, vol. 6, no. 6, pp. 1415–1424, Nov. 2014, doi: 10.4161/mabs.36237.
- [177] Y. Sasaki *et al.*, “Establishment of a novel monoclonal antibody against LGR5”, *Biochem Biophys Res Commun*, vol. 394, no. 3, pp. 498–502, Apr. 2010, doi: 10.1016/j.bbrc.2010.02.166.
- [178] G. Buell *et al.*, “Blockade of Human P2X 7 Receptor Function With a Monoclonal Antibody”, *Blood*, vol. 92, no. 10, pp. 3521–3528, Nov. 1998.
- [179] F. F. Lin *et al.*, “Generation and characterization of fully human monoclonal antibodies against human Orai1 for autoimmune diseases”, *Journal of Pharmacology and Experimental Therapeutics*, vol. 345, no. 2, pp. 225–238, May 2013, doi: 10.1124/jpet.112.202788.
- [180] G. L. Harris, M. B. Creason, G. B. Brulte, and D. R. Herr, “In vitro and in vivo antagonism of a g protein-coupled receptor (S1P3) with a novel blocking monoclonal antibody”, *PLoS One*, vol. 7, no. 4, Apr. 2012, doi: 10.1371/journal.pone.0035129.
- [181] H. Yan *et al.*, “Fully human monoclonal antibodies antagonizing the glucagon receptor improve glucose homeostasis in mice and monkeys”, *Journal of Pharmacology and Experimental Therapeutics*, vol. 329, no. 1, pp. 102–111, Apr. 2009, doi: 10.1124/jpet.108.147009.

Appendix–A

Generation of a poly–epitope antigen and a stable cell line to raise and screen antibody against TLS2

Design and production of pcDNA5_TLS2–EGFP recombinant plasmid

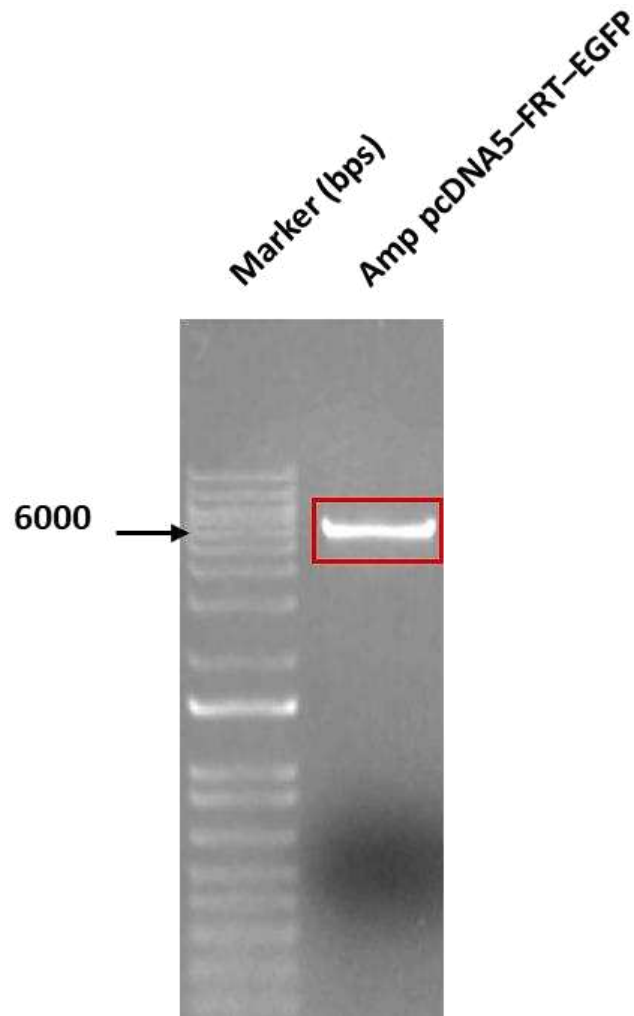


Figure A–1: Quality evaluation of the pcDNA5–FRT–EGFP recombinant plasmid amplification product. The red square highlights the presence of a band with dimension comparable to those expected for the amplified pcDNA5–FRT–EGFP vector (5808bps), which will be subsequently purified through QIAquick Gel Extraction Kit.

Design and production of pcDNA5_TLS2-EGFP recombinant plasmid

Table A-1: Bands generated through the enzymatic digestion of TLS2Full synthetic plasmid and amplified pcDNA5-EGFP vector.

Plasmids/Vector	Restriction enzymes	Generated bands	Band of interest
TLS2Full	HindIII + BamHI	6037bps + 1914bps	1914bps (insert)
pcDNA5-FRT-EGFP	HindIII + BamHI + AP	5730bps + 25bps+ 15bps	5730bps (vector)

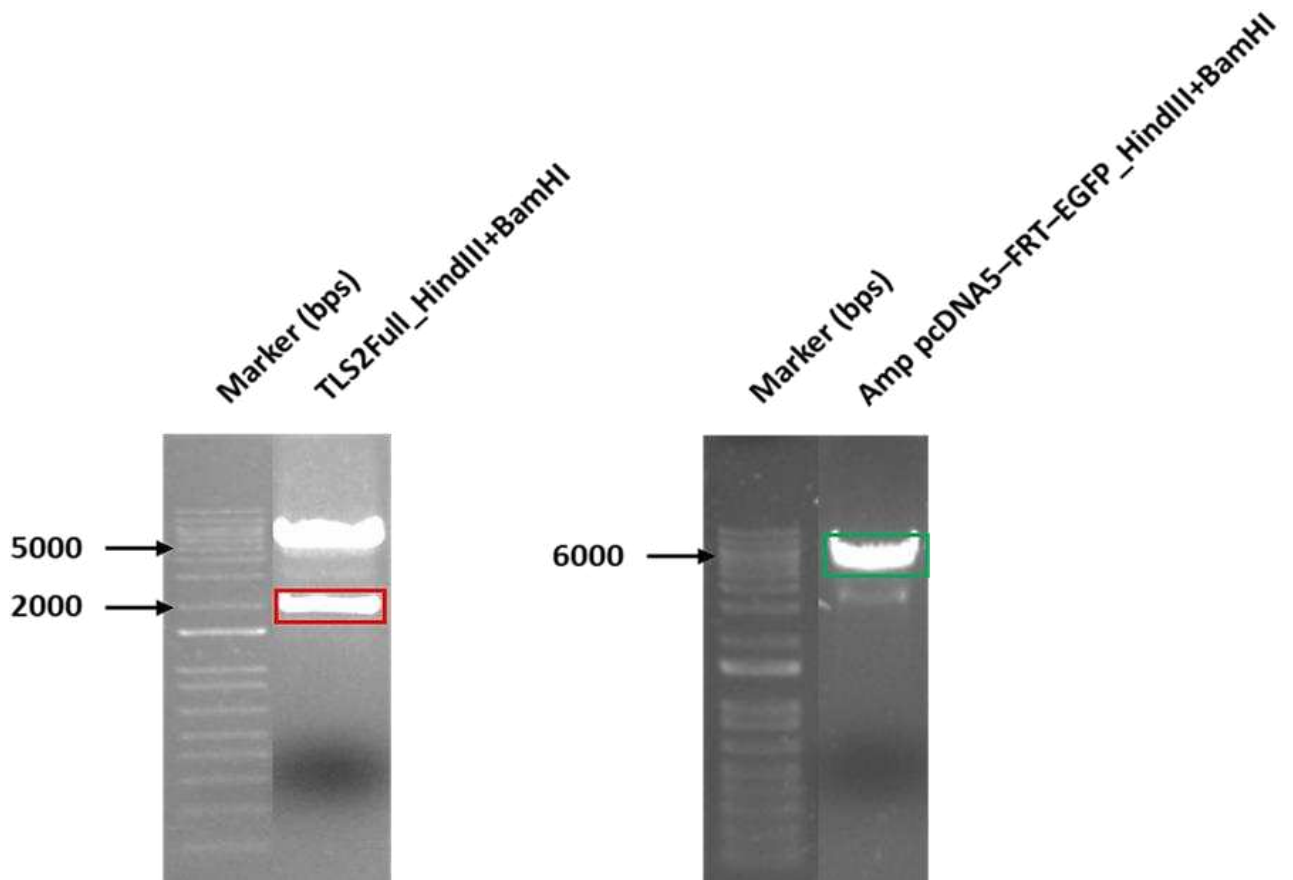


Figure A-2: *TLS2Full synthetic plasmid and pcDNA5-FRT-EGFP amplified vector digested with HindIII + BamHI restriction enzymes. The red square highlights the band corresponding to TLS2Full_HindIII+BamHI insert (1914bps), while the green square highlights the band corresponding to pcDNA5-FRT-EGFP_HindIII+BamHI vector (5730bps), which will be subsequently purified through QIAquick Gel Extraction Kit.*

Design and production of pcDNA5_TLS2-EGFP recombinant plasmid

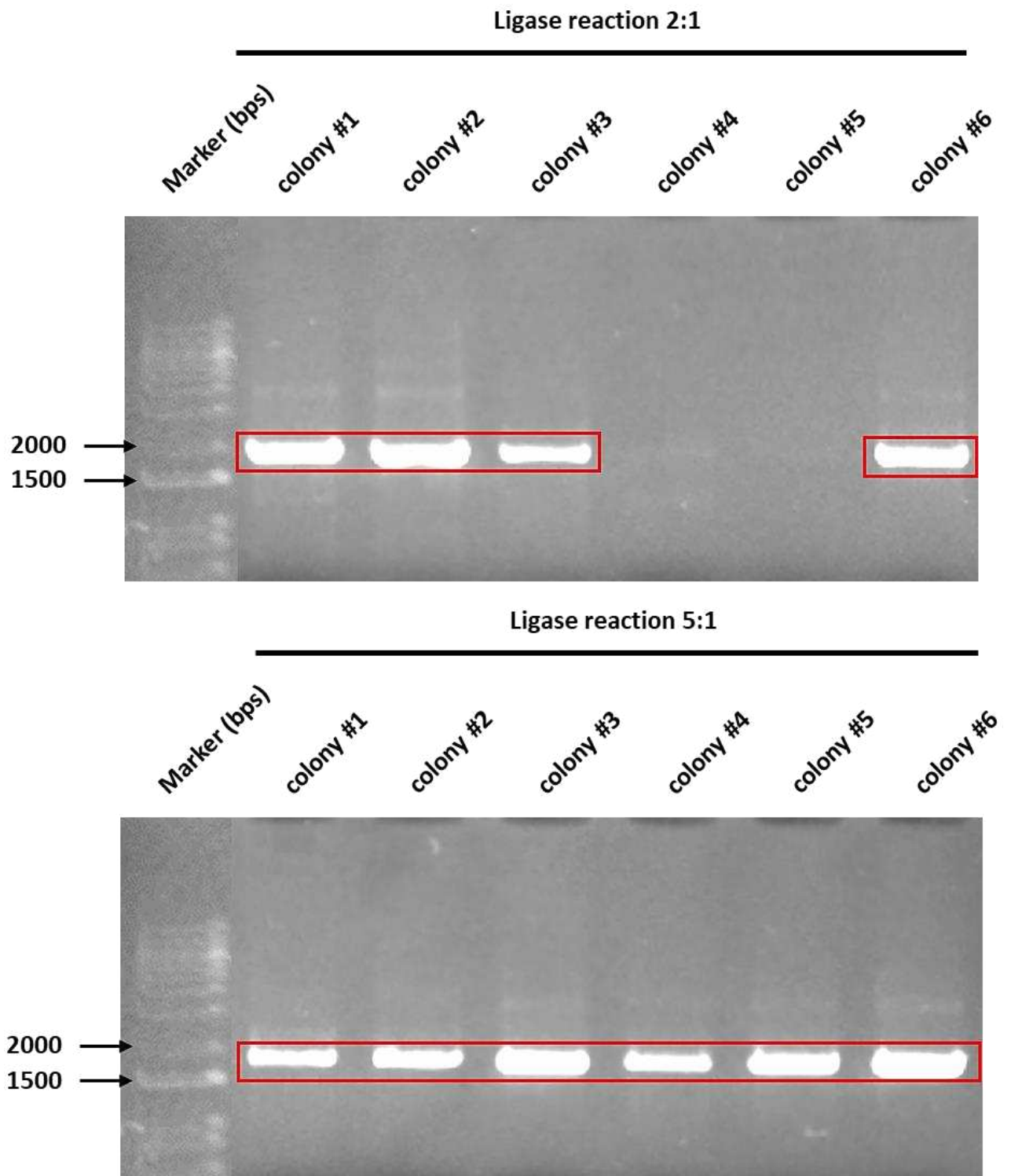


Figure A-3: Colony PCR for the screening of DH5 α colonies transformed with pcDNA5_TLS2-EGFP recombinant plasmid. The red squares highlight the bands corresponding to TLS2Full insert specific amplification product (1920bps).

Appendix–B

Revised approach to generate monoclonal antibodies recognizing conformational extracellular epitopes of TLS2

Design and production of pcDNA3.4_TLS2Loop4–6His recombinant plasmid

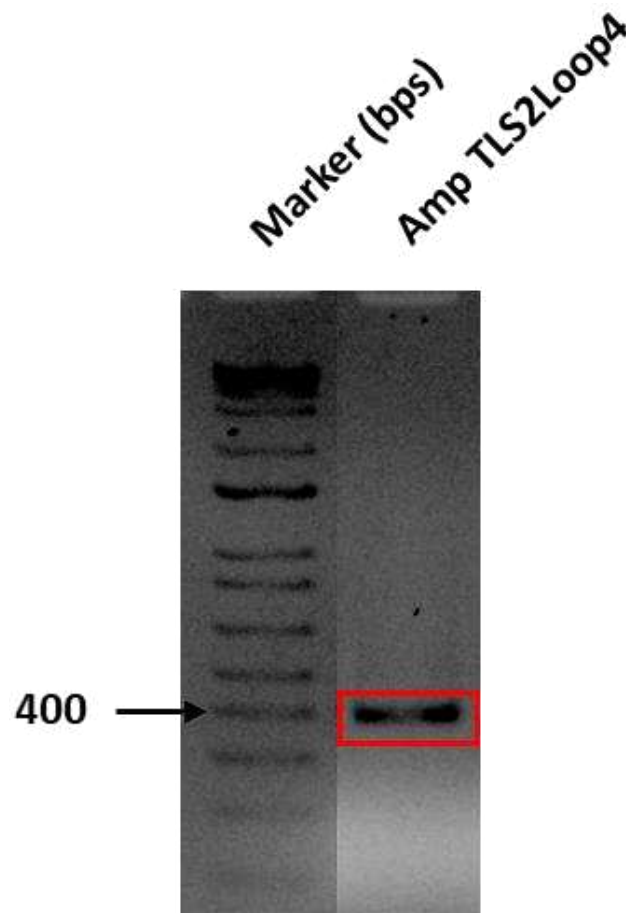


Figure B–1: Quality evaluation of the TLS2Loop4 synthetic DNA string amplification product. The red square highlights the presence of a band with dimension comparable to those expected for the amplified TLS2Loop4 insert (403bps), which will be subsequently purified through QIAquick Gel Extraction Kit.

Design and production of pcDNA3.4_TLS2Loop4-6His recombinant plasmid

Table B-1: Bands generated through the enzymatic digestion of amplified TLS2Loop4 insert and pcDNA3.4-6His synthetic plasmid.

DNA string/plasmid	Restriction enzymes	Generated bands	Band of interest
TLS2Loop4	HindIII + BamHI	352bps + 27bps + 24bps	352bps (insert)
pcDNA3.4-6His	HindIII + BamHI + AP	6046bps + 37bps	6046bps (vector)

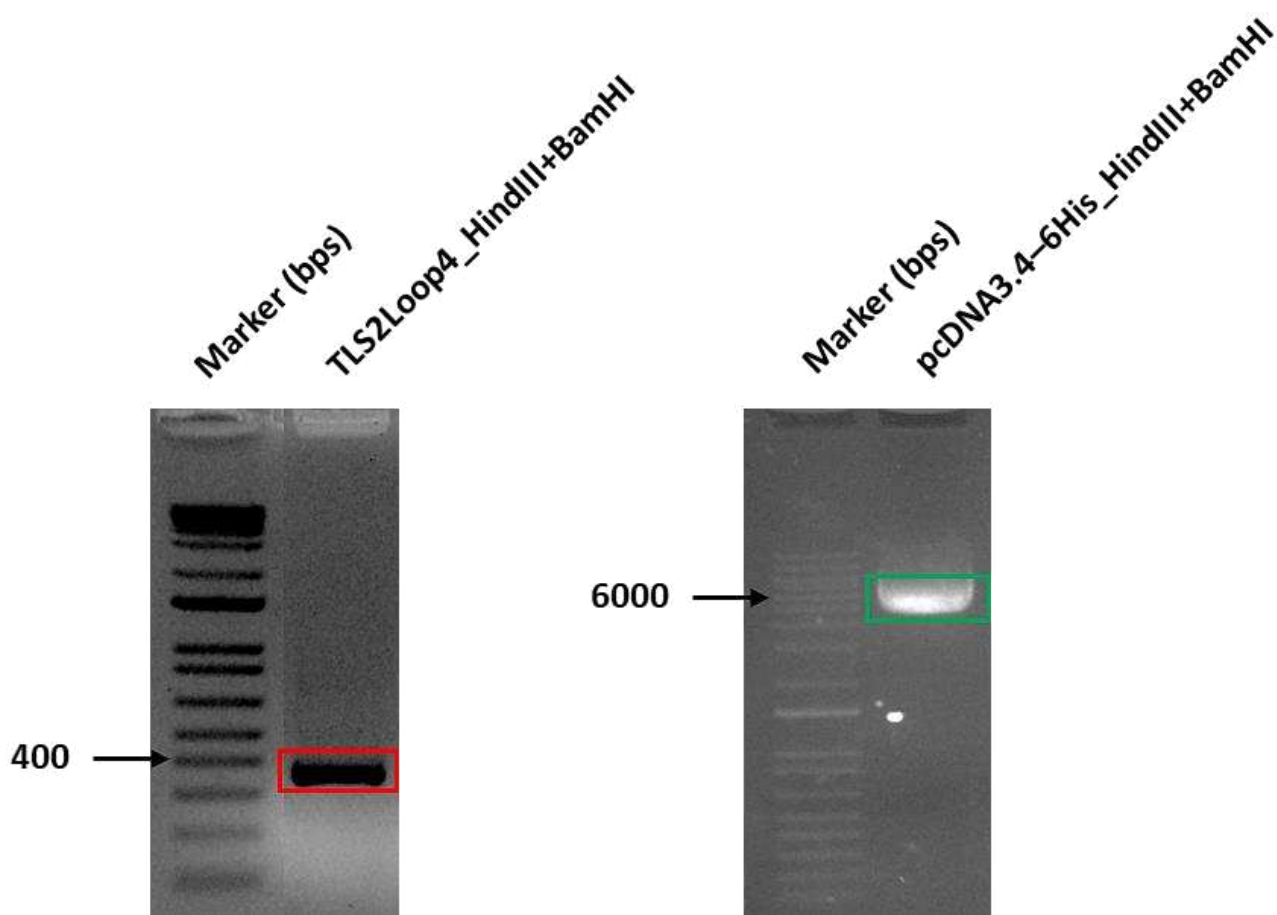


Figure B-2: Amplified TLS2Loop4 insert and pcDNA3.4-6His synthetic plasmid digested with HindIII + BamHI restriction enzymes. The red square highlights the band corresponding to TLS2Loop4_HindIII+BamHI insert (352bps), while the green square highlights the band corresponding to pcDNA3.4-6His_HindIII+BamHI vector (6046ps), which will be subsequently purified through QIAquick Gel Extraction Kit.

Design and production of pcDNA3.4_TLS2Loop4-6His recombinant plasmid

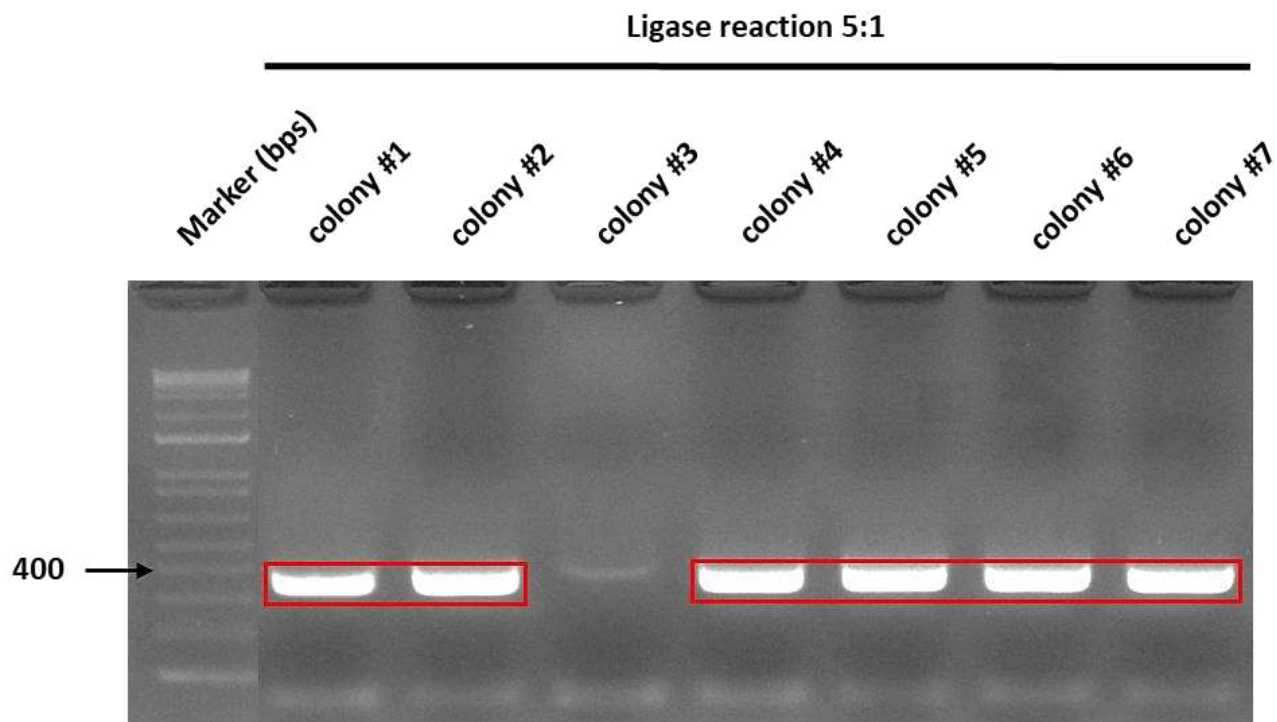


Figure B-3: Colony PCR for the screening of DH5a colonies transformed with pcDNA3.4_TLS2Loop4-6His recombinant plasmid. The red squares highlight the bands corresponding to TLS2Loop4 insert specific amplification product (367bps).

Design and production of a recombinant plasmid allowing the separate expression of TLS2 and EGFP from the same transcript (pcDNA5_TLS2–IRES–EGFP)

Table B-2: Bands generated through the enzymatic digestion of pAAV.CMV.Luc.IRES.EGFP.SV40 synthetic plasmid and pcDNA5_TLS2–EGFP recombinant plasmid.

Plasmids	Restriction enzymes	Generated bands	Band of interest
pAAV.CMV.Luc.IRES.EGFP.SV40	BamHI + NotI	6305bps + 1316bps	1316bps (insert)
pcDNA5_TLS2–EGFP	BamHI + NotI + AP	6916bps + 728bps	6916bps (vector)

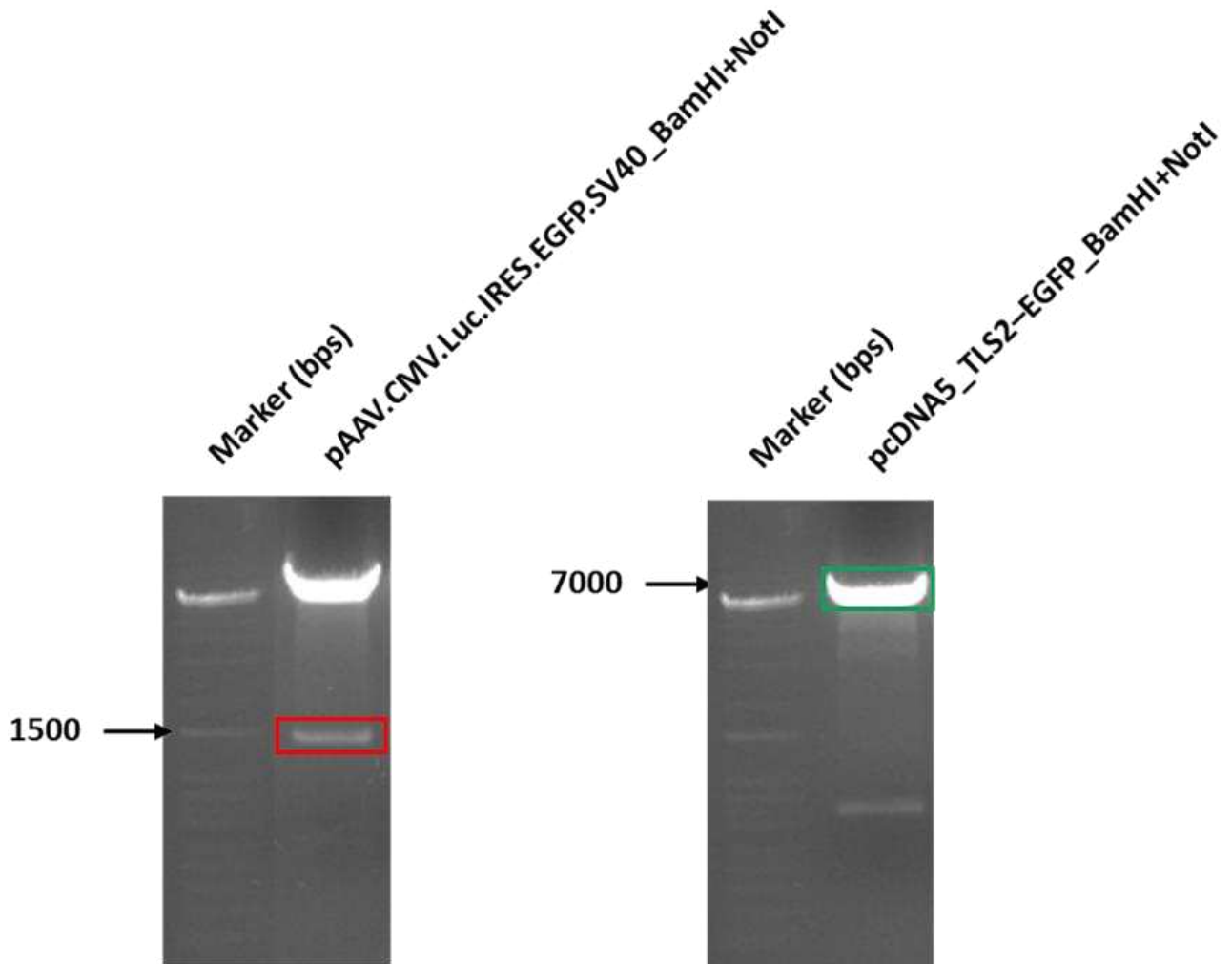


Figure B-4: pAAV.CMV.Luc.IRES.EGFP.SV40 synthetic plasmid and pcDNA5_TLS2–EGFP recombinant plasmid digested with BamHI + NotI restriction enzymes. The red square highlights the band corresponding to pIRES–EGFP_BamHI+NotI insert (1316bps), while the green square highlights the band corresponding to pcDNA5_TLS2nostop_BamHI+NotI vector (6916bps), which will be subsequently purified through QIAquick Gel Extraction Kit.

Design and production of a recombinant plasmid allowing the separate expression of TLS2 and EGFP from the same transcript (pcDNA5_TLS2-IRES-EGFP)

Table B-3: Bands generated through the enzymatic digestion of pcDNA5_TLS2nostop-IRES-EGFP recombinant plasmid.

Plasmid	Restriction enzyme	Generated bands
pDNA5_TLS2nostop-IRES-EGFP	HindIII	6082bps + 2150bps

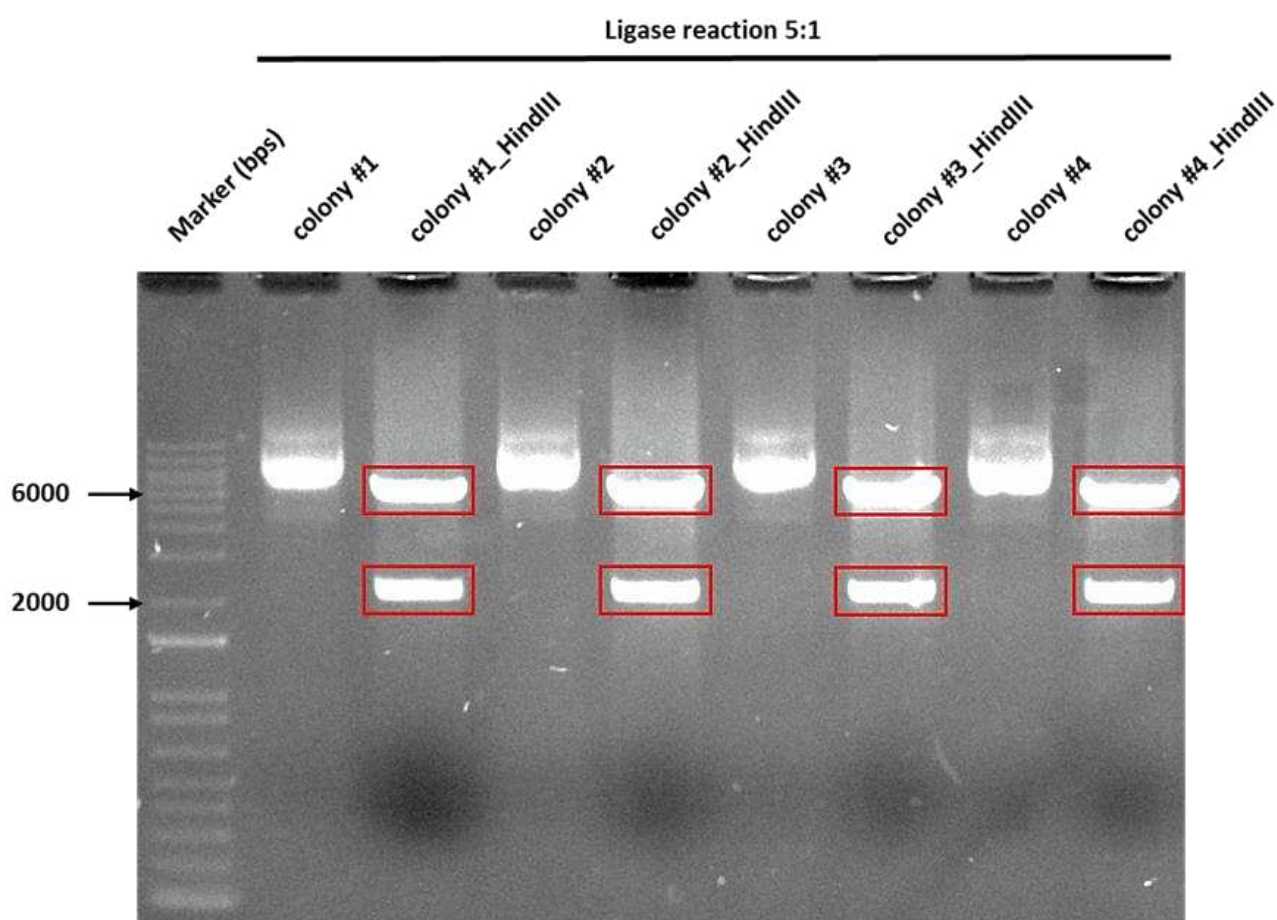


Figure B-5: Control digestion with HindIII restriction enzyme for the screening of DH5α colonies transformed with pcDNA5_TLS2nostop-IRES-EGFP recombinant plasmid. The red squares highlight the bands corresponding to the correct cloning of pIRES-EGFP insert into pcDNA5_TLS2nostop vector (6082bps + 2150bps).

Design and production of a recombinant plasmid allowing the separate expression of TLS2 and EGFP from the same transcript (pcDNA5_TLS2-IRES-EGFP)

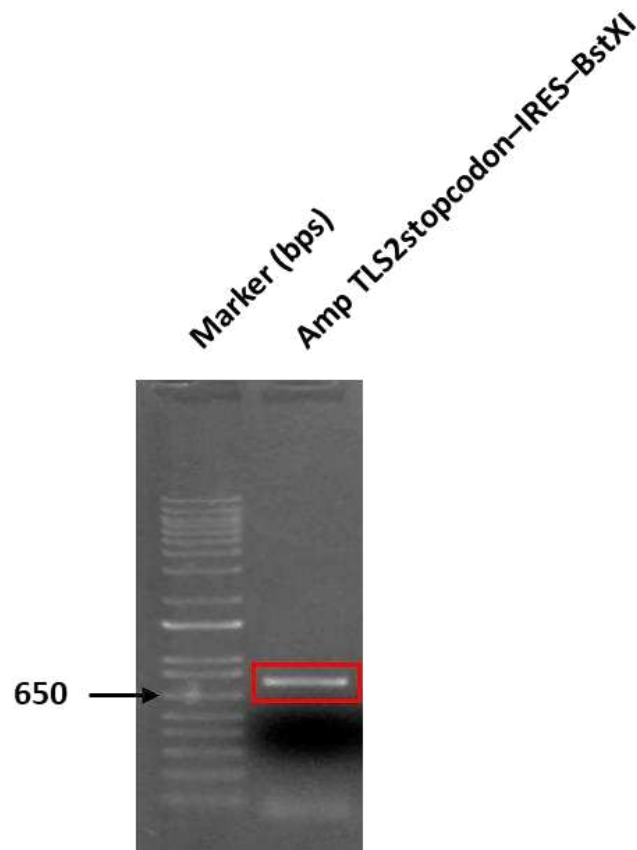


Figure B-6: *Quality evaluation of the TLS2stopcodon-IRES-BstXI synthetic DNA string amplification product. The red square highlights the presence of a band with dimension comparable to those expected for the amplified TLS2stopcodon-IRES-BstXI insert (701bps), which will be subsequently purified through QIAquick Gel Extraction Kit.*

Design and production of a recombinant plasmid allowing the separate expression of TLS2 and EGFP from the same transcript (pcDNA5_TLS2-IRES-EGFP)

Table B-4: Bands generated through the enzymatic digestion of amplified TLS2stopcodon-IRES-BstXI insert and pcDNA5_TLS2nostop-IRES-EGFP recombinant plasmid.

DNA string/plasmid	Restriction enzyme	Generated bands	Band of interest
TLS2stopcodon-IRES-BstXI	BstXI	659bps + 25bps + 17bps	659bps (insert)
pcDNA5_TLS2nostop-IRES-EGFP	BstXI	7573bps + 659bps	7562bps (vector)

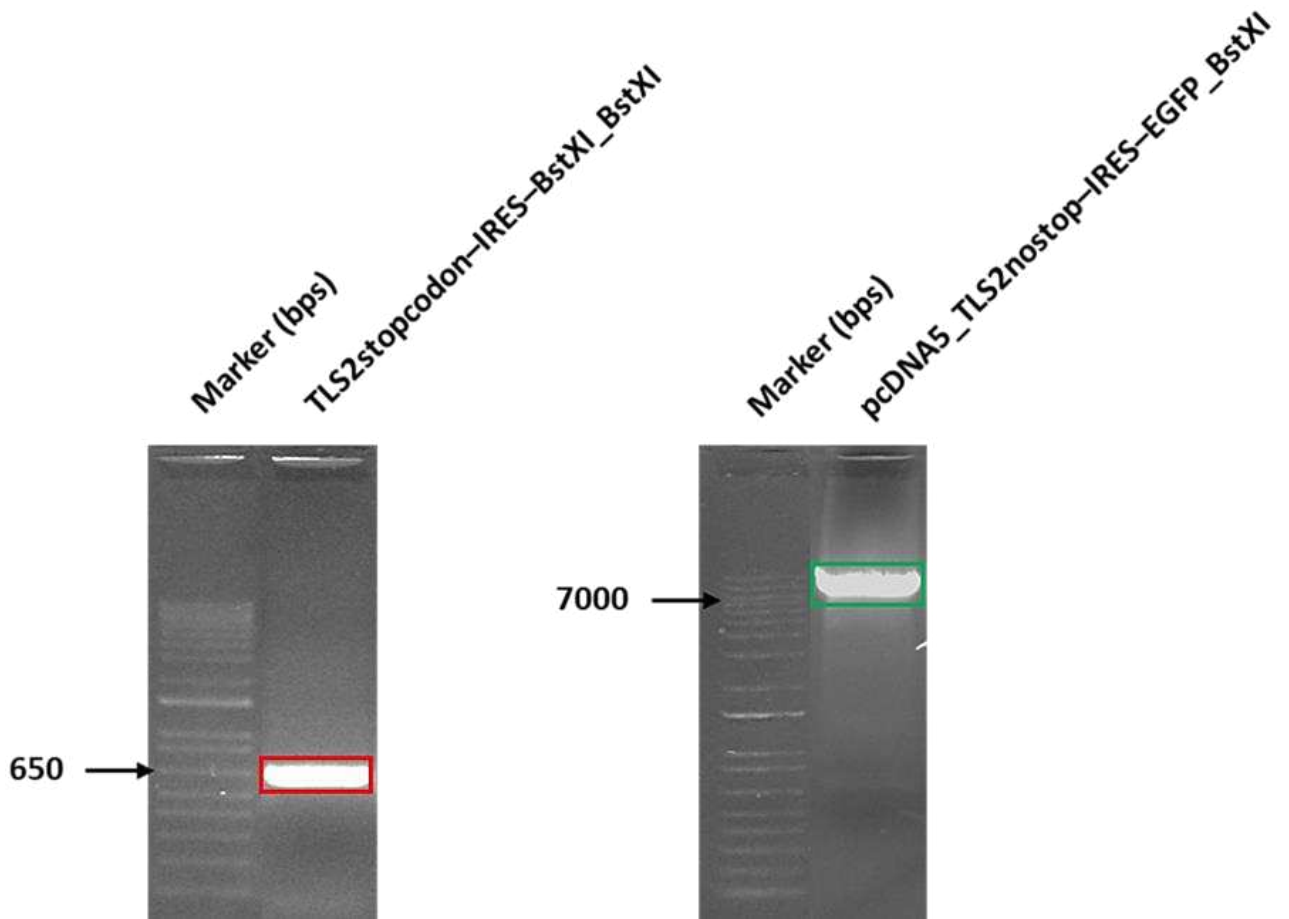


Figure B-7: Amplified TLS2stopcodon-IRES-BstXI insert and pcDNA5_TLS2nostop-IRES-EGFP recombinant plasmid digested with BstXI restriction enzyme. The red square highlights the band corresponding to TLS2stopcodon-IRES_BstXI insert (659bps), while the green square highlights the band corresponding to pcDNA5_TLS2nostop-IRES-EGFP_BstXI vector (7562bps), which will be subsequently purified through QIAquick Gel Extraction Kit.

Design and production of a recombinant plasmid allowing the separate expression of TLS2 and EGFP from the same transcript (pcDNA5_TLS2-IRES-EGFP)

Table B-5: Bands generated through the enzymatic digestion of pcDNA5_TLS2-IRES-EGFP recombinant plasmid.

Plasmid	Restriction enzyme	Generated bands
pcDNA5_TLS2-IRES-EGFP	XhoI	6904bps + 1328bps

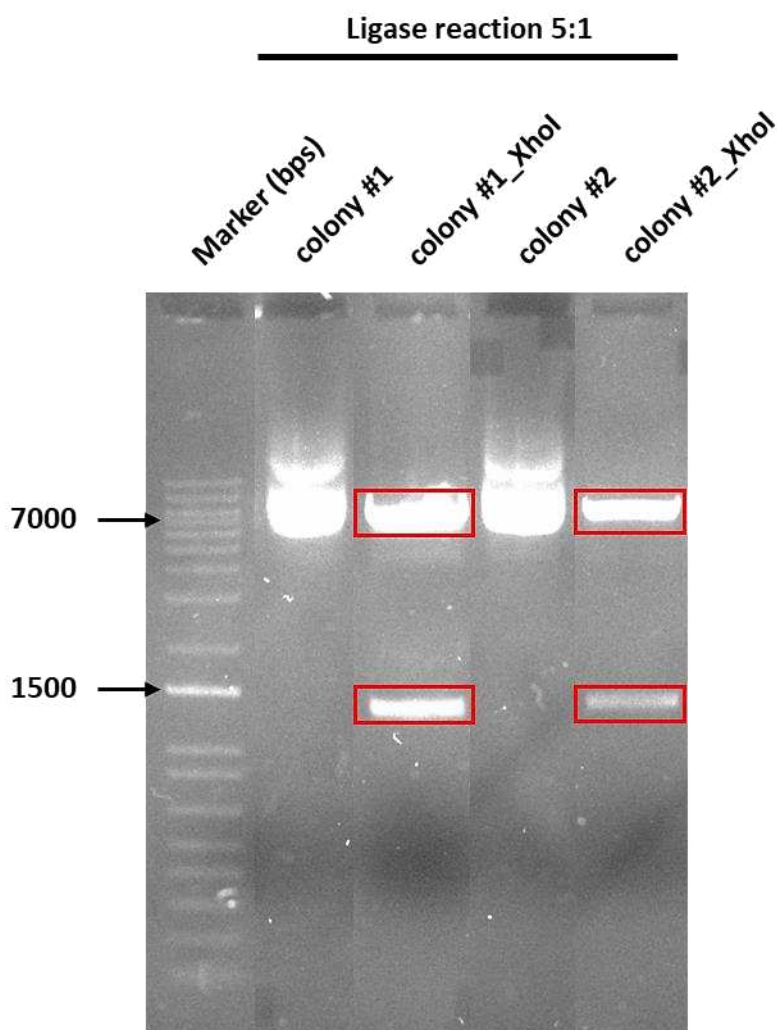


Figure B-8: Control digestion with XhoI restriction enzyme for the screening of DH5a colonies transformed with pcDNA5_TLS2-IRES-EGFP recombinant plasmid. The red squares highlight the bands corresponding to the correct cloning of TLS2stopcodon-IRES insert into pcDNA5_TLS2nostop-IRES-EGFP vector (6904bps + 1328bps).

Design and production of pcDNA3.4_cMyc-AP2 recombinant plasmid

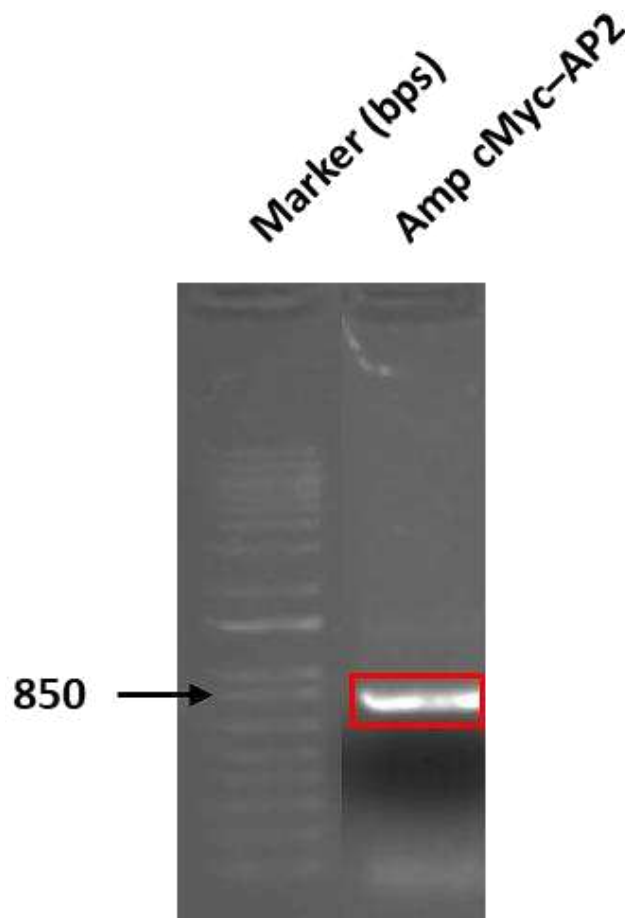


Figure B-9: Quality evaluation of the cMyc-AP2 synthetic DNA string amplification product. The red square highlights the presence of a band with dimension comparable to those expected for the amplified cMyc-AP2 insert (812bps), which will be subsequently purified through QIAquick Gel Extraction Kit.

Design and production of pcDNA3.4_cMyc-AP2 recombinant plasmid

Table B-6: Bands generated through the enzymatic digestion of amplified cMyc-AP2 insert and customized pcDNA3.4 plasmid.

DNA string/plasmid	Restriction enzymes	Generated bands	Band of interest
cMyc-AP2	HindIII + NotI	734bps + 51bps + 27bps	734bps (insert)
Customized pcDNA3.4	HindIII + NotI + AP	6037bps + 18bps	6037bps (vector)

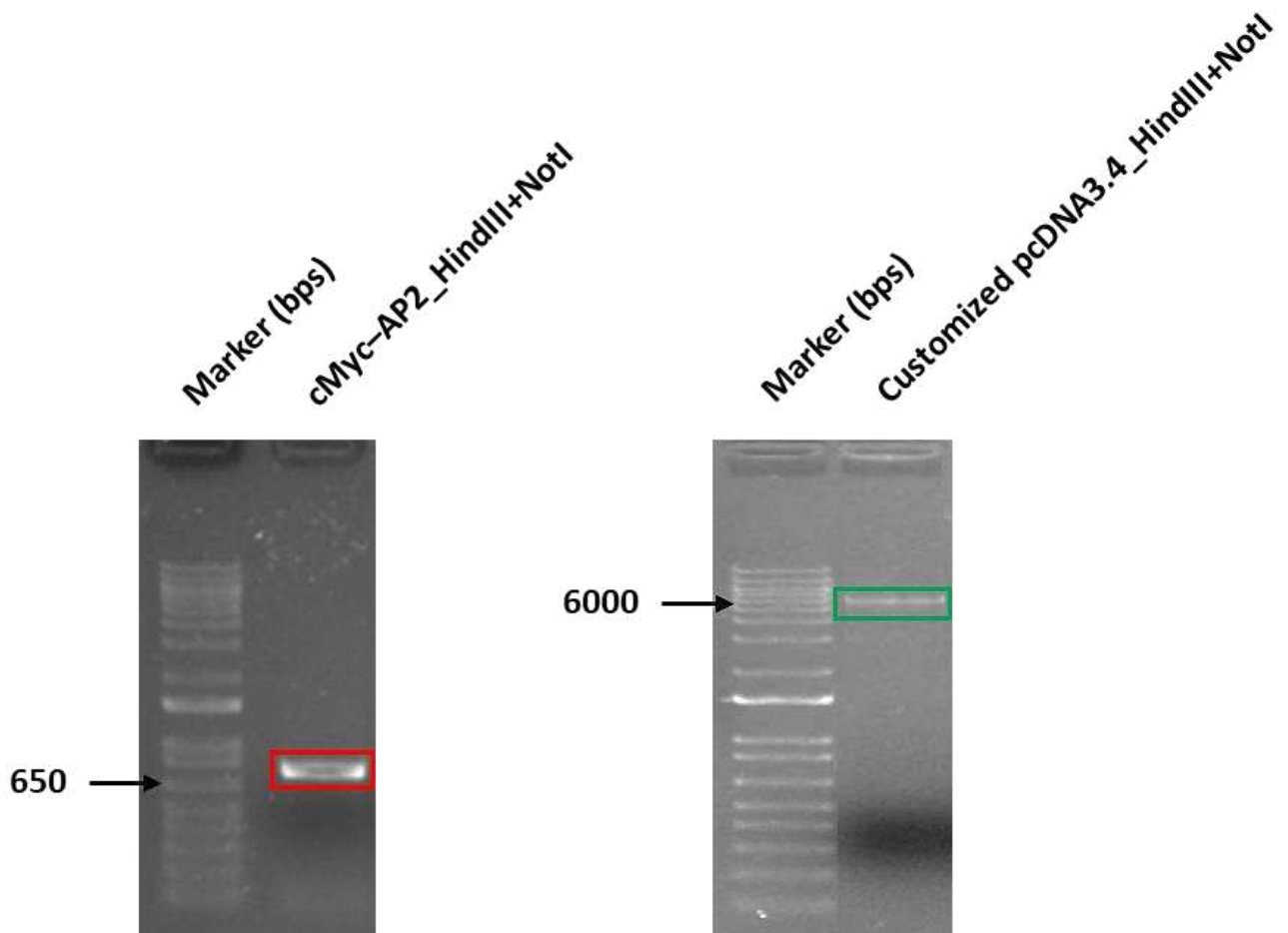


Figure B-10: Amplified cMyc-AP2 insert and customized pcDNA3.4 plasmid digested with HindIII + NotI restriction enzymes. The red square highlights the band corresponding to cMyc-AP2_HindIII+NotI insert (734bps), while the green square highlights the band corresponding to pcDNA3.4_HindIII+NotI vector (6037bps), which will be subsequently purified through QIAquick Gel Extraction Kit.

Design and production of pcDNA3.4_cMyc-AP2 recombinant plasmid

Table B-7: Bands generated through the enzymatic digestion of pcDNA3.4_cMyc-AP2 recombinant plasmid.

Plasmid	Restriction enzymes	Generated bands
pcDNA3.4_cMyc-AP2	XbaI + NotI	5998bps + 753bps

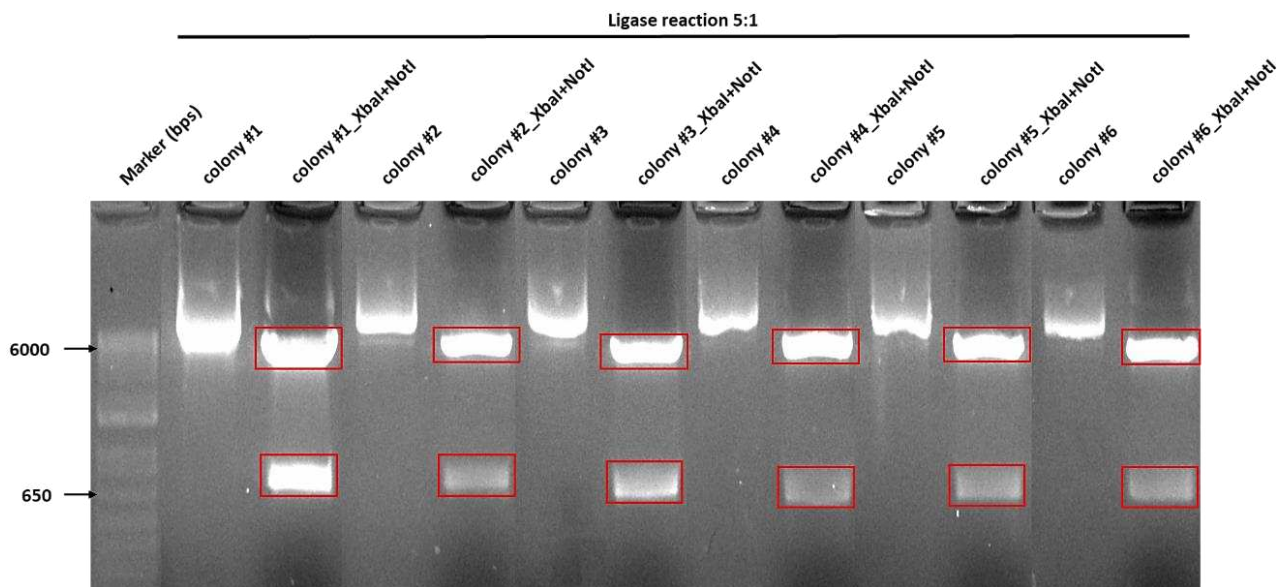


Figure B-11: Control digestion with XbaI and NotI restriction enzymes for the screening of DH5a colonies transformed with pcDNA3.4_cMyc-AP2 recombinant plasmid. The red squares highlight the bands corresponding to the correct cloning of cMyc-AP2 insert into pcDNA3.4 vector (5998bps + 753bps).

Recovery of VH and VL coding sequences from single antigen-specific ASCs and “minigenes” assembly

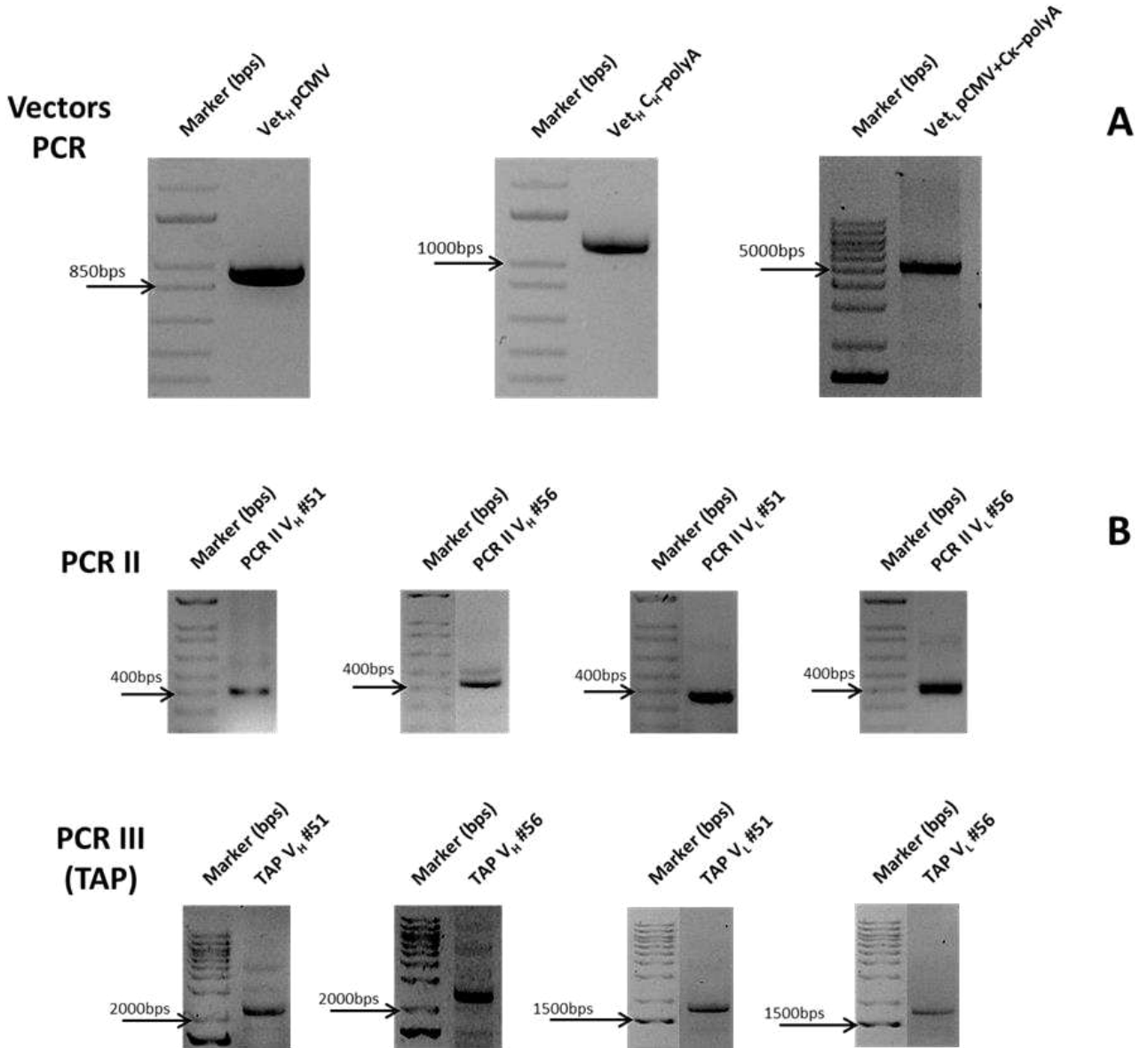


Figure B-12: PCR amplification products for the creation of the human CMV promoter and human constant region fragment fused to a BGH poly-A signal (A); PCR II and PCR III (TAP) amplification products for the creation of complete mAb#51 and mAb#56 TAP V_H/V_L chimeric minigenes (B).

V_H and V_L sequences cloning into expression vectors

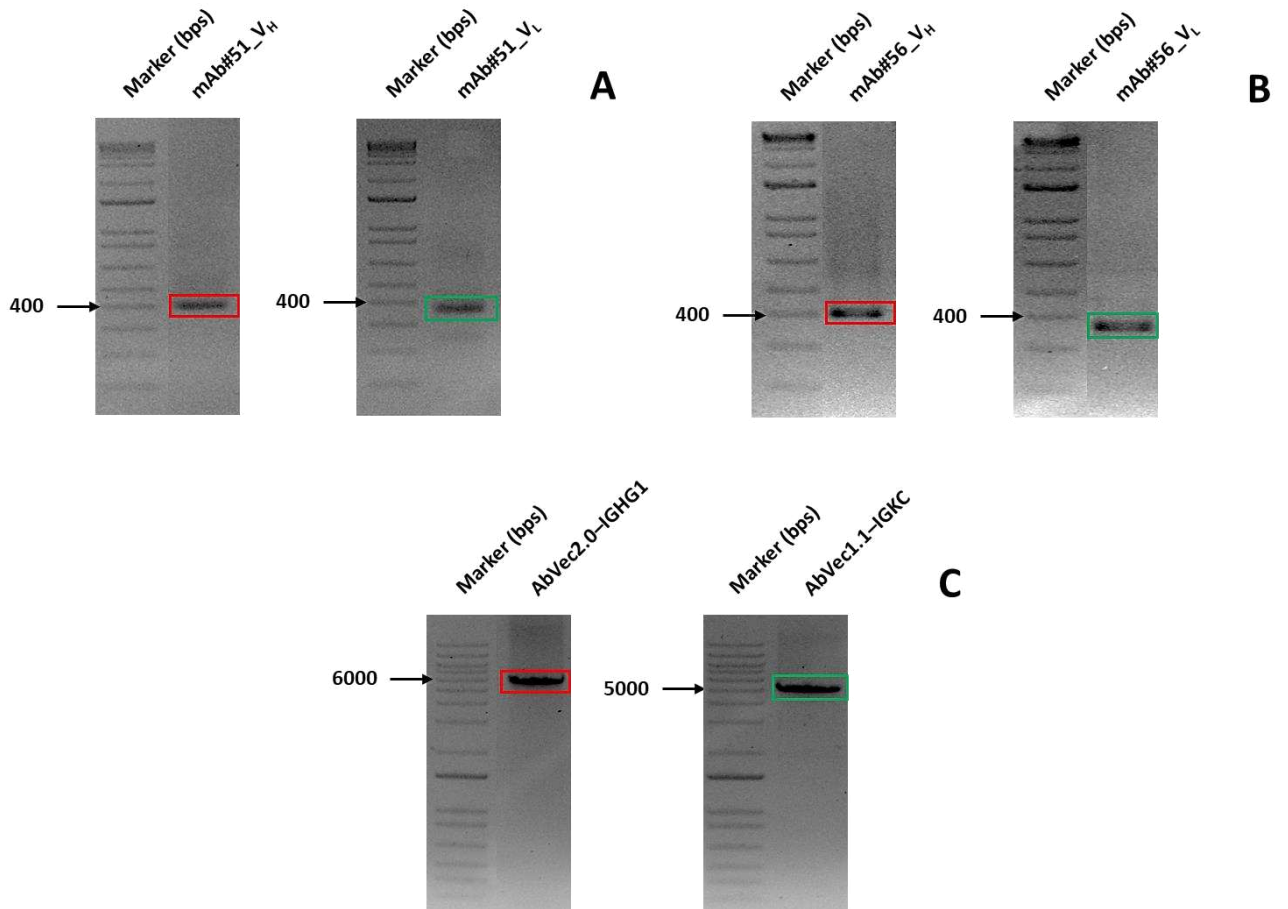


Figure B-13: Quality evaluation of mAb#51 PCR II products PIPE-amplification. The red and green squares highlight the presence of a band with dimension comparable to those expected for the amplified mAb_{V_H} and mAb_{V_L} inserts, respectively (A). Quality evaluation of mAb#56 PCR II products PIPE-amplification. The red and green squares highlight the presence of a band with dimension comparable to those expected for the amplified mAb_{V_H} and mAb_{V_L} inserts, respectively (B). Quality evaluation of AbVec2.0-IGHG1 and AbVec1.1-IGKC plasmids PIPE-amplification. The red and green squares highlight the presence of a band with dimension comparable to those expected for the amplified AbVec2.0-IGHG1 and AbVec1.1-IGKC vectors, respectively (C).

V_H and V_L sequences cloning into expression vectors

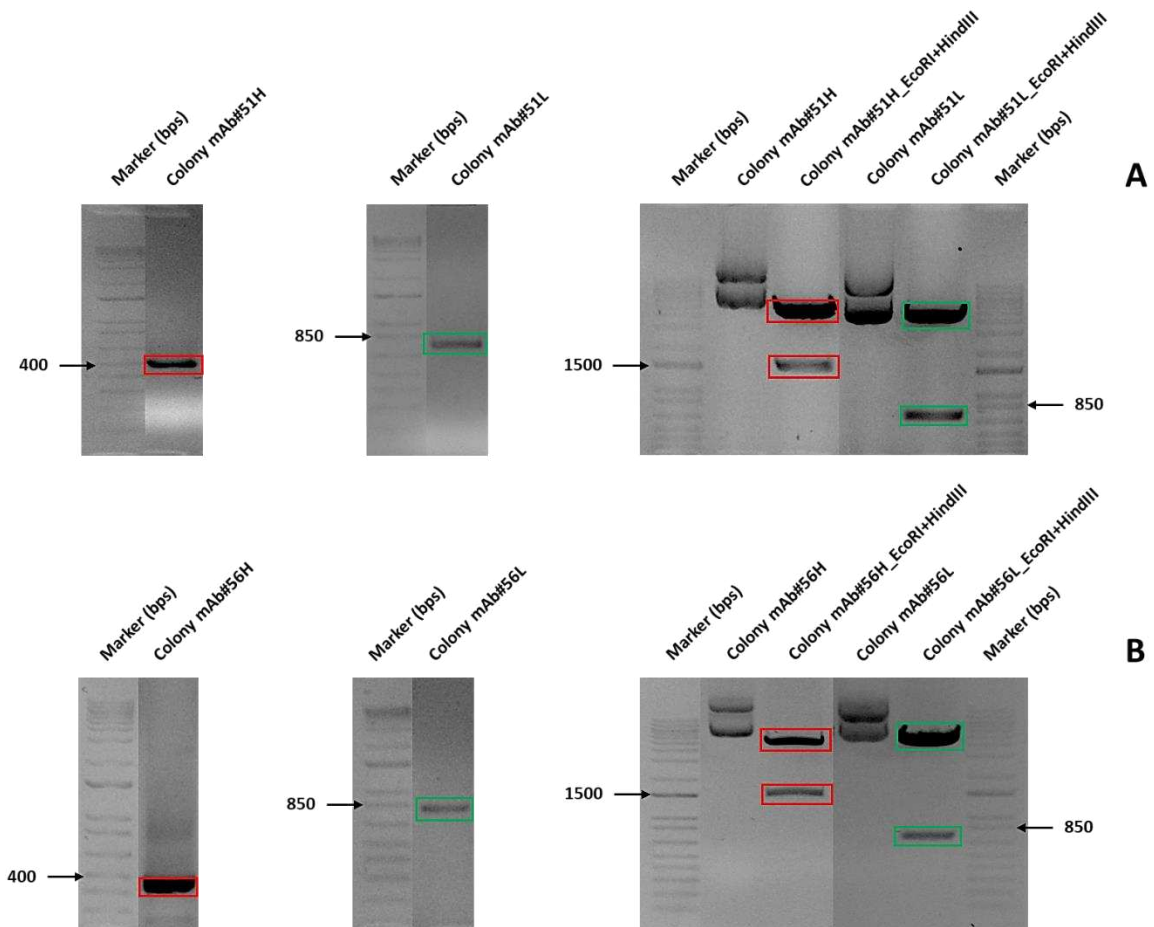


Figure B-14: Colony PCR and control digestion with *EcoRI* and *HindIII* restriction enzymes for the screening of *Mach1* colonies transformed with *mAb#51H/L* insert + *AbVec2.0-IGHG1/AbVec1.1-IGKC* vector. The red square and green squares highlight the bands corresponding to the correct cloning of *mAb#51_{VH/VL}* insert into *AbVec2.0-IGHG1/AbVec1.1-IGKC* vector, respectively (A). Colony PCR and control digestion with *EcoRI* and *HindIII* restriction enzymes for the screening of *Mach1* colonies transformed with *mAb#56H/L* insert + *AbVec2.0-IGHG1/AbVec1.1-IGKC* vector. The red square and green squares highlight the bands corresponding to the correct cloning of *mAb#56_{VH/VL}* insert into *AbVec2.0-IGHG1/AbVec1.1-IGKC* vector, respectively (B).